



HAL
open science

Contributions for enabling high data rate applications in low-power networks

Moufida Maimour

► **To cite this version:**

Moufida Maimour. Contributions for enabling high data rate applications in low-power networks. Networking and Internet Architecture [cs.NI]. Université de Lorraine, 2023. tel-04253876

HAL Id: tel-04253876

<https://hal.science/tel-04253876>

Submitted on 23 Oct 2023

HAL is a multi-disciplinary open access archive for the deposit and dissemination of scientific research documents, whether they are published or not. The documents may come from teaching and research institutions in France or abroad, or from public or private research centers.

L'archive ouverte pluridisciplinaire **HAL**, est destinée au dépôt et à la diffusion de documents scientifiques de niveau recherche, publiés ou non, émanant des établissements d'enseignement et de recherche français ou étrangers, des laboratoires publics ou privés.

Contributions for Enabling High Data Rate Applications in Low-power Networks

Habilitation à Diriger les Recherches

présentée et soutenue publiquement le 19 octobre 2023

pour l'obtention d'une

Habilitation de l'Université de Lorraine

(mention Automatique, Traitement du Signal et des Images, Génie Informatique)

par

Moufida MAIMOUR

Composition du jury :

Président :	William DERIGENT	Professeur, Université de Lorraine, France
Rapporteurs :	Marilyne CHETTO Karim DJOUANI Arkady ZASLAVSKY	Professeure, Université de Nantes, Nantes, France Professeur, Université Paris Est, Créteil, France Professeur, Deakin University, Australie
Examineurs :	Noureddine DOGHMANE Eric RONDEAU Pascale VICAT-BLANC	Professeur, Université Badji Mokhtar, Annaba, Algérie Professeur, Université de Lorraine, France Directrice de Recherche, INRIA, France



This document ...

Before you stands my dissertation, titled "Contributions for Enabling High Data Rate Applications in Low-power Networks", written to fulfill the requirements for my HDR¹ at the University of Lorraine, France. The manuscript is organized into three main parts. The first part, "State of the Art and Main Contributions", provides a detailed overview of my research activities conducted at CRAN² since 2004. It highlights the key contributions and outcomes of my work during this period. The second part focuses on my scientific project for the coming years titled "Digital Twin from Manufacture to Nature - Network Perspective", outlining the main direction and objectives of my future research. Lastly, the third part contains my Curriculum Vitae, providing a summary of my professional background including academic qualifications, teaching experience and research activities.

While my research work at CRAN continues to be centered around communication networks, there has been a noteworthy shift in my research interests from my earlier work. During my thesis, I investigated issues related to *Multicast* communication in the Internet, with a particular emphasis on its application in *Grid Computing*, a concept introduced in the mid-1990s. *The Cloud* can be viewed as a shift in emphasis from an infrastructure that provides resources (*The Grid*) to an economy-driven model that strives to offer abstract resources and services. In my thesis, I used *Active Networks*, an emerging concept at that time, to provide network services to guarantee fully reliable data transfer. Active networks played a key role in introducing programmable functions into the network and is considered a precursor to *Software-Defined Networking* (SDN). Since joining CRAN, my research direction has evolved towards *Wireless Sensor Networks* (WSN).

The inherent constraints of a WSN in terms of energy, bandwidth, processing and storage means, have restricted its scope to the deployment of relatively low rate event-driven applications where a limited amount of data is transferred. However, there is a growing class of WSN applications that involve high data rate sensing and reporting. Modern applications are witnessing an increase in the number of sensors and their data acquisition frequency. Some of these applications produce continuous and intensive sampling, possibly from multiple sensors, of relatively small data. Others rely on fine grained resolution sensing, where a single sample constitutes a substantial amount of data, as it is the case of images in *Wireless Video Sensor Networks* (WVSN). High data rate applications pose unique challenging problems in constrained networks. Large amount of data to be transmitted with high reporting rates consumes an order of magnitude of resources. Intensive traffic loads generated by such applications are prone to losses and network congestion. Moreover, the low-power and low-rate radios of sensor nodes are unable to provide sufficient bandwidth. Therefore effective solutions are essential to offer a good quality of service (QoS) as well as a satisfactory quality of experience (QoE), despite the limited resources of a WSN.

To handle high data rate applications, I considered the design of multipath routing protocols to exploit the high density of WSN to raise the network capacity. As storage means are limited at sensors, routing state at intermediate nodes needs to be kept as small as possible. To populate and maintain its routing state, protocols in adhoc networks rely heavily on flooding to discover routes. This results in substantial

¹Habilitation à Diriger les Recherches

²Centre de Recherche en Automatique de Nancy - Center for Research in Automation of Nancy

overhead that consumes scarce resources such as bandwidth and energy, ultimately impacting the network lifetime. A low-state, low-overhead yet efficient multipath routing protocol is presented in Chapter 1, along with a practical adaptation to standard IEEE 802.15.4 network layers, namely, ZigBee and 6LoWPAN³.

Multipath routing is a good candidate to allow for bandwidth aggregation but its effectiveness is hindered by the shared nature of the wireless medium, particularly when faced with high load traffic. The simultaneous utilization of adjacent paths with high transmission rates leads to significant interpath interference, thereby increasing the likelihood of packet transmission failures caused by collisions along the active paths. Chapter 2 reports on the research made to construct a set of maximally zone-disjoint paths that minimize interpath interference to increase throughput and achieve load balancing features. The research undertaken focused on proposing interference-aware multipath routing protocols, wherein careful consideration was given to assessing and comparing different adopted methodologies based on a unified model. This comprehensive analysis aimed to provide insights into the strengths and limitations of each approach, ultimately contributing to the advancement of multipath routing techniques in WSNs.

In addition to multipath routing, self-organization mechanisms based on clustering techniques have also been employed to enhance network efficiency and prolong its lifetime. This enables the implementation of a hierarchical routing, which addresses the issue of control messages flooding while reducing the routing state. In Chapter 3, clustering techniques are examined from the perspective of data routing. A combination of a recognized routing paradigm in sensor networks *Directed Diffusion* with an energy-efficient and load-balanced cluster formation algorithm is presented.

The resource-intensive tasks associated with WWSNs, such as video capture, encoding, and transmission, present unique and demanding challenges. Bandwidth scarcity poses a major hurdle in WWSNs, given the limited capabilities of low-power and cost-effective sensors equipped with low-range radios. To address this challenge, leveraging multiple non-interfering paths in conjunction with a self-organization mechanism offers a potential solution. However, even with optimal sensor placement and interference-free communication, the capacity of a WSN remains limited, making it difficult to provide sufficient bandwidth to fulfill the requirements of data-intensive applications. In the WWSN context, relying on sensors to deliver all the captured visual data is inefficient. Consequently, in-network data reduction becomes crucial to minimize transmissions and reduce energy expenditure.

Low-cost lossy compression techniques provide a means to reduce the volume of data to deliver, but it comes at the expense of introducing additional distortion. Moreover, wireless transmissions are prone to packet losses, resulting in missing portions in the transmitted images, further deteriorating their quality and making them challenging to be used effectively. Chapter 4 presents a complete and efficient encoding-transmission-reconstruction chain. The absence of performance evaluation tools that consider both quantitative (QoS) and qualitative (QoE) assessment of video transmission protocols in highly constrained networks motivated the development of a dedicated tool. This tool allows experimentation in simulated environments as well as in real-world testbeds.

The obtained results demonstrated that employing low-cost image compression techniques, along with the utilization of multiple paths and traffic prioritization, can significantly improve the quality of received images. While compressing captured images helps reduce the amount of data to be transmitted, it remains substantial for networks with constrained resources. Therefore, further reduction at the source is necessary. One effective approach to mitigate this issue is to transmit only the *Regions of Interest* (ROI) within an image. This approach strikes a balance between achieving high accuracy and optimizing limited resources in the network. Chapter 5 provides an overview of the research conducted to provide efficient and low-cost techniques for ROI extraction.

WSNs play a crucial role as a foundational component of the rapidly expanding *Internet of Things* (IoT). The distributed nature and the significant scale of the IoT make it complex and difficult to model accurately.

³IPv6 Low power Wireless Personal Area Networks

Therefore, providing services that meet stringent requirements becomes inherently challenging. Despite the significant growth of the IoT, a universal architecture has yet to be established. International standardization efforts are currently underway, with various bodies competing to find a global and viable solution to what scientists summarize in *5Vs*: *volume, velocity, variety, veracity and value*. Recent advancements in GPU technology and cloud computing have propelled machine learning to the forefront, offering solutions to complex and challenging problems across diverse domains. This development, along with the rise of big data analytics, has fueled the revival of the *Digital Twin* concept. In Chapter 6, I present my future research project, which primarily focuses on *Knowledge-Defined Networks* (KDN) from a digital twinning perspective. The objective is to achieve the added value, in the sense of "knowledge", that has been absent in my previous work, both in terms of application and network-related data. Accordingly, the aim is to build a holistic digital twinning architecture where the communication network is tightly integrated along with other system components. This research aims to investigate two use cases with distinct requirements, namely the *Industrial Internet of Things* (IIoT) and the *Internet of Multimedia Things* (IoMT).



Contents

I	State of the Art and Main Contributions	1
1	Small-state Low-overhead Multipath Routing	3
1.1	Routing in Adhoc and WSNs	3
1.2	Multipath Prefix Routing (MPR)	6
1.3	MPR Applied to ZigBee	12
1.4	6LoWPAN adaptation of MPR	17
1.5	Conclusion	23
2	Interference Aware Multipath Routing	25
2.1	Interference Aware Routing Metrics	25
2.2	Interference Aware Multipath Routing Overview	28
2.3	Generic Multipath Protocols Description	30
2.4	Performance Evaluation Setup and Metrics	32
2.5	Concurrent Versus Incremental Paths Discovery	34
2.6	Impact of Interference Aware Metrics	41
2.7	Conclusion	43
3	Energy Efficient Passive Clustering	45
3.1	Clustering in WSNs	45
3.2	Energy Efficient Passive Clustering	48
3.3	Simulation Results	52
3.4	Conclusion	58
4	Toward Efficient Video Transmission in Constrained Networks	61
4.1	QoE Video Transmission Evaluation in Constrained Networks	62
4.2	Video Multipath Routing for 6LoWPAN	75
4.3	DL-based Image Restoration	82
4.4	Conclusion	88
5	RoI Reduction Strategies for Constrained Networks	89
5.1	Block-based movIng Region Detection (BIRD)	90
5.2	Multi-Level Region Detection Scheme	96
5.3	Conclusion	106
II	Scientific Project	107
6	Digital Twin from Manufacture to Nature - Network Perspective	109
6.1	DT-based KD-WSN	111
6.2	Digital Twinning and Communication Networks	113

6.3	Digital Twin Modeling and Placement	114
6.4	From Industrial to Natural Environment Digital Twinning	116
6.5	Knowledge Extraction for Natural Environment Surveillance	119
6.6	TSCH Communication Scheduling	120
6.7	Project Timeliness and Positioning	123
III	Curriculum Vitae	127
7	Curriculum Vitae	129
7.1	Summary of Teaching/Administrative Activities	131
7.2	Supervision Activities and PhD Panel Participation	134
7.3	Scientific Projects	138
7.4	Editorial Activities and Community Services	141
7.5	Publications and Scientific production	143
	Bibliography	151

Part I

State of the Art and Main Contributions

Chapter 1

Small-state Low-overhead Multipath Routing

Routing is the process by which a node decides on which link a message has to be sent to reach its destination. To do so, routing protocols make use of route information or *routing state* maintained at intermediate nodes. As storage means are limited at sensor nodes, routing state at intermediate nodes needs to be kept as small as possible. Since WSN¹ are infrastructureless, control messages are required and are usually flooded in the network to discover and maintain routing state. This results in substantial overhead that consumes bandwidth and energy, precious resources in WSNs, which affects the network lifetime. Therefore, control traffic has to be significantly reduced in WSN's routing protocols.

In this chapter, is presented MPR² [MB16], a multipath routing protocol where efficiency is pursued while route state as well as the control traffic overhead are maintained as low as possible. Section 1.1 gives a brief overview of main routing methods and strategies developed for adhoc networks in general and WSNs in particular. Then, Section 1.2 presents the MPR protocol along with two labeling schemes for practical implementation. Finally, Sections 1.3 and 1.4 report on MPR practical adaptation to the IEEE 802.15.4 standard network layers, namely, ZigBee in the context of Bidai's Thesis [Bid13] and 6LoWPAN³ in the context of Kettouche's Thesis [Ket22].

1.1 Routing in Adhoc and WSNs

With respect to routing protocols in adhoc networks, an abundant literature already exists. Many methods and strategies have been proposed that we can classify based on different criteria. Figure 1.1 sums up main classes and schemes that are taken up in what follows which is far from being a comprehensive survey.

1.1.1 Proactive or Reactive Route Discovery

Depending on when the path discovery takes place, a routing protocol is either *reactive*, *proactive* or even *hybrid* if it combines both strategies. In the proactive variant, each node maintains a routing table that indicates for each possible destination, the link on which transmit a given message. This is the case of protocols like DSDV⁴ [PB94]). Routes are built and maintained a priori regardless of their actual use. This approach relies on massive flooding of control messages in order to maintain up-to-date routing tables. These control packets incur significant overhead which wastes the already scarce resources in WSNs. It

¹Wireless Sensor Networks

²Multipath Prefix Routing

³IPv6 Low power Wireless Personal Area Networks

⁴Destination-Sequenced Distance-Vector

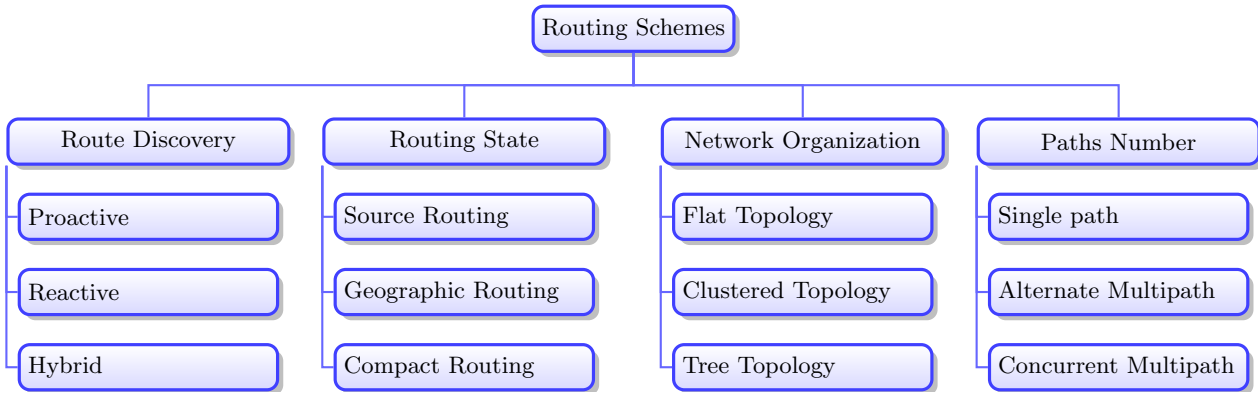


Figure 1.1: Main Routing Schemes in Adhoc Networks

mainly consumes energy and reduces the amount of bandwidth that should be reserved for useful data transfer. As a result, proactive protocols are not suitable to WSNs especially dynamic dense ones. This is even more problematic in the context of high data rate applications where a minimum bandwidth has to be granted to usefully data transmission rather than control traffic.

In order to limit the amount of control messages, reactive (on-demand) routing protocols, such as AODV⁵ [CP99], build their routes as needed. This is why, reactive routing has been considered as more suitable to WSNs than proactive ones. A *source* node willing to send data but does not have the route information, triggers a route request (RREQ) message in order to find its route to the sink. RREQs are broadcast hop by hop toward the sink. Based on the received RREQs, the sink chooses one path and sends the corresponding information back to the source using a route reply (RREP) message. This latter process is commonly called *route reinforcement*.

1.1.2 Compact Routing

Since sensors have very limited memory space, *Routing state* has to be maintained as small as possible. DSR⁶ [JMB01] does not require the maintenance of any routing table but still be inefficient in terms of bandwidth utilization since it also relies on flooding. Geographic routing protocols make use of location information to limit the route discovery flooding to a geographic area around the destination (GEAR⁷ [YYG01]) or to guide packet forwarding through a simple greedy forwarding (GPSR⁸ [KK00]). In this latter, each node forwards the packet to a neighbor closer to the destination than itself, until ultimately the packet reaches the destination. Geographic routing needs only $O(1)$ state per node however additional hardware or resource-hungry localization algorithms are required. Issues related to real-world environments still an open research question in geographic routing such as bypassing holes and obstacles [LWM22].

Compact routing [LT95] is another alternative technique for routing where a reduced routing table can be used provided that nodes are appropriately labeled. Interval routing is one of the most important compact routing that first introduced by Santoro & Khatib [SK85] for tree networks and subsequently extended by Leeuwen & Tan [LT83] to other network topologies. Interval routing requires tables of size $O(d)$ where d is the degree of a node. Each link (channel or neighbor) is associated with an interval of integers. The link is selected if the destination address is within the interval. S4 protocol⁹ proposed in [MWQ⁺07] adopts compact routing for WSNs. It builds on the work of Thorup and Zwick [TZ01] with some changes to meet the requirement of a practical implementation. S4 selects $O(\sqrt{N})$ nodes as beacons where N is the size of the network. Each node forms a virtual local cluster consisting of nodes whose distances to the present node

⁵Adhoc on-demand distance vector

⁶Dynamic Source Routing

⁷Geographical Energy Aware Routing

⁸Greedy Perimeter Stateless Routing

⁹small state and small stretch

Algorithm 1: Prefix Routing Algorithm (PR)

Input: This node's id (c), destination id(d)
Output: The next hop node (x)

```

if  $d == c$  then
  | return
end
if  $c$  is an ancestor of  $d$  then
  |  $x$  is the child with the longest prefix( $d,x$ )
else
  |  $x = parent(c)$ 
end

```

are within their distances to the closest beacons. A node maintains the shortest-path routes to all nodes within its cluster as well as the shortest-path routes to all the beacon nodes. Thus, to reach a destination node outside its cluster, a source node first routes toward the beacon closest to the destination node. While S4 does well at bounding the maximal routing stretch, it requires $O(\sqrt{N})$ node state and maintenance traffic, which may be significant for very large networks and for some constrained sensor node platforms.

1.1.3 Hierarchical Routing

From network organization perspective, a routing protocol can be qualified as *flat* or *hierarchical*. One popular flat-based routing in WSN are data-centric protocols, I mention Directed Diffusion [IGE⁺03] as its extension to become hierarchical was considered as part of Zeghilet Thesis [Zeg13]. This will be discussed in chapter 3.

In a flat topology, each node plays the same role and has the same functionality as other sensor nodes in the network. As opposed to a flat organization, hierarchical organization allows more scalability and is naturally more suitable to typical communication mode in WSNs known as *convergecast*. Data transfer is from multiple sources to a particular sink (*many-to-one*), rather than from one entity to another. Furthermore, with respect to compact routing, a hierarchy endowed with an appropriate labeling scheme allows an efficient data gathering by the Sink. It has been proven that using a Depth-First Scheme (DFS) to label nodes in the tree (resulting in an interval routing) allows an optimum routing [LT83], that is, it allows to find the shortest path (in terms of number of traversed links) to the tree root. However, interval tree routing often provides fragile routing paths and is hardly applicable in dynamic networks. A single hop failure may result in recomputing all the assigned labels in the tree.

To overcome the poor adaptability of the classical interval routing to dynamic changes in the network topology, one can make use of a different compact routing scheme called *prefix routing* [BLT93]. Prefix routing is more robust to topology changes since precedence information is explicitly available. The tree root is labeled by the empty string. Each node in the tree is labeled by a string such that a parent label is a substring of each of its children labels. A node is selected as the next hop if its label has the longest matching prefix of the destination node label (Algorithm 1). Authors of [IS07] developed a framework called HR¹⁰ that uses a kind of prefix routing on top of a multi-level clustered topology where the hierarchy is built in a bottom-up approach (from leaves to the root). They evaluate the implementation of their framework in TOSSIM and on a 60-node test-bed. They demonstrate that from the practical perspective HR can offer low routing stretch despite only logarithmic routing state.

¹⁰Hierarchical Routing

1.1.4 Multipath Routing

Multipath routing protocols [SGG13] enable a source node to discover several paths towards the destination. Traditionally, multipath routing was targeted to failure tolerance. Additional paths are maintained to serve as backup on primary path failure using disjoint [SSK⁺07] or non-disjoint paths [GGSE01]. Multiple discovered paths can also be used to concurrently transmit data. Data intended to the sink is split into multiple streams each routed on a different path. Splitting network traffic over several paths leads to more reliability by alleviating congestion [MPA08], introducing redundancy (MMSPEED¹¹ [FLE06] or using network coding [WDHN04] techniques. Furthermore, concurrent multipath allows bandwidth aggregation [Mai08] [MB16]. Finally, load distribution in multipath routing can result in even energy consumption among sensors which improves the network lifetime by delaying the appearance of network partition [LW06, MLWSW07].

Multiple paths discovery is performed either concurrently or incrementally (Chapter 2). In concurrent paths discovery approach, all the required paths are built using one RREQ flooding. The most important issue in this approach is whether a given RREQ is to be rebroadcast or dropped by an intermediate node. In fact, it appears that when dropping all duplicate packets (same source address and same sequence number), the probability to find node-disjoint paths is almost zero since generated paths are mostly overlapped [LG01, WH01a]. In the iterative paths discovery approach, the source sends its first RREQ to build one path and sends subsequent RREQs each time it receives an RREP with a new disjoint path until the required number of paths is achieved.

1.2 Multipath Prefix Routing (MPR)

MPR builds and maintains multiple disjoint paths from one sensor to the sink. It relies on an already built spanning tree rooted at the sink and assumes that a prefix labeling scheme is available along with this tree. MPR is both proactive and reactive multipath routing protocol. It is proactive since at least one path can be inferred from the tree structure. It is reactive since if required, it will build additional paths based on a very light discovery process. From the one hand, heavy control traffic inherent to reactive routing is reduced and on the other hand, overhead due to routing tables exchange is avoided as it is the case in proactive routing. Moreover, the use of prefix tree routing reduces the size of routing tables in the sensor nodes in addition to help in ensuring paths disjointness. Unlike S4 [MWQ⁺07] and HR [IS07], the aim is to build multiple disjoint paths to the sink rather than one path to other nodes in the network.

1.2.1 Network Model, Assumptions and Definitions

The sensor network is modeled as a graph $G(V, E)$ composed of a set of vertices (sensor nodes) V and a set of edges (links) E . G is assumed to be an undirected connected graph. That is, edges (u, v) and (v, u) are the same and implies that u and v are in the radio transmission range of each other. This assumption is a necessary condition to be able to use reverse paths. Let $T(V, E_T)$ be the spanning tree of the connected undirected graph G rooted at a specific vertex $r \in V$ referred to as the *tree root* and corresponds to the sensor network *sink*. In order to build the spanning tree, a *building-up Method* can be adopted [Lou05]. A path from node u to node v is noted $P(u \rightarrow v) = (u, w_1, w_2, \dots, w_{n-1}, w_n, v)$ where w_i ($i = 1..n$) are its intermediate nodes. $P(u)$ is used to designate the path from node u to the tree root. The unique¹² path that connects a node u to the tree root using only links in the spanning tree T is called interchangeably, the *child-parent* or the *tree path* of u and is noted $P_T(u)$. Moreover, an operator " \rightarrow " is defined to designate the operation that allows to concatenate two paths P and P' so that $P \rightarrow P'$ designates the path where the last vertex of P is connected to the first vertex of P' .

¹¹Multipath Multi-Speed

¹²paths in trees are unique. If we assume that another path exists, this would lead to a cycle in T which is in contradiction to tree definition.

Table 1.1: Notations

Notation	Description
$G(V, E)$	network graph.
$T(V, E_T)$	the spanning tree of G rooted at sensor network sink r .
$P(u \rightarrow v)$	path from u to v .
$P(u)$	path from node u to the tree root.
$P_T(u)$	path from node u to the tree root using only links in the spanning tree T .
$P \rightarrow P'$	the path that results from concatenating P and P' in this order.
$\pi(v)$	v 's parent.
$dg(u)$	u 's degree in G .
d_u	u 's depth in T .
$l(u)$	u 's label.
$prefix_k(u)$	the first k symbols of the string $l(u)$: $prefix(u) = prefix_1(u)$.
$prefix(u, v)$	the first similar symbols in u and v .
H	tree height, $H \geq 2$.
W	tree width, $W \geq 2$.
\mathcal{T}_u	The MPR subtree rooted at u where $\pi(u) = r$.

The parent of a node v in T is noted $\pi(v)$ and a *descendant* u of a node v is a node such that v is in the tree path (using only tree links) from u to the root of T . We say also that v is an *ancestor* of u . Two children of the same node are called *siblings*. The tree that consists of a node $t \in T$ and all of its descendants is called a *subtree* rooted at t . The subtree corresponding to the root node r is the entire tree T . The *depth* of a node is the length (number of hops) of its tree path to the root. The tree root has a depth 0 and a non-root node has a non-zero depth which equals its parent's depth plus one. The height of the tree H is defined as the maximum depth among all the tree nodes. The term *degree* of a node is used to designate the total number of its adjacent links or neighbors and $dg(u)$ denotes the degree of node u in G .

In WSN, it is very difficult to build a global addressing scheme. In this work, a labeling scheme as the one used in prefix routing [BLT93, WS99] is adopted to reduce the size of routing tables. Each node is labeled by a string from an alphabet $\Sigma = \{s_i, i \in [1, W], W \geq 2\}$ where W is the tree width which is the maximum number of children a parent can have in T . The tree is then said to be a W -ary tree. The root is labeled by the empty string λ which is by definition the prefix of all strings built from Σ . For a parent with label L , the k^{th} child is labeled by $L||s_k$ where $||$ is a concatenation operator. In what follows, the assigned label to a node u located at depth d_u in T is noted $l(u)$. $prefix_k(u)$ consists in the first k symbols of the string $l(u)$ and $prefix$ is used instead of $prefix_1$. The substring that corresponds to the first similar symbols in u and v is noted $prefix(u, v)$. If $u = v$ then $prefix(u, v) = l(u) = l(v)$, otherwise $w = prefix(u, v)$ if $\exists w \in \{s_i\}^*, \exists u', v' \in \{s_i\}^+ : u = wu' \wedge v = wv' \wedge prefix(u') \neq prefix(v')$. w can be empty then we write $prefix(u, v) = \lambda$. Table 1.1 summarizes the main notations.

The aim of MPR is to build multiple disjoint paths [RCP23] from one node in the sensor network to the sink. MPR relies on an already built spanning tree $T(V, E_T)$ rooted at the sink $r \in V$ and assumes that a labeling scheme as the one introduced in Section 1.1.3 is available. The tree is assumed to have both width and height of at least 2. At any time, a sensor is assumed to maintain an up-to-date neighbors table. This latter can be built upon initialization of the network and updated periodically to adapt to network topology changes. Without loss of generality and for seek of clarity, we consider the case of one source s with depth d_s in T willing to transmit data via multiple paths to the sink (r) which is not directly reachable from s ; Otherwise, MPR considers the obvious path where s transmits directly to r .

MPR adopts a hybrid approach to build and maintain its paths. From the one hand, it is a proactive routing protocol since at least one path can be inferred from the tree structure. One path that can be used without any discovery process is $P_T(s)$, the tree path from s to r . On the other hand, MPR is a reactive routing

protocol since, if required, it builds additional paths based on a very light discovery process based on the tree structure, its labeling and neighbors tables. Prior to giving details about the paths discovery mechanism, we give the following definitions and lemmas :

Definition 1. (Paths disjointness) Two paths $P(a)$ and $P(a')$ from two different nodes a and a' respectively to the tree root r are said to be disjoint if their only common node is r . If the two paths have the same source $s = a = a'$ then there are two common nodes s and r .

Definition 2. (MPRS) An MPR subtree (MPRS) of T is a subtree rooted at one of the child nodes of the sink r . An MPRS rooted at u is noted \mathcal{T}_u and is said to be busy if its root (u) belongs to an already established path.

Lemma 1.¹³ An MPRS of T rooted at u is uniquely identified by one symbol from Σ which is the u 's label. We have $\forall v \in \mathcal{T}_u : \text{prefix}(v) = \text{prefix}(u) = l(u)$

Definition 3. (MPR-neighbor) Neighbors u and v are said to be MPR-neighbors if and only if each of them belongs to a different MPRS. We say also that u is an MPR-neighbor of node v and vice versa.

Lemma 2. Assume two neighbor nodes u and v . If $\text{prefix}(u) \neq \text{prefix}(v)$ or equivalently $\text{prefix}(u, v) = \lambda$ then nodes u and v are MPR-neighbors.

Definition 4. (MPRN) The MPR-node of a given path (from s to r) is the first node in this path that belongs to a non busy MPRS. The MPRN of the tree path from a source s is its own parent $\pi(s)$.

Basically, a built path \mathcal{P} in MPR is the concatenation of a discovered path $P(s \rightarrow m)$ and a tree path $P_T(m)$ where m is the MPRN of this path. The idea behind MPR is to discover the first portion of the path then reuse an already established tree path. The discovery phase is detailed in Section 1.2.2. At this stage, it is worth noting that in addition to the tree path $P_T(s)$ and thanks to the MPRN notion, MPR is able to use proactively the path $(s) \rightarrow P_T(w)$ if there is a node w that is an MPR-neighbor of s .

Figure 1.2 illustrates MPR on a simple topology where solid and dashed lines represent respectively the tree links (E_T) and the neighboring links. The nodes are labeled using strings from the alphabet $\Sigma = \{1, 2, 3\}$. Paths used by the source s to forward data to the sink r are represented using arrowed lines. In this example, two paths can be used immediately, the tree path $\mathcal{P}_1 = P_T(s)$ and the path $\mathcal{P}_2 = (s) \rightarrow P_T(i)$ with i as the MPRN. In fact, i is an MPR-neighbor of s since they belong to two different MPRSs and the i 's MPRS is not busy. The third path $\mathcal{P}_3 = (s, j) \rightarrow P_T(f)$ requires a discovery phase to build its first portion (s, j) since j belongs to the same MPRS as s . Based on definition 4, nodes e, i and f are respectively the MPRN of paths $\mathcal{P}_1, \mathcal{P}_2$ and \mathcal{P}_3 .

1.2.2 Paths Discovery and Maintenance

Paths Disjointness. As stated before and thanks to the proactive property of MPR, the source is able to immediately start transmitting data on at least one path. Whenever the application requires more paths, a light discovery process can be initiated by the source using explore messages. The labeling scheme is of great importance in achieving a light discovery process in MPR. Labeling contributes in ensuring that two paths are disjoint without a complete discovery as it is the case of reactive routing protocols where request messages have to be forwarded from a node to another until achieving the final destination. The following theorem sets the disjointness criterion between two tree paths :

Theorem 1. Two tree paths $P_T(a)$ and $P_T(a')$ where $a \neq a'$ are node-disjoint if and only if their respective nodes (except the root) belong to a different MPRS.

Corollary 1. Two tree paths $P_T(a)$ and $P_T(a')$ are node disjoint if and only if $\text{prefix}(a) \neq \text{prefix}(a')$ or equivalently $\text{prefix}(a, a') = \lambda$.

¹³Different proofs related to this chapter can be found in [MB16]

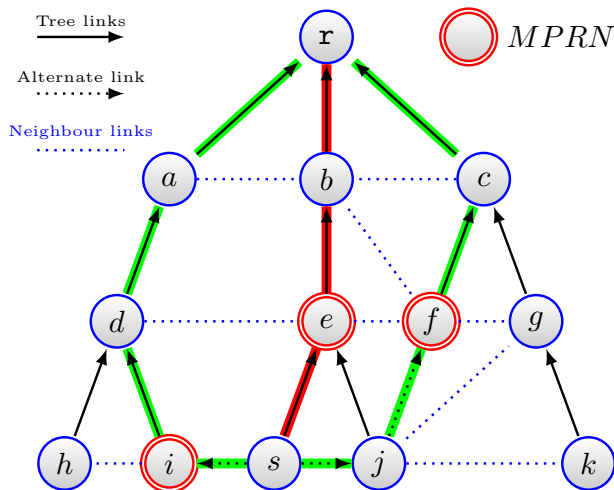


Figure 1.2: Illustrative MPR Example.

Corollary 2. *Each MPRS contains only one disjoint path to the root.*

Paths Discovery. In order to build the first portion of a path in MPR, a lightweight discovery process is initiated by the source using explore messages. An explore message (*ExploreMsg*) is forwarded from a *candidate* node to another based on specific rules using unicast. A *candidate* node is a node that may lead to the root via a disjoint path¹⁴. In order to ensure paths disjointness, an *ExploreMsg* carries a list \mathcal{ML} that contains the prefix of the currently used MPRSs. Two cases are possible :

- The explore message reaches an MPRN which means that a disjoint path exists. This path is the one followed by the *ExploreMsg* augmented by the tree path of the MPRN to the root. The MPRN sends a Response message (*ResponseMsg*) with the prefix of the MPRS it belongs to back to the source using the *ExploreMsg* reverse path. Upon the reception of the response message, the source updates the list \mathcal{ML} accordingly and if required by the application begins forwarding data packets via the neighbor on which the discovery was initiated. A node determines whether it is an MPRN for the path followed by an *ExploreMsg* simply by checking the absence of its prefix in the \mathcal{ML} carried by the *ExploreMsg*. If $prefix(c) \notin \mathcal{ML}$ then c is an MPRN.
- The explore message arrives at a node from which there is no forwarding candidates. This node sends an *ErrorMsg* on the explore message reverse path toward the source. Upon the reception of the *ErrorMsg*, this node neighbor marks it as a *non-candidate* node and tries to discover a new path by sending an *ExploreMsg* to a candidate node if available; otherwise it forwards the *ErrorMsg* back to the source. Likewise, the source marks the neighbor from which it receives an *ErrorMsg* as a *non-candidate*. A neighbor node is marked as a *non-candidate* for a given duration and at least for this discovery phase.

In both cases, if another candidate is available then the source can initiate another discovery phase mainly if the required number of paths is not achieved. In order to avoid infinite wait, the source triggers a new path discovery by issuing an *ExploreMsg* toward another candidate if no *ResponseMsg* is received within a determined duration. Note that the discovery process can be stopped as soon as the maximum possible number of disjoint paths is reached. Indeed, the number of node-disjoint paths is dictated by the network connectivity. It is limited by the minimum number of neighbors among the source and sink nodes. We can at most build $\min(dg(r), dg(s))$ paths. The source stops sending explore messages as soon as the number of built paths achieves $dg(s)$ the value of its own degree in G . One can implement a mechanism that allows the source to know the degree of the sink so it can stop earlier the discovery process if $dg(r) < dg(s)$. Note also that marking nodes as *non-candidate* allows limiting the number of sent explore messages.

¹⁴A discussion of the case where multiple candidate nodes are available can be found in [MB16]

In Figure 1.2, the third path \mathcal{P}_3 is discovered as follows. An *ExploreMsg* is sent to node j since it is the only available candidate (node i is already in use by path \mathcal{P}_2). Upon the reception of the *ExploreMsg*, j has to choose among candidate nodes f , g and k . Here, we assume that we take the decision to rather choose an MPR-neighbor which allows to find immediately a disjoint path if the corresponding MPRS is not busy. If two MPR-neighbors are available then the one with the smallest depth is chosen. In this latter case, shortest paths are privileged. Applying these two rules leads to choose node f as the next recipient of the *ExploreMsg*. Other rules can be applied in order to get paths with different properties and/or based on other metrics than the number of hops. For instance the path $(s, j, k) \rightarrow P_T(g)$ for which node g is the MPRN allows to get a longer path which nevertheless presents less interference, with the tree path \mathcal{P}_1 , than the path $(s, j) \rightarrow P_T(f)$ with f as MPRN. The maximum number of paths is achieved since $dg(s) = 3$. The source stops sending explore messages and the resulting forwarding nodes list is $\{e, i, j\}$ and $\mathcal{ML} = \{2, 1, 3\}$.

Paths Maintenance. MPR functioning builds on a tree structure in addition to up-to-date neighbors tables which both can be affected by network dynamics mainly due to node or link failure. Neighbors tables can be maintained using periodic exchange of hello messages. In order to maintain the tree structure, orphan nodes that occur after a parent node is dead for instance, have to be able to join a new parent in the vicinity. Association and disassociation procedures as those provided by the IEEE 802.15.4 MAC sub-layer [80211] can be adopted to build and maintain the tree structure. The prefix labeling is updated accordingly such that a node that joins a new parent gets the label of its parent plus its sibling rank. The prefix routing still operate correctly as opposed to interval routing where labels have to be recomputed to handle such changes in the tree topology.

Hello messages allow also to detect whether the next node in a path is still alive for routing. Moreover, link or node failure in a path can be detected in the absence of an ACK for a data packet after a certain number of retries if an ACK-based transmission is used. When an intermediate node detects a link failure, it issues a failure message (*FailureMsg*) back to the source. On the reception of this message, the source and the intermediate nodes stop sending data packets. *FailureMsg* may include in its header the sequence number of the last sent data packet so the source can retransmit it if full reliability is required by the application. The source may also redistribute the failed path traffic on the other paths. Meanwhile, the node that detects the failure issues an *ExploreMsg* if any candidate node is available in the vicinity ; otherwise it triggers an *ErrorMsg* back to the source.

Algorithm 2 summarizes the main operations related to the paths discovery and maintenance. The source records the available paths using a list of forwarding nodes and their corresponding MPRN nodes (only using their prefixes). An intermediate node records in its memory the identity of the next node to which send a received data packet.

1.2.3 MPR Prefix Labeling Overhead

In order to implement MPR prefix labeling, we propose to use either a fixed-length or a variable-length labeling schemes. In the former, all nodes' labels are of the same length whereas in the latter, a node's label length depends on its depth in the tree. In both schemes, an alphabet Σ composed of $W + 1$ symbols is required for a W -ary tree where each node has at most W children ($W \geq 2$). In a fixed-length labeling scheme (*FLS*), one more symbol is required to complete the label so all labels are composed of H symbols. In a variable-length labeling scheme (*VLS*), the additional symbol indicates the end of the label. Let $\Sigma = \{0, 1, 2, \dots, W\}$ and $\Sigma^* = \Sigma - \{0\}$.

Definition 5. (FLS) In fixed-length labeling scheme (*FLS*), a node $u \in V$ located at depth $d > 0$ of the spanning tree T is labeled with $l(u)$:

$$l(u) = s_1 || s_2 || \dots || s_d || 0 \dots 0 \quad (1.1)$$

Algorithm 2: - MPR Paths Discovery and Maintenance

Data: This node's id (c), the list of MPRSs already in use maintained by the source (\mathcal{ML})**ExploreMsg packet processing (intermediate node)**Mark the last crossed node as the *previous node***if** $prefix(c) \notin ExploreMsg.ML$ **then** // I am an MPRN

- | Send a *ResponseMsg* packet on the *ExploreMsg* reverse path with $ResponseMsg.MPRS = prefix(c)$

else if *no candidate node* **then**

- | Send an *ErrorMsg* on the *ExploreMsg* reverse path

else // there is a candidate node

- | Forward the *ExploreMsg* packet to a candidate node

end**ResponseMsg packet processing****if** *I am the source* **then**

- | Add the last crossed node to the list of the forwarding nodes and add $ResponseMsg.MPRS$ to \mathcal{ML}

- | Start, if required, forwarding data packets via the corresponding neighbour

- | Send, if required, another *ExploreMsg* if another candidate is available

else

- | // intermediate node

- | Mark the last crossed node as the *next node* in the currently built path

- | Forward on the *ExploreMsg* reverse path

end**ErrorMsg packet processing****if** *I am the the first crossed node* **then**

- | Mark the last crossed node as a *non-candidate* node

end**if** *no candidate node* **then**

- | Send an *ErrorMsg* on the *ExploreMsg* reverse path

else

- | // there is a candidate node

- | Forward the *ExploreMsg* packet to a candidate node

end**FailureMsg packet processing**

Stop sending data packets

if *I am the source* **then**

- | Start data transmission on a backup path if any

else

- | // intermediate node

- | Forward *FailureMsg* toward the source on the reverse path

end

where $s_i \in \Sigma^*$ gives u 's sibling rank. $(H - d)$ 0s are added to obtain an H -symbol label. The root gets the label composed of H null symbols.

Definition 6. (VLS) In variable-length labeling scheme (VLS), a node $u \in V$ located at depth $d > 0$ of the spanning tree T is labeled with $l(u)$:

$$l(u) = \begin{cases} s_1||s_2||\dots||s_d||0 & \text{if } d < H \\ s_1||s_2||\dots||s_{H-1}||s_H & \text{if } d = H \end{cases} \quad (1.2)$$

The root gets the label composed of one null symbol 0.

These labeling schemes are to compare with a flat addressing scheme defined as follows :

Definition 7. (FS) In a flat addressing scheme (FS), a node $u \in V$ is assigned a unique address from $[0 .. \lceil \log|V| \rceil]$ where $|V|$ is the number of nodes in the tree T .

Theorem 2. In a perfect W -ary tree ($W \geq 2$)¹⁵, both FLS and VLS have a maximum label size of $H \lceil \log(W + 1) \rceil$ with at most $H - 1$ additional bits with respect to the FS addressing scheme.

Corollary 3. In a perfect W -ary tree ($W \geq 2$), an FLS or a VLS label size is at most twice the size of an FS address.

Figure 1.3 shows the ratio of additional bits induced by FLS and VLS with respect to FS in a full W -ary tree as the number of nodes increases. When the tree width is set then the worst case for FLS and VLS consists in having only two routers per level i.e. $R = 2$. Figures 1.3a and 1.3b plot the ratio of additional bits when $w = 3$ allowing a tree width in the range $[4, 7]$. The number of routers per level is set to $R = 2$ (worst case) and $R = 4$. In Figures 1.3c, w is set to 4 allowing 8 to 15 children. We always observe that the number of additional bits increases with the number of nodes. Note that FLS and VLS labels size may be 3 times an FS address when $R = 2$. Nevertheless, in the context of WSN an adhoc network, any node is likely to be a router. Thus, the number of routers per level is more likely to be equal to the tree width which leads to a perfect tree rather than a full tree.

1.3 MPR Applied to ZigBee

The ZigBee Standard [Zig04] provides the network layer specifications to be implemented on top of the PHY and MAC layers standardized by the IEEE 802.15.4 [80211]. The two standards are tightly coupled to provide the consumer standardization for low-power and low-rate wireless communication devices. With respect to ZigBee, there is no much research on routing dedicated to the ZigBee network layer. The focus was only on AODV and tree routing defined in the ZigBee standard. The aim of most previous work was to improve and enhance the tree routing for ZigBee cluster-tree and mesh networks. Shortcuts to find paths with less hop count than the tree path are chiefly done through the use of neighbors tables [KKP⁺07, SR15]. Authors of [HPCK07, TPLT09, QSH09] additionally used network addresses to take shortcuts without incurring extra overhead. In particular, ETR¹⁶ [QSH09] intended to achieve certain balance between performance and cost by improving the hop-counts of the ZigBee Tree Routing with minor additional complexity. In addition to neighbors table, authors utilize the structured address assignment scheme of the ZigBee standard.

The IEEE 802.15.4 MAC layer defines two types of nodes : Reduced Function Devices (RFDs) that can act only as end devices and Fully Functional Devices (FFDs) able to operate as a coordinator or a router. The ZigBee network layer extends the basic star topology of an IEEE 802.15.4 PAN to a tree topology where the root, called ZigBee coordinator (ZC), and all internal nodes called ZigBee routers (ZRs) are FFDs. RFDs can only be leaf nodes and are called ZigBee End Devices (ZEDs). The ZC is responsible for initiating the

¹⁵A perfect W -ary tree is a full W -ary tree in which all leaf nodes are at the same depth. In a full W -ary tree, the root and each internal node in the tree has either 0 or W children

¹⁶Enhanced Tree Routing

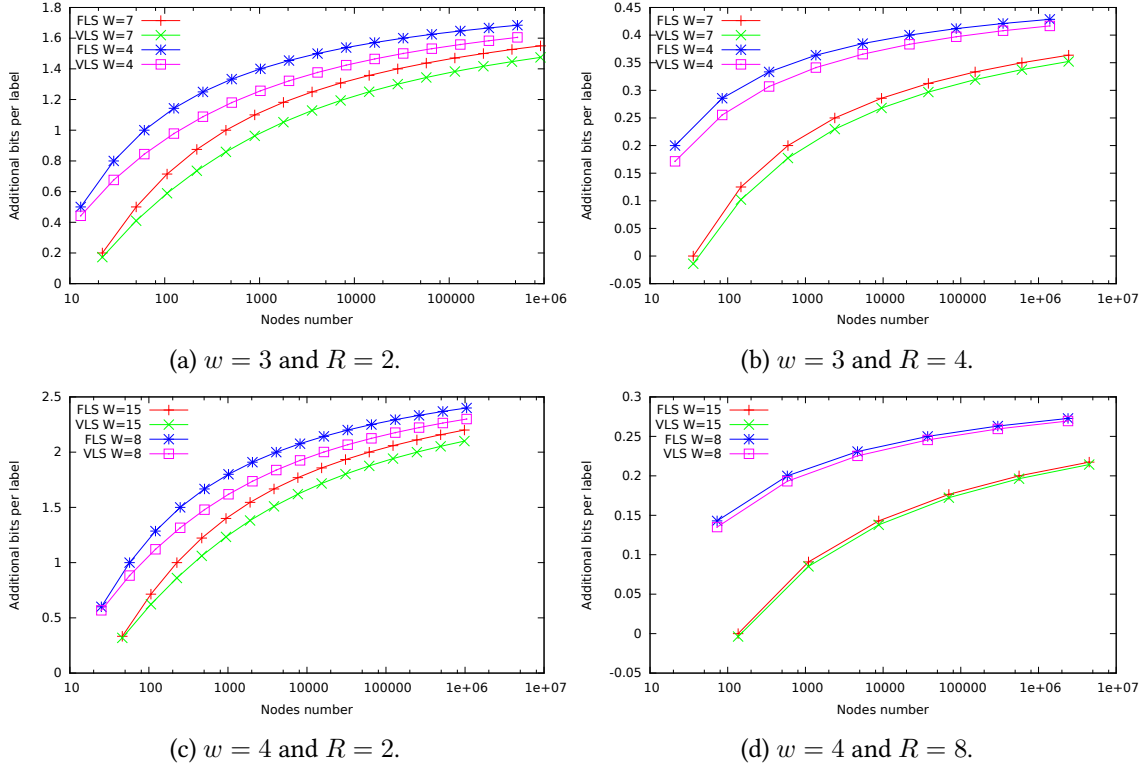


Figure 1.3: Ratio of additional number of bits in *VLS* and *FLS* with respect to *FS* in a full W -ary Tree.

formation of the tree topology. Parent-child relationships are established when a ZR or a ZED joins the network.

1.3.1 ZigBee Addressing Scheme

The ZigBee network layer specifies a distributed algorithm for address assignment. The ZC fixes three parameters (L_m, C_m, R_m) related to the tree topology : L_m is the maximum depth of the tree, C_m and R_m are respectively the maximum number of children and child routers a parent can have in the tree. Note that $C_m \geq R_m$, the ZC has depth 0 and that devices at depth L_m can only be ZEDs. Based on its depth d , a parent node distributes to each of its child routers an address sub-block of size $Cskip(d)$, $d = 0, 1, \dots, (L_m - 1)$ given by :

$$Cskip(d) = \begin{cases} 1 + C_m \cdot (L_m - d - 1) & \text{if } R_m = 1 \\ \frac{1 + C_m - R_m - C_m \cdot R_m^{(L_m - d - 1)}}{1 - R_m} & \text{otherwise} \end{cases} \quad (1.3)$$

The k^{th} router device gets the address :

$$A_k = A_p + (k - 1) Cskip(d) + 1 \quad (1 \leq k \leq R_m) \quad (1.4)$$

and the n^{th} end devices gets the address :

$$A_n = A_p + R_m Cskip(d) + n \quad (1 \leq n \leq C_m - R_m) \quad (1.5)$$

1.3.2 ZigBee Tree Routing

When the tree topology is adopted, the ZigBee standard provides tree routing (ZTR) which is a kind of interval routing since a given interval of addresses is located downstream one node as a result of the ZigBee

addressing scheme. Routing paths are directly inferred from network addresses based on the parent-child relationships. When a packet is received by a ZR with address A_c and depth d , it decides on whether the next hop node for the destination address A_d is up or down the tree by applying the routing rules of Algorithm 3. ZTR is simple to implement and is lighter in terms of memory and processing requirements than an AODV-like routing. Thus it is more suitable for the ZigBee limited resources devices.

Algorithm 3: - ZigBee Tree Routing Algorithm (ZTR)

Input: This router depth (d), this router address (A_c), this router's parent address (A_p), destination address (A_d).

Output: The next hop node address (A_x)

```

if  $A_d \in ]A_c, A_c + Cskip(d - 1)[$  then // the destination is downstream

  if  $A_d > A_c + R_m \cdot Cskip(d)$  then // the destination is a child : the
    packet is directly sent to this child

    |  $A_x = A_d$ 
  else
    | // The packet is forwarded down to an ancestor of the
    | destination
    |  $A_x = A_c + 1 + \lfloor \frac{A_d - A_c - 1}{Cskip(d)} \rfloor \cdot Cskip(d)$ 
  end
else
  | // The destination is upstream : the packet is forwarded to this
  | node parent
  |  $A_x = A_p$ 
end

```

In ZTR, communication is limited to parent-child links in the tree. As a consequence, routing paths could be longer because packets follow the hierarchical tree topology to the destination even if the destination is located nearby. Shortcuts are possible to improve interval routing stretch as stated before. ZTR often provides fragile routing paths and is hardly applicable in dynamic networks. A single hop failure producing an orphan node may result in recomputing all the assigned labels in the tree. Rather, in a prefix routing schemes, the orphan nodes gets simply the concatenation of its new parent's label and its new sibling rank. In this section, we show how a prefix routing label can be assigned to a ZigBee node so the ZTR can be replaced by a prefix tree routing that is more robust to topology changes. Furthermore, prefix routing labels allows the implementation of our multipath routing protocol (MPR) in ZigBee networks.

1.3.3 ZigBee Multipath Prefix Routing (ZMPR)

The cluster-tree topology is assumed to be rooted at the sink that plays the role of the coordinator. As for MPR, ZMPR [BMH12, BHM11] considers building multiple paths from one node to the sink. Multiple paths allows either the use of an alternative path if the tree path is broken or their simultaneous use to increase the available bandwidth in the presence of a high data rate reporting. ZMPR is applied on a steady state network where all the devices are well associated to their parent devices. ZMPR discovery and maintenance phases are similar to those of MPR. Prefix labels assignment can be performed in two ways :

- Make advantage of the association procedure specified in the ZigBee standard. The *Association Response Command* can be used to carry the prefix label of the parent node to the joining (child) node.
- Compute the prefix labels from the already ZigBee assigned addresses. For a given node u at depth $d_u \in [1, L_m]$, each element s_k ($1 \leq k \leq d_u$) of its label can be computed using the following formula

proposed by [QSH09] :

$$s_k = \begin{cases} \lfloor \frac{A - k - \sum_{i=1}^{k-1} Cskip(i-1)(s_i^c - 1)}{Cskip(k-1)} \rfloor + 1 & \text{if ZR} \\ A - k + 1 + R_M(1 - Cskip(k-1)) - \sum_{i=1}^{k-1} (s_i - 1)Cskip(i-1) & \text{if ZD} \end{cases} \quad (1.6)$$

where A is the ZigBee network address of node u and $Cskip(d)$ is given by Equation (1.3).

In the first method, an additional field has to be added in the *Association Response Command*. Its size depends on the largest possible label in the tree. In the second method, some computations are necessary and consumes resources even if they can be optimized. The nature of the network and the application requirements dictate the use of one method rather than an other.

In ZigBee, a neighbors table is maintained so to implement MPR, we need only to extend this table to meet our needs. A ZigBee neighbors table entry already includes the 64-bit MAC address of the neighbor and a relationship type. This latter field can be encoded on one byte and the ZigBee standard specifies only 4 relationship types, namely : parent, child, sibling and none. We propose to use 4 bits to encode other relationship types. The 4 remaining bits can be used to encode the state field. In this way no extra fields are introduced to the ZigBee neighbors table.

Illustrative Example. Figure 1.4 shows a network topology with parameters $(L_m, C_m, R_m) = (3, 4, 4)$ where all the sensor nodes are evenly distributed on a square-shaped area. The sink is the ZC located at the center. The transmission range (Tr) chosen in this topology allows to cover at least three neighbors and at most eight neighbors. The $Cskip$ values are respectively 21, 5 and 1 at depths 0, 1 and 2 (Equation (1.3)). For a given node, we give, separated by a comma, the ZigBee address (interval label that results from Equations (1.4)-(1.5)) and the prefix label using *VLS*.

In this example, the source node s is at depth 3 and has ZigBee address 4 and nodes a, c, b, f and k as neighbors. The prefix label of s is 112 (node s is the second child of b which is the first child of a which is the first child of the root r (PAN)). As shown in Figure 1.4, three node-disjoint paths are established from s to r . The first one is the classical path based on parent-child links and is the shortest one $\mathcal{P}_1 = P_T(s) = (s, b, a, r)$. To construct the second path, node s takes c as its next-hop node since c is an MPR-neighbor of s since $prefix(c) \neq prefix(s)$. Thus $\mathcal{P}_2 = (s) \rightarrow P_T(c)$. The establishment of the third path requires a discovery phase through node k that is the last remaining neighbor as the next-hop. k sends the *ExploreMsg* to y rather than x since y is located at a lower depth. y in turn sends the *ExploreMsg* to z that is an MPR-neighbor that belongs to a non busy MPRS. The resulting node-disjoint path is $\mathcal{P}_3 = (s, k, y) \rightarrow P_T(z)$.

1.3.4 ZMPR Performance Evaluation

To get more insight on the behavior of our proposed multipath routing in the context of the ZigBee technology, simulations were performed using ns2 [ns2]. ZMPR is compared with the classical proactive ZigBee tree routing (ZTR) and a reactive node disjoint multipath routing based on AODV called MAODV [BKH08]. Simulations were performed on a sensor network topology similar to the one of Figure 1.4 consisting of static sensor nodes ranging from 25 to 189 deployed in a square sensor field. The sink is located at the center of the area and sensor nodes are deployed in a rhombic lattice with 10 meters separating two adjacent nodes located at the same row or column of the grid. Main simulation parameters are summarized in Table 1.2. Each simulation lasts at least 120 seconds and repeated 20 times. Simulation results are averaged to produce mean values for different metrics to assess the performances of the simulated protocols.

Figure 1.5a shows the total number of exchanged control messages required to build multiple paths as a function of network size. This is done to evaluate the control messages overhead of ZMPR compared to a table-based multipath routing protocol MAODV. In both protocols, the routing overhead increases with

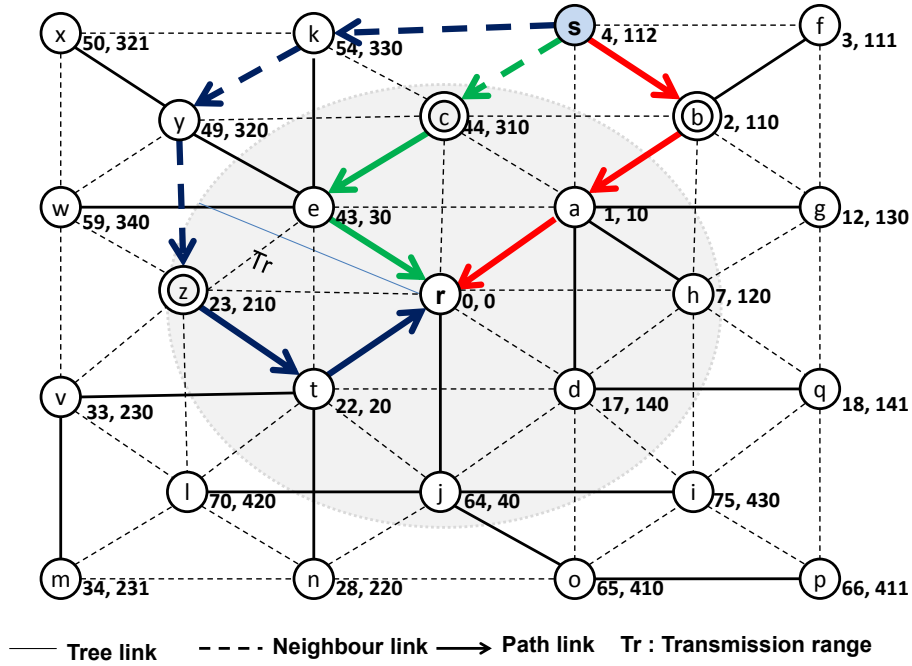


Figure 1.4: Rhombic lattice topology.

Table 1.2: Simulation Parameters

Parameter	Values
(L_m, C_m, R_m)	(7, 4, 4)
Number of nodes	25, 49, 100, 189
Distance between adjacent nodes	10 m
Transmission range (Tr)	11 m, 15 m
Packet payload	80 bytes
Transmission rate	1280 bps, 32 Kbps
Initial energy	0.5 J
Transmission power	42 mW
Reception power	59.1 mW
Idle power	60 μ W

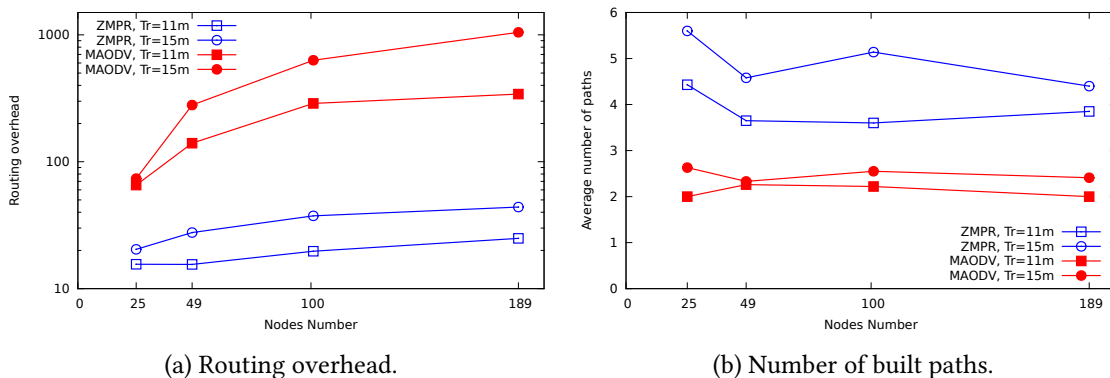


Figure 1.5: ZMPR vs. MAODV.

the number of nodes in the network. In fact, when the number of nodes increases, the source randomly chosen is likely to be located at a higher depth and consequently the number of control messages increases. However, unlike MAODV that makes broadcasts to build its paths, ZMPR finds node-disjoint paths with a very limited overhead.

Figure 1.5b that plots the average number of node-disjoint paths built by ZMPR and MAODV when the network size increases, shows that the number of paths depends on the network connectivity rather than the number of nodes in the network. When the transmission range is higher (15 m instead of 11 m), the degree of both the source and the sink are more likely to increase. As a result, the number of built paths increases as well. Note that ZMPR is able to build more paths than MAODV. This is due to the fact that the former uses unicast explore/response messages while the latter is based on RREQ/RREP broadcast which augments collisions and so the ratio of successful received control RREQ/RREP messages.

Figure 1.6a shows the average length (hop count) of paths built by ZMPR compared to ZTR as the number of nodes varies. It is clear that when the network size increases the average length of paths increases too. However, the average path length in ZMPR is almost shorter than the tree path (ZTR) mainly when the network density is higher ($Tr = 15m$). This is mainly due to the fact that the tree path comprises only tree links while other paths can be shortened through the use of neighbor relationships a node can have. This results in reduced delays in data routing to the sink.

From an energy perspective, unlike single path tree routing, multipath routing allows spreading energy utilization across a larger number of nodes. This feature leads to a higher network lifetime. Figure 1.6b shows the percentage of average consumed energy per routing node in the network under different network sizes. Energy consumption increases with the network size since the number of involved nodes in routing increases. Independently of the transmission range value, ZMPR consumes less energy than ZTR.

In order to evaluate the benefit of multipath routing in terms of throughput, in a 189-node topology, the transmission rate is risen to 50 packets per second giving a useful transmission rate of 32 Kbps. Figures 1.6c-1.6d plot the network throughput variation during 120 seconds of simulation. Multipath routing outperforms single path routing especially when the transmission range is set to 11 m where a 18% improvement with respect to ZTR is achieved. When the transmission range increases, the improvement is only about 10% since ZMPR is more affected by interference when the transmission range is higher (15 m). The problem of multipath routing interference is considered in details in Chapter 2.

1.4 6LoWPAN adaptation of MPR

RPL [ABV⁺12] is the IETF standardized IPv6 Routing Protocol for Low-power and lossy networks (LLNs). Based on an objective function, each node chooses a set of parents with one designated as the preferred

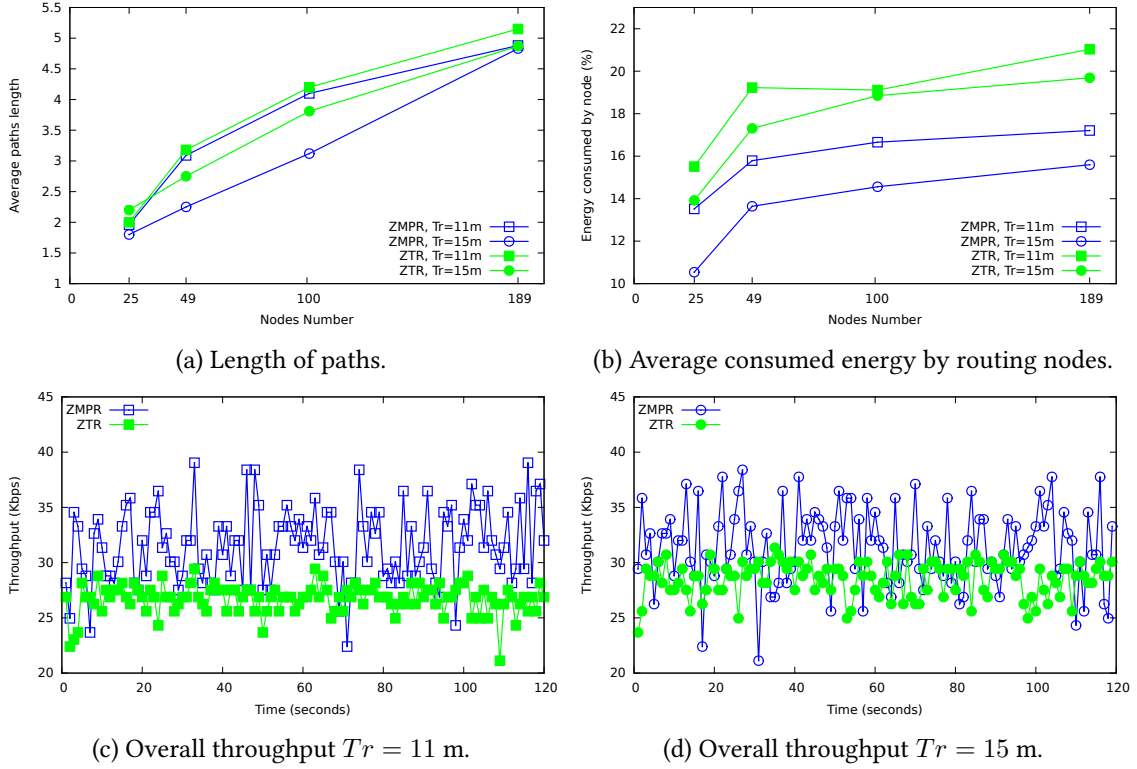


Figure 1.6: ZMPR vs. ZTR.

parent which results in a DODAG structure rooted at the *Sink*. Packets intended for the Sink are forwarded to the preferred parent. Two objective functions namely, $MRHOF$ ¹⁷ [VKP⁺12] and $OF0$ ¹⁸ [Thu12] are predefined. The former is based on ETX¹⁹ metric [DABM03] and the latter on the number of hops. The DODAG structure is maintained through the use of ICMPv6 control packets. The *DODAG Information Object* (DIO) is used to maintain the DODAG structure as it carries information that allows to select a parents set. Each node computes its *rank*, representing its position within the DODAG, using the OF. The preferred parent for a node is the one that allows obtaining the lowest rank.

Since RPL was chiefly designed to meet the requirements of LLNs, the major effort is made on handling low data rate traffic. However, modern applications are increasingly involving high speed sensing and reporting due to the growing number of sensors along with higher data acquisition frequency. Under heavy traffic, RPL may suffer from severe congestion [KKPB16]. As a result, high data loss rates, significant energy expenditure and a bad QoE are experienced especially when real time video delivery is required [KMD19]. [TYM17] emphasized the fact that the produced DAGs based on objective functions may not utilize the full network capacity and proposed to combine RPL object function with backpressure routing. New objective functions were also proposed in the literature to allow better performance in the context of multimedia applications [ASM15, MK18, BL20].

With regard to high data rate applications, routing protocols need to leverage the WSN density to augment its capacity by implying more nodes in the data transfer. Multipath routing is a good candidate to allow for bandwidth aggregation [BM14b] especially in dense networks [Mai18a]. Load distribution in multipath routing can result in even energy consumption among sensors which improves the network lifetime by delaying the appearance of network partition. RPL multipath extension has already been considered in the literature mainly for scalar data reporting and mostly make use of braided (non-disjoint) paths [ITN15,

¹⁷Minimum Rank with Hysteresis Objective Function

¹⁸Objective Function Zero

¹⁹Expected Transmission Count

[TMHW16, LJKPM21]. Additional RPL paths may serve for backup [ANT19], balance traffic when bottleneck nodes are identified [LGB⁺13, ITN15, MT14, ZWY17], improve reliability through replication [LJKPM21] or avoid/control network congestion [LRK⁺17, WZZW18, TMHW16].

All the above multipath routing are opportunistic and have one hop look-ahead. They are targeted to low data rate applications and mostly employ braided (non-disjoint) paths. In this section, an MPR-like multipath extension of RPL, called DM-RPL²⁰, is presented. Existing RPL control messages are used to insure disjointness rather than leveraging the multi-instance opportunity provided by RPL as done in [BBKS20]. In [ELJP⁺20], complete disjointness can be achieved using a detection mechanism at a common node during data transfer. This is allowed by the fact that these routes are used in a replication scenario. In DM-RPL, disjointness is guaranteed before data transmission, hence allowing for load-balancing strategies.

1.4.1 Disjoint Multipath RPL (DM-RPL)

High data rate applications such as multimedia ones are bandwidth demanding. Simultaneous use of multiple disjoint paths is a promising solution to offer additional bandwidth to ensure a good QoS/QoE. In [KMD22, KMD21a, KMD21b], we proposed to augment RPL without incurring much more overhead in such a way multiple disjoint paths are made available for a given source. This is why we build on the already existing DODAG structure maintained by RPL. In RPL, each node x maintains its set of parents, one being designated as the preferred parent, we refer to as $\pi(x)$. When a node has to send a data packet to the Sink, it transfers it to its preferred parent. The so formed path, noted $P^+(x)$ and called the *RPL path*²¹.

The main challenge in an RPL-based multipath routing is to guarantee disjointness while keeping the related overhead as low as possible. In DM-RPL, Theorem²² 3 (below, based on lemma 3) is used to guarantee the disjointness of paths used by one source :

Lemma 3. *In $T(V, E_T)$, a subtree T_x contains one and only one disjoint path from a source $s \in T_x$ to the root r . This path (and the corresponding subtree) can be uniquely identified by the ID of the subroot x .*

Theorem 3. *Let u and v be two nodes in $T(V, E_T)$. If u and v belong to two different subtrees, then their respective RPL paths $P^+(u)$ and $P^+(v)$ are node disjoint : $u \in T_x \wedge v \in T_y \wedge x \neq y \Rightarrow P^+(u) \cap P^+(v) = \emptyset$*

Each subtree in T contains one and only one disjoint path. For a given source s , to obtain disjoint paths, in addition to its RPL path $P^+(s)$, it has to designate alternate parents from disjoint subtrees. An alternate parent v (Figure 1.7), for instance, can be used by the source s as the next node in another path. Node v forwards received packets via its RPL path $P^+(v)$. To be able to identify the subtree to which belong each node (based on Lemma 3), we need to propagate the ID of each subroot downward. We suggest to do that using a new field, we call *PID* (Path ID), in DIO messages. When a DIO from the DODAG root is received, a subroot inserts its ID in the *PID* field before advertising the obtained DIO to its neighbors. Upon the reception of a DIO by a regular node (other than root and subroots), it updates its parents list as suggested by default RPL but additionally it records their *PID* before broadcasting it as it is. When the process converges, each node will get its PID and hence will be aware of its subroot, the last node before the root as well as the parents leading to the root via disjoint paths. It is worth noting that DM-RPL correctness relies on the uniqueness of the *PID*. This can be achieved using any addressing (naming) scheme where simply the address of the subroot is used. The main concern is to keep the *PID* length as short as possible, this is why we consider an *ID* instead of the whole (IPv6) address.

To illustrate how DM-RPL operates to propagate *PIDs* downward using DIO messages, thus allowing the use of multiple disjoint routes, a simple topology with a DODAG structure are shown in Figure 1.8(a). In this example, we note the presence of three subtrees rooted at nodes 1, 2 and 3, direct children of the root r . These nodes have chosen r as their preferred parent after receiving a DIO from it. Before broadcasting

²⁰Disjoint Multipath RPL

²¹same as $P_T(x)$ in Table 1.1

²²Proofs are available in [KMD22]

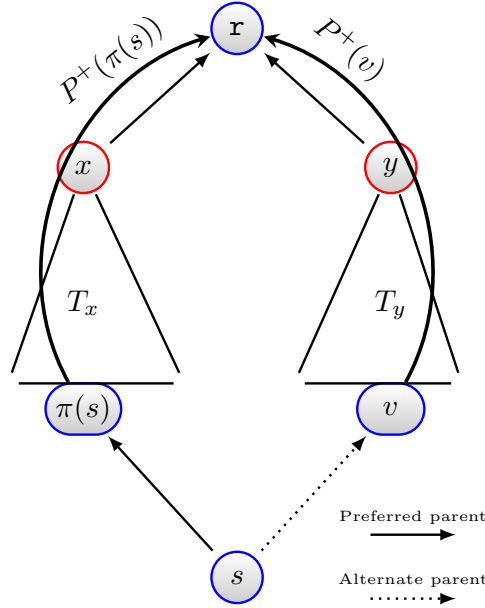


Figure 1.7: Paths Disjointness

a DIO, each subroot inserts its ID in the PID field. Regular nodes (i.e. 4, 5, 6 and 7), upon the reception of such modified DIO, update the list of their parents and keep track of the corresponding PID of each parent. Node 6, for instance, has two disjoint paths via 2 and 3 respectively. Node 7 can benefit from three paths, the red one is the RPL path and the two green are the alternate paths.

1.4.2 DM-RPL Disjoint Paths Discovery Procedure

The above described mechanism allows to know if a path via a given alternate parent is disjoint from an RPL path. However, it does not guarantee the existence of disjoint paths for a given source. Figure 1.8(b) illustrates one scenario where all the parents of node 7 have the same PID . This is likely to be the case in RPL which is commonly known as the *Thundering Herd Phenomenon* [HJL17] that occurs mainly when a node with a small rank attracts much more nodes. This motivates introducing the DM-RPL disjoint paths discovery procedure. A node x willing to send data using multiple disjoint paths that has only parents with the same PID, enters the disjoint paths discovery procedure upon the reception of Δ consecutive DIO messages. Whenever, no new PIDs are obtained during this period, the next DIO is propagated with the flag field set to $\pi(x)$, the preferred parent of this node. On the reception of a such DIO, an alternate parent (node $y \neq \pi(x)$) will replace its preferred parent by another one with a different PID than its own. For instance, in Figure 1.8(b), nodes 4 and 6 change their preferred parent from 2 to 1 and 3 respectively as their PID is different from their current one (i.e. 2). We thus come across the same case as in Figure 1.8(a).

To avoid that replacing preferred parents is made by all the neighbors which may lead to lower quality unstable paths, a parameter $\alpha \in \{0, \dots, 10\}$ is introduced to control the trade-off between the number of disjoint paths and their quality. As the path via the preferred parent is the best one according to the adopted RPL objective function, changing to an alternate parent is not always beneficial. Hence, it is required that the change only takes place if the quality of the path via the alternate parent is above a specified threshold. Upon the reception of a DIO with a non zero flag field, an alternate parent pull a random integer from $\{0, \dots, 9\}$. If it is less than α , then it keeps its preferred parent ; otherwise, it replaces it by the best alternate parent among those with a different PID than its current PID. The parameter α controls the mean ratio of the source alternate parents that have drawn to change their preferred parent. The probability that an alternate parent changes its parent is $1 - \alpha/10$. For instance, when $\alpha = 0$, all the alternate parents change their preferred parents to obtain a different PID. In a dense network where a node is likely to have a large number of neighbors, it is more interesting to increase the value of α as to bound the number of

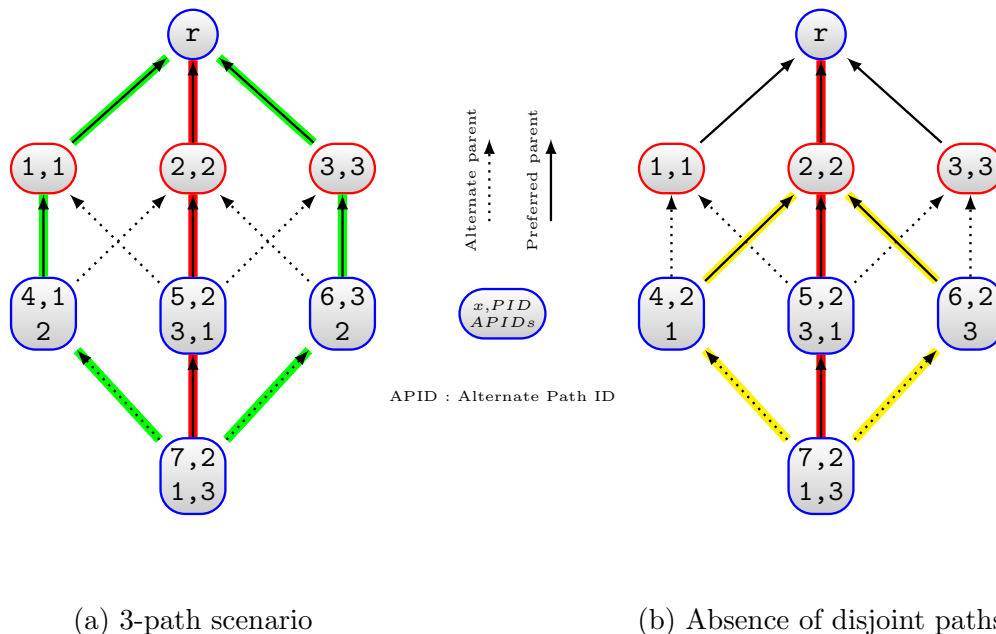


Figure 1.8: Illustrative examples

alternate parents that change their preferred parent. Increasing the number of paths through preferred parents substitution would lead to lower quality (possibly longer) paths which may result in a decrease of the multipath overall performance. Let reconsider Figure 1.8(b). Assume that α is set to 5 and that nodes 4 and 6 pull 2 and 7 respectively, then node 4 will keep its PID while node 6 will change its preferred parent from 2 to 3. In this case, we obtain two disjoint paths instead of three. Algorithm 4 summarizes the main actions of DM-RPL.

1.4.3 DM-RPL Preliminary Evaluation

To get insight into the performances of the proposed disjoint multipath extension, extensive simulations using Cooja [RQADG16] were performed, the Contiki network simulator. The purpose of this preliminary analysis is to study some properties of the proposed multipath discovery procedure with respect to its parameters α and Δ . Further analysis of DM-RPL is carried out in Section 4.2. Simulations were performed on a 25-node random topology in a $120m$ -side square area. The transmission range is set to $45m$ which results in a mean degree (number of neighbors) of 3.2 for each node. The source node obtained at least two paths in more than 50% of the simulations for $\Delta = 5$. When the DM-RPL disjoint path discovery procedure is triggered, the source is able to get at least two paths in all the simulations when $\alpha = 0$. When α is increased to 3, 5 and 7, the source gets at least two paths in 88%, 76% and 53% of cases respectively.

Figure 1.9 shows the distribution (minimum, maximum, interquartile, median and mean) of the required time to get the second path when the DM-RPL disjoint discovery procedure is triggered for different values of Δ and α . The number of built paths is depicted using black squares when α is varied. As expected, the number of paths decreases when α is increased. Moreover, the required time to get a second path increases with Δ . Although in half of the cases, this delay remains below 50 sec, it can rise to high values. Note that this delay bounds depend on the min/max DIO intervals set to their default values (4 sec and 17.5 min, respectively) in our simulations. When these latter are set to lower values, we can consider rising Δ . In order to reduce the convergence time, one can consider the use of the DIS-Trickle mechanism in a selective (both temporal and spatial) way to accelerate the convergence of the multipath routing.

Algorithm 4: DM-RPL**Data:**

x is this node and $\Pi(x)$ is its parents set;

$\pi(x) \in \Pi(x)$ is the x 's preferred parent. Let $\Pi^*(x) = \Pi(x) - \pi(x)$;

$\Delta \geq 2$, the minimum number of DIO a source receives before entering the DM-RPL disjoint paths discovery procedure;

$\alpha \in 0..10$, a trade-off parameter that mainly controls the replacement of the preferred parent;

Each regular node maintains an additional field PID for each parent entry in the neighbors table.

This is referred to as $y.PID$ for $y \in \Pi(x)$;

Result: Two disjoint paths for a given source. The generalization to more paths is straightforward

The root broadcasts the initial DIO message with $DIO.PID \leftarrow 0$ and $DIO.flag \leftarrow 0$;

Upon the reception of a DIO :

handle the DIO as in default RPL

if $\pi(x) = r$ **then** // I am a subroot

 | broadcast the DIO with $DIO.PID \leftarrow x$

end

if $\pi(x) \neq r$ **then** // I am a regular node

 | **if** $DIO.flag = 0$ **then**

 | broadcast the DIO as it is : $DIO.PID$ field set to this node subroot

 | **else** // Enter the DM-RPL disjoint paths discovery procedure

 | pull a random integer number $rdm \in 0..9$;

 | **if** $rdm \geq \alpha$ **then**

 | let y^* be the best parent of x in $\Pi^*(x)$ with $y.PID \neq x.PID$, then $\pi(x) \leftarrow y^*$;

 | broadcast the next DIO with $DIO.PID \leftarrow y^*.PID$

 | **end**

 | **end**

end

A source (regular) node willing to transmit data using multipath :

The first path is the one that follows the preferred parent i.e. via $\pi(x)$;

$countDIO \leftarrow 1$;

if $\exists y \in \Pi^*(x)$ with $y.PID \neq x.PID$ **then**

 | choose the best parent y^* to be the next hop for the second disjoint path

else

 | wait for a new DIO;

 | $countDIO \leftarrow countDIO + 1$;

 | **if** $countDIO < \Delta$ **then**

 | **if** $\exists y \in \Pi^*(x)$ with $y.PID \neq x.PID$ **then**

 | choose the best y^* to be the next hop for the second disjoint path

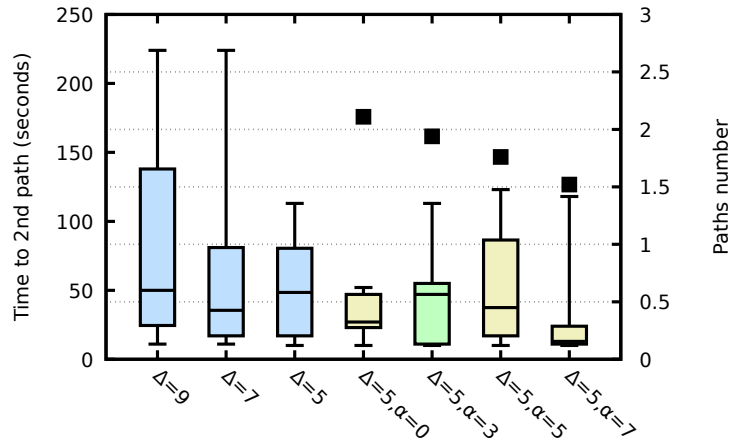
 | **end**

 | **else** // Trigger DM-RPL disjoint paths discovery procedure

 | broadcast the next DIO with $DIO.flag \leftarrow \pi(x)$

 | **end**

end

Figure 1.9: DM-RPL parameters (α and Δ) impact

1.5 Conclusion

Multipath routing when well designed allows the emergence of new applications with higher requirements in terms of quality of service and robustness. In this chapter, I reported on the design of a disjoint multipath routing protocol (MPR) that utilises an already built hierarchy rooted at the sink to build extra paths in addition to the tree path. This is achieved through the use of prefix routing in addition to neighbours information maintained at each node of the network. MPR is a hybrid routing protocol where at least one path is proactively discovered and others can be built using a light discovery process. As a result, the control traffic overhead is limited while maintaining the route state as low as possible.

MPR is a good candidate to be implemented in constrained networks. Practical adaptations to the IEEE 802.15.4 standard network layers, namely, ZigBee and 6LoWPAN have been proposed. Simulation results showed mainly its limited overhead in terms of control messages compared to a table-based multipath protocol. Despite the obtained results, there is still room for improvement mainly with respect to the interpath interference that may have severe impact on the performance of multipath routing. This issue will be dealt with in the next chapter.

Chapter 2

Interference Aware Multipath Routing

With regard to high data rate applications, routing protocols need to exploit the high density of WSN to raise the network capacity by involving more nodes using multiple paths. Multipath routing is a good candidate to allow for bandwidth aggregation. This is impeded by the shared nature of the wireless medium especially in the presence of high load traffic. Simultaneous utilization of adjacent paths with high transmission rates results in significant interpath interference, which increases the probability of packet transmission failures due to collisions along the active paths. As a result, a set of maximally zone-disjoint paths that minimize interpath as well as intrapath wireless interference need to be discovered to increase throughput and achieve load balancing features.

One promising approach to mitigate interference, without requiring special hardware support, is to design routing protocols that incorporate new metrics to consider the potential interference that routes may encounter. Interference aware routing metrics have received a keen interest in the literature on wireless mesh networks [JJKD09]. Section 2.1 overviews main interference-aware routing metrics in the literature. Interference aware multipath routing related work is presented in Section 2.2. Based on this state of the art, generic protocols to evaluate are derived and described in Section 2.3. The aim is not to propose yet another multipath routing protocol, but to compare existing strategies to build non interfering paths and to assess the advantage the incremental discovery approach can make when integrating interference-aware metrics. The network simulation model is presented in Section 2.4. Performance evaluation results are presented in Sections 2.5 and 2.6. In the former, the focus is on comparing two paths discovery strategies. In the latter, the impact of using seven interference aware metrics on the performance of the iterative path discovery mechanism is studied.

2.1 Interference Aware Routing Metrics

Building additional paths while others are in service allows to capture the potential interference level of the former with respect to the latter using interference aware metrics. The metrics considered in this study are chosen based on the following criteria. First, since not all metrics benefit from channel diversity, for fairness purposes, the radio is assumed to operate on a single channel. Moreover, multichannel integration, usually results in non isotonic metrics [SBM06, BPCM09] which require employing a virtual network with isotonicity verified in order to be able to use Bellman-Ford or Dijkstra's algorithms. Therefore, if a metric includes a multichannel component, the latter will not be considered in this study. Second, a selected metric has to be of a reasonable complexity to be suitable to WSN. Finally, the selected metrics are the most representative of those found in the literature. Overall, interference aware routing can be classified into two categories, namely *active* and *passive* monitoring metrics. As opposed to the latter, the former require periodic probing messages to assess the amount of the potential interference a link may experience.

2.1.1 Active Monitoring Metrics

Expected Transmission Count (ETX) [DABM03]. ETX measures the link loss ratio using the expected number of transmissions, counting retransmissions, needed to successfully receive a unicast packet through a link. The path metric is the summation of each link ETX in the path and the one with the minimum metric value is selected. A node u computes the ETX of the link to a node v using the delivery ratio of probes sent on the forward (p_f) and reverse (p_r) directions. These delivery ratios are, respectively, the fraction of successfully received probes from u announced by v and the fraction of successfully received probes from v , at the same period. The ETX of link $l(u, v)$ is given by :

$$ETX_l = \frac{1}{p_f \times p_r} \quad (2.1)$$

ETX is bidirectional and appropriately handles asymmetry by incorporating loss ratios in both direction. Measurements on a wireless test-bed show that ETX penalizes routes with more hops which have lower throughput due to interference between different hops of the same path [DABM03]. Although ETX does very well in homogeneous environments, it does not perform well in environments with different data rates. This is due to the small size of probes compared to typical data packets in addition to the fact that it does not consider the data rate at which the packets are transmitted. Moreover, ETX does not capture the interference experienced by the links completely since the periodic probes are sent at a slow interval (usually 1 sec) which does not reflect how busy a link is [SBM06].

Interference AWARE (iAWARE) [SBM06]. Routing metric iAWARE has two components. The first one is based on the physical interference model where SNR¹ and SINR² are used to continuously reproduce neighboring interference variations. In the physical model, a communication between nodes u and v on the link $l(u, v)$ is successful if the SINR at the receiver v is above a certain threshold. The second component, not considered here, exploits the channel diversity to find paths with least intra-flow interference. In iAWARE, link l Expected Transmission Time [DPZ04], ETT_l is weighted with its *interference ratio*, IR_l , to capture the interference experienced by the link from its neighbors :

$$iAWARE_l = \frac{ETT_l}{IR_l} \quad (2.2)$$

ETT metric estimates the time a data packet requires to be transmitted successfully to each neighbor. It improves upon ETX by capturing the data rate used by each link : $ETT_l = ETX_l \times S/B$ where the number of expected transmissions is multiplied by the link bandwidth giving the time required to transmit the packet. S is the size of the used packet and B is the bandwidth (raw data rate) of the link.

The *interference ratio* IR_l of a link l is defined as the minimum of the *interference ratio* of its nodes u and v : $IR_l = \min(IR_l(u), IR_l(v))$. For node u in the link $l(u, v)$, we have :

$$IR_l(u) = \frac{SINR_l(u)}{SNR_l(u)} = \frac{N}{N + \sum_{w \in \eta(u)-v} \tau(w) P_u(w)} \quad (2.3)$$

where N is the background noise. $P_u(w)$ denotes the signal strength of a packet from node u to node w . $\eta(u)$ denotes the set of nodes from which u can hear a packet and $\tau(w)$ is the normalized rate at which node w generates traffic averaged over a period of time. $\tau(w)$ is 1 when node w sends out packets at the full data rate supported. $\tau(w)$ is used to weight the signal strength from an interfering node w as $\tau(w)$ gives the fraction of time node w occupies the channel. The cumulative path metric $iAWARE(p)$ of a path p is defined as $iAWARE(p) = \sum_{l \in P} iAWARE_l$.

iAWARE gives more importance to ETT than interference. Moreover, iAWARE only considers interference at the physical layer and does not capture the interference at the MAC layer. The required measurements

¹Signal to Noise Ratio

²Signal to Interference and Noise Ratio

of the SNR, the signal strength and the background noise are not easy to obtain unless a cross-layer method is employed. This results also in considering all heard packets by the routing layer of a node even if they were not intended to this node.

Interferer Neighbors Count (INX) [LBB09]. INX routing metric is improved on the basis of ETX. It takes into account interference through measuring the sum of the transmission rates of the links that can interfere with the transmission on link l as :

$$INX_l = ETX_l \times \sum_{j \in S_l} r_j \quad (2.4)$$

where r_j is the data rate of link. ETX_l is the expected transmission time of link l . S_l is the set of interfering links. For a given path p , $INX(p) = \sum_{l \in p} INX_l / N$ where N is the number of links in the WSN.

2.1.2 Passive Monitoring Metrics

All active monitoring metrics overviewed in the previous section are based on ETX. Therefore, probing packets are exchanged to acquire delivery ratio of each link in both directions. Since probe messages are usually shorter than data packets, a node may experience higher losses for actual packets [DABM03]. Moreover, the number of broadcast probes in an n -node network is $O(n)$ which causes additional overhead especially in dense networks. Due to the restricted resources of WSN, passive monitoring is desirable to help acquiring measurements without introducing extra overhead disturbing the normal operation in the network. Providing sufficiently accurate interference metric without active monitoring is challenging.

Contention aware transmission time (CATT) [GS08]. CATT takes into account the effect of interferers on the transmission time of packets over the interfered link. It depicts the intra-path and inter-path interference as well as the traffic load in a uniform way by adding up the delays of the interfering neighbor links that are one and two hops away. CATT of link l is defined as :

$$CATT_l = \sum_{j \in N_l} \frac{L_j}{R_j} \quad (2.5)$$

where L_j is the packet size of link j ; it is set to the same value for all packets in the network. R_j is the data rate of link j . N_l is the set of links (including l) whose transmission can interfere with the transmission on link l . The CATT associated to a path p is $CATT(p) = \sum_{l \in p} CATT_l$

Metric for INterference and channel Diversity (MIND) [BPCM09]. MIND is an interference aware routing metric that relies on passive measurements to depict interference and traffic load. Like iAWARE, it is composed of two components. One that concerns inter-path interference and the other exploits channel diversity to limit intra-path interference. When considering one channel, MIND employs the interference ratio as done in iAWARE (Section 2.1.1) to capture the experienced interference based on the physical interference model. Additionally, as the Channel Busy Time (CBT) provides a more precise way of measuring traffic load [WC07], CBT is also considered. That is :

$$MIND(p) = \sum_{l \in p} (1 - IR_l) \times \tau \times CBT_l \quad (2.6)$$

where IR_l is the interference ratio of link l (Section 2.1.1) and τ is a configurable parameter used to provide a higher weight to interference. CBT is defined by : $CBT = (TotalTime - IdleTime) / TotalTime$

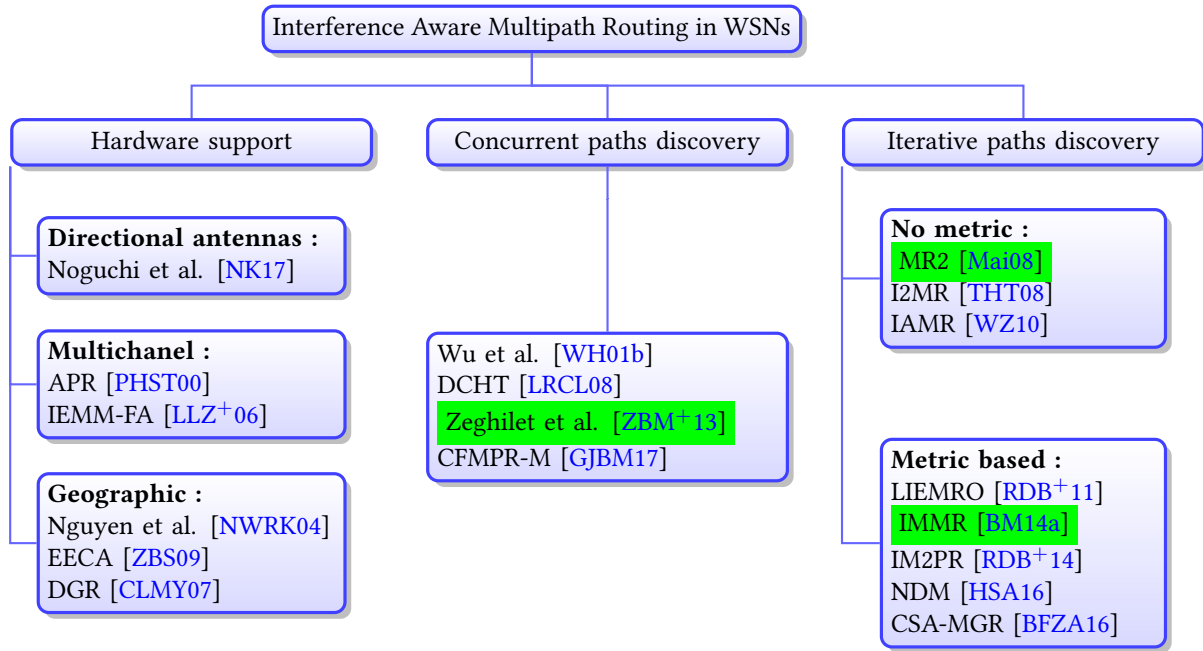


Figure 2.1: Interference Aware Multipath Routing

2.2 Interference Aware Multipath Routing Overview

Building an interference-free routing topology is not a trivial task. There have been in the literature, several proposals dealing with the interference problem in the context of routing protocols especially multipath ones. Basically, interference aware multipath routing can be split into three main classes (Figure 2.1). The first one benefits from the support of special hardware to get rid of interference. When such specific hardware facilities are costly or simply not available, there were basically two main approaches to minimize interference depending on whether the discovery of multiple routes is performed concurrently or iteratively.

2.2.1 Special Hardware Support

Minimal interference between paths can be achieved using directional antennas where the transmission beam of a node can be set in a particular direction. In [NK17], a zone-disjoint shortest multipath routing algorithm is proposed where directional antennas are used to select maximally disjoint paths. When multiple channels are available, interference can be minimized through an appropriate selection of orthogonal channels. As a result, the capacity of the network is improved as more links can operate simultaneously using non overlapping channels. APR³ [PHST00] is one example of multichannel multipath routing. In the particular case of WSN, multi-frequency characteristic of CC2420 radio have been leveraged in [LLZ+06] to minimize interference and energy consumption of multiple paths.

Geographic routing is one of the most obvious techniques allowing the construction of non-interfering paths. Routes are built so they are physically separated thanks to location information available at nodes. Nguyen et al. [NWRK04] draw inspiration from electric field lines to select physically separated paths for multipath load balancing. EECA⁴ [ZBS09] is another multipath routing protocol that uses the location information of all the sensor nodes to establish two paths in both sides of the direct line between the source-destination pair. DGR⁵ [CLMY07] is a geographical interference-aware routing protocol which constructs

³Alternate Path Routing

⁴Energy-Efficient and Collision-Aware Multipath Routing Protocol

⁵Directional Geographical Routing

two non-interfering paths based on the angle deviation method to control paths direction. GEAM⁶ [LC13] makes use of localization information to divide the network into districts for individual paths.

Despite the efficiency of these solutions to construct non-interfering paths, they still require special hardware facility. Hardware-dependent routing may not be cost-effective in low-cost wireless sensor nodes especially in dense networks. The use of directional antennas in convergecast, the main communication pattern in WSN, may not provide the expected performances as shown in [TMP16]. Multichannel approach, although quite suitable for mesh networks, it still needs more efforts to be recognized as suitable solution for WSN with high data rates. This mainly includes the design of efficient channel scheduling strategies that does not introduce significant switch overhead. Moreover, multichannel integration usually results in non isotonic metrics [SBM06, BPCM09] which introduce more complexity in a distributed routing protocol. Finally, in the absence of positioning system, localization algorithms may impose significant overhead in terms of communication and computational complexity.

2.2.2 Interference-aware Concurrent Multipath Routing

One of the first proposed metrics to characterize inter-path interference in multipath routing is the *route coupling* metric [PHST00]. It describes the average number of nodes in a path that are blocked for receiving packets while a node on another path is transmitting. However, to pick paths with minimum interference, the network connectivity graph has to be established which incurs significant additional calculations especially in dense WSNs.

Wu et al. [WH01b] introduced the *correlation factor (CF)* metric to measure the relative degree of inter-path Independence. The correlation factor of two node-disjoint paths is defined as the number of the links connecting the two paths. If there is no link between two node-disjoint paths, we say the two node-disjoint paths are unrelated. A link (u, v) is said to be connecting two paths P_1 and P_2 if $(u \in P_1$ and $v \in P_2)$ or $(u \in P_2$ and $v \in P_1)$. The total correlation factor of a set of multiple paths is defined as the sum of the correlation factor of each pair of paths. A DSR [JMB01] based interference aware multipath routing is proposed based on this metric. Node-disjoint paths with a small correlation factor are built while taking care of getting small length difference between them. To compute the correlation factor, each RREP message brings additionally neighborhood information of the advertised route.

Piggybacking neighborhood information in the control messages that serve the route discovery is also adopted in our work [ZBM⁺13] where instead of RREP messages, RREQs are used to convey neighborhood information. Based on these latter, the sink selects paths with the least common neighbors so nodes that are in the neighborhood of a chosen path are prevented from being used in other paths. A similar mechanism is used in CFMPR-M⁷ [GJBM17]. The main concern about this approach is that topology reporting through RREQ/RREP messages may cause large control overhead in large and dense networks especially when the source is in charge of path selection.

DCHT (Delay-Constrained High Throughput) [LRCL08] follows the basics of Directed Diffusion [IGE⁺03] with multipath extension. To maximize the throughput and improve the delay performance, instead of pure delay, it introduces a path cost metric that consists in a weighted product of the ETX (§ 2.1.1) and the delay. In [LRCL08], it is suggested to compute ETX based on SNR read from each exploratory packet at intermediate nodes. The ETX of the two previous hops is considered to ensure intra-path interference. It is worth noting that the authors do not provide the method to obtain SNR measures. Results show that DCHT applied to video streaming over WSNs obtains higher throughput than its single path counterpart (EDGE [LKLL07]). However, there was no comparison with another interference aware multipath routing protocol. One limitation of DCHT is that it considers more link quality and focuses on intra-path rather than inter-path interference in multipath routing.

⁶Geographic Energy-Aware non-interfering Multipath

⁷Correlation-Free MultiPath Routing protocol for multimedia

2.2.3 Interference-aware Iterative Paths Discovery

Iterative paths discovery allows obtaining low inter-path interference either by explicitly preventing nodes that might interfere with an already built path from being considered in subsequent paths construction, or by using an adequate interference-aware metric. The former approach was first adopted in the context of WSNs in MR2⁸ protocol I proposed in [Mai08]. During the reinforcement phase, RREPs are also used to put nodes surrounding the selected path in a passive mode where the radio can be switched off. In addition to reducing the inter-path interference, this allows energy saving. With respect to interference awareness, I2MR⁹ [THT08] follows the same principle but requires the availability of location information at both the source and the destination.

Nodes exclusion can be done up to two-hop neighbors of intermediate nodes of an already built path. This is done to consider the fact that the interference range can reach twice the communication range [ZHKS04]. This is the case of IAMR¹⁰ [WZ10] where the shortest path as well as its one-hop neighborhood are marked. Afterwards, two paths surrounding the marked area are built. It is worth noting that two-hop neighbors marking is likely to increase paths length which may result in more losses requiring a large buffer at the sink to reorder packets.

Iterative paths discovery can benefit from the use of an interference aware metric. Using an ETX-based cost metric, LIEMRO¹¹ [RDB⁺11] makes use of the iterative approach to discover multiple paths. To avoid interference, LIEMRO makes use of flowing packets overhearing mechanism to eliminate paths with higher interference. In IMMR¹² [BM14a] (Bidai's Thesis [Bid13]), we made use of flowing packets overhearing to assess the amount of interference between already built paths to choose the less interfering ones. In IMMR, multiple paths are built incrementally based on an already established spanning tree rooted at the sink. The first path consists in the tree path that follows the child-parent links until the sink is reached. Subsequent paths are discovered based on a metric called *Interference Level (IL)* for which the estimation is based on the overhearing of data packets that already circulate in the vicinity as well as potential path explore messages.

Like IMMR and in an attempt to allow (almost) concurrent multipath discovery, authors in [RDB⁺14] suggest to build a minimum cost recovery tree and propose IM2PR¹³. The first path construction is initiated by sending an RREQ by the source toward the sink following the tree structure. Subsequent RREQs to build additional paths are delayed in order to assess their interference degree with already built ones. A node is chosen to be in the current path to build based on the number of its neighbors that are in the other active paths.

More recently, the iterative approach is once again adopted by NDM¹⁴ [HSA16] and CSA-MGR¹⁵ [BFZA16]. In the former, hop count and correlation metrics are combined to build less interfering backup paths with respect to a primary path. In the latter, paths are built using location information and the banish state, equivalent to the passive mode in MR2 [Mai08]. A metric called *the number of common neighbors* is introduced to reduce the number of banished nodes.

2.3 Generic Multipath Protocols Description

The first protocol consists in a concurrent multipath routing, referred to as *MP*, in which only one request/reply session is performed and multiple paths are built at once. The second one consists in an iterative (incremental) approach, referred to as *INC* where only one path is built at once. The third one referred to

⁸Maximally Radio-disjoint Multipath Routing

⁹Interference-Minimized Multipath Routing

¹⁰Interference Aware Multipath Routing

¹¹Low-Interference Energy-Efficient Multipath Routing Protocol

¹²Interference-Minimized Multipath Routing

¹³Interference-Minimized Multipath Routing Protocol

¹⁴Neighbor-Disjoint Multipath

¹⁵Carrier Sense Aware Multipath Geographic Routing Protocol

as *IM2R* is a variant of *INC* that integrates an interference aware metric. The Last one is a modified version of *MR2* [Mai08] referred to as *M2R2* where nodes surrounding an already built path are put in a passive mode.

The selected multipath protocols are on-demand reactive routing protocols where the source willing to send data triggers route requests in order to find paths to the sink. The selected paths are sent to the source by the sink using route reply messages. When the source has data packets to send but does not have the route information to the sink, it transmits an RREQ packet that contains the source ID. When a node other than the sink receives an RREQ, it appends its ID to the list of traversed nodes before re-broadcasting the packet. This technique is called *path accumulation* in [GBRP03] and allows the selection of disjoint paths as well as route loops avoidance. RREPs also carry the whole path information between the source and the destination and are broadcast throughout the advertised path instead of being unicast in order to consider non symmetric links since the reverse path does not necessarily exist. Based on a received RREP, each intermediate node maintains a route table that indicates the path to the sink. The source maintains a similar table with multiple entries, one per built path. Finally, each node in the network has to maintain an up-to-date neighbors table. In what follows, particular behavior of each considered multipath protocols is described.

2.3.1 Concurrent Paths Discovery (MP)

In concurrent paths discovery, all paths are built using one RREQ flooding. An important point to consider is RREQ strategy suppression at intermediate nodes since dropping all duplicate RREQs may reduce drastically the probability to find multiple disjoint paths. Thus, RREQ caching and rebroadcast are required in multipath routing. In [LG01], the authors propose to forward duplicate packets that traversed an incoming link different from the link from which the first RREQ is received, and whose hop count is not larger than that of the first received RREQ. In [WH01a], RREQ messages are cached at intermediate nodes. When a node receives a route query message, if received for the first time or the path included in this query message is node-disjoint with the paths included in previously cached path records, then the node will cache and broadcast it again.

Even if both described methods increase the flooding cost, RREQ caching and rebroadcast are required to allow the construction of node-disjoint routes. In MP, we adopt another RREQ caching and suppression strategy. On the reception of a new RREQ, an intermediate node records its sequence number, the corresponding path ID and the cost of this path from the source until this node in a *path record*. An RREQ is considered as a *duplicate* (as opposed to a new one) if both its sequence number and path ID have already been recorded. A duplicate RREQ is simply discarded if it carries a bigger path cost ; otherwise it is rebroadcast and the corresponding path record is updated with the new cost. Our suppression strategy generates less RREQs than the one adopted in [LG01]. With respect to [WH01a], more RREQs are broadcast but more node-disjoint paths can be discovered with less storage capabilities at intermediate nodes.

When the sink receives a route request, it sets a timer. Each time it receives an RREQ, it records the conveyed path nodes along with the corresponding cost. On timeout, the sink chooses the required number of disjoint paths with the least cost. Afterwards, an RREP per selected path is sent back to the source. On the reception of an RREP, an intermediate node that belongs to this RREP path sets its routing entry. Finally, when the RREP reaches the source, an entry is added to its routing table.

2.3.2 Iterative Paths Discovery (INC)

In the iterative paths discovery approach, the source sends a first RREQ to build one route and transmits subsequent ones each time it receives an RREP with a new disjoint path whenever the needed number of paths is not achieved. As opposed to the concurrent approach, this requires that RREQ and RREP messages contain an additional field that gives the rank of the built path. Additionally, only one path record with the list of its nodes is maintained at the intermediate nodes.

When an intermediate node, that does not belong to another path, receives an RREQ, it checks if it is the first time it receives such RREQ. If so, the newly received path is saved with its cost and a timer is set to allow the reception of other RREQs with paths having better cost. During the timer period, subsequent RREQs are considered by the intermediate node if they convey a lower cost and the path record is updated. On timeout, an RREQ is sent using broadcast. It conveys information on the best path among those advertised by the received RREQs during the timer period.

Upon the reception of an RREQ, the sink records the conveyed path and sets a timer for a given period to consider subsequent RREQs. Each time the sink receives an RREQ with a better cost, it replaces its path record. On timeout, the sink selects one path with the best cost metric value. An RREP that contains the elected path record is sent back to the source. When an RREP is received by an intermediate node that belongs to the advertised path, an entry is set in the routing table using the information provided by this RREP. Otherwise, the RREP is ignored. Finally, upon the reception of the RREP, the source adds an entry to its routing table.

2.3.3 Interference Aware Metric-based Incremental Multipath Routing (IM2R)

Like INC, IM2R follows the same incremental path discovery strategy. In addition to the traditional hop count (HC) metric, to be interference aware, metrics defined in Section 2.1, namely ETX, iAWARE, INX, CATT and MIND are implemented along with the incremental multipath routing. Moreover, we also considered the metric used in DCHT presented in Section 2.2.2 that we refer to as *ETX3* as it considers three-hop ETX value.

All ETX based metrics require that each entry in the neighbors table is extended to maintain for each neighbor, the number of received probes from this neighbor and those received by the neighbor from this node. In turn, iAWARE and MIND require to record additionally, the receive power from each neighbor, an estimation of its neighbor's transmission rate as well as the interference ration (IR) of its links. Finally, ETX3 requires three cost fields in RREQs to keep ETX measures for the three last hops.

2.3.4 Iterative Paths Discovery with Neighbors Marking (M2R2)

M2R2 is a modified version of our interference-aware protocol MR2 [Mai08] where RREQs transmission is initiated by the source instead of the sink. Compared to INC, M2R2 operates in the same way except that nodes that are in the transmission range of the advertised path nodes have to switch to a passive mode. This is triggered by the reception of an RREP. This is another difference with MR2 where a dedicated message is used for this purpose. In fact, in M2R2, a node is able to know if it is a neighbor of a given path by checking the path field of the received RREP and its own neighbors table. Note that neighbors of the sink or the source can not switch to passive mode to allow multiple paths discovery.

Passive nodes are prevented from taking part in the route discovery process. Any received control message (RREQ or RREP) is ignored. In order to save energy, passive nodes can simply be put in a sleep state where the radio is switched off or configured with a low duty cycle depending on the application requirements. Only one-hop neighbors are put in passive mode. Doing so for two-hop neighbors may result in longer paths that are prone to more losses. Moreover, the sink needs to maintain large reception buffers to reorder packets.

2.4 Performance Evaluation Setup and Metrics

Using Castalia [B⁺11], a wireless sensor network Omnet++ based simulator, I implemented the generic multipath routing protocols, namely MP, INC, IM2R and M2R2. Metrics ETX, iAWARE, INX, ETX3, CATT and MIND were implemented along with IM2R as well as hop count (HC) metric in order to assess their impact on its performance. In active monitoring metrics, probes are sent every one second and ETX value is computed every 10 seconds. To model interference, the additive interference model provided by Castalia

Table 2.1: Simulation Parameters

Number of sensors	225, 324, 400 , 529, 625, 729, 900.
Transmission rate	20, 25 , 30 , 35, 40, 45, 50, 60, 70, 80 pps.
Data packet payload	64 , 96, 128, 160, 192, 224 bytes.
Node average degree	20, 12 , 8.
Transmission power	0 dBm
Transmission range	46.42 m (average)
Collision model	Additive interference
Active metrics	ETX, iAWARE, INX
Passive metrics	HC, ETX3, CATT, MIND

is adopted along with a contention based CSMA MAC layer. source. Each scenario is simulated several times using different simulation seeds. Simulation parameters are summed up in Table 2.1.

Each sensor is equipped with a CC2420 radio that operates at 250 Kbps transmitting at a power of 0 dBm which results in a transmission range of about 46.42 meters. Nodes are deployed in a randomized grid and spaced in a way to obtain a given mean node degree. I considered high, intermediate and low network densities that correspond respectively to an average node degree of 20, 12 and 8. The sink and the source are placed respectively at the lower left and the upper right corners of the sensors area.

Most experiments were limited to the case of two paths even if more paths can be discovered. This is sufficient to emphasize the performances of each variant with respect to each other. Obtained results can be generalized to more paths as well as for the case of multiple sources. Unless stated otherwise, I report on the simulation results performed with 400 nodes where the source transmits 64-byte data packets on two paths. The transmission rate is equally distributed on the paths. When results are provided using box plots. Each box displays the metric distribution (minimum, maximum, interquartile, median and mean).

The performance evaluation metrics used are :

- **Reliability.** Even if reliability is mainly a matter of the transport layer, the routing layer must still do its best. In this performance evaluation, data reliability is assessed using the PDR¹⁶ defined as the percentage of the number of data packets successfully received by the sink with respect to the total number of sent messages by the source node.
- **Path Length** is given by the number of its hops. It can be used to evaluate the average delay required for a packet to reach its destination as delay is largely related to the number of traversed links.
- **Paths Success Variance** helps evaluate the contribution of each of the built paths. It is computed based on their achieved PDR with respect to the whole success ratio.
- **Throughput** is computed using the amount of useful data (payload) received by the sink without considering the different headers of the transmitted packets.
- **Number of failures due to interference** counts for the percentage of packets failed to be received due to interference with respect to the total number of transmitted packets by the source and intermediate nodes. This metric allows assessing more precisely the behavior of each protocol with respect to interference.
- **Paths Correlation Factor (§ 2.2.2)** allows to evaluate the correlation between paths and is computed off-line based on the network connectivity graph. Failures due to interference are mainly caused by paths that are close to each other.
- **Paths Discovery Overhead.** Compared to single path routing protocols, path discovery is more challenging in multipath routing protocols. In order to evaluate the efficiency of a multipath routing protocol, one has to consider the amount of overhead incurred by the different control messages such as RREQ and RREP as well as the potential hello messages to maintain neighborhood information.

¹⁶Packet Delivery Ratio

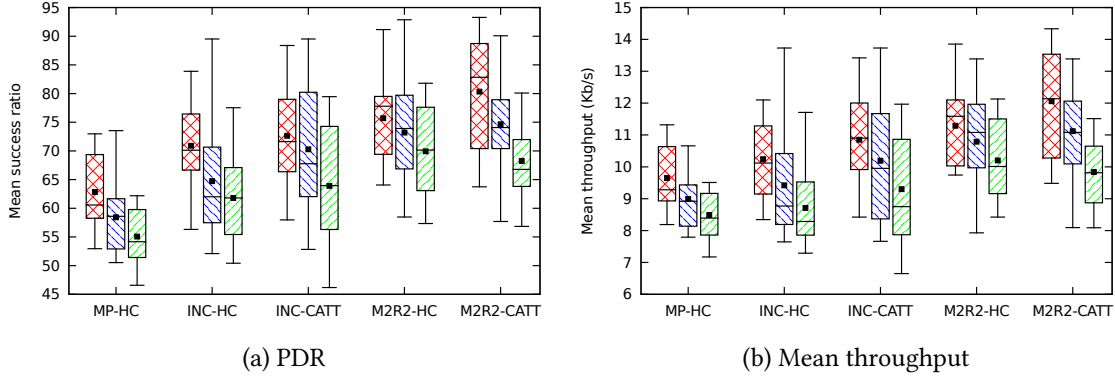


Figure 2.2: Achieved PDR and throughput for different densities.

2.5 Concurrent Versus Incremental Paths Discovery

In this section, are considered, variants of the implemented protocols combined to HC and CATT metrics : MP-HC, INC-HC, INC-CATT, M2R2-HC and M2R2-CATT. CATT metric is considered only for INC and M2R2 protocols as it is designed to assess interference that results from other existing flows making it not suitable to the concurrent path discovery. CATT choice is motivated by its low complexity and its non intrusive estimation method. More results can be found in [Mai18a].

2.5.1 Reliability

Figure 2.2a shows success ratio distribution for each protocol with three boxes that result from experiments using (left to right) high, intermediate and low network densities. Independently of the route discovery mechanism, denser networks provide better performances. This can be explained by the fact that in a denser network, the built paths are shorter in terms of the number of traversed nodes. Figure 2.3a shows that the path length increases when the network density decreases since the sensor area becomes larger. When the number of traversed nodes increases, loss probability increases. Moreover, independently of the network density, iterative paths discovery (INC and M2R2) exhibits better performances than the concurrent approach (MP). For both implemented metrics, M2R2 provides the best success ratios. CATT allows better success ratio in average but can result in less performances when combined with INC. The minimum success ratio can drop as low as the one obtained in MP. This is due to the fact that CATT tends to build longer paths as it favors nodes with less potential interfering links in the vicinity at the expense of increasing path lengths. The throughput results as shown in Figure 2.2b confirm those obtained in terms of PDR. In average, MP achieves the smallest throughput, whereas the four other protocols achieve higher values.

Figure 2.3a shows that regardless of the used metric, both INC and M2R2 produce longer paths compared to MP. In M2R2, excluding nodes surrounding already built paths makes subsequent paths even longer than those generated by INC. CATT produces longer paths than HC. MP builds the shortest paths because of its RREQs suppression strategy : the sink selects the paths based on a larger number of RREQs which increases the probability of selecting the shortest ones. The carried experiments show that the first chosen path in MP is in average shorter than those selected first in INC and M2R2. Figure 2.3b plots the built paths success variance. As can be seen, MP presents the highest variance values (up to 16) which indicates that the achieved success ratios by one of the two paths exhibits better performances than the other one. On the contrary, M2R2-CATT exhibits a variance close to zero. As a result, even if paths are longer in the iterative discovery approach, the success ratio is higher and is almost equally distributed among built paths.

Figure 2.4a plots the percentage of packets failed to be received due to interference. MP generates more failures while M2R2 exhibits less interference compared to INC. With respect to the used metric, CATT

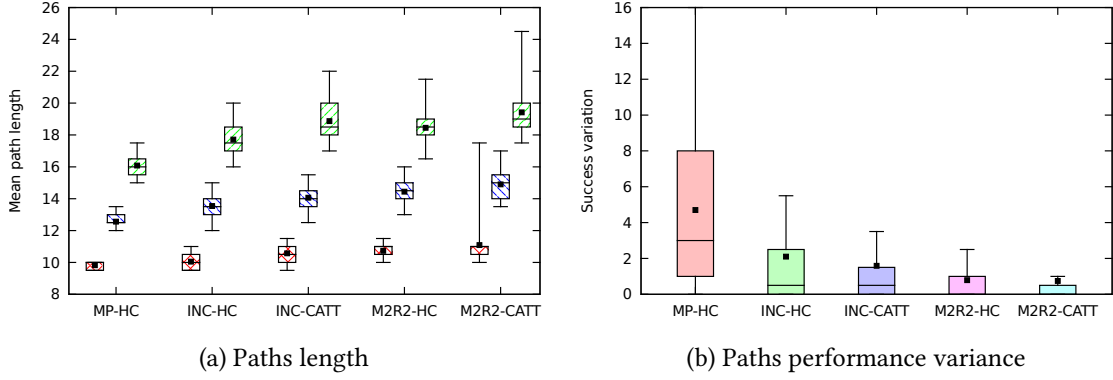


Figure 2.3: Paths characteristics.

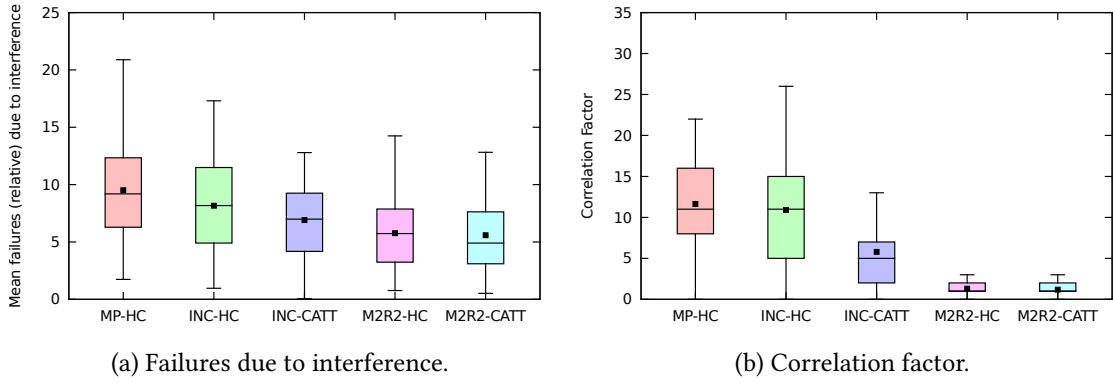


Figure 2.4: Failures and Paths Correlation.

produces less interference than HC. Failures due to interference are mainly caused by paths that are close to each other. Figure 2.4b plots the correlation factor and shows that the built paths in MP and INC are the most correlated compared to the three other protocols. Paths built by M2R2, however, are the less correlated and often present a near zero correlation factor.

2.5.2 Paths Discovery Overhead

Figure 2.5a plots the normalized number of RREQs received by the different sensors in the path discovery phase. As opposed to the iterative paths discovery, there is an implosion of the number of the exchanged RREQs in MP. This is inherent to the RREQ suppression strategy used in which a minimum of RREQs have to be forwarded ; otherwise the probability to find disjoint paths is dramatically reduced. This problem does not exist in the iterative discovery approach since paths are discovered sequentially. The least number of RREQs is obtained in M2R2 where nodes are put in passive mode and hence do not receive or process any RREQ.

Figure 2.5b shows the normalized number of received RREPs. Even though, one RREP is sent by the sink for each chosen path in all the evaluated variants, note that their overall number varies. The passive mode strategy allows M2R2 to generate the smallest number of RREPs. INC produces more RREPs than M2R2 and MP. With respect to MP, INC paths are longer (Figure 2.3a) which produces more RREPs to be forwarded by intermediate nodes back to the source. This is still the case when paths number is increased from 2 to 6 as shown in Figure 2.6a that plots the amount of exchanged RREPs for MP-HC (concurrent) and INC-HC (incremental) as a function of the number of built paths. The observed higher overhead in terms of RREPs in IM2R is due to the fact that paths built by the incremental multipath routing are likely to be longer as depicted in Figure 2.6b. This results in more RREPs to be exchanged along each path from the sink to the source. However, with respect to the concurrent discovery in MP, this overhead in the incremental

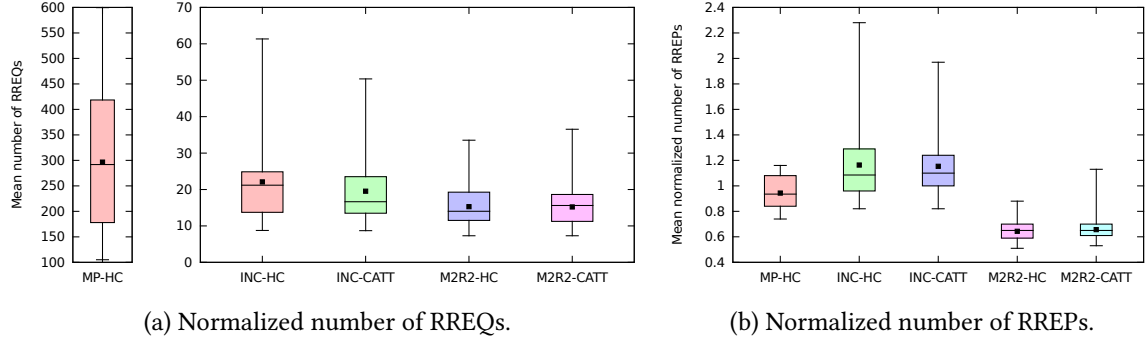


Figure 2.5: Control Messages Overhead.

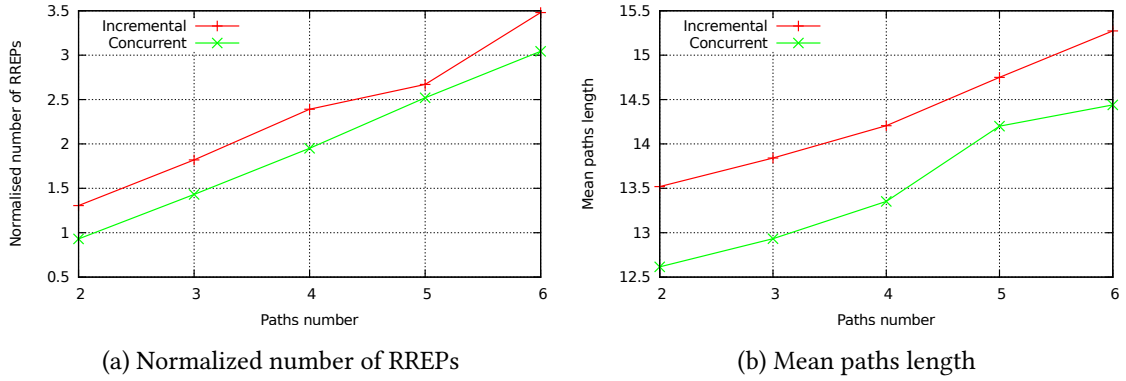


Figure 2.6: Concurrent (MP) vs. incremental (INC) multipath routing

approach, drops from 39% of additional RREPs for two built paths to 14% when the number of paths is risen to 6.

2.5.3 Varying the Network Size

Figure 2.7a shows the evolution of the PDR when the number of sensor nodes is varied. Once again, MP provides the least success ratio while M2R2 exhibits the best performances. The INC routing allows better results with respect to MP since its paths are less correlated as depicted in Figure 2.7b. The rationale behind is that when RREQs are sent to build the second path, data packets are already flowing through the first one. Thus, RREQs are likely to be lost in the vicinity of this latter due to interference. As a result, INC routing takes advantage from the overhearing property of the wireless media. This is even more true when an interference aware metric such as CATT is used. In fact, CATT counts for data packets that already flows through active paths.

Moreover, Figure 2.7a shows that the performances of M2R2 using either HC or CATT are almost the same. This means that the interference-zone marking strategy of M2R2 is a good mean to avoid interference and that an interference-aware metric can be left out. As shown in Figure 2.7b, M2R2 builds the least correlated paths where the correlation factor is close to zero and almost constant when the network size increases.

2.5.4 Impact of Data Packets Size and Data Rate

Figure 2.8a plots the achieved PDR when increasing packets payload. We observe that the ratio of successfully received packets by the sink decreases as the packets payload increases. This is due to the fact that larger packets are more likely to produce interference. This is confirmed in Figure 2.8b that confirms the correlation between the achieved PDR and the amount of failures due to interference. M2R2 protocol allows more successful transmissions whatever the used metric while MP exhibits the poorest performances.

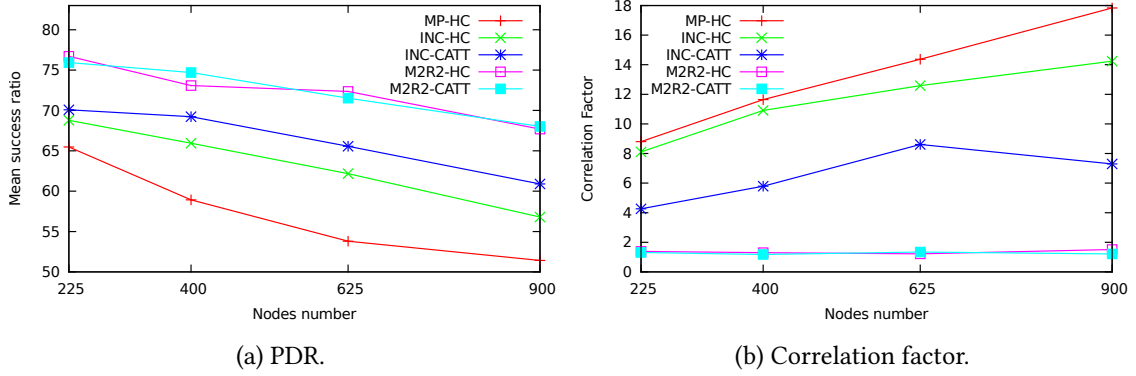


Figure 2.7: Varying the network size.

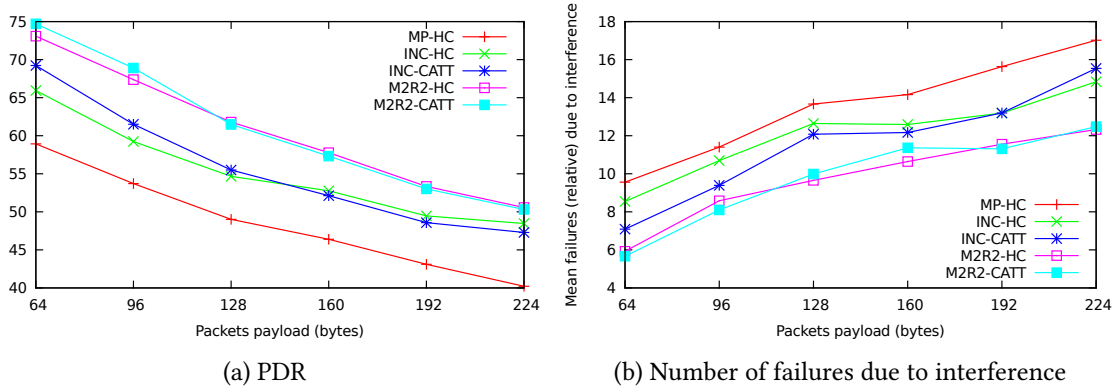


Figure 2.8: Varying the data packet size.

INC-HC may behave better than INC-CATT with large packets. In fact, packets are transmitted on the first path when the second one discovery is in progress. The related RREQs experience more losses due to interference with first path data packets. These losses are more likely to appear in the vicinity of the first path, already in use. The same behavior is also observed when the transmission rate increases.

When the data transmission rate is varied, almost the same behavior is obtained for all protocols. As shown in Figure 2.9a, M2R2 achieves the highest PDRs and MP the lowest ones. Moreover, INC-HC can achieve the same performances as INC-CATT when rising the data rate. A high transmission rate on the first path rises the number of failures due to interference during the discovery of the second path. RREQs related to less correlated paths are more likely to achieve the sink. In terms of achieved throughput as depicted in Figure 2.9b, M2R2 achieves the best performances while MP the worst ones. The throughput achieves its maximum when the transmission rate is set to 40 pps. Then, it decreases with the transmission rate. This means that rate adjusting through a transport level congestion control is critical to achieve optimal performances. In terms of achievable throughput, CATT obtains higher performances than the HC metric in both M2R2 and INC protocols.

2.5.5 Comparing with Single Path

Here, the potential performance enhancement of the simulated multipath protocols with two and three paths compared to a single path routing is assessed. Figure 2.10a shows the mean gain obtained in terms of the PDR when two paths are used. It can be seen that the improvement increases when the network size is bigger or equivalently when the path length increases. The PDR decreases with the network size and thus the improvement is more important since the number of traversed nodes is larger. Looking at the performances of each of the considered protocols, almost, no improvement is achieved in MP when two paths are employed instead of one. With respect to single path routing, multipath protocols that consider

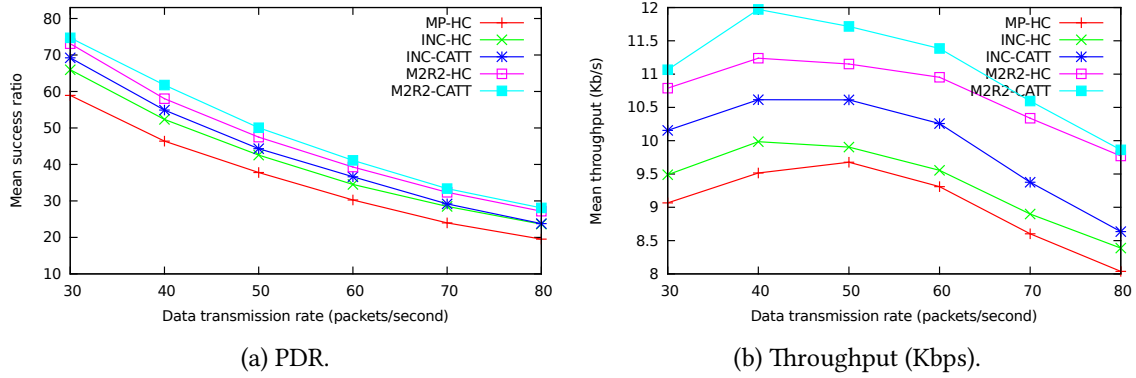


Figure 2.9: Varying the data rate.

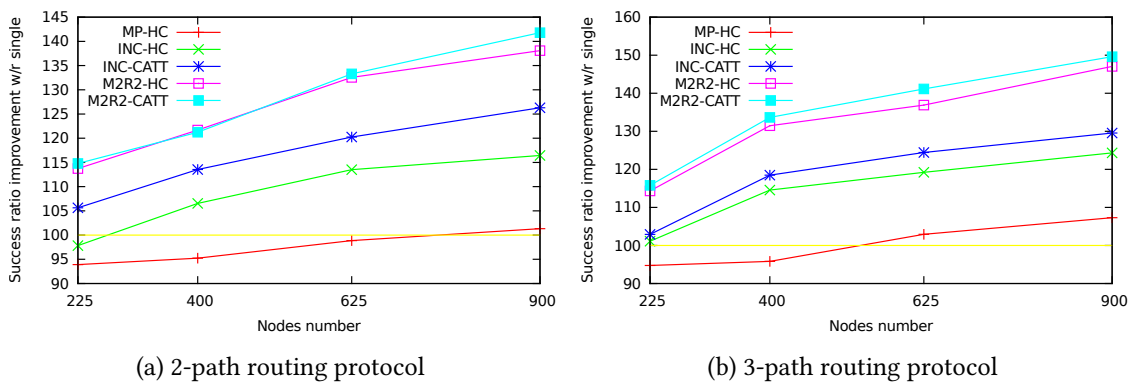


Figure 2.10: Success ratio improvement over single path.

interpath interference using either an interference metric such as INC-CATT or using a zone marking strategy such as the one employed in M2R2, achieve better performances.

Figure 2.10b shows the improvement when three paths are used instead of one. The same observations can be made while noting that, in most cases, a higher improvement is achieved with three paths. Figure 2.11 plots the achieved improvement in terms of the PDR for a 900-node network. For each protocol, the first and the second box summarize the improvement using respectively two and three paths over single path routing. It can be seen that interference-aware protocols allow better success ratio using multiple paths over single path routing for all the performed simulations. The improvement in MP-HC and INC-HC is less obvious. Compared to MP, INC-HC allows better performances since it may take advantage of overhearing.

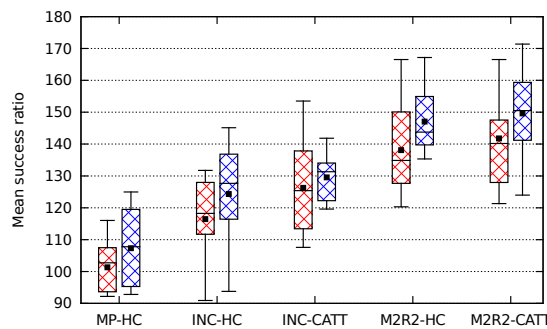


Figure 2.11: Success ratio improvement using 2 and 3 paths over single path in a 900-node network.

Table 2.2: Results obtained with four paths.

Protocol	PDR	Path length	Failures due to interference
Single	60.52%	13	1%
MP	60.71%	14	16.6%
INC-HC	63.31%	14.25	13.38%
INC-CATT	77.44%	15.25	10.71%
M2R2-HC	89.00%	15.25	6.64%
M2R2-CATT	81.13%	16	7.02%

Table 2.3: Success percentage to handle multiple sources.

Protocol	2 sources		3 sources		4 sources	
MP	194	97%	188	94%	155	77.5%
INC	164	82%	111	55.5%	90	45%
M2R2	98	49%	40	20%	10	5%

2.5.6 Increasing the Number of Paths

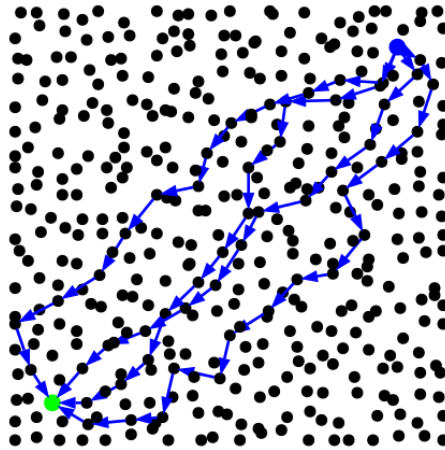
Table 2.2 summarizes the obtained results using a representative topology with default settings when four paths are built. Figure 2.12 shows the built paths when four paths are built by each of the five protocols in the representative topology. The blue and green nodes are respectively the selected source and sink. Obtained results show that MP does not improve the PDR when building two and even three paths with respect to single-path routing. Four paths are needed to achieve slightly higher performances. Similar but slightly higher performances are achieved in INC-HC where three instead of four paths are required to outperform the single path routing protocol. Figures 2.12a-2.12b) show that the built paths may cross and are highly correlated.

When the interference-aware metric CATT is used by INC routing protocol, the built paths (Figure 2.12c) are less correlated and the obtained PDR is higher than in single path. Figures 2.12d-2.12e show that the built paths in M2R2 routing protocol using HC and CATT metrics respectively are less correlated than in the other protocols. When the number of built paths is risen respectively to three and four, the improvement is more significant. The PDR is higher using HC in M2R2 when the number of paths exceeds two. As already emphasized, the CATT metric is likely to build longer paths which increases the probability of losses. Moreover, the M2R2 strategy of interference-zone marking allows the construction of less correlated paths.

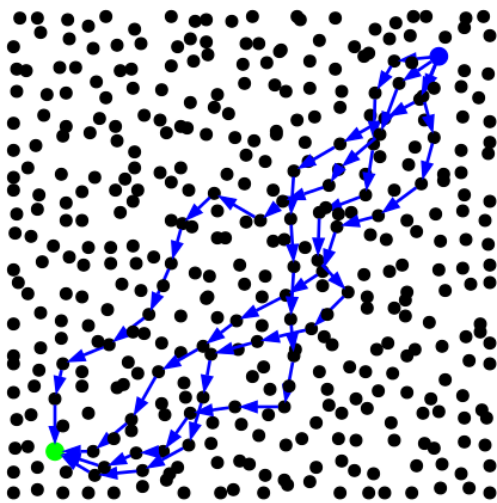
2.5.7 Handling Multiple Sources

In order to assess the ability of each protocol to handle multiple sources, simulations were performed with 2, 3 and 4 sources. The worst case where all of them are located near each other in the upper right of the sensor field is considered. Each source has to transmit data packets using at least two paths. 200 simulations are performed for each protocol and the number of successful ones as well as the corresponding percentage are reported in Table 2.3. M2R2 exhibits the least successful number of simulations that drops to 5% when the number of sources is raised to 4. This issue can be solved by allowing some passive nodes to take part in routing other sources data. Based on the nature of flows, a best trade-off has to be found between handling more flows in the network and their achievable performances. MP succeeds in handling more sources since there is no constraint in building paths except paths disjointness. Due to the iterative nature of INC, more RREQ/RREP losses are experienced which reduces the number of built paths for the considered sources.

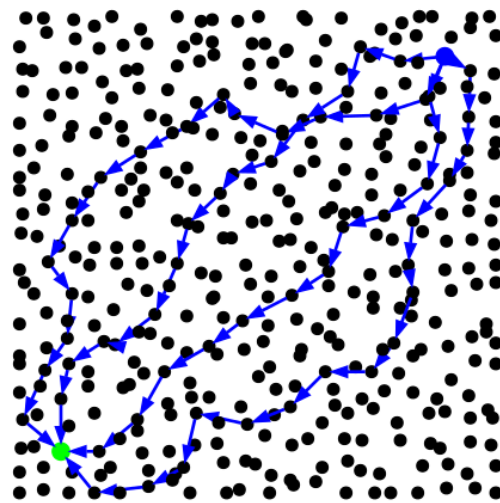
Figure 2.13 presents the mean PDR in the presence of respectively one, two and three sources. It can be seen that their relative performances are the same whatever the number of the sources is. M2R2 and MP exhibit respectively the highest and the lowest success ratios. When increasing the number of sources, the



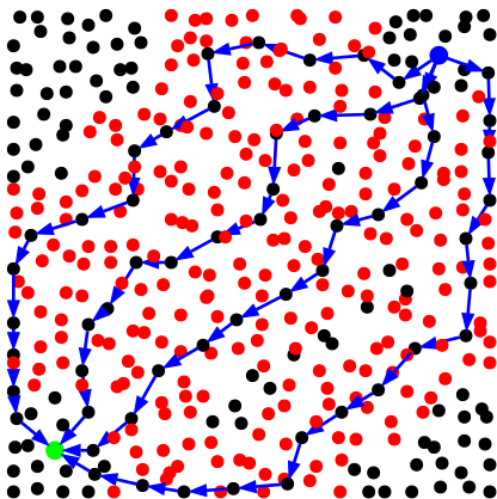
(a) MP - mean PDR : 60.71%, mean path length : 14 hops, ratio of failures due to interference :16.6%



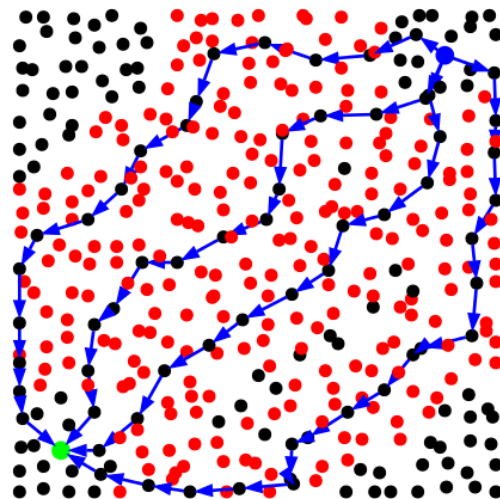
(b) INC-HC with PDR : 63.31%, mean path length : 14.25 hops, ratio of failures due to interference : 13.38%



(c) INC-CATT with PDR : 77.44% and mean path length : 15.25, ratio of failures due to interference : 10.71%



(d) M2R2-HC with PDR : 89.00% and mean path length : 15.25, ratio of failures due to interference : 6.64%



(e) M2R2-CATT with PDR : 81.13% and mean path length : 16, ratio of failures due to interference : 7.02%

Figure 2.12: Multipath topologies with four paths.

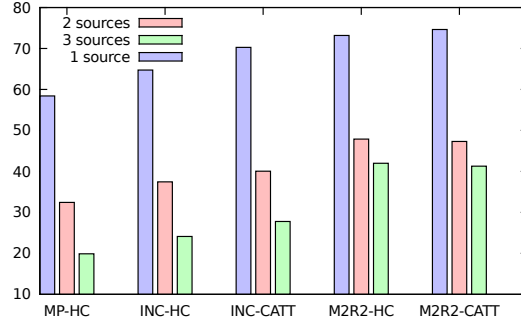


Figure 2.13: PDR with one, two and three sources.

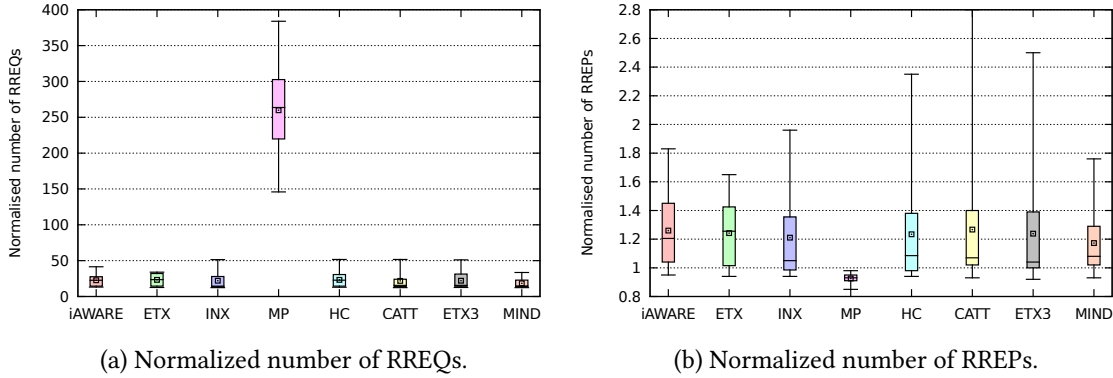


Figure 2.14: Control messages

success ratio decreases for all protocols. However, as shown in the plots, it fastly decreases in MP compared to INC and M2R2.

2.6 Impact of Interference Aware Metrics

The aim of this section is to assess the advantage the incremental discovery approach can make when integrating interference aware metrics [Mai20a]. More results can be found in [Mai20b].

2.6.1 Routing Overhead Versus Reliability

Figure 2.14 plots the normalized number of control messages exchanged during the path discovery phase for MP and IM2R combined with the different implemented metrics that occur at the x-axis. The obtained results confirm those obtained and interpreted in Section 2.5.2. The problem of RREQ implosion does not exist in IM2R whatever the used metric since paths are discovered sequentially. However, the iterative discovery produces more, but moderate proportions, RREPs than MP.

From Figure 2.15a, two main observations can be made. First, while generating the least amount of routing overhead, passive monitoring metrics (except ETX3) and even HC allow better performances in IM2R when compared to MP. Second, IM2R combined with active monitoring metrics exhibits poor performances when compared to MP. This is mainly due to the periodic probes used in active monitoring which consume bandwidth. All active monitoring metrics are based on ETX that measures link quality rather than its experienced interference. Similar results are obtained in terms of achieved throughput. The poor performance of ETX3 when compared to other passive monitoring metrics can be explained by the fact that ETX3 deals with intra-path instead of inter-path interference. In fact, ETX3 builds the paths with the highest correlation factor as shown in Figure 2.15b. Despite that active monitoring metrics build less interfering paths, they achieve less performances when compared to MP. Among all metrics, CATT allows to build the least

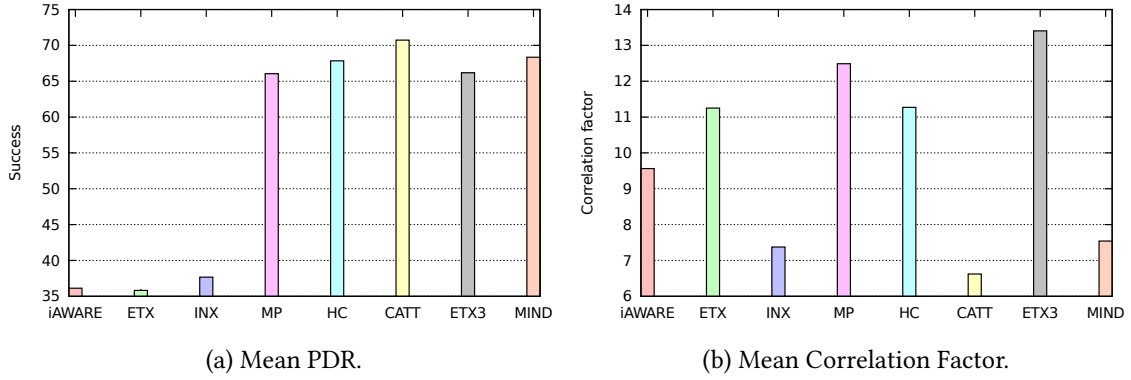


Figure 2.15: Performances in a 400-node network and a transmission rate of 25 packets per second

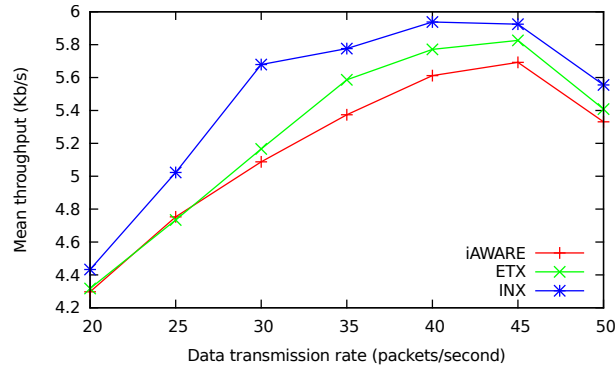


Figure 2.16: Mean throughput for active metrics as the data rate is varied.

correlated paths which confirms the highest obtained performances. Finally, Figure 2.15b confirms that less correlated paths are likely to be longer which justifies the amount of additional RREPs exchanged.

2.6.2 Active Monitoring Metrics

To get more insight on the performance of active monitoring metrics when compared to each other, I performed simulations for different data transmission rates. Figure 2.16 plots the mean throughput achieved by IM2R using iAWARE, ETX and INX as a function of the transmission rate. ETX achieves higher throughput than iAWARE when the data transmission rate is increased and INX outperforms both ETX and iAWARE metrics. This is mainly due to the fact that INX allows to build the least correlated paths as shown in Figure 2.15b. Besides, iAWARE paths are less correlated than those produced with ETX. Nevertheless, the achieved throughput by iAWARE is not superior. The reason behind that is the additional overhead introduced by the technique of packet pairs [Kes91] to estimate ETT values required by iAWARE. Furthermore, employing ETT may also lead to links quality to be overestimated [BCM11]. Finally, iAWARE paths are more correlated than INX ones and hence iAWARE is less interference aware. This is due to the fact that iAWARE only considers interference at the physical level and does not capture interference at the MAC layer [GS08].

2.6.3 Passive Monitoring Metrics

Figure 2.17a depicts the evolution of the PDR for IM2R when passive monitoring metrics are employed as a function of the number of nodes ranging from 225 to 729. As can be expected, the PDR decreases with the network size as the sink and the source become more distant from each other. Thus, the number of transmission and failures increases since traversed routes are longer. Regardless the network size, as opposed to ETX3, MIND and CATT allow higher PDR than the traditional HC metric. The main reason for

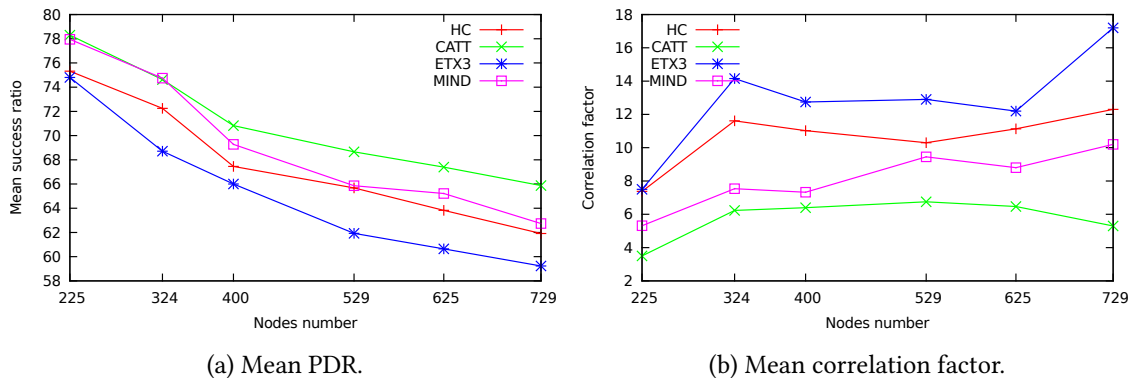


Figure 2.17: Performances of passive metrics as the network size is varied.

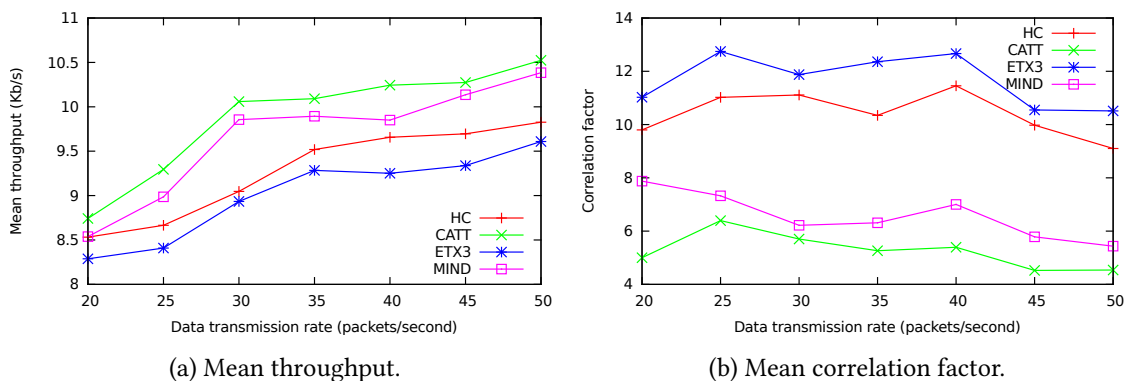


Figure 2.18: Performances of passive metrics as the data rate is varied.

the above observations is that paths produced by CATT and MIND are less correlated than those of HC, that is in turn less correlated when ETX3 is employed as a metric. This is confirmed in Figure 2.17b that plots the average value of the correlation factor of the built paths. IM2R routing using HC takes advantage from the overhearing property. When RREQs are broadcast to establish the following path, data packets are already flowing through the first path. Due to interference with this latter, second path RREQs are most likely to be lost in the vicinity of the first path. As a result, these RREQs have lower probability to reach the sink and hence the second path is more likely to be less interfering with the first one.

When the data transmission rate varies, almost the same behavior is observed for the different evaluated passive metrics. As shown in Figure 2.18a, CATT achieves the highest throughput. CATT is able to estimate the interference degree in the neighborhood (up to two links away) of a path in a more accurate manner. MIND allows to build less interfering paths than HC since it considers how busy is the channel in the vicinity. The use of CBT instead of ETT allows MIND to build less interfering paths than iAWARE (Figure 2.15b). ETX3 achieves the worst throughput since it considers more link quality and intra-path rather than inter-path interference. Once again, the mean correlation factor depicted in Figure 2.18b for different loads confirms that the achieved throughput depends on the degree of correlation of built paths. In fact, CATT builds the least interfering paths while ETX3 paths are more correlated even when compared to the HC metric.

2.7 Conclusion

Multipath routing holds a great potential to provide sufficient bandwidth to high data rate applications. To achieve this aim, a multipath routing protocol has to be carefully designed and the problem of interpath as well as intrapath interference have to be considered. In this chapter, the focus was on the performance

evaluation of the iterative paths discovery approach as opposed to the traditional concurrent multipath routing. Different variants of multipath protocols were simulated and evaluated using different performance metrics.

Extensive simulations showed that concurrent multipath routing introduces significant routing overhead when compared to the incremental approach. Even without interference awareness (using hop count as a metric), incremental multipath achieves higher performances thanks to packets overhearing. Naturally, incremental multipath is obviously more suitable to integrate and take benefit of interference aware metrics. The iterative approach allows better performances when used jointly with an interference-aware metric such as CATT or when an interference-zone marking strategy is employed. This latter, used in M2R2, appears to exhibit the best performances in terms of success ratio, achieved throughput, control messages overhead as well as energy consumption at the expense of the number of flows that can be handled simultaneously.

Even if active monitoring metrics are able to build less interfering paths, they still obtain poor performances in terms of throughput and success ratio. This is due to the bandwidth overhead introduced by the probe messages required to estimate ETX and/or ETT component in the corresponding metrics. Passive monitoring metrics, except ETX3, enable better performances when compared to active ones. The best performance can be obtained using CATT followed by MIND. With respect to metric estimation complexity, CATT is once again the best candidate and is well suited for WSN in which nodes are characterized by their scarce resources.

The obtained performances can be further improved when the interference-aware multipath routing is jointly used with an appropriate transport protocol that effectively manages the source transmission rate. Additionally, self-organization mechanisms based on clustering techniques, which will be discussed in the next chapter, can also be utilized to improve the overall performance.

Chapter 3

Energy Efficient Passive Clustering

Previously, hierarchical routing has been raised as a potential solution to control message flooding problem and minimize routing state (Section 1.1.3). In this chapter, self-organization mechanisms based on clustering techniques are considered from the perspective of data routing to achieve high network lifetime by balancing and reducing energy expenditure. First, main clustering concepts and strategies are summarized in Section 3.1. Then, the main contribution of Zeghilet's thesis [Zeg13], an energy efficient clustering protocol, is presented in Section 3.2. This protocol has undergone extensive evaluation for both scalar and video data transport. Main obtained results are provided in Section 3.3.

3.1 Clustering in WSNs

Flat routing protocols are quite effective in relatively small networks. However, they scale very bad to large and dense networks since, typically, all nodes are alive and generate more processing and bandwidth usage. Hierarchical routing that relies on maintaining a hierarchy in the network topology emerged as an inevitable solution to the problem of scalability in the context of WSNs. In hierarchical based routing, nodes play different roles in the network and typically are organized into clusters. Clustering (Figure 3.1) is the method by which sensor nodes in a network organize themselves into groups according to specific requirements or metrics. Each group or cluster has a leader referred to as *clusterhead* (CH) and other ordinary member nodes (MNs). The clusterheads can be organized into more hierarchical levels. Clustering allows a hierarchical architecture with more scalability, less consumed energy and thus longer lifetime for the whole network. This is due mainly to the fact that most of the sensing, data processing and communication activities can be performed within clusters. Numerous are WSN applications that require simply an aggregate value to be reported to the sink. In such applications, data aggregation at the clusterheads helps to alleviate congestion and save energy.

From a routing perspective, clustering allows to split data transmission into *intra-cluster* (within a cluster) and *inter-cluster* (between clusterheads and every clusterhead and the sink) communication. This separation leads to significant energy saving since the radio unit is the major energy consumer in a sensor node in addition to smaller dissemination latency. In fact, member nodes are only allowed to communicate with their respective clusterhead, which is responsible for relaying the data to the sink with possible aggregation and fusion operations. Moreover, this separation allows to reduce routing tables at both member nodes and clusterheads in addition to possible spatial reuse of communication bandwidth.

Intra-cluster Communications. In very dense networks, a subset of nodes may be put into the low-power sleep mode provided that these nodes are chosen without affecting the network coverage and connectivity. In this context, a clusterhead can efficiently schedule its member nodes states. Furthermore, medium access collision can be prevented within a cluster if a round-robin strategy is applied among the

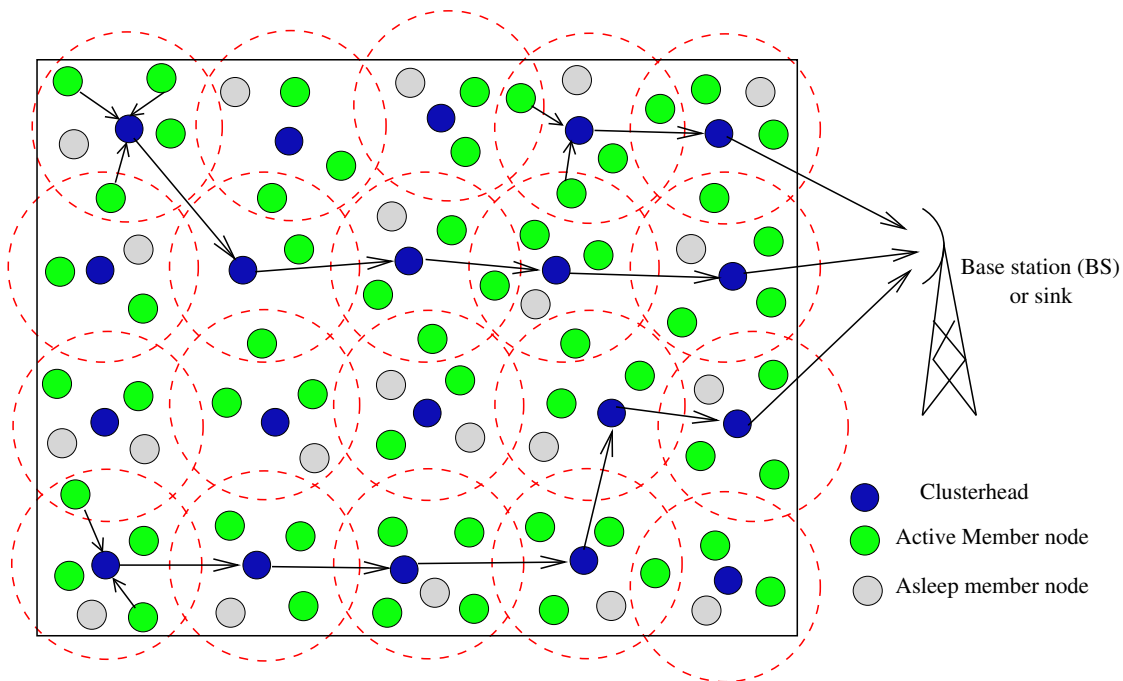


Figure 3.1: Cluster Based Hierarchy

member nodes. Collisions may require that nodes retransmit their data thus wasting more energy.

Most of the earlier work on clustering assume direct (one-hop) communication between member nodes and their respective clusterheads. This is the case of LEACH¹ [LEA00] and HEED² [YF04]. All the member nodes are at most two hops away from each other (Figure 3.2a). One-hop clusters makes selection and propagation of clusterheads easy, however, multi-hop intra-cluster connectivity is sometimes required, in particular for limited radio ranges and large networks with limited clusterhead count. Multi-hop routing within a cluster (Figure 3.2b) has already been proposed in wireless adhoc networks [LG95]. WSN clustering algorithms like DWEHC³ [DHC05] allow multi-hop intra-cluster routing.

¹Low Energy Adaptive Clustering Hierarchy
²Hybrid Energy-Efficient Distributed Clustering
³Distributed Energy Efficient Hierarchical Clustering

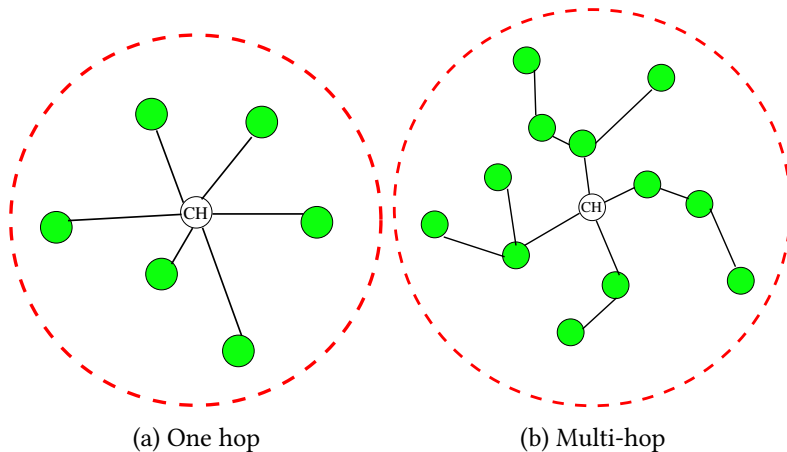


Figure 3.2: Intra-cluster communications

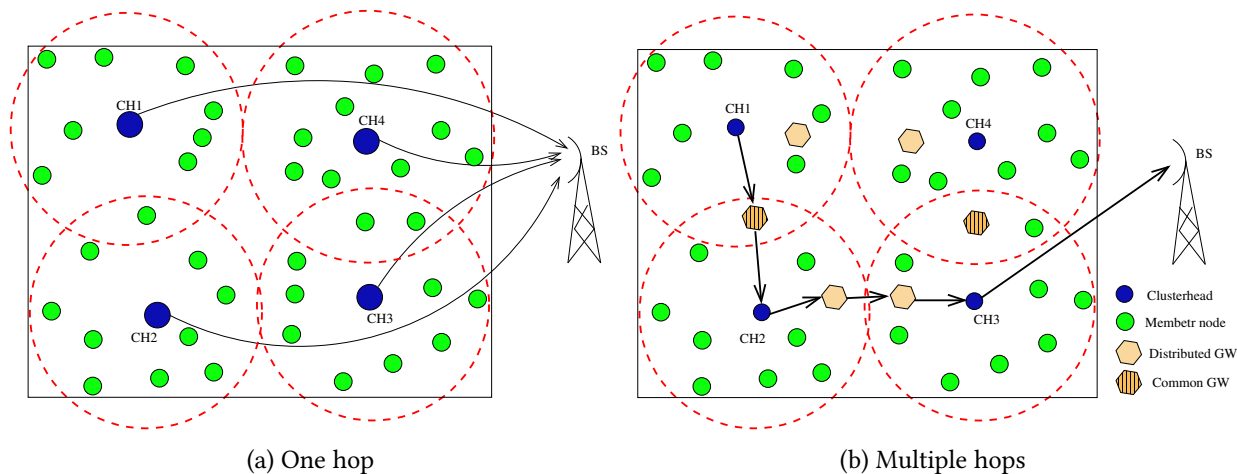


Figure 3.3: Route toward the sink

Inter-cluster Routing. Earlier cluster-based routing protocols such as LEACH assume that the clusterheads have long communication ranges allowing direct connection between every clusterhead and the sink (Figure 3.3a). Although simple, this approach is not only inefficient in terms of energy consumption, it is based on unrealistic assumption. The sink is usually located far away from the sensing area and is often not directly reachable to all nodes due to signal propagation problems. A more realistic approach is multihop inter-cluster routing that had shown to be more energy efficient [MR04]. Sensed data are relayed from one clusterhead to another until reaching the sink. As an example, ECDS⁴ [ATM13] allows multi-hop inter-cluster routing in addition to K -hop intra-cluster communication.

Direct communication between clusterheads is not always possible especially for large clusters. In this case (Figure 3.3b), ordinary nodes located between two clusterheads could act as *gateways* (GW) allowing the clusterheads to reach each other. A gateway node is either *common* or *distributed*. A common gateway is located within the transmission range of two clusterheads and thus, allows two-hop communication between these clusterheads. When two clusterheads do not have a common gateway, they can reach each other in at least three hops via two distributed gateways located in their respective clusters. A distributed gateway is only reachable by one clusterhead and by another distributed gateway of the second clusterhead cluster.

Cluster Head Designation Strategies. When sensor nodes location is known, clusterheads can be pre-designated before even deploying the network as done in PANEL⁵ [BS10]. Although PANEL allows a better load balancing, CHs pre-designation is not suitable to dynamic networks. The probabilistic approach adopted by earlier protocols such as LEACH allows each node to take the initiative to become a CH with a given probability. This random election does not ensure the quality of communication between each node and its CH nor a fair distribution of the load between the different nodes of the network. Parameters like energy (HEED) or quality of links should be considered (ECDS). Clusterheads selection is performed on-demand [GBS19, AM19] instead of performing clustering in every round in.

Energy Efficiency and Load Balancing. Minimizing energy consumption on a per sensor basis is not sufficient to get longer network lifetime, a global strategy with load-balancing is required. Two main approaches allow for energy efficient load balancing, namely *clusterhead rotation* and *unequal clustering*. *Role rotation* is mainly motivated by the heavy burden put on clusterheads induced by both intra and inter-cluster communications in addition to possible in-network processing such as aggregation and fusion. Even if clusterheads are equipped with more powerful and durable batteries, this heavy burden could result in

⁴Energy-Constrained minimum Dominating Set-based clustering

⁵Position-based Aggregator Node Election

fast battery depletion at the clusterheads and thus shorter lifetime compared to other sensor nodes. This is one possible load unfairness situation that may occur in cluster-based routing.

In order to give each clusterhead equivalent burden in the network, many algorithms focus on balancing the intra-cluster traffic load through the formation of nearly equal size (uniform) clusters. In fact, in clusters of comparable coverage and node density, the intra-cluster traffic volume is more likely to be the same for all clusters. One possible solution to this issue is to form unequal clusters [AP19] depending on how far is a clusterhead from the sink as done in [SH05, GP16]. The rationale behind this is that main spent energy by a clusterhead is due to both inter-cluster and intra-cluster communication and hence have to be considered jointly. On the one hand, intra-cluster communication cost is proportional to the number of member nodes in a cluster. On the other hand, in a multihop network, inter-cluster communication cost depends on the experienced forwarding load by a given clusterhead. In the many-to-one communication pattern of WSN, the closer to the sink, the greater forwarding load a clusterhead have to handle. As a consequence, more uniform load distribution among clusterheads in a network can be achieved through smaller clusters near the sink.

Passive Clustering. Most of the proposed cluster-based routing protocols rely on already formed clusters. Afterwards, the inter-cluster communication is generally ensured using traditional flooding among only clusterheads or by recursively executing the clustering algorithm to obtain a hierarchy of clusterheads routed at the sink. They were qualified as *pre-established* cluster-based routing algorithms [MZL10]. Protocols that build clusters based on packets flowing in the network without a priori construction are qualified as *on-demand* cluster-based algorithms. On-demand clustering by exploiting existing traffic to piggyback cluster-related information, eliminates major control overhead of traditional clustering protocols. Besides, there is no startup latency even if there is a transient period before getting maximum performances. This is done in PC⁶ [KG02, VDP22] by introducing two innovative mechanisms for the cluster formation: “*first Declaration wins*” rule and “*gateway selection heuristic*”. With the “*first Declaration wins*” rule, a node that first claims to be a clusterhead *rules* the rest of nodes in its clustered area. The “*gateway selection heuristic*” provides a procedure to elect the minimal number of gateways. The algorithm defines several states in which a node can be. At cold start, all nodes are in the initial state. Nodes can keep internal states such as *clusterhead-ready* or *gateway-ready* to express their readiness to be respectively a clusterhead or gateway. A candidate node finalizes its role of a clusterhead, a gateway (common or distributed) or an ordinary node.

3.2 Energy Efficient Passive Clustering

The reactive nature of PC motivated its combination with on demand routing protocols to mainly achieve energy efficiency [HKK⁺04]. The main idea of the combination, we refer to as PCDD⁷, is to save energy by preventing ordinary nodes from participating in the flooding phases known to be very costly. Under different network sizes and loads, the combination achieves better performances in terms of delivery ratio and average dissipated energy. However, the energy expenditure of the flooding nodes will be much higher than those of ordinary nodes. This may cause a premature death of the network due to the lack of connectivity caused by rapid energy dissipation at critical nodes (CH and GW). This problem can be chiefly attributed to the lack of load balancing between the nodes that belong to a given cluster. In fact, topology construction in PC is done according to the lowest ID. The drawback of doing so is its bias towards nodes with smaller IDs leading to their battery drainage. Assume that three nodes 1, 2 and 3 (with same initial amount of energy) are contending to be a flooding node as shown in Figure 3.4a. If we use PC algorithm, node 1 will be selected to be a CH since it has the smallest ID. Even if we consider energy as done in [MAH07], a CH will keep its role until it exhausts its whole energy.

⁶Passive Clustering

⁷Passive Clustering Directed Diffusion

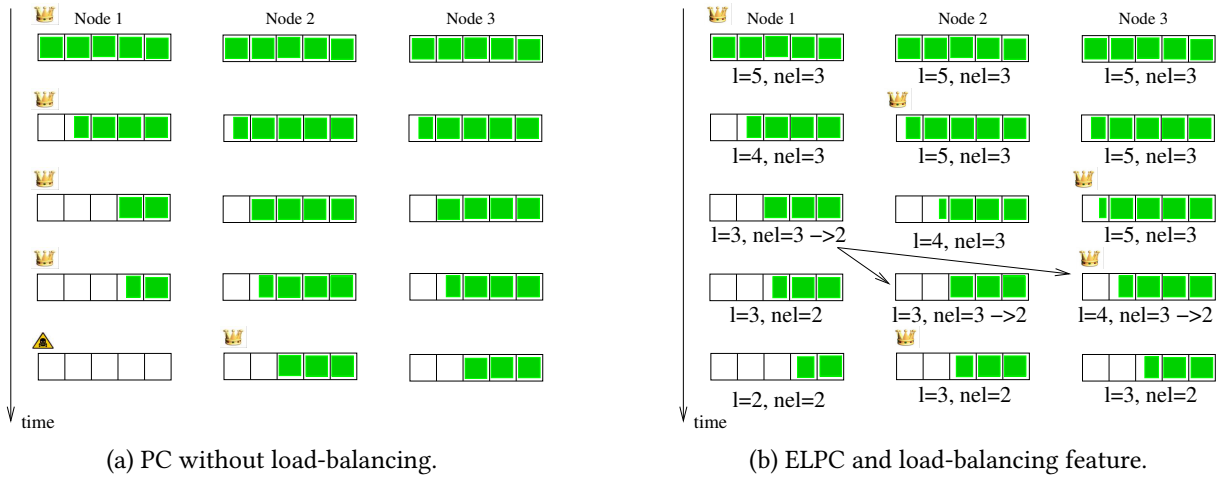


Figure 3.4: PC versus ELPC [ZMLB12]

The problem of flooding and the absence of load balancing of PC has been examined in the context of Zeghilet's thesis [Zeg13] for Directed Diffusion (DD) [IGE⁺03]. In what follows, DD is summarized before presenting an energy-efficient PCDD.

3.2.1 Directed Diffusion (DD)

Directed Diffusion (DD) [IGE⁺03] is the most popular data-centric routing protocol in the literature, proposed to deal with the lack of a globally assigned identifiers scheme in WSN. The main idea is that data is routed based on its content rather than using routes based on unique identifiers of nodes in the sensor network. Directed Diffusion aims at diffusing data through sensor nodes by using a naming scheme for the data. It is query-based and suggests the use of attribute-value pairs for the data. In order to create a query, the sink sends an interest defined using a list of attribute-value pairs such as name of objects, interval, duration, geographical area, etc.

The interest is broadcast by a sink through its neighbors. Each node receiving the interest caches it for later use. As soon as a sensor node detects an event that matches one of the interests in its cache, it calculates a gradient for each neighbor node that delivers the matching interest. Thus, the gradients are setup from sensors to the sink. A gradient is a reply link to a neighbor from which the interest was received. Hence, by utilizing interest and gradients, paths are established between sink and sources. The sink reinforces one or more paths by sending the same interest on the selected paths with a higher event rate. In addition to route discovery mechanisms, in-network processing may be employed to aggregate data to increase efficiency.

The on-demand nature of DD in constructing paths enables robustness and energy saving. Data caching and aggregation also make big benefit in terms of energy consumption and delay reduction. However, DD can not support time-sensitive traffic nor perform energy-balancing to increase network lifetime. This is due to the fact that it makes use of the same small set of paths in the routing phase which can lead to the exhaustion of nodes on these paths and cause network partition.

3.2.2 Energy Level-based Passive Clustering (ELPC)

The main purpose of ELPC [ZMLB12] is to achieve energy efficiency in terms of network lifetime, not only in terms of energy consumption. This is done through alternating flooding nodes role (clusterheads and gateways) among nodes depending on their energy. The aim of doing so is to have the same amount of energy at all the nodes at a given time which increases substantially the whole network lifetime. In ELPC, each node's battery is split into levels. One can make a correspondence between different energy levels of a node and virtual sub-batteries it consumed sequentially. The energy level (l) of a node can be computed

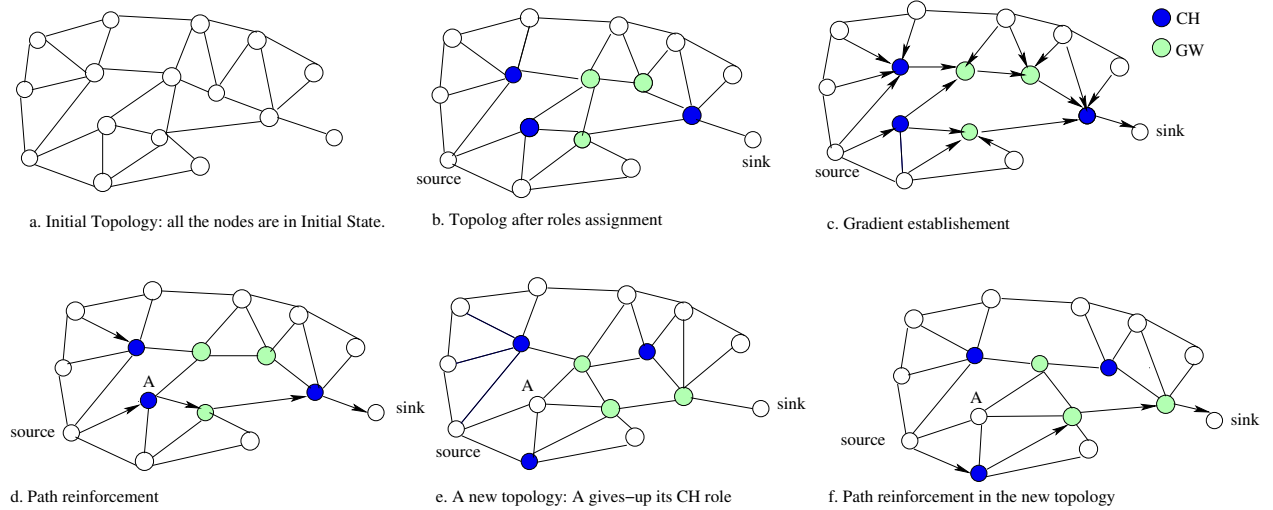


Figure 3.5: ELPC illustrated

using :

$$l = \left\lceil L \frac{E_r}{E_i} \right\rceil \quad (3.1)$$

where E_r is the remaining energy, E_i is the initial one and L is the considered number of levels.

We introduced the notion of *candidature* to be a clusterhead or a gateway by defining the *network energy level (nel)* parameter. A node is not allowed to declare itself as a clusterhead (or a gateway) if its energy level is below this parameter. A clusterhead (or a gateway) can keep its role as long as its energy level is higher than the *nel*. Otherwise, it gives up its role and passes to the *initial* or *ordinary* state depending on whether or not it is aware of the presence of a clusterhead in its vicinity.

Finding a meaningful value for the network energy level is non-trivial. It depends on the energy level of the network nodes and can be viewed as the minimum level of energy necessary for a node to be a clusterhead or a gateway. We suggested to take an initial value that corresponds to the half of the battery charge. This value is decreased locally each time the condition to be a clusterhead is not satisfied. The local network energy level is then propagated within outgoing packets header. The local *nel* value is updated each time a node receives a smaller *nel* value.

The same states suggested in [KG02] are used. A node starts by setting itself to the *initial* state. Nodes form and maintain the clustering topology by changing their internal and external states based on outgoing messages. When sending the next message, a node announces its external state that becomes visible in the network. Algorithm 5 summarizes how PC is modified to allow load-balancing feature depending on nodes energy levels.

Figure 3.4b illustrates the same example of Figure 3.4a with ELPC applied. The number of levels is chosen to be 5 for all the three nodes and the *nel* is initially set to 3 corresponding to the half of battery charge. It can be seen that the clusterhead role is alternated between the three nodes depending on their energy levels. When two nodes have the same energy level, then the nodes' identities are used to solve conflict in declaring roles. At step 3, note that node 1 decreases its *nel* to 2 (since $l = nel$) and propagates this new value to its neighbors so all nodes can have same estimation of the network energy level. It is straightforward that using ELPC, the network lifetime is enhanced as energy consumption is fairly distribution on nodes.

Figure 3.5 shows the establishment of routing structures of directed diffusion when this latter is used in combination with ELPC. Initially, all nodes in the network are in the *initial* state. Nodes will use the first interest messages to establish the new topology as described in the algorithms. A possible topology is illustrated in Figure 3.5(a-b). After establishing the gradient (c) and path reinforcement (d), the source begins

Algorithm 5: ELPC**Data:****CH-L, GW-L, ORD-L, INIT-L** : the list of, respectively, clusterheads, gateways, ordinary nodes, nodes in initial state, known to this node.**give-up** : when set, this node wants to give-up its role**Initialization phase****begin**

```

| state ← initial
| while true do
|   wait for receiving/sending a message
| end

```

end**Incoming message processing****begin**

```

| give_up ← false
| if msg.nel < nel then
|   nel ← msg.nel
| if msg.give-up then
|   delete the node from lists and updates its
|   state
|   return
| if msg.state == CH then
|   if state == CH then
|     if l < msg.level then
|       give_up ← true; add CH to CH-L;
|     else if l == msg.level then
|       use nodes' Ids to solve conflict (if
|       any)
|     else
|       add CH to CH-L; check lists; return
|   else
|     add the CH to CH-L; check lists;
|     recalculate my state
|   end
| if (msg.state == GW) then
|   add the gateway to the corresponding list
|   and update its state
| if (state == initial) AND
|   (msg.state ≠ CH) then
|   state ← CH_Ready

```

end**Outgoing message processing****begin**

```

| if give_up == true then
|   give_up ← false
|   if CH_list is not empty then
|     state ← Ordinary
|   else
|     state ← initial
|   end
| if state == CH_Ready then
|   if l > nel then
|     state ← CH
|   else
|     decrease nel
|     if CH_list is empty then
|       state ← CH
|   end
| if state == GW_Ready then
|   if l > nel then
|     state ← GW
|   else
|     decrease nel
|     if GW-L is empty then
|       state ← GW
|   end
| if (state == CH) OR (state == GW) then
|   if l < nel then
|     give_up ← true
|     if CH_list is not empty then
|       state ← Ordinary
|     else
|       state ← Initial
|   end
|   update msg fields
|   send msg

```

end

sending the sensed data. When the energy level falls under the network energy level at node A, it gives-up its role of clusterhead (d). Thus, a new topology is established (e). This is done using next circulating messages in the network (data messages, interests, exploratory data). The resulting passive clustering can be applied to any routing protocol in sensor networks as they mostly rely on flooding and particularly with DD. This not only reduces energy consumption, it also increases the whole network survivability.

Consider a network region with one cluster and say $k, k \geq 1$ potential candidates to be a clusterhead. Let E_L be the amount of energy per level, assumed to be the same for all the region sensors. Let E_i be the available energy at a sensor i in the beginning of the session where $E_1 \leq E_2 \leq \dots \leq E_{k-1} \leq E_k$. A *round* is defined as the time interval during which a given candidate is a clusterhead. Let P be the power dissipation of a sensor when it is a clusterhead.

In PCDD, the number of rounds is k since each candidate becomes a clusterhead once. Each round lasts E_i/P when sensor i is the clusterhead in this round. Given that a region lifetime is defined as the time until the first candidate dies, the PCDD lifetime corresponds to the duration of the first round. Since, it is the candidate with largest amount of energy (k) who is elected for the first round, then this region lifetime in PCDD can be given by :

$$\Lambda^{PCDD} = \frac{E_k}{P} \quad (3.2)$$

In ELPC, the number of rounds is $\sum_{i=1}^k E_i/E_L$ and each candidate (i) becomes a clusterhead E_i/E_L times. This is because each round consists in exhausting a level (E_L) of energy. It comes that each round lasts E_L/P . When the first clusterhead is died (the k th one with the largest amount of energy at the beginning of the session), it remains one level of energy for the $(k-1)$ other candidates and this region lifetime can be computed as follows :

$$\Lambda^{ELPC} = \frac{E_L}{P} \left(\sum_{i=1}^{k-1} (E_i/E_L - 1) + E_k/E_L \right)$$

Equivalently :

$$\Lambda^{ELPC} = \frac{1}{P} \left(\sum_{i=1}^k E_i - (k-1)E_L \right) \quad (3.3)$$

Note that $E_i = E_L$ when $L = 1$ and that $\forall i = 1, k-1 : E_i \geq E_L$. Then we can write the following :

$$\sum_{i=1}^{k-1} E_i \geq (k-1)E_L$$

giving :

$$\sum_{i=1}^k E_i \geq E_k + (k-1)E_L$$

Dividing by P , it follows that $\Lambda^{ELPC} \geq \Lambda^{PCDD}$ and that $\Lambda^{ELPC} > \Lambda^{PCDD}$ when $L > 1$ and $k > 1$. This means that if we have only one level of energy ($L = 1$) or just one potential candidate to be a clusterhead ($k = 1$), ELPC behaves exactly like PCDD. To get better performances in ELPC, we need naturally to have more than one level of energy and more than one potential candidate so the network connectivity is ensured for longer time.

3.3 Simulation Results

In order to assess the performances of the proposed clustering algorithm, ELPC is implemented using ns2 [ns2] and compared to the original DD and PCDD (DD with the passive clustering without energy consideration). The “*Two Phase Pull*” diffusion algorithm with its two flooding phases is used. The interest flooding are initiated by the sink and the data messages flooding are performed by a source when events

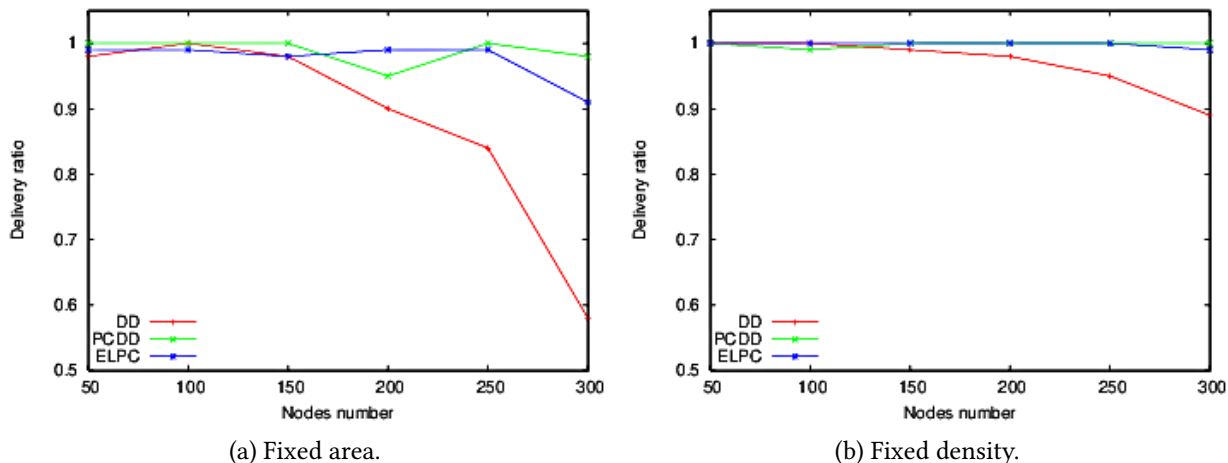


Figure 3.6: Mean PDR.

are detected in the network. Additional fields in the message header are added as attributes to represent the energy level of a node as well as the whole network. The IEEE 802.11 and the two-ray propagation model are adopted. The radio propagation of each sensor node reaches up to 40 meters. Simulation results are averaged over 20 randomly generated topologies.

The number of energy levels is one important parameter to be defined. As the idea is to virtually divide the node's battery, the initial amount of energy has a great effect on this parameter. To evaluate this, simulations with a variable initial energy and different number of levels are performed. Based on the average dissipated energy observed in each simulation, it appears that the number of energy levels depends on the initial amount of energy and that the average amount of energy per level can be set to $5 J$.

ELPC is evaluated when used for scalar data transmission to have general insights on its performance. Then, a focus on its use for video data packets transmissions is considered.

3.3.1 Scalar Data Transport

To examine the effect of network topology on the different solutions, both fixed zone ($160 \times 160 m^2$) area with variable number of nodes and fixed average density with variable zone dimensions are considered in this study.

Packet Delivery Ratio (PDR). Figure 3.6 shows, as a function of the number of nodes, the PDR of the different solutions in the fixed area and fixed density topologies. Passive clustering (in both PCDD and ELPC) provides better performances in terms of PDR that reaches higher values and even 100% in some cases. In fact, when the network size or density increases, more flooded messages are observed in the network. Passive clustering reduces the resulting overhead and keeps the performances of DD as if it were executed in small, low-density networks.

Network Lifetime. Extending the network lifetime is a primary design goal of this work. That is, simulations with nodes assigned insufficient amount of energy are conducted to capture the network lifetime. This latter is estimated using two metrics, (i) the time until the first node dies to see if the energy consumption is fairly distributed in the network ; (ii) the number of events before the network is partitioned, to show the delivery capacity of the network before giving up. As shown in Figure 3.7, the time to network partition decreases as the number of nodes increases. This was expected, as more nodes lead to more floods and hence more energy is consumed in the network. ELPC, however, achieves better performances compared to the two others in both fixed area and fixed density scenarios.

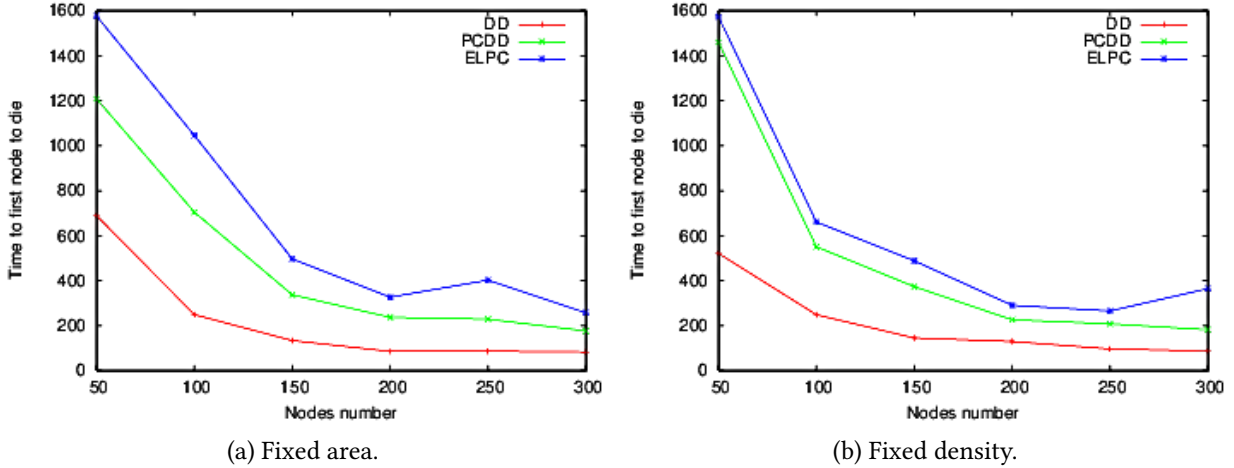


Figure 3.7: Network partition time (s).

3.3.2 Video Transport

With respect to high data rate applications, the main drawback of DD is that it relies heavily on flooding to build and maintain paths. This is very expensive in terms of required resources especially in dense networks. Some work has addressed extending DD to accommodate multimedia applications in WSN. For instance, authors of [LRCL08] proposed a multipath extension of DD where multiple routes are reinforced based on link quality and latency. The resulting algorithm is used for transmitting video traces generated by Multiple Description Coding [Goy01]. This section reports on the obtained results that show the value of the proposed clustering strategy to DD when used to transport video traffic.

In this study, fixed area topologies where the sensors field ($160 \times 160 m^2$) is populated by a number ranging from 100 to 500 nodes are considered. A video sensor is assumed to capture and transmit the "Hall Monitor" video sequence that lasts 10 seconds and consists of 300 frames in CIF resolution (352×288). The video sequence is encoded in MPEG4 with a target bit rate of $128 Kbps$ and a Group of Pictures (GOP) of 30. Only I (intra) and P (predicted) frames were generated in video traces using EvalVid [KRW03]. The reference (or the sent video) PSNR⁸ obtained is 29.70 dB.

The video clip is sent twice. This is done in order to get more insight into both the transient and steady phases of passive clustering in PCDD and ELPC. Each simulation runs until network partition (no way to reach the sink from the video source) or all the data packets composing the two clips are received by the sink. Both sufficient and insufficient energy experiments are considered. In the former, nodes have sufficient amount of energy such that the source is able to send all the video clip considered. This allows to mainly assess the average dissipated energy per correctly received information. In the latter, the amount of energy at nodes is chosen so it is smaller than the minimum required energy in the three protocols. This allows to assess the network lifetime based on the time at which the sink receives the last data packet from the video source.

Overall Performances. The object of this section is to present overall performances related to the entire simulation time from sending the first packet of the first clip until the last packet of the second clip. Figure 3.8 shows the energy gain obtained in PCDD and ELPC with respect to DD with sufficient energy. Passive clustering allows energy saving in both ELPC and PCDD where they at most consume 45% of what DD consumes for 100-node network. When increasing the network size, the gain is much higher mainly with ELPC. This is because more data packets are delivered in ELPC compared to PCDD as will be shown later.

⁸Peak Signal to Noise Ratio computed using formula (4.2)

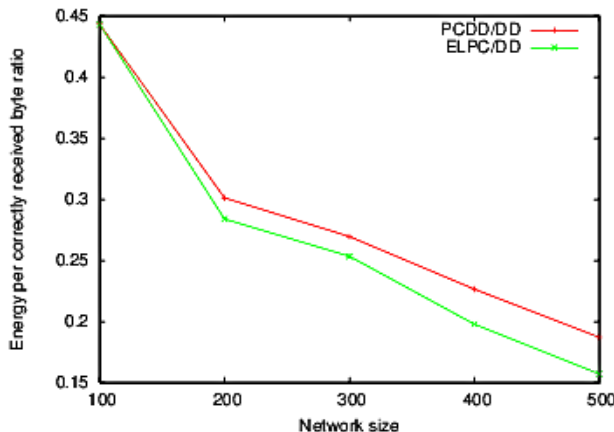


Figure 3.8: Energy ratio per correctly received byte (sufficient energy)

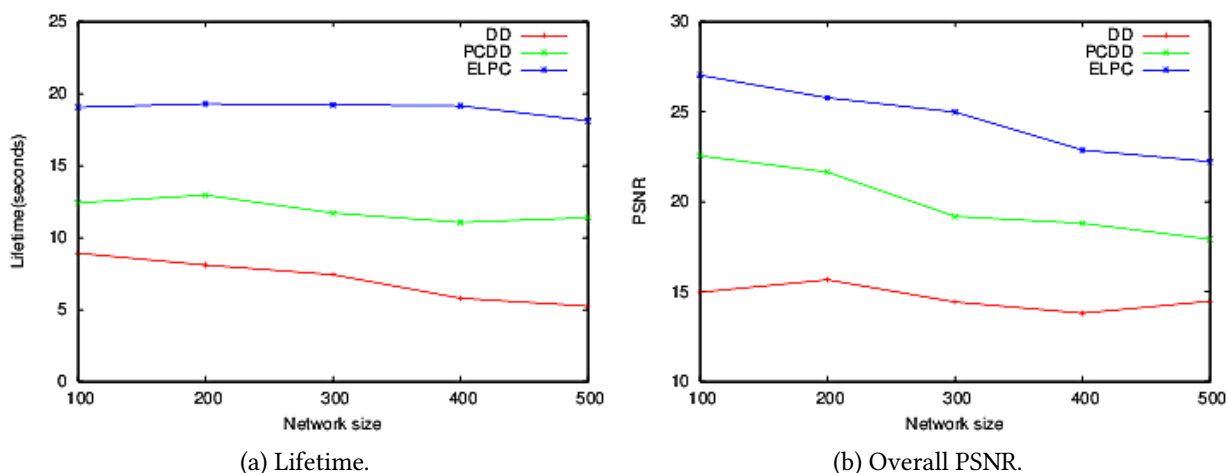


Figure 3.9: Overall Performance (insufficient energy).

The network lifetime, for the three protocols, slightly decreases when its size increases as shown in Figure 3.9a. A larger number of nodes results in more floods and subsequently a larger amount of energy is consumed in the network. ELPC achieves better performances since almost the two clips are received and the network lifetime is estimated to be nearly the duration of the two clips. However, PCDD and DD best lifetime does not exceed 13 and 9 seconds respectively. Regarding video quality, ELPC outperforms both DD and PCDD mainly for insufficient energy scenarios as shown in Figure 3.9b. Video quality decreases with the network size since more losses are experienced which affect the quality of received video. For sufficient energy as shown in Figure 3.10, ELPC and PCDD present nearly the same performances. Enough energy does not allow distinguishing the two protocols.

First Clip Period. Here, the focus is on the transient phase of the three protocols mainly PCDD and ELPC since clusters formation needs a given period of time to completely converge. It is worth saying that first clip related results (mainly for PCDD and ELPC) are nearly the same for both sufficient and insufficient energy scenarios since the amount of available energy is chosen (even in insufficient energy case) so at least a minimum number of the first clip frames are received by the sink.

Figure 3.11 shows, for a selected simulation run, the evolution of the PSNR on a per frame basis. To consider only the impact of network transmission on the video quality, the reference PSNR (REF) that corresponds to the measured quality of the sent video is also plotted. It is clear that both PCDD and ELPC outperform DD thanks to the clustering mechanism that reduces flooding. Similar PSNR values to the reference PSNR

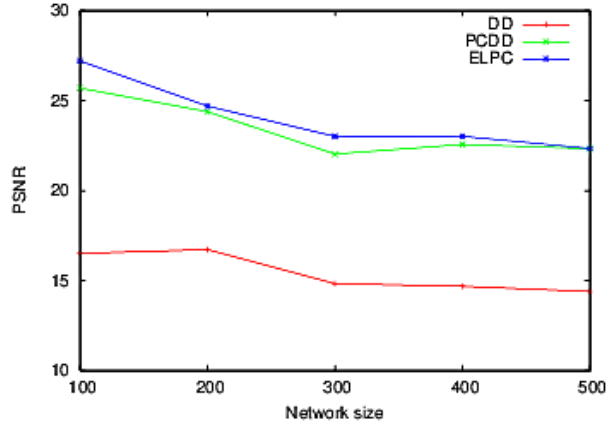


Figure 3.10: Overall PSNR (sufficient energy).

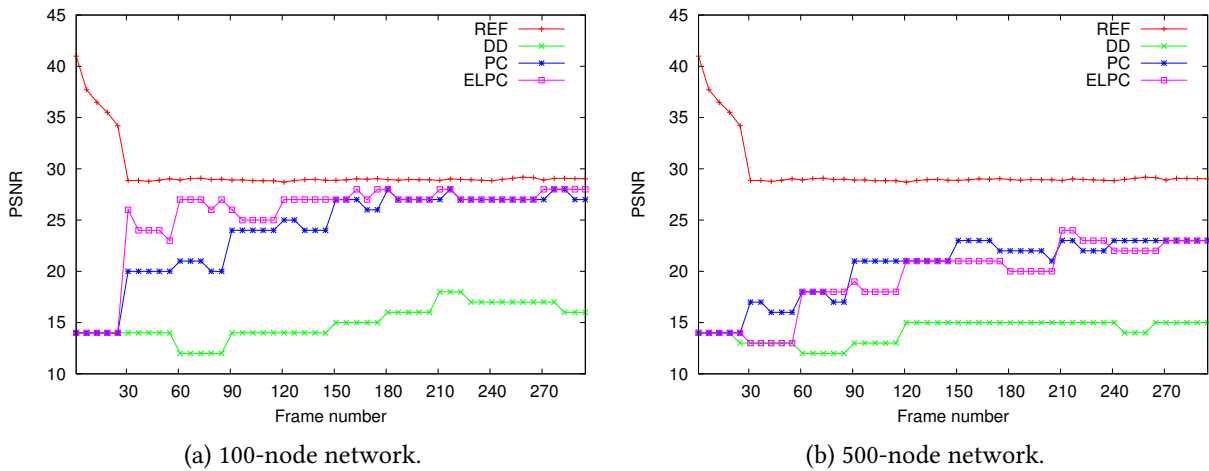


Figure 3.11: Mean PSNR per frame in the first clip video

except for the first 30 frames where ELPC and PCDD perform as poorly as DD. These 30 frames correspond exactly to the first transmitted GOP. Their bad quality can be explained by the presence of a transitional period where the clusters are not formed yet in ELPC as it behaves as DD at the beginning. Many messages are lost as the routing paths are not properly established.

The mean PSNR obtained with ELPC is of about 26.31 dB for 100-node network while it is of only 16.03 dB for DD. Note that the mean PSNR of the transmitted video is 29.7 dB. DD is unable to reach a PSNR greater than 18 dB which is very bad as can be observed in Figure 3.12. The video quality improvement of ELPC compared to DD is noteworthy. For instance, the best achieved quality in DD corresponds to $PSNR = 14.1$ dB for which, we can note the bad quality especially compared to the one of ELPC (with a PSNR of 27.56 dB). This can be explained by losses caused by messages dropped due to congestion in the network as large number of flooding are performed according to DD conception. For a 500-node network, similar results are obtained when comparing the three protocols however with lower PSNR values due to scalability issues especially for DD.

Second Clip Period. Figure 3.13a plots the mean PSNR obtained at the sink as function of the number of sensor nodes with sufficient energy. The first thing to note is that even with sufficient energy, DD performs very bad with a PSNR less than 19 dB. In what follows, only ELPC and PCDD are considered. As shown in Figure 3.13, ELPC allows better video quality in terms of mean PSNR with respect to PCDD regardless of initial amount of energy available at the sensor nodes. The difference is mainly observed in insufficient

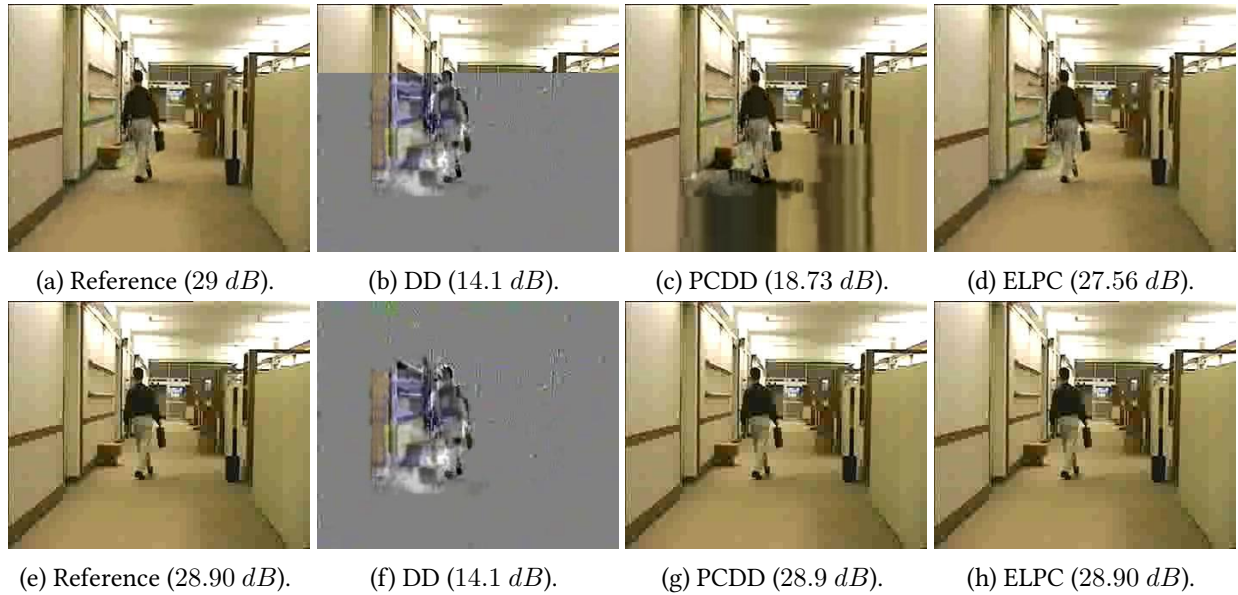


Figure 3.12: Frames 60 & 61 from the first clip with corresponding PSNR

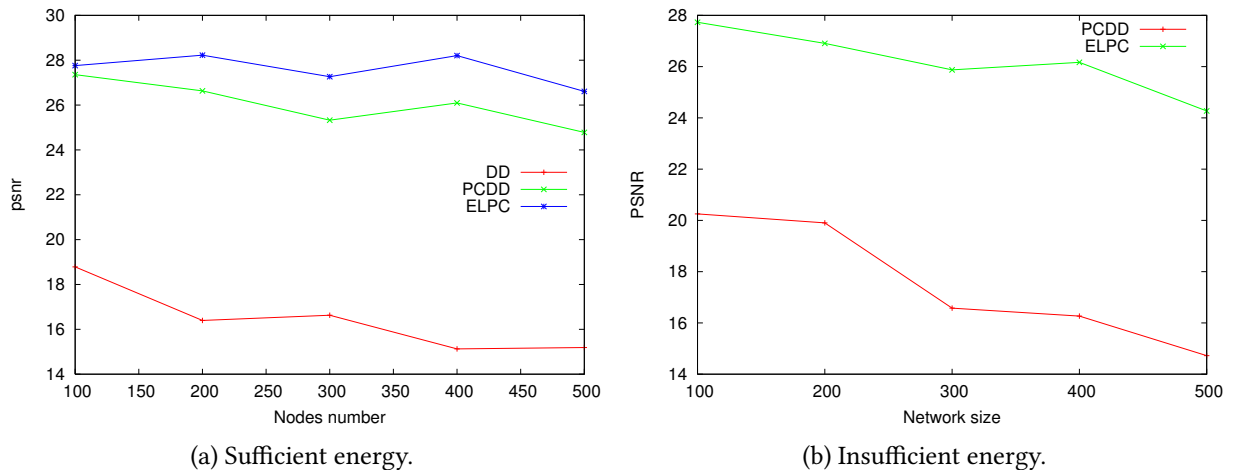


Figure 3.13: Mean PSNR of the second clip

energy cases. Figure 3.13b shows that PCDD achieves at most a mean PSNR of 20.25 dB for a 100-node network while ELPC mean PSNR is 27.73 dB. Even if the network size is increased to reach 500 nodes, ELPC obtains a mean PSNR of 24.27 dB.

Figure 3.14 plots the mean PSNR on a per-frame basis for a 300-node network with sufficient and insufficient energy. In both cases, ELPC outperforms PCDD especially for insufficient energy simulations where ELPC achieves a mean PSNR of 25.87 dB while PCDD a mean PSNR of only 16.57 dB suffering from higher loss rates. We can see that in ELPC, the frames keep a fair PSNR until almost the end of the clip as the network lifetime is longer.

Figure 3.15 shows frames number 30, 60 and 90 as received by the sink in insufficient energy simulations in PCDD and ELPC as well as the reference ones (as sent from the source). The three frames correspond to the last frames of the three first GOPs. This allows assessing video quality using the worst frame in a GOP just before receiving a new I-frame that could increase considerably the observed PSNR. ELPC allows higher quality with respect to PCDD. Besides, it achieves approximately the same quality of the reference frames. For instance the frame 30 is received with only a PSNR of 14.20 dB with very bad quality in PCDD

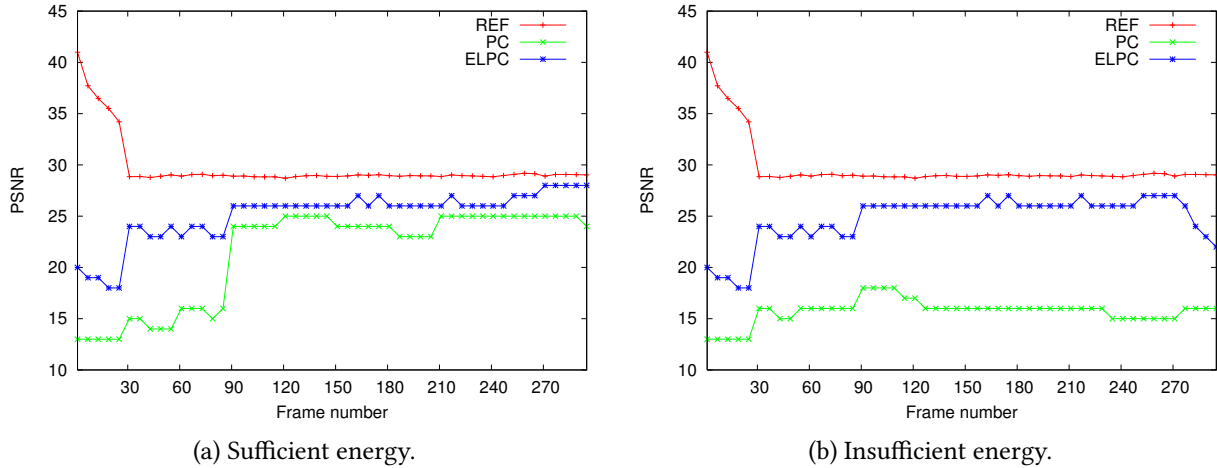


Figure 3.14: Mean PSNR per frame in the second clip video for a 300-node network.

while it is received with a PSNR of 29.21 dB. An other important observation is that frames 60 and 90 are nearly the same for PCDD. This means that very few data arrived at the sink from the third GOP. In the corresponding simulation scenario, the last received packet using PCDD corresponds to the 69th frame of the second clip. In the same simulation scenario, no frame from the second clip is received using DD.

3.4 Conclusion

In this chapter, a novel approach that combines a well-known routing paradigm (DD) in sensor networks with an energy-efficient cluster formation algorithm is presented. This combination offers improved network survivability and data delivery ratio, particularly when dealing with limited energy resources. With respect to high data rate video applications, the performance of the proposed load-balanced clustering technique can be further improved if combined with a multipath routing protocol that enables bandwidth aggregation. However, the capacity of a WSN remains limited, making it difficult to provide sufficient bandwidth to meet the requirements of data-intensive applications. Relying on sensors to deliver all the captured visual data is inefficient. Consequently, in-network data reduction becomes crucial to minimize transmissions and reduce energy expenditure. These aspects will be explored and discussed in the upcoming chapters.

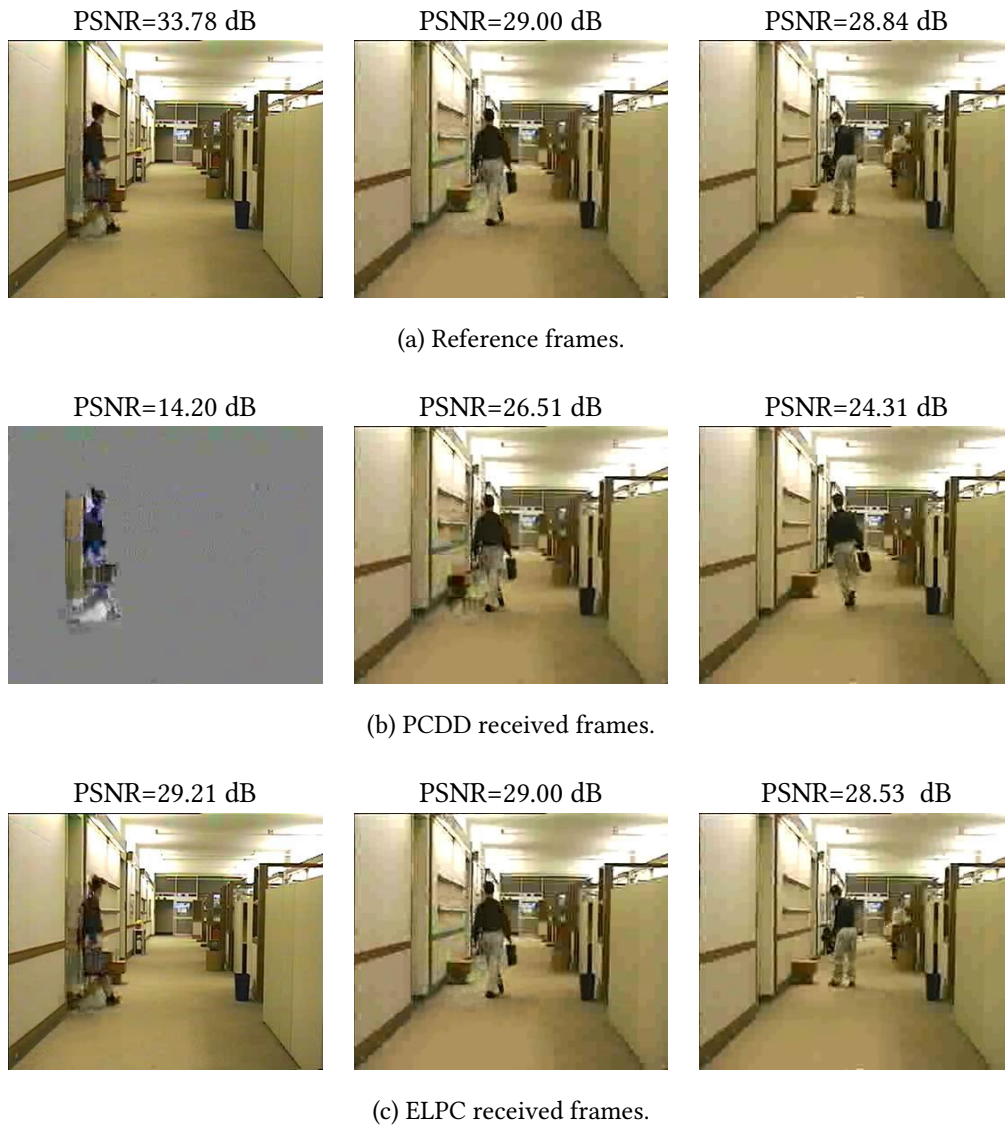


Figure 3.15: Sample of received frames (30, 60 and 90) from the second clip with insufficient energy.

Chapter 4

Toward Efficient Video Transmission in Constrained Networks

The emergence of low-cost and low-power visual modules [TBZBO12, ARS15] fostered the development of wireless video sensor networks (WVSN) and paved the way to a plethora of applications, mainly in monitoring and surveillance fields. However, WVSNs generate unique challenging problems as the capture, the encoding and the transmission of video flows are resource-intensive, coupled with the constraints of energy, bandwidth, processing, and storage in the underlying network infrastructure. As a result, significant efforts have to be devoted to designing and developing new algorithms and protocols that optimize the utilization of limited network resources while ensuring a high quality of service for end users [LKHL19, BPO⁺22, CN22].

Bandwidth scarcity has always been a significant challenge in WVSNs due to the limited radio capabilities of low-power and low-cost sensors [LDFH⁺06]. To address this issue, network protocols need to be designed to provide sufficient bandwidth for high data rate transmissions. One approach is to leverage multiple non-interfering paths to increase bandwidth capacity (Chapter 2). Paths diversity in WVSNs is commonly used to prioritize packets based on their relative importance, allowing for the implementation of appropriate dropping policies to match the available bandwidth [PTK08, EYG⁺16]. Besides, higher quality paths can be dedicated to transmitting more relevant visual data [Mai07, LA10, JBM12, HCWW14].

Despite optimal placement and interference-free communications, it remains challenging to provide sufficient bandwidth to meet the requirements of data-intensive WVSN applications, given the inherent limitations of wireless network capacity [GK00]. Relying on sensors to deliver all captured visual data is inefficient and impractical. In our work [BM14a], we demonstrated that an interference-aware multipath routing approach can double the overall throughput. However, achieving acceptable video quality remains difficult, even when capturing and transmitting at only 6 *fps* a gray-scale low resolution video clip compressed using MPEG-4. As a result, in-network data reduction is more than necessary to lower transmissions and corresponding energy expenditure.

Low-cost lossy compression offers a means to reduce the amount of data to deliver, but at the cost of introducing additional distortion. Moreover, wireless transmissions are prone to losses that induce holes in the images, further degrading their quality and usability. In this chapter, a complete efficient encoding-transmission-reconstruction chain is proposed. The absence of tools that allow both quantitative (QoS) and qualitative (QoE) evaluation of video transmission protocols in highly constrained networks has motivated the development of a more suitable tool. This latter is presented in Section 4.1. In addition to the use of a low complexity image compression method, an appropriate packetization scheme is proposed. This tool is used to evaluate the performance of a multipath routing protocol in Section 4.2. At the destination, more powerful resources are leveraged to apply deep learning models to compensate for the distortion caused by

Table 4.1: Summary Table of Existing Tools

Tool	Evalvid [KRW03]	Sim-LIT [ORSHDF ⁺ 11]	WVSN Model [Pha12]	Wise-MNet++ [SC17]	M3WSN [RZS ⁺ 13]	Joined-JPEG [ATM ⁺ 14]	EvalVSN [BMK14]	SenseVid [Mai18b]
Language	C	C++	C++	C++	C++	C++	Matlab	C++
Open source	✓		✓	✓				✓
Video support	✓			✓	✓		✓	✓
Codec	MPEG-4,H.263/4	custom	custom	N/A	MPEG-4,H.263/4	JPEG/2000	custom	custom
Bit stream		✓	✓	✓		✓		
Simulator	ns2	Tossim	Castalia	Castalia	Castalia	Castalia	ns2	cooja
Real testbed	✓	✓					✓	✓
QoE metrics	PSNR,SSIM	PSNR	PSNR	PSNR,SSIM	PSNR,SSIM	PSNR	PSNR,SSIM	PSNR,SSIM
Other metrics	loss, delay, jitter	loss	energy	energy	loss, delay, jitter	delay, energy	loss	loss, energy, delay

the adopted lossy compression as well as to fill in the holes induced by packet losses. Section 4.3 describes the used models and presents the main obtained results.

4.1 QoE Video Transmission Evaluation in Constrained Networks

Network researchers usually make use of discrete event network simulators such as ns2 [ns2] and OM-NeT++ [omn] to develop and evaluate their algorithms and protocols. Compared to a real WSN testbed, network simulators are good means to easily test protocols in a large scale with very limited cost. However, with respect to WVSN, pure simulation testing may not accurately reproduce real-life scenarios and may not provide appropriate metrics to assess proposed protocols and/or video encoding techniques. Metrics such as packet loss ratio, throughput, delay and jitter remain pure network related metrics that provide only limited insight into the video quality perceived by a human and do not reflect its associated subjective factors. One step forward to achieve more accurate assessment of network proposals is to be able to estimate the received image/video quality. Human perception can be evaluated using Quality of Experience (QoE) metrics such as structural similarity index (SSIM) [WBSS04]. This requires simulated experiments to be performed using actual encoders, decoders and video data.

EvalVid [KRW03] provides a set of tools, that allows researchers to carry out simulations of real video sequences transmission. EvalVid takes the video traffic trace approach to characterize a video sequence where trace files with limited size are produced rather than using actual video bit stream [SRK04]. Since EvalVid was developed to be used in less constrained networks, no energy model is provided. Moreover, the supported encoders, namely, MPEG-4, H.263 or H.264 are resources-hungry and as a result are not adapted to constrained networks. These codecs concentrate the most computational complexity at the encoder while video sensors have neither sufficient processing power nor enough energy to perform complex compression algorithms. Various tools, as summarized in Table 4.1, have taken into account constrained networks.

WVSN model [Pha12], Sim-LIT¹ [ORSHDF⁺11] and Joined-JPEG [ATM⁺14] are based on the bit stream method that does not allow their easy use in other simulation or real experiment environment. M3WSN² [RZS⁺13] is based on a traffic trace approach however it is highly dependent on the Castalia simulator and can not be used in other simulation environments. EvalVSN [BMK14] developed using Matlab, follows the same principle of EvalVid [KRW03] by adopting the traffic trace method. It implements a modified version of MPEG-2 similar to the one proposed in [AAMS08] but additionally provides different DCT implementations. An application module that allows the use of EvalVSN with more realistic loss patterns is provided in the ns2 [ns2] simulation environment. EvalVSN supports video transmission since it implements inter-frame coding. However, in addition to not providing an energy related metric, it suffers from a heavy execution time as well as poor performances. The existing transmission evaluation tools either consider video sequences along with codecs that are unsuitable for WSN or make use of low cost compression methods for still images without inter-frame coding required for efficient video transmission. SenseVid is a step forward in the development of an open source video transmission and evaluation tool

¹SIMulator for Lossy Image Transmission

²Mobile MultiMedia Wireless Sensor Network

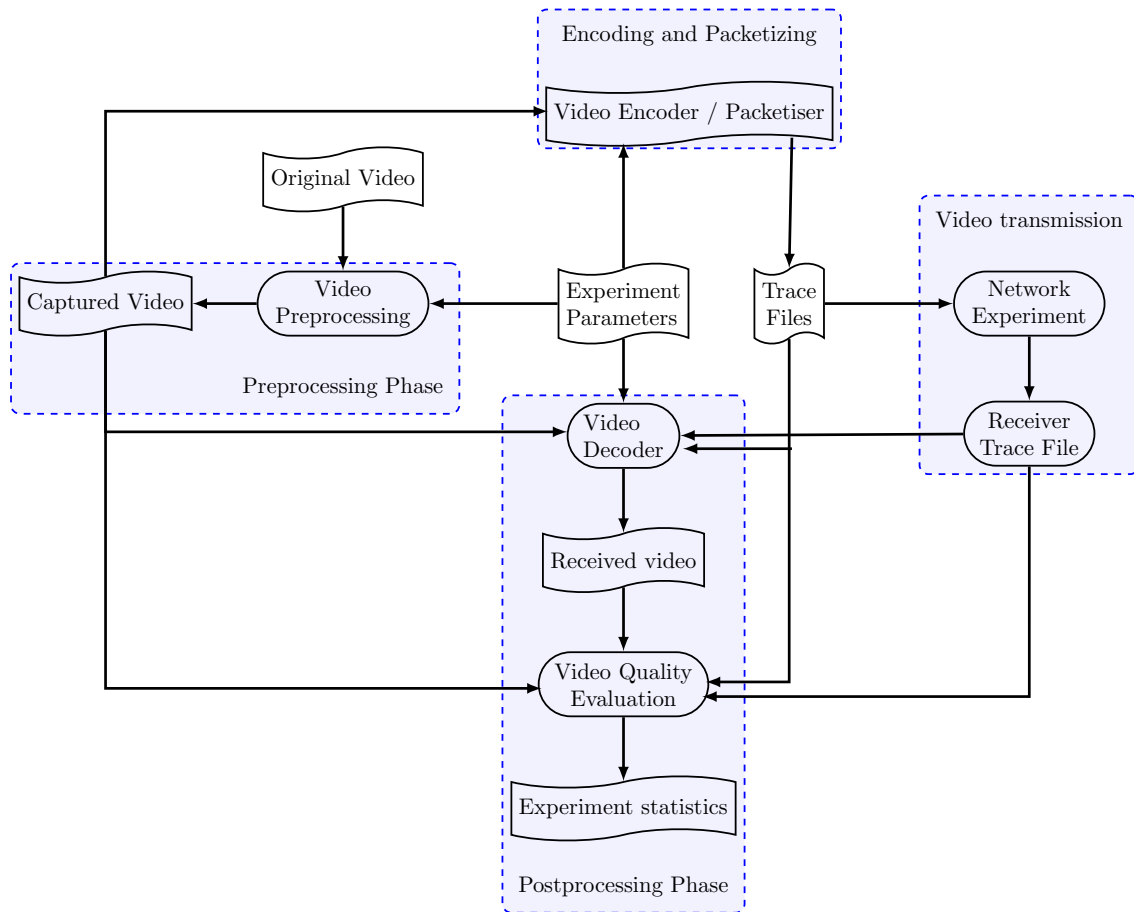


Figure 4.1: SenseVid Architecture

targeted to WSN. It (Figure 4.1) follows the main principle behind EvalVid where the interface with the real or simulation-based experiment is ensured through the use of traffic trace files. Based on the user's parameters, the encoder/packetizer module generates two trace files. The first is the frame trace file (*st-frame*) that records required information about the encoded frames. The second is the sender trace file (*st-packet*) that provides the sender application with the required information about the data packets to be sent. The receiver application records the delivered data packets in a receiver trace file (*rt-packet*). Based on this file, SenseVid reconstructs the video clip allowing its subjective assessment by the user. In addition, it generates statistics (both QoS and QoE metrics) on the conducted experiment.

In order to be able to use reference video sequences such as those available at [yuv] while being able to make them more realistic with respect to WSN characteristics, an optional preprocessing phase is introduced. The video preprocessing module allows to resize the video frames mainly to a lower resolution in order to reduce the required transmission rate. For the same purposes, the video original FFC³ can be lowered. Besides low energy intra-frame compression, a low complexity inter-frame encoding is provided to allow efficient support of video flows. SenseVid implements a fine-grained energy model that estimates the required energy to capture and encode each frame. Finally, SenseVid allows to differentiate priority levels of the data to transmit in order to adapt to network constraints and dynamics. After describing the main functionalities of SenseVid, some numerical results are provided in Section 4.1.4. Sections 4.1.5 gives use scenarios in a simulation environment (cooja [RQADG16]) as well as in a real sensor testbed (IoT-LAB [ABF⁺15]). More results can be found in [Mai18b].

³Frame Frequency Capture

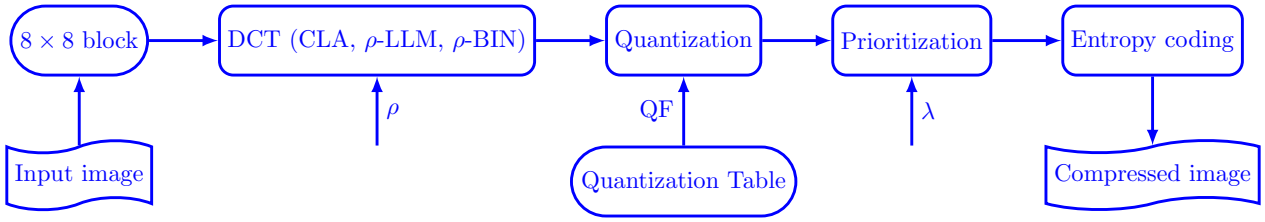


Figure 4.2: M-frame block encoding sequence

4.1.1 Video Encoder/Packetizer Module

Based on the user parameters, the video encoder/packetizer module compresses the captured video clip and generates the sender trace files. It converts the captured frames to gray scale where each pixel is encoded using 8 bits with range $[0, 255]$. A low energy compression algorithm that considers both spatial and temporal redundancy in a video sequence is implemented. A frame is either intra-coded and qualified as a *main frame* (M-frame) or inter-coded with respect to the previous M-frame in which case it is referred to as a *secondary frame* (S-frame). The first frame is always encoded as an M-frame. A subsequent frame is encoded as a main or a secondary frame based on a user parameter $\gamma \in [0, V_{peak}]$, the GOP coefficient, that allows to control the GOP of the resulting compressed video. $V_{peak} = 255$ is the maximum mean square error two frames can have. For each frame, the mean square error (MSE) with respect to the previous M-frame is computed. If $MSE > \gamma^2$ then the frame is considered to be sufficiently different from the previous M-frame and thus is M-encoded ; otherwise, it is S-encoded.

Main Frame Encoding

As depicted in Figure 4.2, each M-frame is first decomposed into blocks of 8×8 each of which is shifted from range $[0, 255]$ to signed integers range $[-128, 127]$. Then, a DCT is applied on each block. However, DCT computation consumes at least 60% of the whole power encoder [TPD02]. Therefore, a considerable effort has been made in reducing the DCT computational complexity [SA18]. In order to meet the requirements of constrained networks, two fast pruned DCTs are implemented in SenseVid, the Loeffler-Ligtenberg-Moschytz DCT (LLM) [LLM89a] and the binDCT-C (BIN) proposed in [Tra99]. Both the square and the triangular patterns of pruned DCT are provided. The square or triangle side length ρ is defined by the user. The default value is set to 8. For comparison purposes, I also implemented the traditional DCT variant, referred to as CLA. The resulting DCT block coefficients are quantized using the JPEG standard quantization matrix. Trade-off between quality level and compression rate can be obtained by selecting a proper quality factor (QF) that allows adjusting the quantization matrix values. The user is able to decide the frame visual quality ranging from the poorest ($QF = 1$) to the best quality ($QF = 100$).

The obtained block (B) is then linearized using the traditional zigzag scan along with an optional prioritization procedure. For an M-frame, priorities range from 0 to 12 and follow the zigzag scan of the block. For the maximum number of priorities ($\lambda = 13$), the first priority level ($l = 0$) contains the DC component (b_{11}) and the following two AC components (b_{12} and b_{21}). The last priority level ($l = 12$) is composed of the last three coefficients of the linearized block : b_{78} , b_{87} and b_{88} . The remaining block coefficients are assigned to levels $l \in [1, 11]$ where coefficient b_{ij} gets priority level $l = i + j - 3$. Figure 4.3 shows the zigzag scan and priority assignment for the square and triangular shapes with $\lambda = 3$ and $\rho = 4$. Finally a lossless entropy encoding is applied. The user can choose among various encoders such as Huffmann and exponential-Golomb [Teu78] with or without RLE⁴.

⁴Run Length Encoding

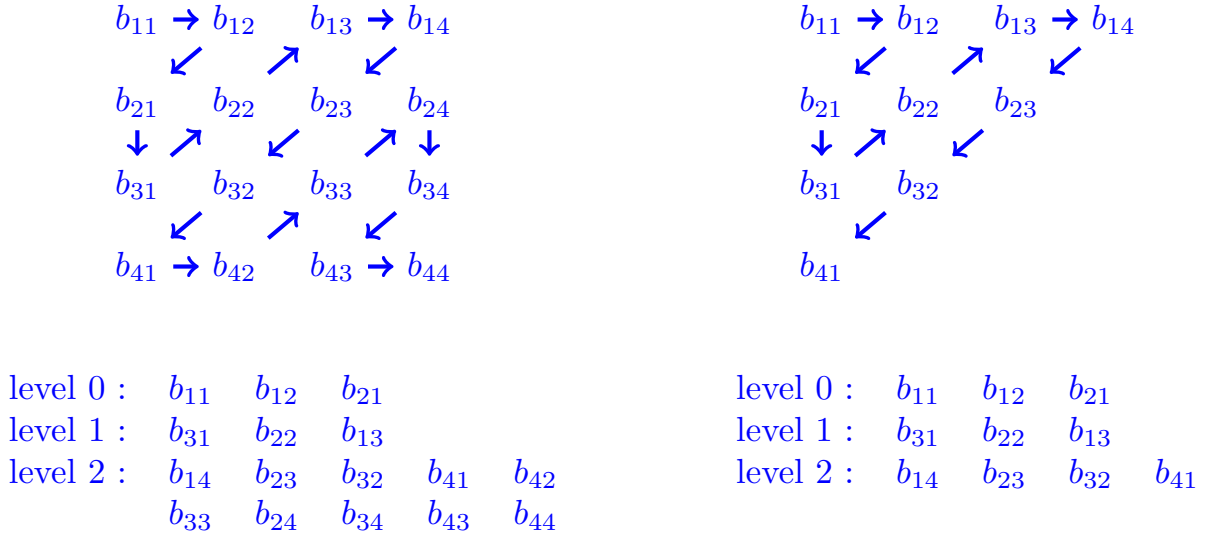


Figure 4.3: Liberation and priority assignment (a) square (b) triangular pruned DCT. $\rho = 4$ and $\lambda = 3$.

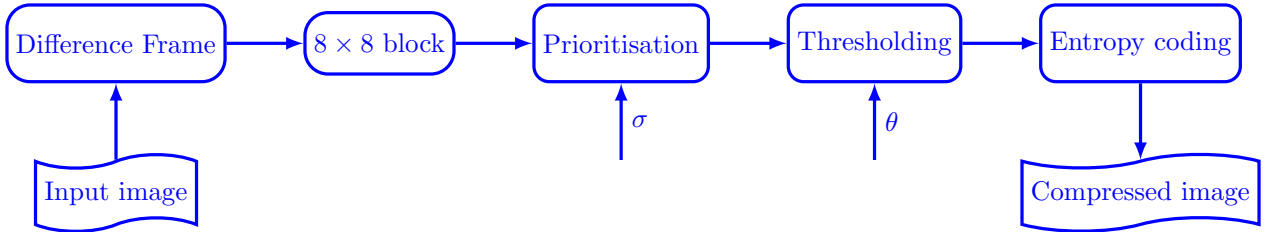


Figure 4.4: S-frame encoding sequence

Secondary Frame Encoding

A secondary frame is inter-coded with respect to the previous main frame. That is, what is encoded is the difference between the current frame and its main frame. The resulting difference blocks with only zero values are ignored. In order to reduce the amount of data to be transmitted, only a subset of the remaining blocks is encoded. Blocks deemed to be similar to the previous M-frame blocks get lower priority, lossy compressed or simply discarded depending on two parameters provided by the user required by the prioritization and the thresholding steps (Figure 4.4).

The prioritization step consists in attributing a priority level (0..4) to each block where 0 is the lowest priority level. Highest priority blocks are those with the least degree of similarity with their related blocks in the previous M-frame. The five priority levels are related to the MOS⁵ ratings and the corresponding mean square $MS = \sum d_{ij}^2 / 64$ of each block of the difference frame (Tables 4.2-4.3). The highest priority is assigned to blocks with $MS > 650$ and the lowest priority to those with $MS < 13$. The rationale behind this is that if a block with a highest priority is missing, then the rebuilt block based on the previous M-encoded block will get a bad quality ($PSNR < 20$ dB). In contrast, loss of blocks with lowest priority does not affect the quality of the rebuilt block that still get an excellent quality ($PSNR > 37$ dB).

To save video sensors and network resources, the user can decide to only encode a subset of the blocks of a given frame by adjusting parameter σ that defines the lowest priority level to consider for the following step (thresholding). The retained blocks by the prioritization step are then thresholded using the *threshold similarity* parameter (θ). All pixels with value less than θ are zeroed. As for the main frame, the last step consists in applying a lossless entropy encoding on the remaining blocks. Since not all blocks are

⁵Mean Opinion Score

Table 4.2: PSNR and QoE correspondence

PSNR	MOS	QoE	Distortion
> 37	5	Excellent	Imperceptible
]31, 37]	4	Good	Just perceptible, but not annoying
]25, 31]	3	Fair	Perceptible and slightly annoying
]20, 25]	2	Poor	Annoying, but not objectionable
< 20	1	Bad	Very annoying and objectionable

Table 4.3: S-frame blocks priorities

MS	PSNR	Priority
< 13	> 37	4
]13, 51]]31, 37]	3
]51, 205]]25, 31]	2
]205, 650]]20, 25]	1
> 650	< 20	0

transmitted, sequence information is included. It is encoded using VLI⁶ with $4 + n$ bits. The first 4 bits give the required number (n) of bits to encode the number using biased representation.

Packetization

The compressed blocks are then packetized. In addition to sequential packetization, I considered scattering the blocks based on a torus automorphism (TA) so as to avoid getting adjacent losses that appear in more or less long chunks depending on the loss rate. A TA is a highly chaotic system that can be used to obtain spatial transformation of the blocks coordinates in a video frame in which the initial position can be recovered by the Sink. Without loss of generality, let I be a square frame composed of $N \times N$ square blocks. Applying a TA transformation on image I_0 , to obtain a new image I_n , consists in relocating every block of I_0 situated in position (x_0, y_0) to a new position (x_n, y_n) in I_n using :

$$\begin{pmatrix} x_n \\ y_n \end{pmatrix} = \begin{pmatrix} 1 & 1 \\ k & k+1 \end{pmatrix}^n \begin{pmatrix} x_0 \\ y_0 \end{pmatrix} \text{ mod } N \quad (4.1)$$

where $k \in \mathbb{N}$ is a parameter of the transformation and $n \in \mathbb{N}$ is the scatter key. The set of points $\{I_0, I_1, I_2, \dots\}$ thereby obtained is called an orbit of the system. Under certain circumstances, an automorphism may have periodic orbits, which means that after T iterations the current frame is equal to the initial one, i.e. : $I_0 = I_T = A^T \times I_0$, where $A = \begin{pmatrix} 1 & 1 \\ k & k+1 \end{pmatrix}$. We can write $I_0 = A^{T-n} \times A^n \times I_0 = A^{T-n} \times I_n$. That is, the Sink is able to reconstruct the initial frame I_0 based on the received one I_n using A^{T-n} , a known matrix.

To avoid complex computations [DFL08], I considered the *Arnold's cat map* [Pet97] where $k = 1$ with a scatter key $n = 8$. The elements of the matrix A^n are pre-computed and stored at the video source to lessen the computation complexity. As opposed to [DFL08] that made pixels scattering, TA is applied on a per block basis to further save energy. Figure 4.5 gives a visual view of the obtained loss patterns at the Sink when adopting a TA-based scattering compared to a sequential packetization with 30% of packets being lost. Gray strokes correspond to the missing blocks in the received image. They are represented in white in the frame binary mask (left). A more even distribution of holes in the scattered packetization can be observed. This helps the reconstruction process at the Sink since filling missing blocks is basically based on neighboring blocks.

4.1.2 Video Decoding and Quality Evaluation

The sender trace file is used by the sender application to get the list of data packets to transmit. At the end of the experiment, a receiver trace file that records the list of the received packets is produced by the receiver application. Potential missing lines with respect to the sender trace correspond to the set of lost packets during transmission. Based on the different trace files in addition to the original captured video, the received frames are decoded considering the potential losses. Statistics on the conducted experiment are generated and recorded in the receiver frame trace file (*rt-frame*). Both network and video quality

⁶Variable-Length Integer

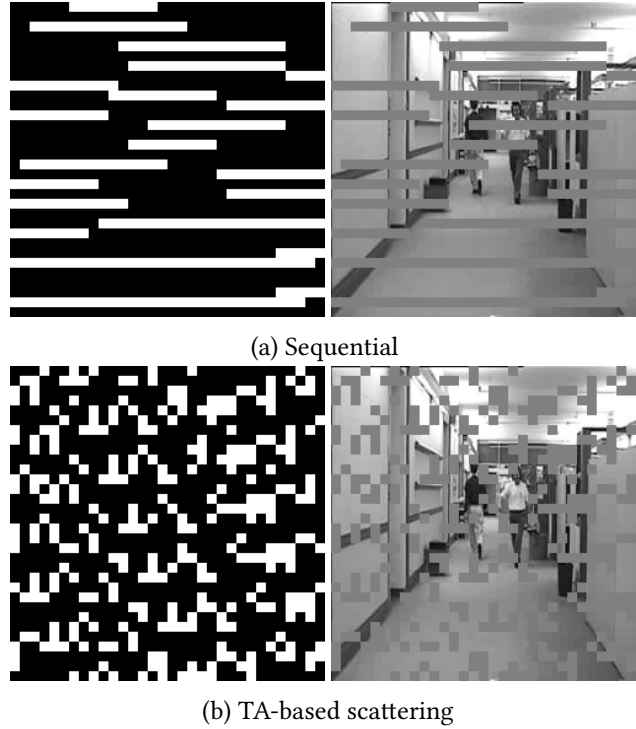


Figure 4.5: Sequential vs. TA-based scattered blocks with 30% loss rate

related metrics are computed in order to quantitatively assess the performances of the user's transmission strategies.

Network-related (QoS) metrics such as losses, delay and jitter can easily be computed using scripts based on the generated trace files. Video-related (QoE) metrics are implemented by the quality evaluation module. PSNR and SSIM metrics are implemented to assess the quality of both the encoded video before transmission (reference PSNR or SSIM) and the received video with respect to the initial lossless encoded video. The PSNR between the sent and the received, possibly distorted video frame is computed using :

$$PSNR = 20 \log \frac{V_{peak}}{MSE} \quad (4.2)$$

where MSE is the mean square error which is the average of the square of the pixel differences of the two images. The SSIM metric is computed as follows :

$$SSIM = \frac{2\mu_x\mu_y + C_1}{\mu_x^2 + \mu_y^2 + C_1} \times \frac{2\sigma_x\sigma_y + C_2}{\sigma_x^2 + \sigma_y^2 + C_2} \times \frac{\sigma_{xy} + C_2/2}{\sigma_x\sigma_y + C_2/2} \quad (4.3)$$

where x and y are two non negative image signals, μ_x , σ_x and μ_y , σ_y are the mean and standard deviation of x and y respectively. σ_{xy} is the sample cross-covariance between x and y . C_1 and C_2 are set respectively to 6.5025 and 58.5225.

4.1.3 Energy Model

In constrained networks where video acquisition and compression require significant computation resources can not be neglected. Therefore, an energy consumption model has to be provided in order to be able to assess the overall cost of video applications from video capture to its delivery to the final destination. Any power consumption model is dependent of the sensor node computation capabilities and instructions set. The developed tool provides parameters for the Atmel Atmega128L, 8-bit micro-controller and allows the user to modify them to meet his target platform characteristics.

Table 4.4: Fast pruned DCT cost for different values of ρ

ρ	LLM DCT						binDCT-C					
	1-D		square 2-D		triangular 2-D		1-D		square 2-D		triangular 2-D	
	Add.	Mul.	Add.	Mul.	Add.	Mul.	Add.	Shift	Add.	Shift	Add.	Shift
8	29	11	464	176	413	152	30	13	480	208	420	172
7	28	11	420	165	348	130	28	12	420	180	346	139
6	26	10	364	140	280	102	28	12	392	168	290	115
5	25	9	325	117	223	77	28	12	364	156	234	91
4	24	9	288	108	169	59	27	11	324	132	174	63
3	23	8	253	88	118	38	19	6	209	66	96	26
2	20	6	200	60	66	18	13	2	130	20	46	6

SenseVid gives separately an estimation of the required energy to capture and to encode each frame. Capturing energy depends mainly on the frame size [RBI⁺05]. The user provides the required energy to capture an 8×8 block and SenseVid computes the overall capturing energy. The compression energy is estimated depending on how a frame is encoded. The compression cost of an M-encoded frame is estimated based on the required power to M-encode one block P_{Mblock} given by :

$$P_{Mblock} = P_{DCT} + P_{quantization} + P_{entropy}$$

where P_{DCT} , $P_{quantization}$ and $P_{entropy}$ are amounts of power consumed by respectively DCT coefficients computation, quantization and entropy coding of one block. P_{DCT} can be computed using :

$$P_{DCT} = \sum_{op} N_{op} * P_{op}$$

where P_{op} is power consumption of operation op (addition, multiplication or shift) that is mainly function of the number of required cycles to execute op , the underlying processor power and clock rate. N_{op} is the required number of operations of type op to compute the DCT. This number depends on the selected DCT as well as its zone size (ρ) and is given by :

$$N_{op}^{\rho} = \begin{cases} (\rho + 8) \times n_{op}^{\rho} & \text{if square DCT} \\ \rho \times n_{op}^{\rho} + \sum_{i=1}^{\rho} n_{op,i} & \text{if triangular DCT} \end{cases}$$

where $n_{op,i}$ is the number of operation of type op required by the 1-D DCT of side length i . Table 4.4 summarizes the number of required operations for the implemented fast pruned LLM and BIN DCT. At this stage, it is worth noting that the cost of operation of type op is differentiated depending on integer (BIN DCT) or float (CLA and LLM) arithmetic. Per block quantitation is estimated as follows :

$$P_{quantization} = \begin{cases} 8^2 \times P_{div} & \text{classical DCT} \\ \rho^2 \times P_{div} & \text{square pruned DCT of side length } \rho \\ \rho \times (\rho - 1) \times P_{div} & \text{triangular pruned DCT of side length } \rho \end{cases}$$

where P_{div} is power consumption due to division operation. Finally, the entropy power is estimated depending on the chosen entropy coder. The default one is exponential-Golomb where the required power to encode a non null value can be given by :

$$P_{EG} = \begin{cases} 9 & \text{if CLZ instruction is available} \\ 3 \times \lfloor \log_2(value + 1) \rfloor + 7 & \text{otherwise} \end{cases}$$

where CLZ is the *Count Leading Zeros* instruction.

4.1.4 Numerical Results

In this section, is assessed, the effect of some parameters on the resulting compressed video sequence without considering its transmission. This is done using two QCIF video clips namely the *hall* and the *flowers* video sequences [yuv] composed respectively of 300 and 250 frames captured at 25 fps. The hall video can be qualified as a low movement sequence with a static background while the flowers video is a medium motion sequence with many small details.

Comparing the DCTs. The two video sequences are considered without any preprocessing. The quality coefficient (QF) is adjusted such that bit rates of 0.5, 1 and 2 bpp are obtained for the five implemented DCTs : the traditional one (CLA), the LLM and BIN using square and triangular patterns (sLLM, tLLM, sBIN and tBIN). The side length ρ is set to 8 and all frames are intra-coded. Figures 4.6a-4.6d depict the obtained video quality (reference SSIM/PSNR) for hall and flowers video clips. Both videos and for any chosen DCT, the lower the compression ratio, the higher is the video quality. Compared to hall, flowers video exhibits low quality for the same compression ratio. This is due to the fact that the former has a static background with a small moving ROI while the latter has many small details and hence a low spatial redundancy.

When comparing the three DCTs, we note that the BIN DCT produces slightly lower quality mainly for the lowest bit rate in the flowers video clip. This is widely offset by the corresponding energy footprint as shown in Figures 4.6e-4.6f. The BIN DCT exhibits the lowest energy expenditure since integer arithmetic requires less processor cycles. As expected, the CLA DCT consumes the largest amount of energy. The triangular pattern in both BIN and LLM results in lower energy cost (about 80% cost reduction) compared to the square pattern.

DCT Zone Size Influence. Here, the DCT zone size ρ is varied to assess its effect on the video quality as well as the corresponding consumed energy. As it presents good image quality while consuming much lower energy compared to CLA and LLM, only the BIN DCT is considered in what follows. Figure 4.7 brings the obtained results when encoding the hall clip as the DCT zone size (ρ) varies from 3 to 8. Plot 4.7a shows that the required energy to encode a frame increases with the DCT zone size as the encoding complexity increases with the number of DCT coefficients to compute. For the same reason, the triangular pattern reduces the amount of consumed energy compared to the square one. Figure 4.7b depicts the obtained SSIM and shows that beyond a given value of ρ the video quality does not improve mainly for the lowest bit rate. When increasing the triangle side size, all non null values are likely to be located at the left top sub-block. The square pattern does not add any significant DCT coefficient. Despite this, the square pattern consumes more energy.

Figure 4.8a plots the video quality as a function of the obtained bit rate for tBIN. For each zone size, the quality coefficient is varied to obtain different bit rates ranging from 0.3 to 2 bpp. The main observation is that, increasing the bit rate does not improve significantly the video quality mainly for small zone sizes. Figure 4.8b plots the SSIM as a function of the consumed energy. A higher energy corresponds to a lower compression ratio (higher bit rate). Note that extra energy can be consumed to obtain less compressed video without improving the video quality. Thus, depending on the chosen side size, the quality coefficient has to be appropriately chosen to obtain the maximum video quality as well as a good compression ratio while consuming less energy. The results show that the quality coefficient has to be set to lower values for lower ρ values and can be increased when $\rho = 8$.

S-frames - Impact of γ , θ and σ . Figure 4.9 depicts using boxes, the distribution of obtained SSIM, bit rate and encoding energy by the 300 frames of the hall video sequence when varying γ and θ . Only the highest priority data are encoded ($\sigma = 0$). As shown in Figure 4.9b, when all frames are intra-coded ($\gamma = 0$), a bit rate of 2.07 bpp is obtained. When γ is increased, the bit rate is reduced. When considering only the S-frames, the bit rate increases with *gamma* as shown in Figure 4.9a. This is due to the fact that a higher value of γ produces more S-frames which exacerbates their difference with the related M-frame. Note that

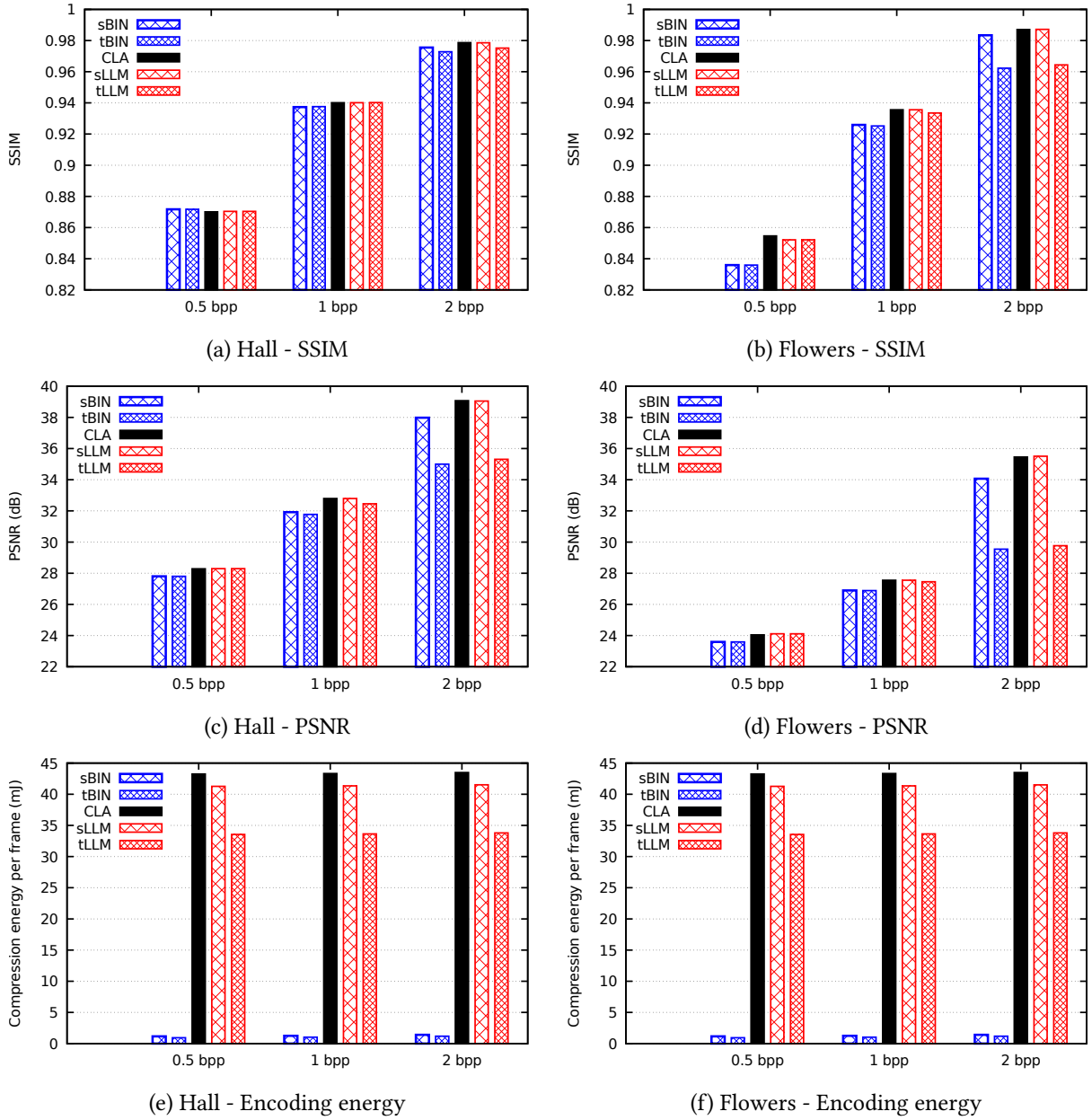


Figure 4.6: Comparing DCTs.

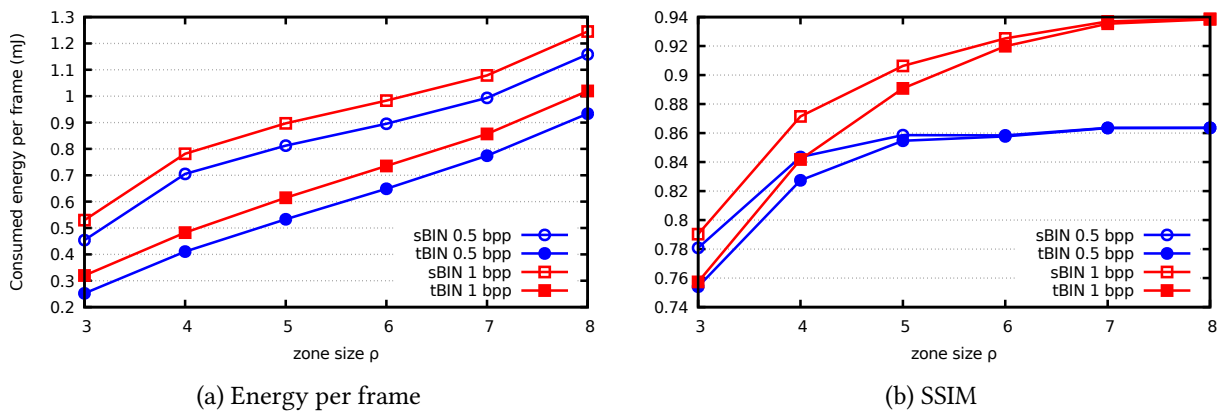


Figure 4.7: Varying the DCT zone size (ρ).

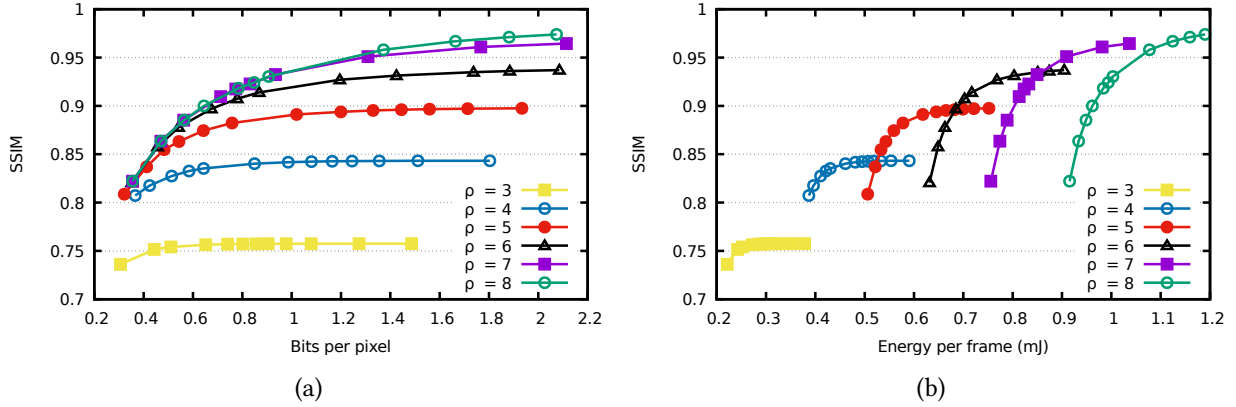


Figure 4.8: Rate distortion - Triangular BIN

some S-frames have null size and that their ratio increases when γ is set to lower values. S-frames are more likely to be very similar to the previous M-frame which increases the number of null values in the difference frame. The thresholding process further increases the number of null frames. Besides, an M-frame has a better quality compared to the following S-frames mainly when γ and θ are set to high values.

When $\gamma = 0$, all frames are intra-coded and requires in average 1.19 mJ to encode each frame as depicted in Figure 4.9f. Energy saving is possible if a subset of frames are inter-coded. Overall, increasing γ allows to reduce the per-frame encoding energy. Compression energy is halved when $\gamma = 18$ and $\theta = 1$. When only S-frames are considered, the mean energy increases since more (non null) values have to be encoded due to the increasing number of S-frames. Thresholding allows to further decrease the consumed energy to encode the S-frames since it generates zero values in the difference frame allowing the lossless encoder to achieve higher compression ratios.

Figure 4.10 plots the obtained results for S-frames when the σ parameter is varied. The highest the number of blocks we consider, the highest are the bit rate and the encoding energy. When all blocks ($\sigma = 4$) are encoded, the mean achieved SSIM is greater than 0.955 at the expense of a bit rate greater than 2 bpp and an encoding energy of approximately 0.9 mJ per frame. If only the highest priority blocks are considered ($\sigma = 0$), the mean achieved SSIM is greater than 0.94 resulting in a good quality video with less than 0.45 bpp average bit rate and about 0.5 mJ encoding energy.

4.1.5 Sample Experimentations

SenseVid traffic trace files can be used in any real testbed or simulated environment. As a first step, I provided Contiki [DGV04] application modules to be used in a real testbed, namely IoT-LAB [ABF⁺15] as well as in Cooja [RQADG16], a simulation environment. The purpose of this section is to give use examples of SenseVid rather than optimizing the transmission process.

IoT-LAB Experiment

IoT-LAB provides large scale WSN testbed with over 2000 wireless sensor nodes with different processor architectures and different wireless chips. The main benefit of SenseVid in a real testbed such as IoT-LAB is that it allows to perform real experiment without having a camera sensor. An application module that allows the transmission of packets based on a traffic trace file is developed. Based on the packet traffic trace, commands to send packets are injected into the sensor platform (sender node) using a python script (client.py) as shown in Figure 4.11. The receiver reports the sequence numbers of correctly received packets that can be retrieved using the netcat (nc) command to produce the receiver trace. This latter can be analyzed using SenseVid on the user's computer to rebuild the received video and compute metrics on the performed experiment.

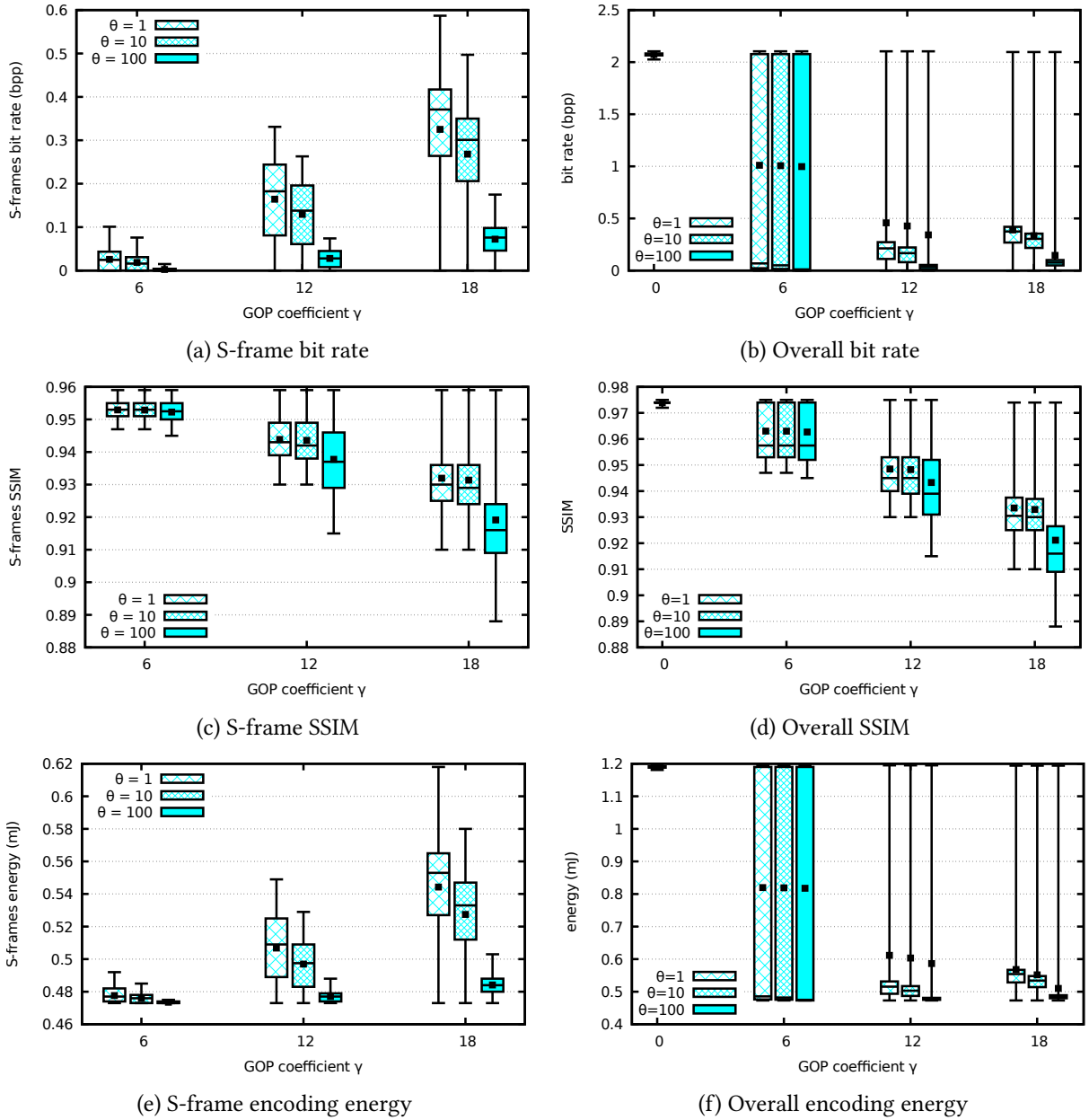


Figure 4.9: Inter-frame coding : impact of θ and γ

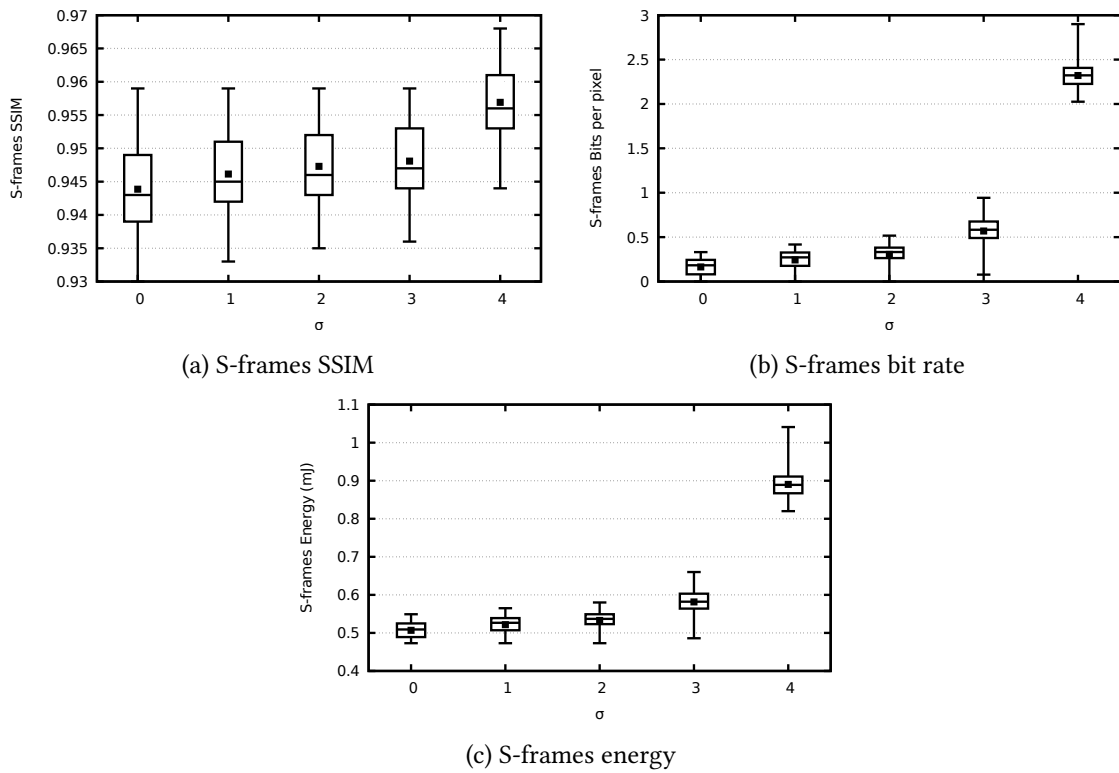


Figure 4.10: Inter-frame coding : impact of σ

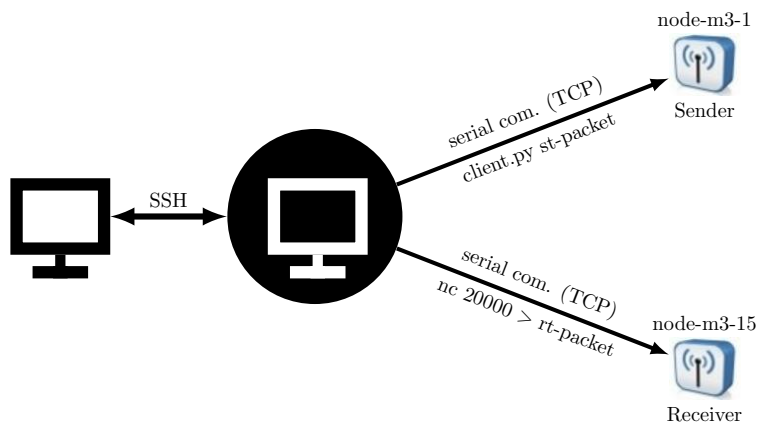


Figure 4.11: IoT-LAB sample configuration with SenseVid.

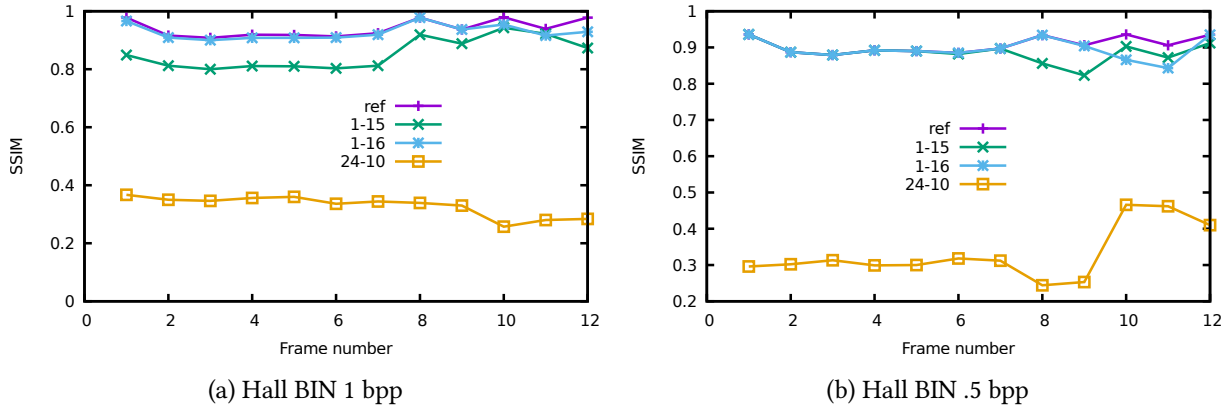


Figure 4.12: IoT-LAB experiment : Frames quality

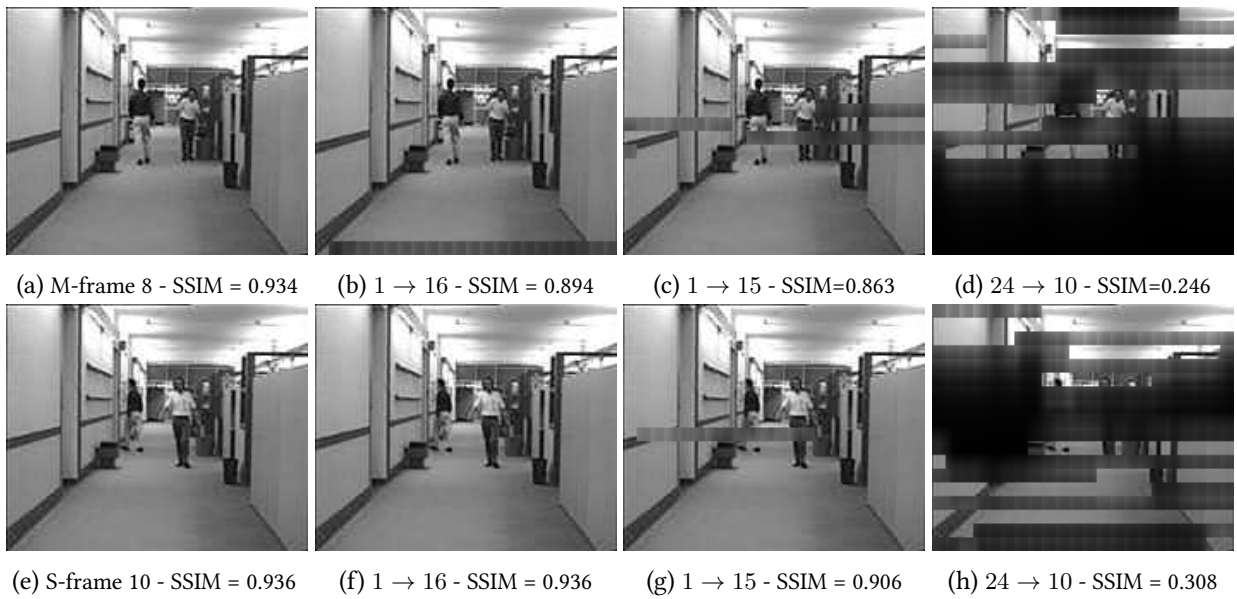


Figure 4.13: Sent (reference) and received frames in the three IoT-LAB experiments

My first experiments on top of IoT-LAB testbed made use of M3 open nodes (ARM Cortex M3, 32-bits MCU and 802.15.4 PHY standard) where the transmission of the hall video clip is emulated. Sender and receiver pairs are chosen among the nodes m3-1, m3-10, m3-15, m3-16 and m3-24 so different loss rates are obtained. Average success rates obtained for pairs (m3-1 → m3-16), (m3-1 → m3-15) and (m3-24 → m3-10) are respectively of about 98%, 91% and 33%. The hall video is considered with an FFC of 1 fps giving 12 captured frames. The GOP coefficient $\gamma = 22$ results in 4 M-frames and 8 S-frames with sequence "MSSSSSMSMSM" where the i^{th} character gives the type of the i^{th} frame. S-frames thresholding parameter is set to 10.

Figure 4.12 plots the achieved SSIM by the different frames as well as the reference SSIM. Connection m3-24 → m3-10 exhibits more losses than the other two connections resulting in the lowest video quality. Figure 4.13 shows frames 8 and 10 before their transmission (first column) then when received by nodes m3-15, m3-16 and m3-10 respectively. We can easily observe the good quality of received frames by node m3-16. Because of the high experienced loss ratio, node m3-10 receives bad quality frames.

Cooja Collect Application Scenario

In this experiment, the aim is to evaluate the effect of sending different priority levels of an M-frame using the RIME collect application. A simple linear topology with 4 Tmote Sky nodes [Mot] is used here data

Table 4.5: IoT-LAB Experiments Settings

Video characteristics	half QCIF (88×72) captured at 1 FPS (12 frames)
DCT	tBIN with side size $\rho = 8$
GOP coefficient	$\gamma = 15$ giving sequence "MMMMMSMMSMSS"
M-frames levels number	$\lambda = 0..6$
S-frame parameters	threshold $\theta = 20$, maximum level $\sigma = 4$

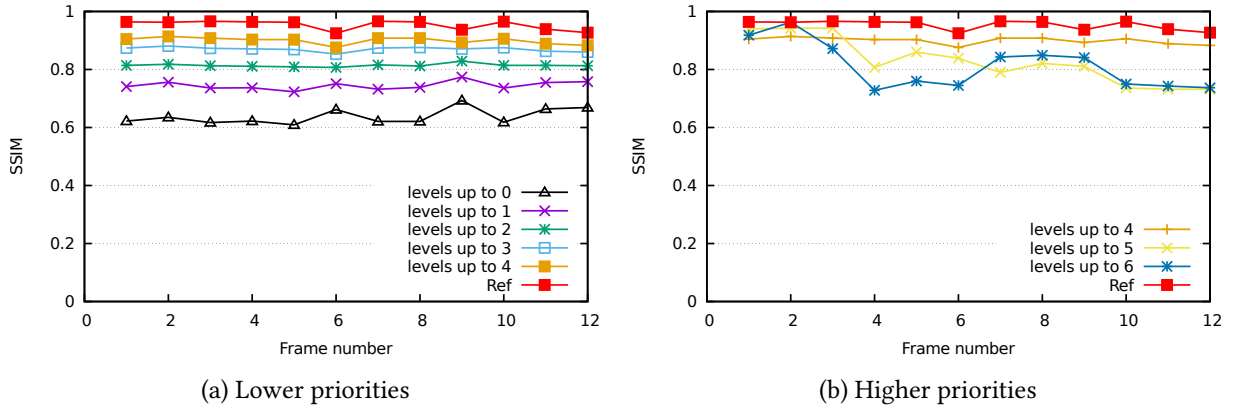


Figure 4.14: SSIM Hall - Cooja

packets have to cross two intermediate nodes from the source to the sink. This simulation parameters are summarized in Table 4.5. Figure 4.14 plots the achieved quality by the hall video frames when a some levels of an M-frame are transmitted. Figure 4.14a shows that when increasing the maximum priority level to transmit, the quality of each frame is improved. However when it is set to 5 and 6, the quality deteriorates as shown in Figure 4.14b because the transmission rate is risen to maintain real time transmission. When sending up to level 4, there is no loss. The sink experiences 16% and 23% of losses when sending up to level 5 and 6 respectively. This means that the amount of data to transmit can be adapted to network dynamics through priority levels tuning. This results are well illustrated in Figure 4.15 that shows frame 5 (M-encoded) as it would be rebuilt by the sink with their respective quality.

4.2 Video Multipath Routing for 6LoWPAN

Despite the fact that RPL (§ 1.4) almost meets the requirements of LLNs to handle scalar data routing, it still far from being able to allow real time streaming of video flows. Visual sensors with limited resources have to deal with large amount of data to capture, encode and transmit. These tasks result in significant power consumption while sensor nodes are equipped with limited batteries capacity. Authors of [ASM15] considered video traffic routing using RPL and proposed a new objective function called *Green-RPL* in an attempt to minimize energy consumption while assuring a required quality of service. Simulation results show that *Green-RPL* outperforms *ETX* and *OF0* in terms of consumed energy, number of delivered packets and delay. However, the performance evaluation does not consider a real video traffic and as a result the user quality of experience is not evaluated either. The work in [MK18] defined another objective function based on the remaining energy. Results show that energy consumption is better distributed among nodes. However, simulations are made using H. 264 (not suited to WSN) multimedia trace [SRK04] where additionally the user QoE is not considered.

Network lifetime can be maximized by minimizing the radio activity characterized by its high power consumption in the transmit, receive as well as idle listening periods. In order to save energy, radio duty cycling (RDC) protocols are suggested to switch off the radio as much as possible. With respect to visual data, compression is also required before transmission to limit the amount of data to route and hence limit

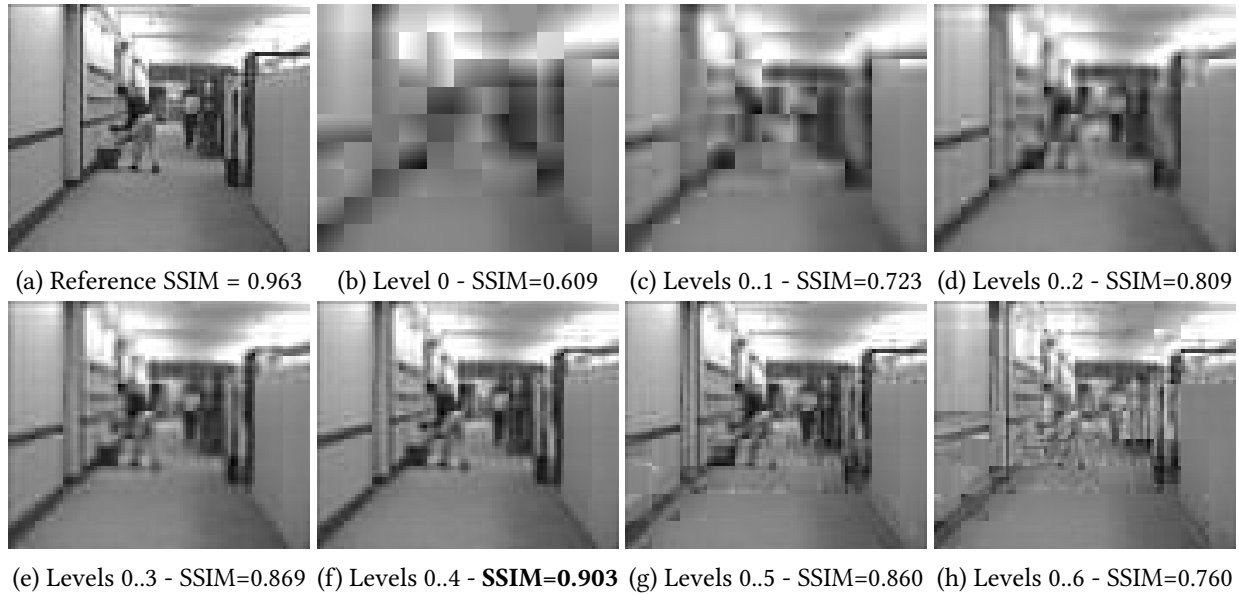


Figure 4.15: Cooja frame 5 : M encoded

power consumption. In the context of Kettouche’s thesis [Ket22], the feasibility of real video streaming using RPL is investigated as will be reported on in Section 4.2.1. The improvement provided by our disjoint multipath routing protocol, DM-RPL (§ 1.4), is assessed in Section 4.2.2. In the following experiments, modified Contiki RPL-UDP server and client applications are used.

4.2.1 RPL Video Transmission

In this work, we mainly addressed radio duty cycling impact on the transmission of low complexity compressed images. We chose ContikiMAC [Dun11] as the radio duty cycling protocol. Duty cycling can be tuned using *Channel Check Rate* (CCR) parameter defined as the frequency a node will listen to the medium to eventually receive data from its neighbors. When some activity is detected the node stays awake to receive data ; otherwise the node goes back to sleep mode for another duty cycling period. We considered a square sensor field of size $90 \times 90 m^2$ where 16 static nodes (Tmote Sky) are deployed in a grid topology. The sink is located at the upper left corner and the video source is located the lower right corner. Transmission range is set to 50 meters resulting in 8 as a maximum node degree (neighbors) and 3 as the minimum number of hops from source to the sink. The sender transmits data packets that result from the encoding of gray scale captured images from the *hall monitor* video clip [yuv] down-sampled to half QCIF resolution. All frames are intra-coded (M-frames) $\gamma = 0$. Instead of 25 frames per second, the frame frequency capture (FFC) is set to values ranging from 10 to 60 frames per minute. Performance evaluation metrics are averaged over at least 10 simulations. Main experiments parameters are summarized in Table 4.6.

Impact of Duty Cycling. Figure 4.16a plots the obtained ratio of successfully delivered packets to the sink when increasing the FFC for different duty cycling settings. We can see that the higher the CCR, the higher the packets delivery ratio. This ratio decreases when increasing the number of captured frames. Figure 4.16b shows the average PSNR and SSIM of received images. With the highest CCR, we are only able to obtain a fair image quality (with a PSNR of at least 20 dB) for a maximum rate of 35 frames per minute. Lower CCR values exhibit very poor image quality.

Figure 4.17a plots the overall depleted power as the number of sent frames per minute is increased. The case $CCR = 128$ where more than 21 mW of overall power is measured, is omitted for clarity. Figure 4.17b plots the depleted power due to radio transmission activities. The main observation is that power consumption does not depend on the transmission rate (FFC). Figure 4.17a shows that the more the CCR, the more

Table 4.6: Simulation Parameters - RPL Video Transmission

Routing protocol	RPL (IPv6)
RPL DiO min/max interval	4 s / 17.5 min
RPL objective function	ETX
MAC	CSMA
Radio Duty Cycling	ContikiMAC, NullRDC
Channel check rates (Hz)	8, 16, 32, 64, 128
Physical	IEEE 802.15.4
Radio active power	75.6 mW
Radio idle power	4.32 mW
Radio listening power	82.8 mW
Video duration	12 seconds
Frame resolution	88x72
FFC (frames/mn)	10, 15 ... 55, 60
Quality Factor	8

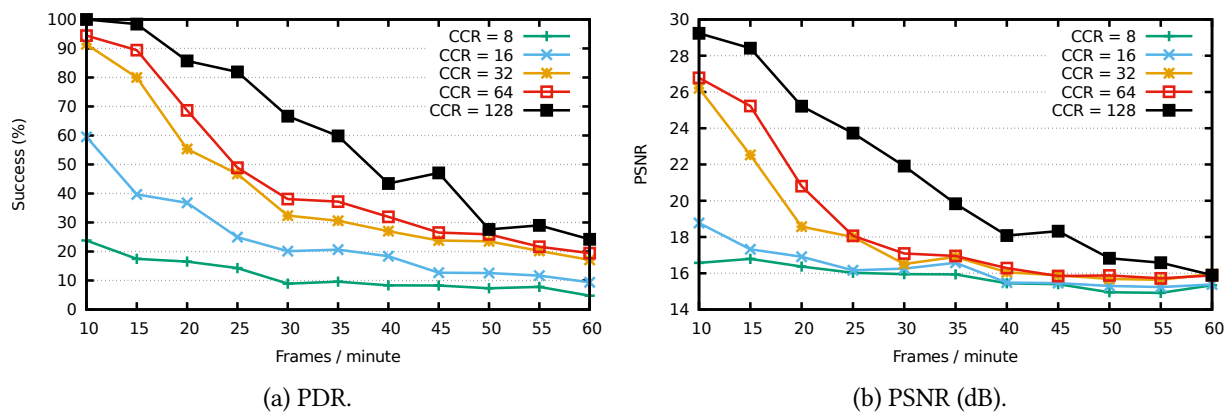


Figure 4.16: Quality of received images.

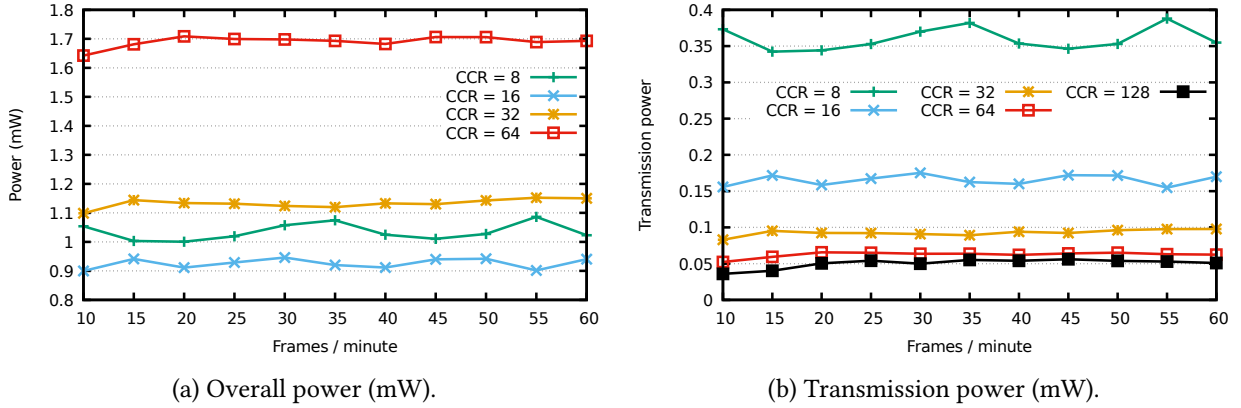


Figure 4.17: Power consumption.

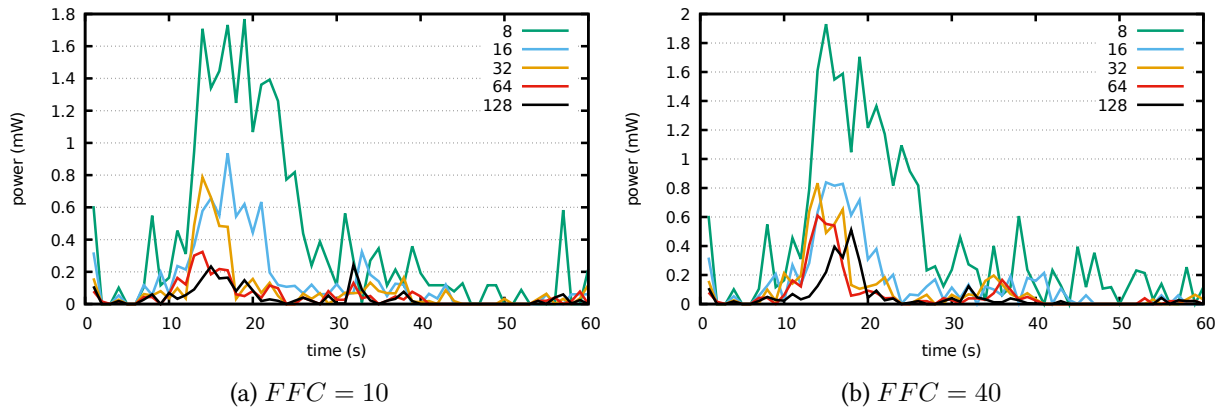


Figure 4.18: Transmission power

consumed energy except for $CCR = 8$. In fact, a CCR set to 16 triggers less energy consumption compared to a CCR of 8. This is due to the fact that in the later case, the number of retransmissions is higher as confirmed in Figure 4.17b. The highest depleted transmission power corresponds to $CCR = 8$ which attests the highest experienced transmission attempts.

Figure 4.18 plots the depleted power due to radio transmission activities as time evolves for an FFC of 10 and 40 frames per minute. Recall that the video lasts 12 seconds and the frames are captured as required by the FFC parameter within this duration. Frames transmission is started approximately around 8 seconds. We observe that the higher the CCR, the lower the interval where power consumption is maximized and the lower the consumed power. For the lowest CCR, transmissions last longer and power consumption achieves much higher values.

4.2.2 DM-RPL Video Transmission

To get insight into the performances of our disjoint multipath extension, we begin by assessing the performance of DM-RPL with respect to standard RPL. Then, real time video frames transmission is considered in real testbed experiments.

DM-RPL versus RPL

In this section, Cooja simulations are performed with the aim of comparing DM-RPL using two paths with default RPL. The sent traffic corresponds to 25 gray-scale images (2 fps) extracted from the 300 frames that composes the *hall monitor* video clip [yuv]. To further fit the LLN limited capacity, images are down-

Table 4.7: Simulation Parameters - DM-RPL versus RPL

Routing protocol	RPL, DM-RPL (IPv6)
Number of sensors	25
Area	120 m × 120 m
Transmission/interference range	45m / 50m
Radio Duty Cycling	ContikiMAC
Channel check rate	128 Hz
Frame resolution	128x128
Frames per second	2
Quality Factor	20

sampled to 128×128 resolution. In these simulations, all the captured images are encoded independently of each other (M-encoded). Two main scenarios are considered. First, all the packets get the same priority and are sent without differentiation. In the second scenario, two levels of priority are used and packets with higher priority are sent twice by the source, each on one path in the case of DM-RPL. Table 4.7 summarizes the main new simulation parameters.

Figure 4.19 presents the results obtained in RPL (1-path) and DM-RPL (2-path) for one (*l1*) and two (*l2*) priority levels when the transmission rate is varied from 1 to 5 packets per second (pps). Only the mean values of the different metrics are plotted, their distribution and more details can be found in [KMD22]. Figure 4.19a show respectively the distribution and mean PDR obtained. While the mean PDR decreases for all scenarios. With two priority levels, we obtain better performances in both RPL and DM-RPL. This is due to the replication of a subset of the data packets which results in an improved reliability. Besides, using two paths allows obtaining higher PDR with or without replication. DM-RPL allows getting more bandwidth thanks to data splitting on two disjoint paths. We observe that the priority-based scenario coupled with multipath routing obtains the highest PDR with values more concentrated around the median.

Figure 4.19c depicts the quality of the received images. When the transmission rate is very low, the obtained quality is close to that of the transmitted (reference) frames mainly for DM-RPL. Note that the reference PSNR and SSIM are respectively 34.0920 dB and 0.9629. When the transmission rate is increased the quality deteriorates due to the experienced losses. We observe, however that the quality is improved when higher priority packets are replicated (*l2*) regardless of the number of used paths. This is more noticeable when two paths are used. Paths diversity reduces losses and important visual data success transmission is likely to be maximized with replication of higher priority packets.

Figure 4.20 shows visual samples of frame 22 with the corresponding PSNR and SSIM when transmitted at 4 pps. The rightmost one is the reference frame transmitted by the source. The other images are those received by the Sink when using the different transmission scenarios. We observe that the image that corresponds to the first scenario (one path and one priority level) is useless. When using two paths along with replication of higher priority packets, we are able to distinguish the man walking in the corridor.

To get some insight on the impact of our transmission strategies on energy, we represent the mean values of the consumed power by the radio for transmission. Figure 4.19d shows that transmitting at a higher rate consumes more energy especially when only one path is used. More interesting, for higher data rates, a significant increase in power consumption when replication is used with RPL while it remains mostly the same with DM-RPL. Our multipath protocol allows obtaining the lowest energy expenditure especially for high data rates. This is mainly due to the absence of retransmissions due to an improved reliability as shown by PDR curves.

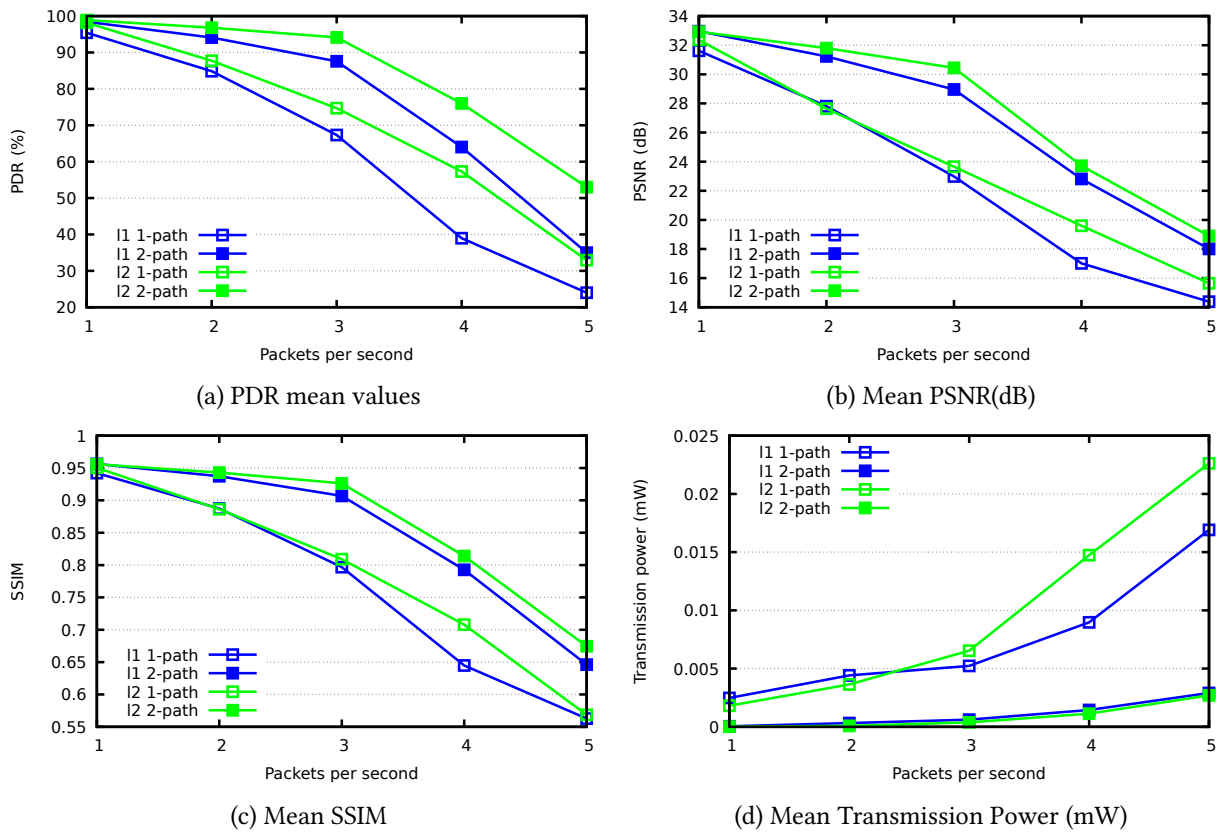


Figure 4.19: Simulation results : DM-RPL vs. RPL

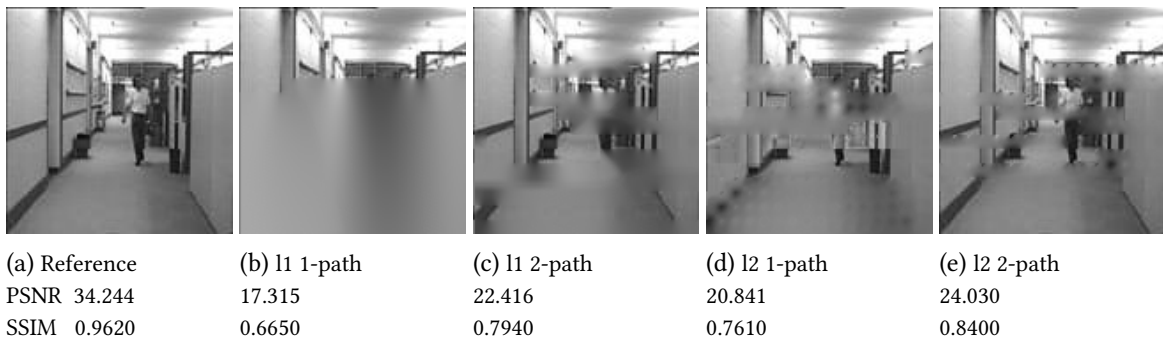


Figure 4.20: Sample images for frame 22 when transmitted at 4 packets per second.

Table 4.8: Transmitted video characteristics (IoT-LAB)

Images number	ref. PSNR (dB)		ref. SSIM		compression (bpp)		bit rate (Kbps)		packets to send		Frames sequence when $g = 15$
	$g = 0$	$g = 15$	$g = 0$	$g = 15$	$g = 0$	$g = 15$	$g = 0$	$g = 15$	$g = 0$	$g = 15$	
9	29.50	28.52	0.9081	0.8980	0.66	0.57	7.8	6.73	99	90	MMMMSMSMS
12	29.50	28.81	0.9010	0.8997	0.66	0.57	10.40	8.98	132	116	MMMMMSMMSMSM
15	29.50	28.05	0.9077	0.8959	0.66	0.52	13.01	10.32	165	140	MSMMMMSMSMSMSSM
18	29.51	28.31	0.9078	0.8960	0.66	0.51	15.6	11.94	198	162	MSMMMMSMSMSMSSMM

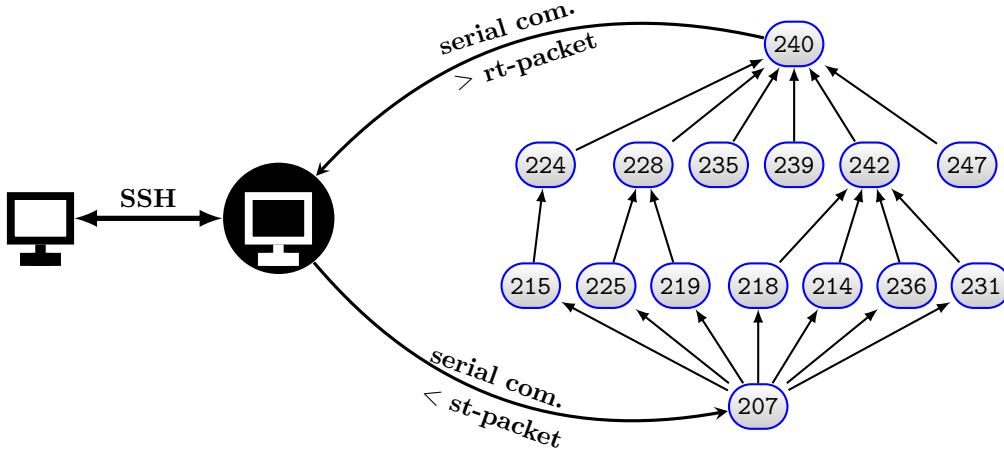


Figure 4.21: IoT-lab Experiment Setup and Interface with SenseVid.

DM-RPL Experimental Results

Here, the focus is on the impact of increasing images frequency capture on real time transmission. To do so and coping with the limitations of the used sensors, only 9 to 18 gray-scale images of the hall monitor video are transmitted and the quality factor is lowered to 5. To further reduce the data transmission rate as shown in Table 4.8, some S-frames are included by setting the GOP coefficient g to 15. σ is set to zero so only their highest priority level data are encoded and transmitted. The threshold similarity θ is set to 1. All the resulting packets are assigned the same priority. 15 M3 open nodes⁷ of IoT-LAB [ABF⁺15] are used. Figure 4.21 shows how transmission instructions based on a sender trace file are given to the source (node 207) that sends in a real time the captured images to the root (node 240). A possible tree structure is also shown where the links are those connecting each node to its preferred parent.

Figure 4.22a shows the mean PDR obtained when RPL and DM-RPL are used to send the two sequences of frames (g_0 and g_{15}). It can be observed that the PDR decreases when the number of images to transmit is increased. This was expected since the data rate transmission is increased. DM-RPL outperforms RPL in terms of PDR whatever the transmission rate. Reducing the transmission rate by inter-coding some frames ($g = 15$) allows achieving higher PDR with respect to the case where all frames are intra-coded ($g = 0$). Figure 4.22b depicts the mean consumed power for the different schemes as the number of captured frames is varied. Compared to RPL, DM-RPL consumes lower amount of energy. This is the consequence of traffic load balancing when using DM-RPL. Lower packet losses are experienced and thus reducing the amount of MAC level retransmissions. This translates in lower energy consumption.

Figure 4.22d shows mean obtained PSNR and SSIM of the received images. Data reduction due to the introduction of S-frames brings lower image quality as shown. The quality is lowered when increasing the transmission rate. The images quality is still fair ($PSNR > 20$) for all schemes when the number of frames does not exceed 12. Using two paths with more data reduction (2-path, g_{15}) allows an acceptable quality even for the highest transmission rate. Note that thanks to data reduction, received images quality

⁷<https://www.iot-lab.info/docs/boards/iot-lab-m3/>

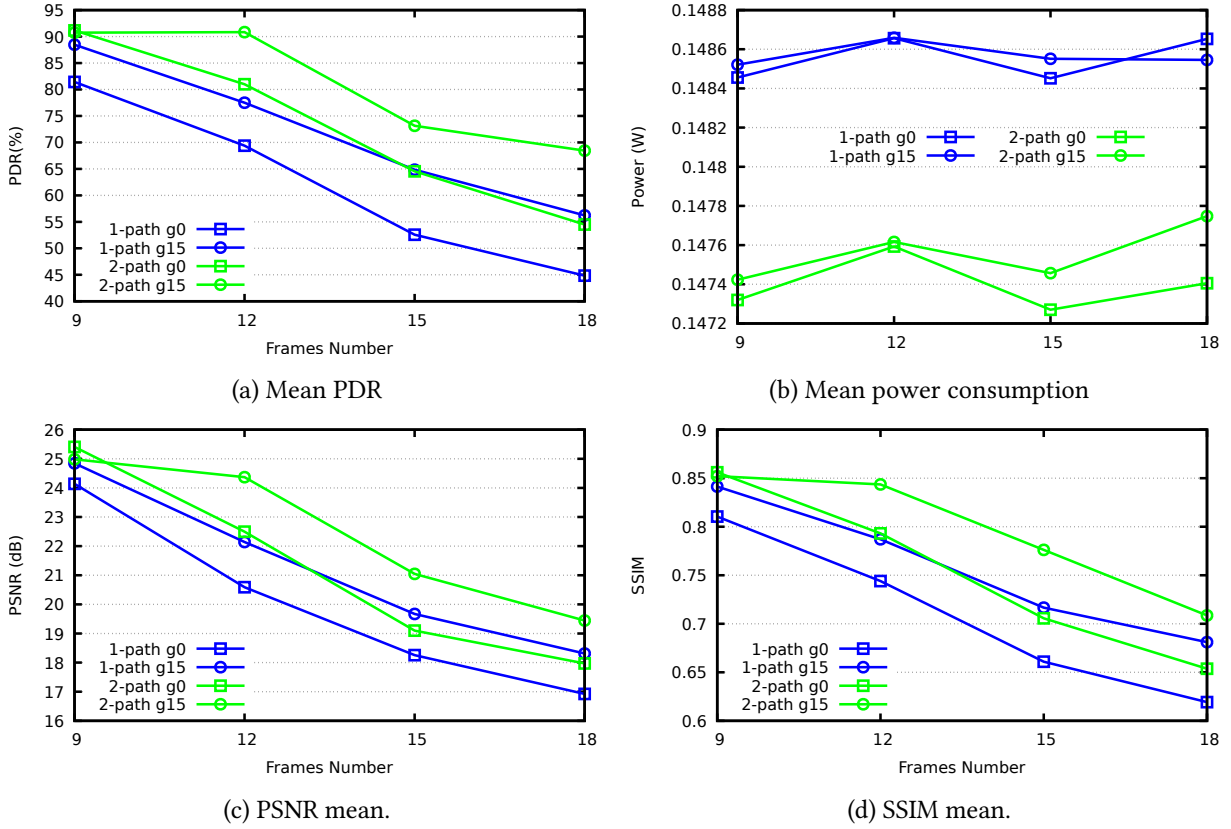


Figure 4.22: IoT-LAB experimental results : DM-RPL vs. RPL

is better when $g = 15$ compared to $g = 0$ even if the corresponding reference values are higher in the latter case. Figure 4.23 shows the third transmitted frame when 12 images are captured and transmitted with samples of the same frame as received by the Sink for the different evaluated schemes. Observing the pictures confirms that data reduction strategy is profitable mainly when two paths are used where both PSNR and SSIM are improved.

4.3 DL-based Image Restoration

In-network data reduction allows to lower the transmissions at the source and, therefore, the energy required to deliver the visual data to its final destination. In Section 4.2.2, captured frames are compressed using a low complexity video encoding, then the video flow is transmitted on two paths along with a priority-based scheme. However, the achieved quality of experience is still perfectible. From the one hand,

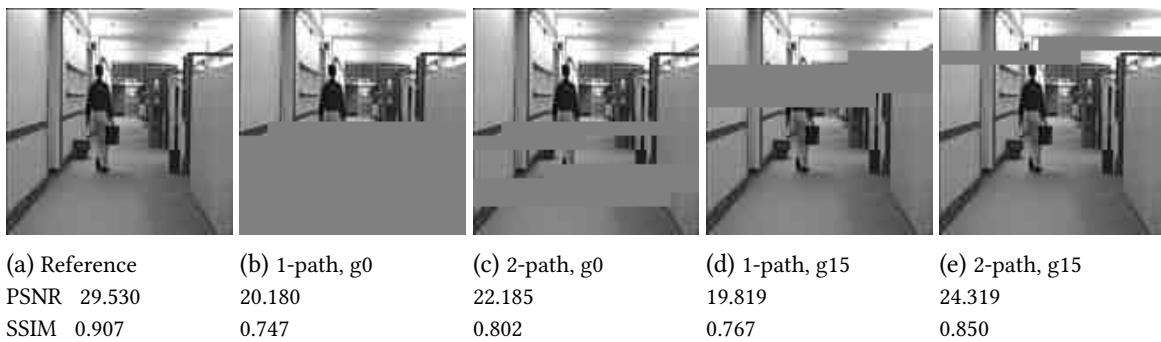


Figure 4.23: Sample images for frame 3 when 12 frames are captured.

the adopted low-cost compression may induce a noticeable distortion due to the high target compression ratio. On the other hand, data packets may experience significant losses causing damaging holes to appear. The closest work to ours is [NSC21] where a DL super-resolution model is leveraged to restore high quality images from degraded images with a high compression ratio. They considered only losses induced by lossy compression while network transmission related losses were not dealt with. The latter are more problematic when considering their exploitation at the end user [BAB20]. In this work the encoding/transmission chain is augmented by a DL-based restoring at the sink that deals with both types of losses in the context of LLNs. The obtained results show the effectiveness of adopting the DL-based restoration especially when adopting the proposed scattered packetization scheme [MSR⁺22].

4.3.1 Image Reconstruction at the Sink

To compensate for the distortion caused by the adopted lossy compression as well as to fill in the holes induced by packet losses, one may rely on the computational power of the Sink for an optimal reconstruction of the received images. A DL-based inpainting model is used to fill in the holes and a CAR⁸ DL model is used to recover losses induced by the compression process. Figure 4.26 illustrates the whole encoding-transmission-reconstruction chain.

DL-based Inpainting

LLNs suffer from high loss rates especially with increased transmission data rates. As a result, received frames are likely to experience a substantial deterioration even with compressed visual data (§ 4.2). When the Sink reconstructs the images based on the received packets, bands of damaged pixels appear. In order to fill in the lost blocks in an image, a DL inpainting technique [LJXY19] that mimics the human behavior is used. Missing parts of an image are repaired while maintaining its consistency based on an overall observation of its structure. In particular, a new coherent semantic attention (CSA) layer is introduced to preserve contextual structure to achieve more effective predictions of missing parts by modeling the semantic relevance between the holes features.

As shown in Figure 4.24, the model is composed of two steps, namely, rough inpainting and refinement inpainting. The first step takes as an input I_{in} , a 256×256 image with holes derived from the ground truth image I_{gt} , and produce the rough prediction I_p . The used rough network consists in the generative network proposed in [IZZE17], composed of 4×4 convolutions with skip connections to match the features from each layer of the encoder and its corresponding layer of the decoder. The second step, the refinement inpainting, takes as an input, the pair (I_p, I_{in}) to output I_r , the final image. The refinement network is composed of an encoder and a decoder with skip connections similarly to the rough part. Each layer of the encoder is made of a 3×3 convolution and a 4×4 dilated convolution except at the fourth layer of the encoder, there is a CSA layer instead of a 4×4 dilated convolution. Finally, the decoder structure is symmetrically similar to the encoder without a CSA layer.

Compression Artifact Reduction (CAR)

As we rely on a lossy compression at the source, the obtained images may suffer from a noticeable distortion especially when targeting higher packet delivery ratios through a higher compression ratio to reduce the amount of data to transmit. In an attempt to recover the lost information due to our lossy compression, we considered the SwinIR model [LCS⁺21]. It is based on the Swin Transformer and comprises three modules (Figure 4.25), namely, shallow feature extraction, deep feature extraction and high-quality image reconstruction. Particularly, the deep feature extraction module is made of multiple residual Swin Transformer blocks (RSTB), each with several Swin Transformer layers together with a residual connection.

⁸Compression Artifact Reduction

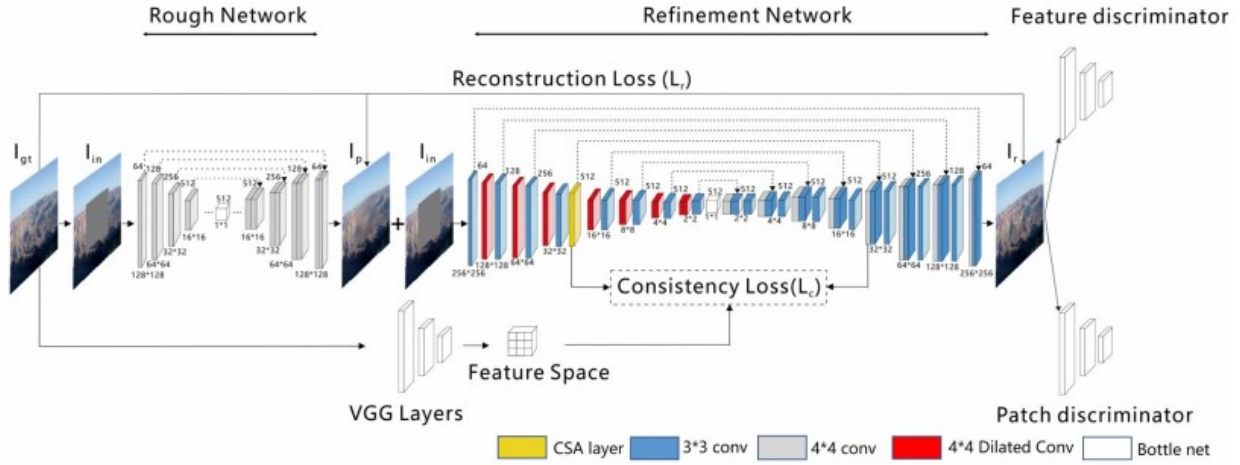


Figure 4.24: The inpainting model (redrawn from [LJXY19])

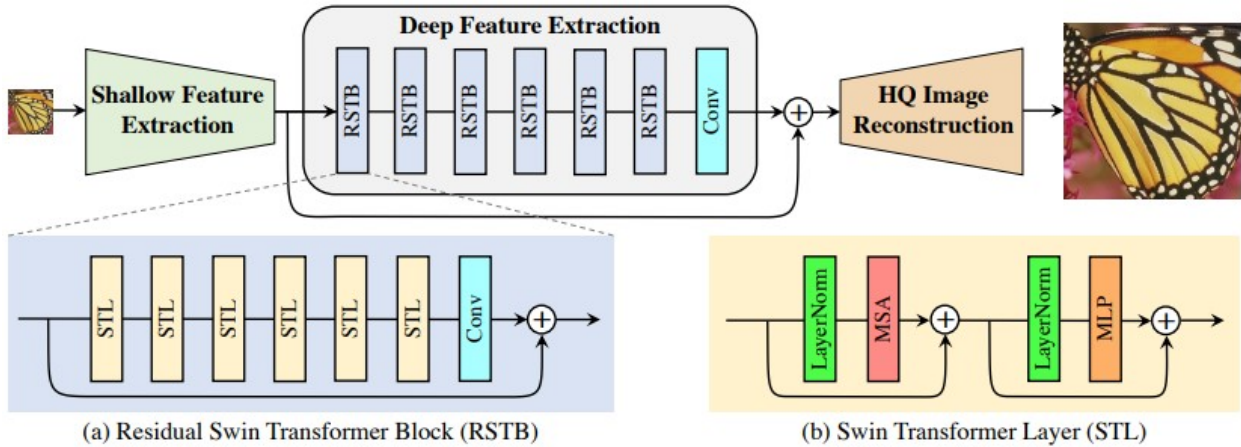


Figure 4.25: SwinIR architecture for image restoration (redrawn from [LCS⁺21])

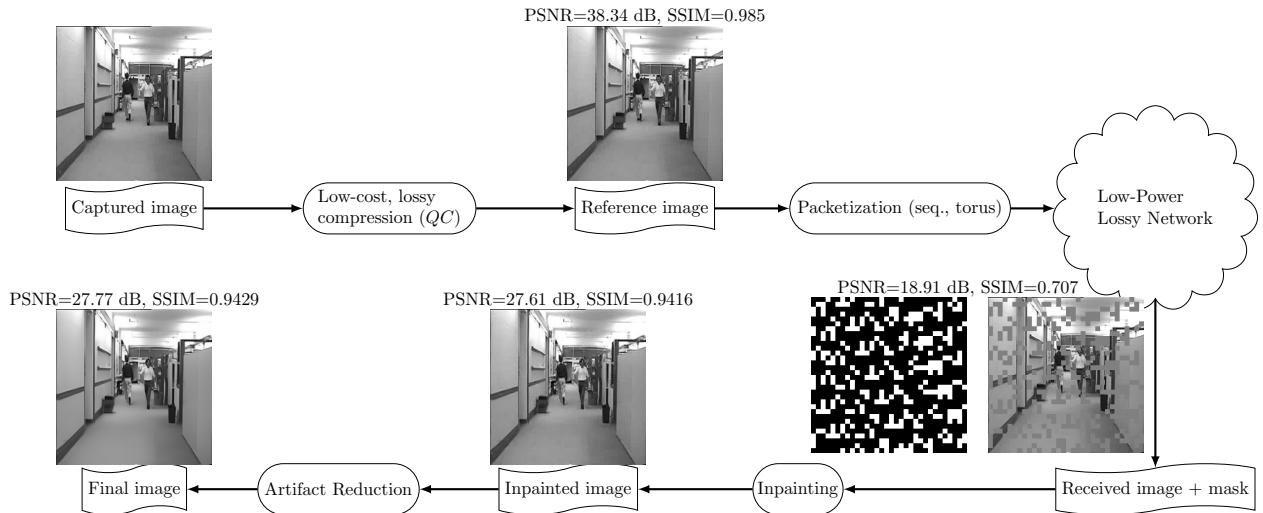


Figure 4.26: Encoding, transmission and reconstruction chain

4.3.2 Results

To carry out the performance evaluation of the proposed chain and its adaptability to LLNs, we made use of SenseVid to generate compressed images using a low-cost compression algorithm. Besides, SenseVid integrates a traditional inpainting solution that consists in a simple and fast algorithm of Telea [Tel04] based on the fast marching method for level set applications. We considered both sequential and scattered packetization.

We used the official PyTorch implementation of the CSA-inpainting model⁹ and the SwinIR model¹⁰ for compression artifact reduction. To train them, we made use of images from *Places* data base [ZLK⁺17] that provides images with losses ranging from 15% to 50%. In order to be more adapted to our gray-scale low-cost lossy compression patterns, we also made use of images generated by the SenseVid tool. To test the trained models, we mainly considered three CIF video clips with different characteristics, namely the hall, flower and coastguard video sequences from [yuv]. The frames are down-sampled to 256×256 and adequate quality coefficients have been applied to obtain compressed images of 0.5 bpp. Transmission losses have been varied from 0 to 30%.

Our tests showed that applying the CAR after the inpainting allows obtaining the best results. Figure 4.26 shows the overall chain applied on a frame from the hall video clip. The transmitted (reference frame) obtains an excellent MOS rating with a $PSNR = 38.34$ dB and an $SSIM = 0.985$. When received by the Sink with 30% of the transmitted packets being lost, the quality is degraded down to a bad quality ($PSNR < 20$). After applying the inpainting, the image is enhanced with a score rising to 3 corresponding to a fair quality. The CAR allows for an additional improvement as can be seen.

Figure 4.27 shows the obtained quality (both PSNR and SSIM metrics) as a function of the experienced packets loss for the three considered video clips. In each plot, are shown, the mean reference quality "Ref" of the transmitted image, mean quality of the received images "Rx", the obtained quality when the Telea inpainting is applied for both sequential "seq." and scattered "TA" packetization and finally when using DL models for restoring the received images. It is worth noting that the reference quality is constant as it concerns the transmitted images and does not depend on the experienced losses and recall that these quality metrics are computed with respect to the raw captured images before compression. Note also that the obtained PSNR is almost the same when losing the same number of packets regardless of the used packetization technique. This is due to the fact that the PSNR is directly related to the number of lost blocks

⁹github.com/KumapowerLIU/CSA-inpainting

¹⁰github.com/JingyunLiang/SwinIR

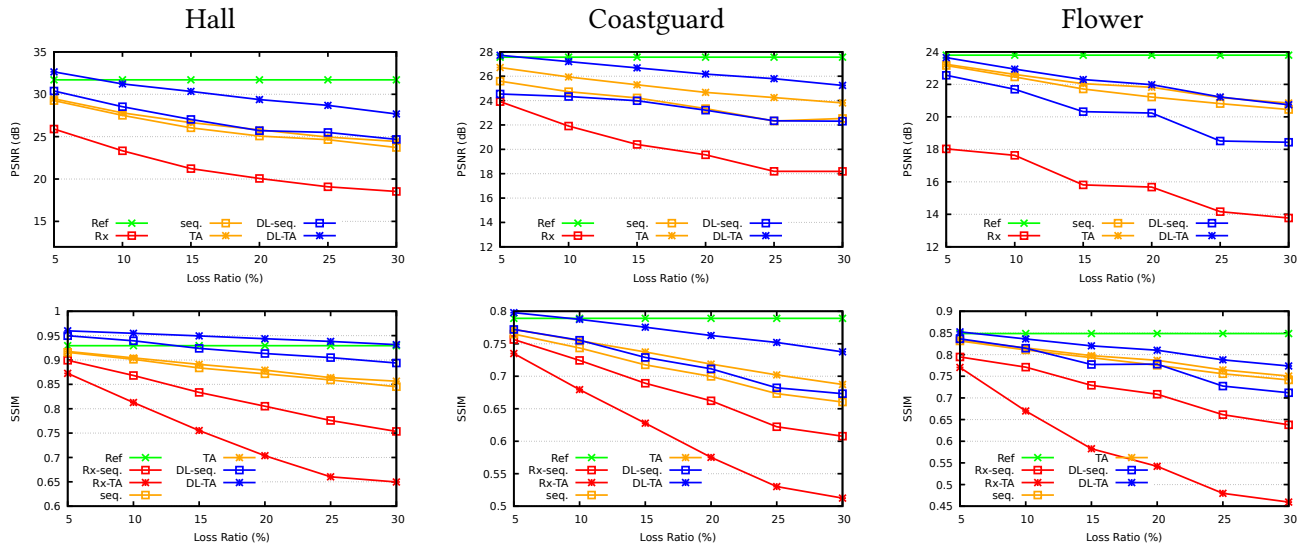


Figure 4.27: Achieved video quality when varying the loss rate.

whatever their distribution. However, separate curves of the received quality are presented for the SSIM that presents different values depending on the blocks distribution. It is known that for the same distortion (PSNR value), the perceived quality can drastically be different [WBSS04]. Figure 4.28 shows a sample frame from the coastguard video clip when transmitted using a sequential versus scattered packetization scheme. We can observe that the received image in the latter (Figure 4.28e) has a slightly higher PSNR but obtains a much lower SSIM value than the former (Figure 4.28b) which confirms the statement made above.

As shown in Figure 4.27, the obtained reference quality is different depending on the video clip considered. We can see that we obtain for the same compression ratio, according to the MOS rating, a good quality (PSNR=31.7 dB) for hall, a fair quality (PSNR=27.57 dB) for coastguard and a poor quality (PSNR=23.8 dB) for flower that exhibits more details and motion than the two other clips. The received frames undergo a degradation in quality that is proportional to the rate of lost data packets during the transmission process. For instance, The hall video clip quality deteriorates to become "fair", "poor" and "bad" from respectively 5%, 10% and 25% of losses. The flower clip suffers from bad quality received video from only 5% experienced losses. Regardless of the employed image restoration method, scattered packetization allows to obtain the best quality. This can be confirmed when comparing the frame in Figure 4.28c (respectively 4.28d) to the one in Figure 4.28f (respectively 4.28g).

The reconstruction process either using the Telea or the DL-based method enhances the quality of the received images in all the considered cases. The amount of improvement varies depending on the characteristics of the video clip being considered. The Hall video clip, characterized by a low motion and less detail, achieves the highest quality improvement mainly when using a scattered packetization along with a DL-based reconstruction. More interestingly, the achieved SSIM is even higher than the reference one. This proves that the DL approach can recover not only the losses due to packet dropping, but also the quality degradation due to lossy compression.

When a scattered packetization is used, applying the DL-based restoration technique allows the highest quality for the three clips whatever the loss rate despite the fact that in terms of SSIM, the quality of the input images is lower especially in flower clip. We note that when sequential packetization is adopted, the traditional Telea method achieves almost the same performances for coastguard and higher results for flower clip. In terms of SSIM, the DL-based restoring achieves better performances. This is due to the fact that the adopted DL models are targeted to improve the SSIM rather than the PSNR.

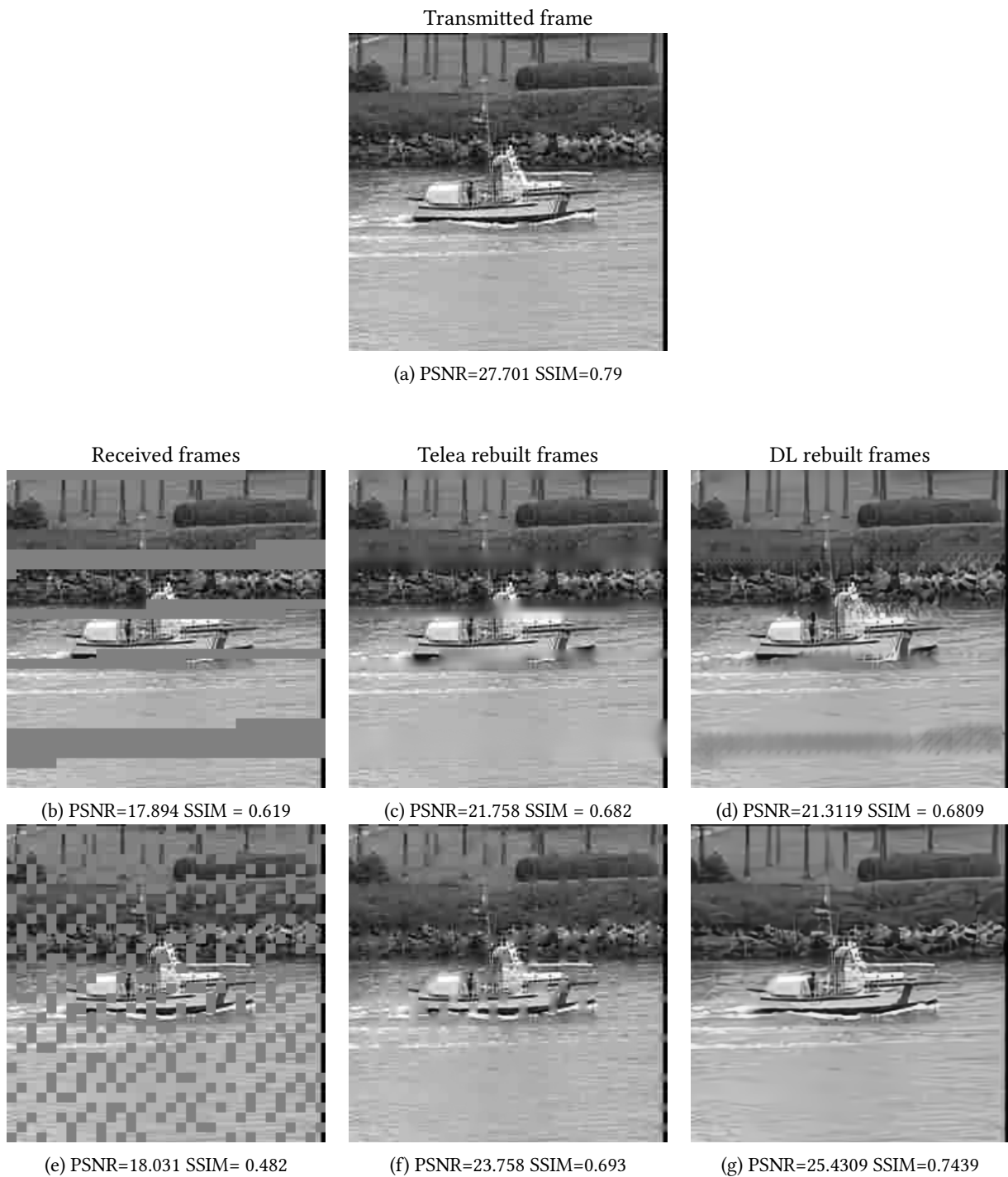


Figure 4.28: A sample frame (coastguard) with 30% lost packets. Sequential (top) and scattered (bottom) packetization.

4.4 Conclusion

Multimedia applications are becoming more and more ubiquitous in our daily life. Their integration into low-power and lossy networks remains a challenging issue. Aiming to achieve a satisfactory quality of service along with a descent quality of experience within the constraints of limited resources, a complete efficient encoding-transmission-reconstruction chain is proposed and evaluated. At the source side, a low complexity image compression method is employed along with an appropriate packetization scheme. At the destination, where more powerful resources are available, deep learning models are leveraged to compensate for the distortion caused by the adopted lossy compression as well as to fill in the gaps induced by packet losses. At the network level, different transmission strategies have been experimented. In particular, a priority-based multipath transmission strategy that shows promising results.

To assess the proposed chain along with the transmission strategies, experiments were carried out on a simulated environment (Cooja) as well as a real testbed (IoT-LAB) using SenseVid. This latter, a traffic trace based transmission and evaluation tool, is developed to address the lack of performance evaluation tools that provide both QoS and QoE assessment metrics and suit the constrained nature of WSN.

Chapter 5

Region of Interest Reduction Strategies for Constrained Networks

Low cost image compression (§ 4.1) and path diversity along with traffic prioritization (§ 4.2) contribute to improving the quality of the received images in constrained networks. While compressing captured images reduce the amount of the data to be transmitted, it is still substantial for networks with limited bandwidth. To address this, further reduction at the source is necessary. One alternative to sending the whole image is to determine and transmit only its *Regions of Interest* (ROI). By focusing on these areas, data processing can be limited to only the most relevant parts of the scene, thereby reducing the computational burden and improving processing efficiency. Besides, ROIs significantly reduce the amount of data that needs to be transmitted while preserving the essential information. However, achieving the right trade-off between data reduction and preserving image quality remains a challenge, and ongoing research [KMM15a, KNM18a, WQB⁺22] aims to further improve this area.

Feature extraction is a commonly used technique for detecting ROI that involves identifying and extracting distinctive features from an image, such as edges, corners, and texture patterns [HAM21]. These features can then be used to distinguish the ROI from the surrounding area. Feature extraction methods often come with a high computational cost, making them impractical for deployment on constrained visual sensor nodes. In [AKMH22], we proposed a low-cost ROI detection technique based on the Sobel edge detector [SF⁺68]. We also proposed a cost-effective edge detection (ED) operation based on the Canny edge detector [SF⁺68], along with a multi-threshold segmentation in [AKHM22]. Moving object detection [TD18] in a frame sequence can help detect ROIs when the background is relatively constant. For instance, background subtraction (BS) approach [GS18, AFT⁺22] involves modeling the background assumed to remain relatively static. Then, the ROI is isolated in a frame by subtracting the static background. However, this technique can be sensitive to lighting changes and may not be effective for detecting stationary ROI. An alternative is to use frame difference (FD) [SM17], a low-cost moving detection technique, that involves subtracting two consecutive frames in a video sequence to identify areas of motion or change. However, it has low accuracy when dealing with noisy backgrounds [KMM15b].

In constrained networks, a good trade-off between high accuracy and limited resources needs to be found [HHHH22, WP18]. To reduce the amount of transmitted data, the quality of non-ROI part of the image is sacrificed by reducing the amount of DCT coefficients [MKZH08b, MKZH08a] or by applying a higher compression ratio [SSC11]. In [KMHD19], the sum of absolute differences (SAD) is used to achieve a low-cost ROI detection/compression. A low-overhead ROI detection that combines ED, FD and SAD techniques is proposed in [KMM15a] along with an energy- and content-aware control scheme to maintain target transmission energy with minimum degradation of the ROI quality under varying wireless channel conditions. Despite all this effort, ROI detection methods still need to be improved to guarantee a high QoE [KMM15b]. This chapter provides an overview of the research work done in the context of Ahcen

Aliouat's thesis [Ali23], which was conducted in collaboration with Annaba University in Algeria under the Tassili HC¹ program. The key aspects of the research and its main findings are outlined. In Section 5.1, an enhanced FD is leveraged to determine ROIs as an improvement of the S-frame coding in SenseVid (§ 4.1). Then, a multi-level ROI detection/compression/transmission strategy is presented in Section 5.2.

To evaluate the efficiency of the proposed strategies, extensive simulations and tests have been performed using sequences from standard datasets, in particular, the *CDnet 2014 dataset* [WJP⁺14]. Key performance metrics derived from the confusion matrix to characterize the classification have been used. Let TP and TN be the number of pixels that are correctly classified as foreground and background (True Negatives) respectively. Similarly, let FP and FN (False Negatives) be the number of pixels that are incorrectly classified as foreground (False Positives) and background (True Positives) respectively. The considered metrics are :

- *Recall* : $Re = TP/(TP + FN)$
- *Specificity or true-positive rate* : $Sp = TPR = TN/(TN + FP)$
- *Precision* : $Pr = TP/(TP + FP)$
- *F-measure* : $Fm = Re \times PR/(Re + Pr)$
- *False-positive rate* : $FPR = FP/(FP + TN) = 1 - Sp$
- *False-negative rate* : $FNR = FN/(TP + FN)$
- *Percentage of wrong classifications* : $PWC(\%) = (FN + FP)/(TP + FN + FP + TN)$
- *Balanced Accuracy* : $BAC = (Re + Sp)/2$

Lower values for PWC , FNR and FPR metrics indicate higher accuracy while higher values for Re , Sp , Pr , BAC and Fm indicate better performance.

The MJPEG encoder is chosen to compress the ROI blocks as it is more space and energy efficient than newer encoders like H.264 and H.265 [Ko18]. These later encoders use motion compensation techniques to reduce temporal redundancy and obtain a better compression ratio, which makes them very computationally expensive [KMM15b]. Besides, the MJPEG encoder is considered "solid" due to the absence of links between frames. If a frame is lost during transmission, the rest of the video will not be compromised, and the error is not propagated to the following frames. This is beneficial in the context of WMSNs, where a hostile channel is presented. Finally, MJPEG can be more appropriate for low and very low image capture frequencies where temporal redundancy becomes less obvious. This is a typical scenario for a WMSN application where the captured and transmitted images are not necessarily part of a video sequence.

5.1 Block-based movIng Region Detection (BIRD)

The main purpose of this work is to propose a ROI detection mechanism that offers a good trade-off between accuracy and complexity. The main idea of BIRD is to leverage the changes between two frames in a captured video based on a simple low-cost difference operation. To reduce the processing cost as well as the required memory to store the entire previous frame, a block-wise rather than a pixel-wise difference is adopted. An activity map that measures each block activity between two frames is built using SAD² [KD18] :

$$\Delta(x, y) = \frac{1}{w^2} \sum_{u=0}^{w-1} \sum_{v=0}^{w-1} |F_n(wx + u, wy + v) - F_m(wx + u, wy + v)|, x \in 0..M/w - 1, y \in 0..N/w - 1 \quad (5.1)$$

where w is the block size, F_n and F_m ($m < n$) are respectively the current and a previously captured frame, both of size $M \times N$. The previous frame is selected based on the activity level and the frame rate of the video. Since a high frame rate creates a low disparity between consecutive frames, it is necessary to select

¹Hubert Curien

²Summation of Absolute Difference

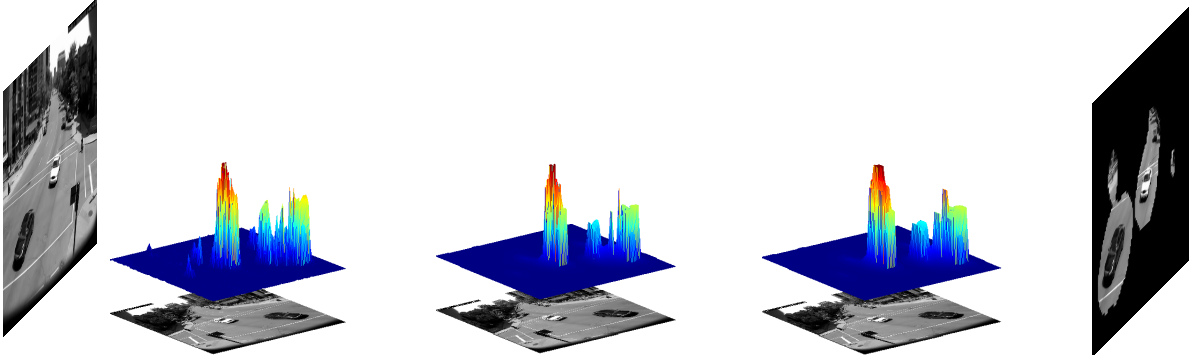


Figure 5.1: FGS eliminates unnecessary activities and ROF enhances the non-zeros scores prior to thresholding

an older frame as a previous frame and vice versa. The obtained activity map is w^2 times less than the input frames size. High scores in Δ indicate moving regions.

To avoid false negatives and improve the detection accuracy, the obtained map scores are processed using a combination of a fast Gaussian smoother and a rank-order filter. That is, FGS³ [MCL⁺14], a Gaussian smoother, is applied on the activity map to smooth the details and noisy parts resulting from the SAD operation. The use of FGS is motivated by its low complexity and rapidity when compared to convolution filters. The resulting smoothed map is then filtered by the maximum rank order filter (ROF) that calculates the envelope of the smoothed map. ROF belongs to a class of easy to implement filters [HM95] and provides a fast and cost-effective solution due to its simple arithmetic operations [KNM18b]. Finally, a binary mask is created with respect to a predefined threshold. The complete scheme of the proposed method is shown in Figure 5.1. In the performance evaluation that follows, the block side w is set to 8 and the ROF window is set to 4. Other settings and more details and results can be found in [AKHM23].

5.1.1 Computational Complexity and Energy Consumption

Let $E_{process}$ be the energy consumption by a visual sensor node to detect a ROI and compress the corresponding data, then we can write :

$$E_{process} = E_{detect} + E_{compress} \quad (5.2)$$

where E_{detect} is the energy cost of the object detection and $E_{compress}$ is the energy cost of ROI compression. We have :

$$E_{detect} = E_{SAD} + E_{FGS} + E_{ROF} + E_{thresh} \quad (5.3)$$

The energy budget is directly proportional to its computational complexity. For a given step s , the necessary energy (E_s) can be estimated using :

$$E_s = \varepsilon_{cycle} \sum_{op} N_{s,op} \times Cycles_{op} \quad (5.4)$$

where $N_{s,op}$ is the required number of operations op (addition, subtraction, division or thresholding) to perform the step s , $Cycles_{op}$ is the number of required cycles to execute operation op and ε_{cycle} is the energy consumption per processing cycle. These two latter parameters depend on the underlying processor. In this chapter, we consider a sensor node equipped with an ARM Cortex M3 micro-controller [Arm18]

³Fast Global Smoother

Table 5.1: Computational budget of each step in BIRD

Step	Operation	# operations
SAD	Addition	$(w^2 - 1) NM/w^2$
	Subtraction	NM/w^2
	Absolute	NM/w^2
	Division	NM/w^2
ROF	Comparison	$6 NM/w^4 - 18M/w^2$
FGS	Multiplication	$6 NM/w^2$
	Division	NM/w^2
Thresholding	Comparison	NM/w^2

operating at 72 MHz with processing power of 23 mW which results in $\varepsilon_{cycle} \approx 0.32\mu\text{J}$. The number of required cycles for addition, subtraction, comparison and absolute operations are considered to be the same : $Cycles_{abs} = Cycles_{sub} = Cycles_{cmp} = Cycles_{add} = 1$ while multiplication and division operations can require up to 2 and 12 cycles respectively. Table 5.1 gives the number of operations for each step.

To estimate the compression energy ($E_{compress}$), we count for the MJPEG cost for each block including the DCT, the quantization and the Huffman coding costs. The model provided in [LKR⁺09] and its slow IJG [LLM89b] variant is adopted as it proved to achieve good performances. It achieves a compression energy cost of 192.28 μJ per block. In a ROI based strategy, compression cost is proportionally related to the number of activity blocks detected that will be coded for each frame.

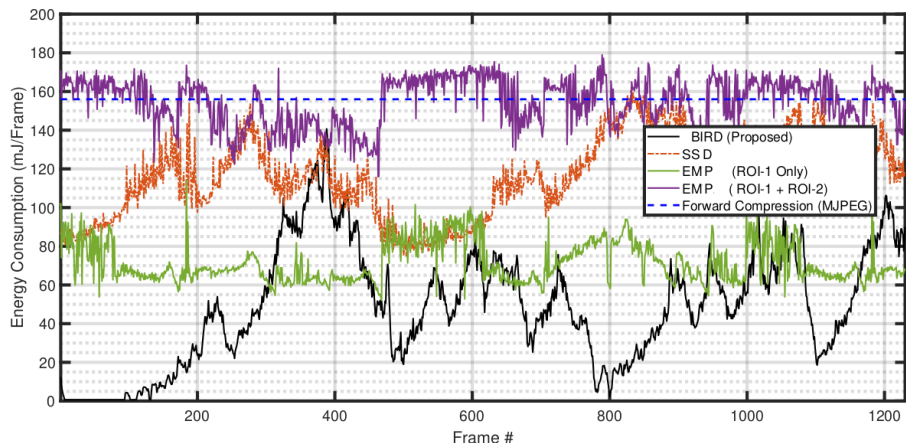
Three sequences are selected to empirically validate BIRD’s accuracy and low-overhead assumptions. *Highway* contains high activity with a number of moving vehicles. The *Pedestrians* sequence is of low activity with relatively high stability in the background. The *Snowfall* sequence is a long sequence that contains moving objects with very high activity in the background (weather conditions). The energy dissipation of BIRD is proportional to the frame size and directly correlated to the number of the blocks in the detected ROI. About 79.29%, 98% and 86.89% of blocks respectively are skipped in the *Highway*, *Snowfall* and *Pedestrians* sequences.

In the detection phase, BIRD [AKHM23], as it adds a moderate extra cost to a basic FD operation (about 38% for extreme cases), it consumes much lower energy than state-of-the art techniques [SG99, SHL⁺12, SHY⁺15, KKK16]. Figure 5.2 illustrates the per-frame energy consumption of the proposed method compared to ROI-based compression methods, namely, [AKHM22] referred to as *EMP* and [AKMH22] referred to as *SSD*. The forward baseline compression (MJPEG) is also plot and shows a constant energy consumption while other methods curves oscillate based on the number of blocks to compress. Despite the good ROI detection of the other techniques, they are weakened by the high energy cost in the detection step. This is due to the adopted edge detection and automatic thresholding techniques in [AKHM22] and [AKMH22] respectively in addition to the use of arithmetic convolution and histogram calculation. BIRD exhibits the lowest energy budget in all scenarios. More than 90% of the energy is saved most of the time.

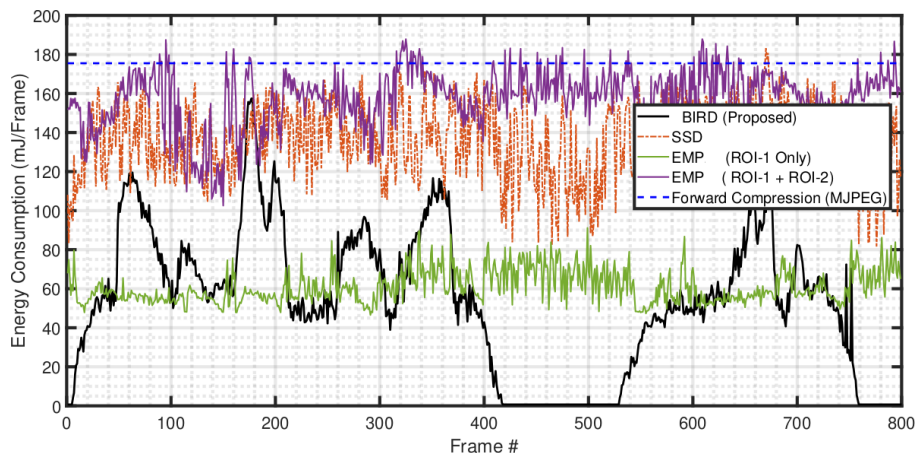
5.1.2 Detection Efficiency Evaluation

First, a qualitative assessment based on visual observation of the obtained masks for moving regions compared to the ground truth masks is considered. Sample frames from seven categories of the *CDnet 2014 dataset* in Figure 5.3 show that BIRD successfully detects blocks in which a significant motion occurs. Objects are entirely detected in all presented frames except for some video sequences (such as the *Sofa* clip) where the algorithm is unable to detect some objects due to their stability. It should be noted, however, that the information about the objects has already been delivered to the destination.

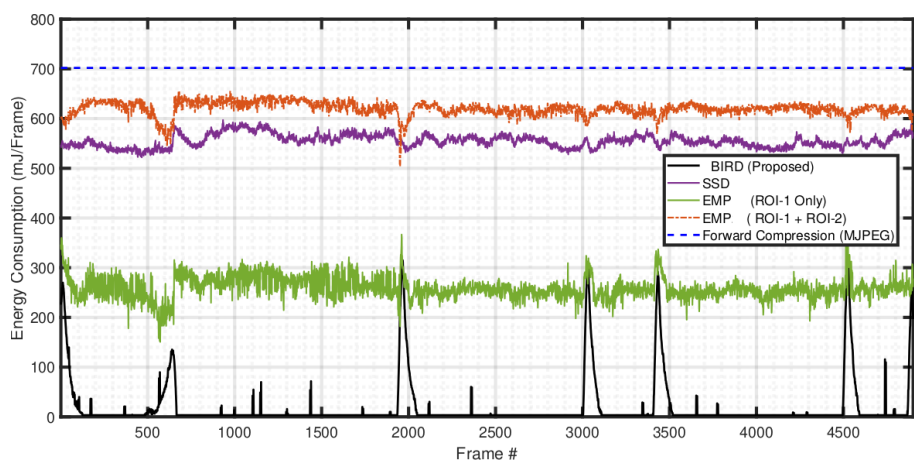
Table 5.2 shows the mean obtained results of BIRD when compared to some state-of-the-art techniques. BIRD shows the best results in terms of recall and FNR metrics and exhibits competitive results in terms of



(a) Highway sequence



(b) Pedestrians sequence



(c) snowfall sequence

Figure 5.2: Per-frame energy dissipation in BIRD.

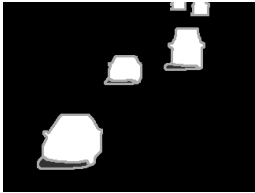
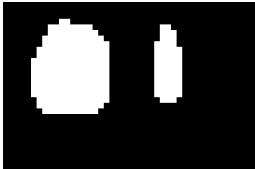
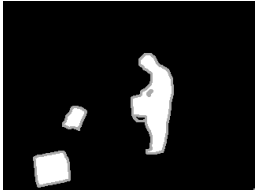
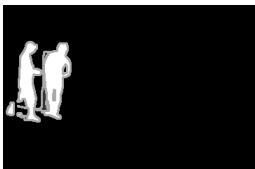
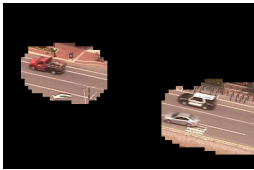
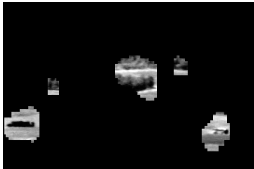
Frame	Original	Ground-truth	Mask	ROI
Baseline : Highway #1475				
Baseline : Pedestrians #476				
Bad Weather : Snow Fall #2784				
Intermittent Motion : Sofa #1185				
Shadow : Bus station #400				
PTZ #1240				
Turbulence #2045				
Night Video #1300				

Figure 5.3: Samples of ROI extraction mask results (CDnet 2014 dataset)

Table 5.2: Comparison of BIRD with classical techniques (CDnet 2014 dataset)

Technique	Recall	Specificity	FPR	FNR	PWC	F-Measure	Precision
KNN [ZVDH06]	0.6650	0.9802	0.0198	0.3350	3.3200	0.5937	0.6788
GMM1 [SG99]	0.6846	0.9750	0.0250	0.3154	3.7667	0.5707	0.6025
KDE [EHD00]	0.7375	0.9519	0.0481	0.2625	5.6262	0.5688	0.5811
MahaD [BJE ⁺ 10]	0.1644	0.9931	0.0069	0.8356	3.4750	0.2267	0.7403
GMM2 [Ziv04]	0.6604	0.9725	0.0275	0.3396	3.9953	0.5566	0.5973
EucD [BJE ⁺ 10]	0.6803	0.9449	0.0551	0.3197	6.5423	0.5161	0.5480
BIRD	0.8084	0.8357	0.1642	0.1915	16.7115	0.1893	0.2678

Table 5.3: CDnet 2014 dataset Category-wise comparison : BIRD vs. [SDE18] & [DGG14]

Category	Recall			Specificity			Balanced Accuracy		
	BIRD	[SDE18]	[DGG14]	BIRD	[SDE18]	[DGG14]	BIRD	[SDE18]	[DGG14]
Dynamic Background	0.7593	0.6436	0.8144	0.9512	0.9962	0.9985	0.8553	0.8199	0.9064
PTZ	0.9662	0.7685	0.3833	0.6443	0.9977	0.9968	0.8053	0.8831	0.6901
Bad Weather	0.9208	0.5647	0.6697	0.8948	0.9985	0.9993	0.9078	0.7816	0.8345
Baseline	0.7619	0.6214	0.8972	0.9437	0.8213	0.9980	0.8528	0.7213	0.9476
Camera Jitter	0.8504	0.4567	0.7436	0.6446	0.9788	0.9931	0.7475	0.7177	0.8683
Intermittent Motion	0.4186	0.5547	0.8324	0.8603	0.9979	0.9911	0.6394	0.7763	0.9118
Low Framerate	0.8161	0.5490	0.6659	0.7905	0.7464	0.9949	0.8033	0.6477	0.8304
Night	0.9455	0.4593	0.4511	0.8374	0.9583	0.9874	0.8915	0.7088	0.7193
Shadow	0.8775	0.8365	0.8786	0.8500	0.9828	0.9910	0.8638	0.9097	0.9348
Thermal	0.7548	0.4650	0.7268	0.8894	0.9647	0.9949	0.8221	0.7148	0.8609
Turbulence	0.8216	0.7421	0.7122	0.8870	0.9883	0.9997	0.8543	0.8652	0.8559
Overall	0.8084	0.6056	0.6608	0.8357	0.9483	0.9948	0.8220	0.7770	0.8509

*bold values are the best category-wise, red and blue values are respectively the best and second best, overall.

specificity. The weakness of the algorithm in the precision and F-measure values can be explained by the adopted block-based technique which detects additional pixels with the moving objects (i.e. high FPR).

Table 5.3 records the results of different sequence categories against those of a DL-based [DGG14] and a block-based object detection [SDE18] methods. The obtained results show a good detection performance of the proposed algorithm with high TP values for different categories. BIRD shows high detection results for some categories and moderate detection performances for others. Recall is high for almost all categories. Good performances are achieved for "dark" sequences (*Night Video*) or those with dynamic background (*PTZ sequence*) categories despite their difficulty. The algorithm presents some weaknesses in full object detection in some categories like intermittent object motion category. While [DGG14] shows superior BAC and specificity values, with an overall BAC of 82%, BIRD still guarantees high accuracy in detecting moving object regions for different categories and variable conditions. Overall, the proposed method provides a good balance between energy saving and detection accuracy.

5.1.3 Impact of Thresholding

Table 5.4 shows the impact of the threshold value on the number of ROI blocks that determines the amount of data to be transmitted to the final destination. It can be seen that the higher the threshold, the lower the number of the blocks of interest. When the background is characterized by a high stability (for example *Pedestrians* sequence), a high threshold is generally preferred since there is a low risk of wrongly including background blocks in the ROI. However, in the presence of noisy and dynamic background (the *Snowing* scene in the *Snow fall* sequence for example), a high number of background blocks can be misclassified. A higher number of ROI blocks is likely to enhance the quality of the reconstructed frames at the destination but at the cost of higher energy and bitrate consumption.

Table 5.4: Ratio of ROI blocks (per frame average) under threshold variation

Threshold	Highway	Pedestrians	Snowfall
1	51,75%	22,75%	154,75%
3	24,25%	10,00%	15,83%
5	20,75%	6,33%	9,17%
7	16,00%	5,00%	7,25%
9	13,33%	4,33%	6,17%
10	12,42%	4,08%	5,67%

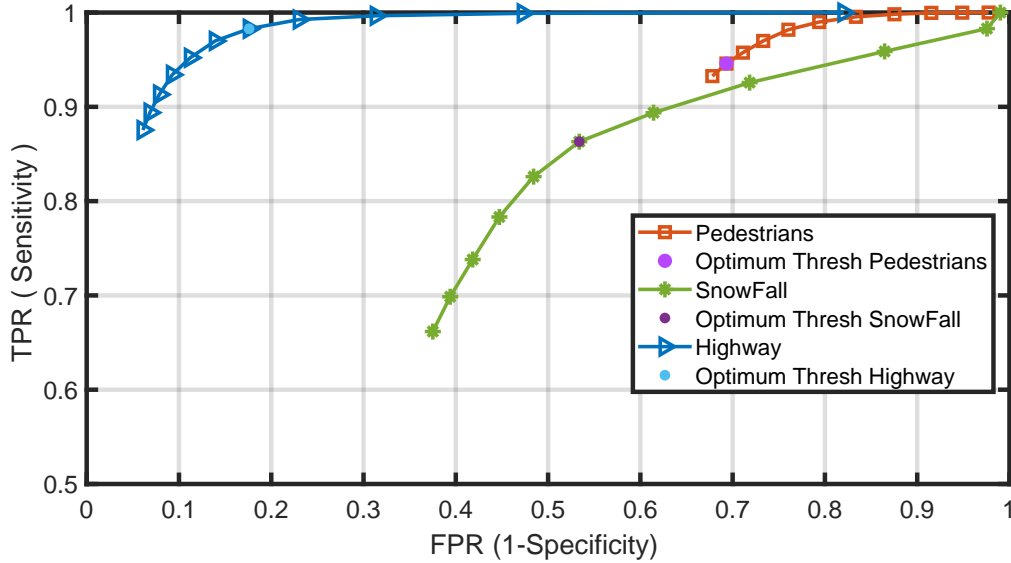


Figure 5.4: ROC curve and optimal thresholds.

Figure 5.4 plots the ROC curve (i.e. TPR against the FPR) when varying the threshold value (0 .. 10). It can be observed that low thresholds imply a high true positive rate. However, this adversely affects the specificity of the detection, since a high number of blocks is wrongly labeled as activity blocks, which results in more data to deliver. The optimum threshold that allows the best tradeoff between TPR and FPR could be estimated by calculating the minimum Gaussian distance between the results of TPR and FPR for the different threshold values : $\min_i \sqrt{(1 - TPR_i)^2 + FPR_i^2}$. It is represented using a filled circle dot in each ROC curve. For instance, the threshold value for an optimal detection accuracy is 9 for the *Pedestrians* sequence. This can significantly save the energy consumption in the sensor node and the bitrate needed for transmission.

5.2 Multi-Level Region Detection Scheme

In this work, an efficient and low cost multi-level ROI detection scheme is proposed. Depending on the importance of each level, a decision is made whether or not to transmit the corresponding region. If so, a compression with an appropriate quality coefficient reflecting the importance of the region is applied on its blocks prior to transmission. Transmitting only a subset but relevant information of each captured image saves energy and bandwidth while allowing for a machine-based recognition with a high level of accuracy at the final destination as will be shown in Section 5.2.3. Without loss of generality and for the sake of clarity, in what follows, a three-level ROI strategy is considered to decide whether a given block in the frame has to be encoded with high or low quality factor or simply discarded.

ROI Detection The proposed ROI detection method aims to classify each frame region based on its activity level. To do so, we introduce the Successive Summation of Absolute Difference (S-SAD) method to compute and classify the activity in the current frame based on a successive summation of different size windowing blocks using Eq. (5.1). First, a SAD between the current frame and a previous frame is calculated on $w_1 \times w_1$ -size non-overlapping blocks. The blocks of the activity map (SAD_{map}) that outshine a threshold value are considered to belong to the $ROI-1$ which presents the *Local Activity Map*. They are shown in white in Figure 5.5(b) where Figure 5.5 illustrates the different steps based on a frame sample. Then, a $w_2 \times w_2$ summation is applied on the obtained SAD_{map} to extract the *Regional Activity Map* R_{map} by substituting w_1 by w_2 in Eq. (5.1). The R_{map} blocks that exceed a threshold value are part of the second region of interest $ROI-2$ depicted in Figure 5.5(c). Finally and following the same principle, we derive the *Global Activity Map* (G_{map}) of the frame by considering a summation of the *Regional Activity Map* using $w_3 \times w_3$ blocks. The thresholding applied on the obtained G_{map} determines the blocks of the third region of interest $ROI-3$ (Figure 5.5(d)). We refer to this final ROI as the global moving region (GMR) which should have the property of including the other regions ($ROI-1 \subset ROI-2 \subset ROI-3$) and thus serves as a mask for the previous ROIs to eliminate all blocks initially classified as part of these regions of interest. The excluded blocks are surrounded in red in Figure 5.5(b)-(c). The final obtained ROIs are shown in three different colors in Figure 5.5(e).

The successive block sizes and the threshold values used in each step have to be appropriately chosen to achieve a good trade-off between computational complexity (large block sizes) and detection precision (small block sizes). According to numerous tests, the block sizes $w = w_1, w_2$ and w_3 are set respectively, to 8, 4 and 2, while the threshold values were set empirically following comprehensive testing and experimentation.

ROI Compression and Transmission. First, the initial frame is completely compressed and sent. This first frame is considered as a background frame at the destination. For the next frames, only the ROI blocks are taken into account for compression and transmission based on their relative importance by considering the following priority classes :

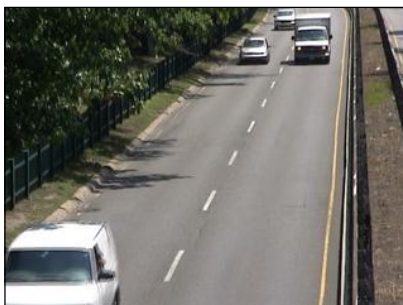
- The first priority class $C_1 = ROI-1$ represents the blocks that are in, and only in the first ROI. Class C_1 blocks having the highest interest are coded with a higher MJPEG quality factor Q_1 before being transmitted ;
- The second priority class $C_2 = ROI-2 - ROI-1$ includes the labeled moving blocks that are in $ROI-2$ but not in $ROI-1$. Class C_2 blocks having a medium interest are coded, prior to their transmission, with a lower MJPEG quality factor $Q_2 < Q_1$;
- The third priority class $C_3 = GMR - ROI-2$ includes the blocks that are in the GMR but are not in $ROI-2$. This class blocks are considered to be of low interest and are simply dropped.

In the performance evaluation, presented herein, the proposed scheme is compared to the method proposed by Kouadria et al. [KMHD19] and the standard MJPEG compression where the quality factor QF is set to 50. In our proposed strategy, Q_1 and Q_2 are set to 50 and 20 to encode the blocks of $ROI-1$ and $ROI-2$ respectively. For more details and results, the reader can refer to [AKM⁺23].

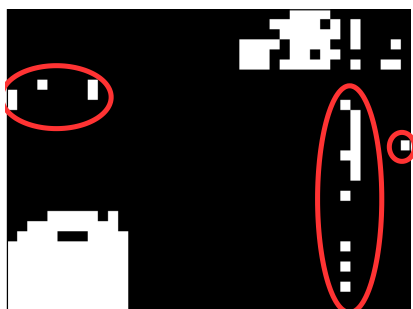
5.2.1 Computational Complexity and Energy Consumption

To show the effectiveness of the proposed strategy in terms of computational complexity, the same model as the one presented in Section 5.1.1 is adopted along with Equations (5.2)-(5.4). That is, the detection energy can be estimated as follows :

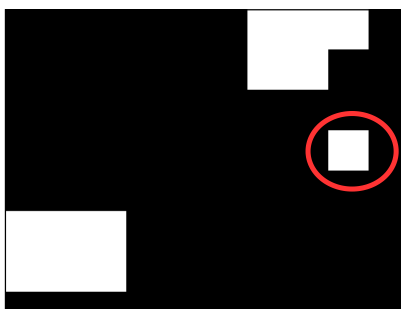
$$E_{detect} = E_{SADmap} + E_{Rmap} + E_{Gmap} + E_{thresh} \quad (5.5)$$



(a) Highway #170



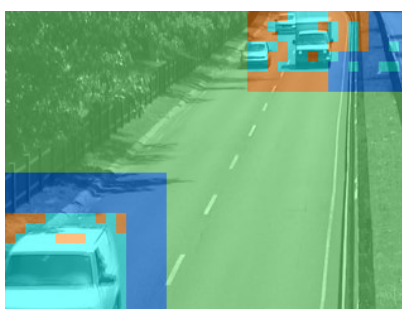
(b) $w_1 \times w_1$ -block SAD_{map} mask



(c) $w_2 \times w_2$ -block R_{map} mask



(d) $w_3 \times w_3$ -block G_{map} mask



(e) Labeled ROIs

Figure 5.5: ROI construction and GMR mask use for extra blocks elimination.

Table 5.5: Computational Cost of each step ($w_2 = w/2$, $w_3 = w/4$)

Step	Operation	Window	# operations
SAD_{map}	Add.	w	$NM(w^2 - 1)/w^2$
	Sub.		NM/w^2
	Abs.		
	Div.		
R_{map}	Add.	$w_2 = w/2$	$4NM/w^4$
	Div.		
G_{map}	Add.	$w_3 = w/4$	$64NM/w^6$
	Div.		
Thresholding	SAD_{map}	w	NM/w^2
	R_{map}	$w_2 = w/2$	
	G_{map}	$w_3 = w/4$	

Table 5.6: Per frame mean energy cost (mJ)

Sequence	Frame Size	E_{detect}	$E_{process}$ mean [min-max]	$E_{detect}/E_{process}$	MJPEG	Energy saving w/r MJPEG
<i>campus</i>	352×288	0.8827	14.24 [0.9 - 211.14]	6.20%	205.92	93.08%
<i>highway</i>	320×240	0.6699	16.02 [0.9 - 53.38]	4.18%	156	89.74%
<i>traffic</i>	160×120	0.1671	20.22 [0.23 - 40.18]	0.83%	39	48.16%

The number of operations needed by each step of the proposed strategy are provided in Table 5.5 and assuming that $w_2 = w/2$ and $w_3 = w/4$, we obtain :

$$E_{detect} = N M \varepsilon_{cycle} \left(\left(1 + \frac{4}{w^2} + \frac{4}{w^4} + \frac{64}{w^6}\right) Cycles_{add} + \left(\frac{1}{w^2} + \frac{4}{w^4} + \frac{64}{w^6}\right) Cycles_{div} \right) \quad (5.6)$$

Table 5.6 reports some numerical results for three video sequences of different frame sizes (*campus*, *highway* and *traffic*) to figure out the extra cost induced by the proposed ROI detection process. The mean consumed energy per frame for the detection phase (E_{detect}) depends on the size of the images and remains moderate as it does not exceed 7% of the overall processing energy. Compared to MJPEG, our strategy allows a significant energy saving which can be as higher as 93% for the *campus* sequence for instance and could achieve 90% or more depending on the amount of activity during the surveillance task for the two other sequences. We note a lower energy saving of about 50% for the *traffic* sequence due mainly to the small size of its frames making the chosen values for w_1 , w_2 and w_3 less adequate, they need to be tuned considering the frame size. The energy gain also depends on the size of the moving objects in the scene since small objects imply small ROIs and thus fewer data to compress and vice versa.

Frames that exhibit a high activity map require much energy consumption, while low activity periods lead to very limited energy usage. A wide statistical spread is observed (ranging from 0.9 mJ for extremely little activity and more than 211 mJ exceeding the MJPEG energy expenditure) reflects a significant variance in energy expenditure in the *campus* sequence. This is attributable to a varying activity level in the different parts of the sequence.

Figure 5.6 shows the evolution of the consumed energy per frame for the three sequences along with the achieved PSNR. The energy curves confirm above findings. The oscillation in energy consumption is directly related to the size of the ROI. It is illustrated that the method yields lower energy consumption than MJPEG that registers a constant high value. The quality of the video is not affected by limiting the amount of processed data to be transmitted as it remains stable in the range 30..35 dB while it allows reducing significantly the overall energy consumption.

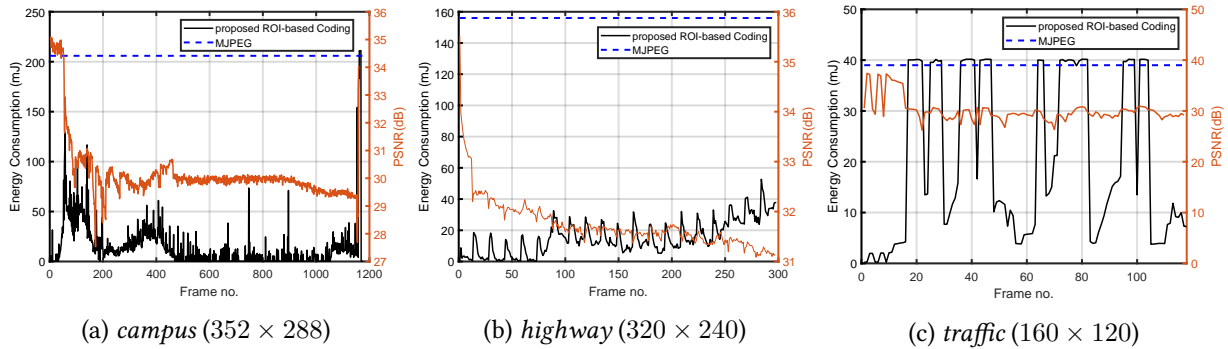


Figure 5.6: Total processing energy and the corresponding PSNR.

5.2.2 ROI Detection Accuracy

Visual Results. Figure 5.7 presents some visual results of the reference frames (before transmission) when applying our multi-level ROI coding compared to [KMHD19] and the standard MJPEG. As can be seen, the whole frame visual quality for our strategy shows better results for all the sequences compared to [KMHD19] and slightly lower than those of MJPEG. The detection of the moving region is almost complete and the classification of the regions of interest into high, medium and lower importance is also satisfactory. Furthermore, based on our experiments, our strategy does not suffer from the error propagation problem encountered in [KMHD19]. This is due to the fact that our method detects larger regions which significantly lowers the probability of a region selection error (loss of context). Our strategy ensures effective detection for different scenarios, both indoor, *laboratory* and *intelligent room* sequences, and outdoor as can be seen in the other sequences. The detection accuracy is not affected by dark background scenario as can be observed in the *Street Corner At Night* sequence. It is also worth noting that the speed of the movement does not affect the detection performance as observed in the results of *laboratory* sequence. This is one key advantage of the adopted frame difference-based detection technique.

Bitrate Gain. Reducing the bitrate saves both transmission energy and network bandwidth which helps avoid or at least limit congestion situations for better delivery conditions. Figure 5.8 plots the amount of data to be transmitted on a per frame basis when adopting our proposed method, MJPEG and [KMHD19]. We can see that the required bitrate for the suggested strategy is slightly higher than in [KMHD19] for most of the sequences. This was expected since the size of ROI in our case is larger but in turn, our strategy ensures the delivery of a higher quality ROI at the expense of a slightly higher bitrate. For instance, with the same quality level, our method requires a mean bitrate of 3.358 kB/s for the *campus* sequence ($fps = 10$), which is 27 times less than the required bitrate when adopting MJPEG (93.06 kB/s) which represents a saving of 96.4%. For the *highway* sequence ($fps = 25$), we achieve a saving of about 76.3% of the required bitrate since it drops from 263.25 kB/s to 62.65 kB/s.

Image Quality assessment. The obtained PSNR, SSIM and VIF⁴ [SB06] scores are reported in Table 5.7 for different video sequences to estimate the information loss resulting from the compression phase. Bold (underlined>) values represent the (second) best results. MJPEG performs the best in terms of both PSNR and VIF for all sequences. This was expected since the entire image is transmitted after being encoded with a high quality factor. Our proposed method gives the second best results for all metrics and outperforms MJPEG in terms of the SSIM measure for specific sequences (*Intelligent room* and *Highway*). This superiority is directly due to the nature of the scene background, which is distinguished by a significant stability. The quality of the background blocks is maintained over time. However, a considerable decrease in the quality of the reconstructed frames for some sequences (such as *Highway II*) is observed. This degradation is due to the low frame rate of the video with significant motion in the scene. The large size of the moving objects

⁴Visual Information Fidelity

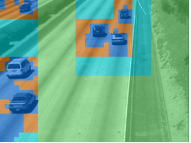
Frame	Original	ROI	Proposed	MJPEG	Kouadria et al. [KMHD19]
Traffic #10			 SSIM=0.9586	 SSIM=0.8992	 SSIM=0.8915
Highway II #484			 SSIM=0.8521	 SSIM=0.9110	 SSIM=0.8397
Intelligent Room #231			 SSIM=0.9287	 SSIM=0.9428	 SSIM=0.9129
Laboratory #806			 SSIM=0.9195	 SSIM=0.9476	 SSIM=0.9023
Street Corner #884			 SSIM=0.9311	 SSIM=0.9891	 SSIM=0.9163

Figure 5.7: Some Visual Results

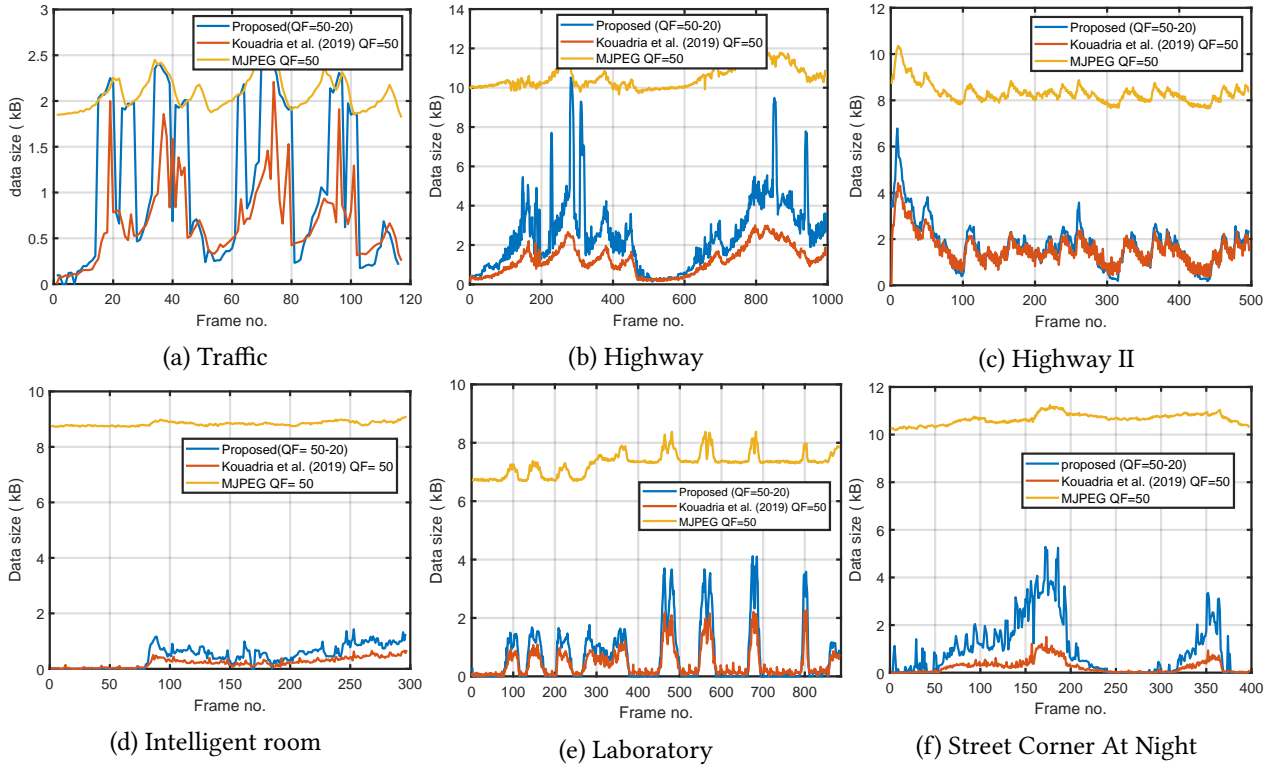


Figure 5.8: Per-frame data quantity to transmit

Table 5.7: Overall mean quality metrics

Sequence	Proposed method			Kouadria et al. [KMHD19]			MJPEG		
	PSNR	SSIM	VIF	PSNR	SSIM	VIF	PSNR	SSIM	VIF
Highway	31.7414	0.7865	0.6042	30.4667	0.7053	0.5385	32.7808	0.7700	0.7351
Highway I	28.8923	0.6716	0.5744	31.8053	0.6138	0.4874	37.9583	0.8374	0.7934
Highway II	28.4600	0.7055	0.4637	29.3400	0.6965	0.4506	33.0100	0.8208	0.7207
campus	31.3614	0.7055	0.4637	29.5200	0.6965	0.4501	35.7400	0.8208	0.7207
Intelligent room	31.7727	0.8036	0.5916	30.4667	0.7053	0.5385	32.7808	0.7700	0.7351
Laboratory	32.1748	0.6214	0.5748	30.9583	0.5894	0.5297	34.6275	0.6790	0.7492
Traffic	30.0569	0.6559	0.6230	28.2246	0.5710	0.5030	30.4093	0.6625	0.6493
Street Corner At Night	33.3932	0.9181	0.9209	32.1294	0.8815	0.8724	42.7939	0.9690	0.9514

may cause inaccurate ROI detection, resulting in a substantial loss of contextual information. Furthermore, a high movement leads to more *ROI-2* zones coded with low quality, which decreases the frame quality.

For a more refined analysis, the image quality metrics are plotted on a per-frame basis in Figures 5.9-5.11. It is clearly shown that the proposed strategy guarantees an acceptable high quality under a very low bitrate. The method registers about 30 dB PSNR or higher for all the sequences as depicted in Figure 5.9. Our strategy shows at most 4 dB lower PSNR values when compared to MJPEG and a higher PSNR, for all the sequences, with respect to [KMHD19]. For the SSIM values, the proposed strategy registers values varying from 0.6 to 1 as shown in Figure 5.10. Most of the first received frames exhibit high SSIM values (above 0.95) which degrade over time. Deterioration is due to the increasing amount of blocks being classified as *ROI-2*, compressed with lower quality. Nevertheless, we still obtain higher SSIM values with respect to [KMHD19]. Similar results are obtained based on the VIF metric as shown in Figure 5.11 with scores almost above 0.4 for the different considered sequences. Some sequences exhibit high degradation in terms of VIF like the *campus* clip that undergoes a degradation as high as 0.4. This is due to the complexity of the corresponding background. The same degradation is noticed in [KMHD19] but with slightly better results

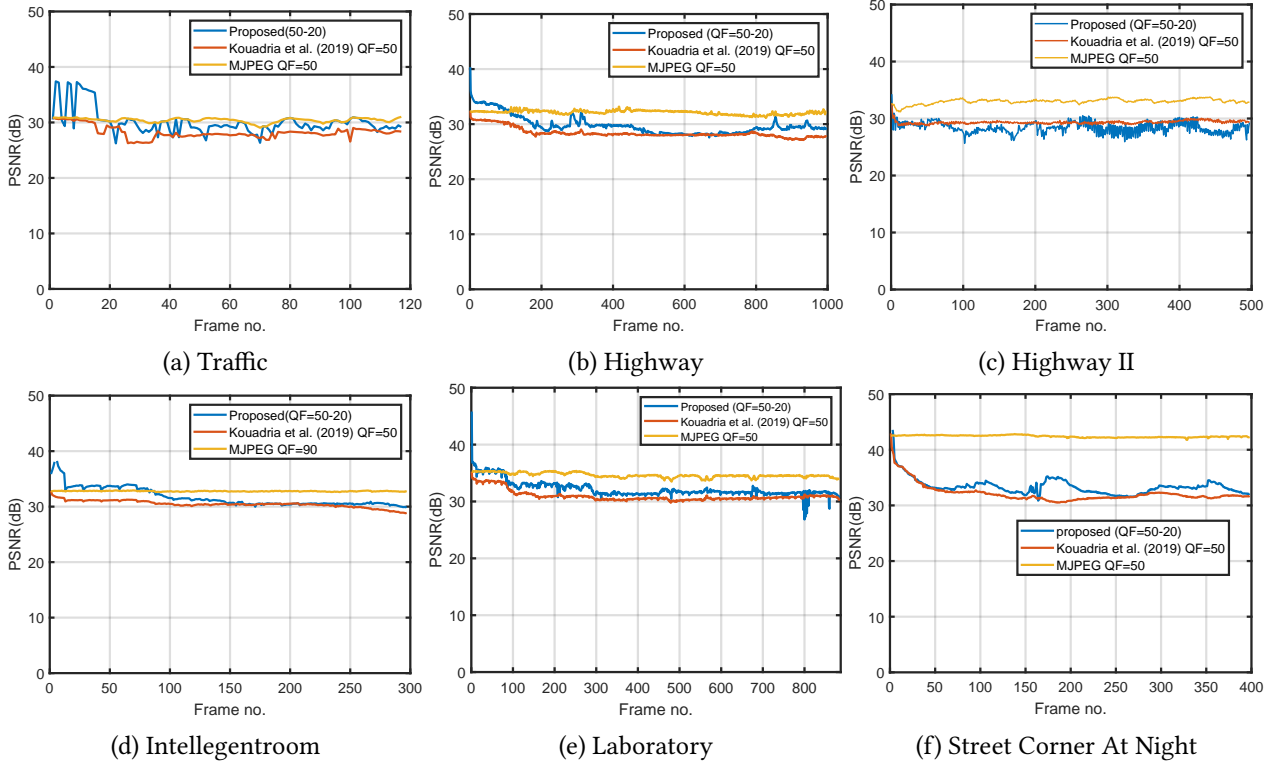


Figure 5.9: PSNR results for different sequences.

for our strategy. Overall, the proposed method outperforms [KMHD19] and is able to ensure an acceptable QoE while lowering the required bitrate with respect to MJPEG.

5.2.3 The Impact of Quality Degradation on Object Recognition

The aim is to assess the efficiency of the proposed strategy in ensuring a high recognition accuracy under a very low bitrate. The real-time object detection system YOLOv3 [ZL20], a machine-based monitoring system, is used on the received frames to extract and recognize the moving objects. It proves to be of a competitive accuracy and speed with a robustness in detecting different types of objects. The recognition accuracy on the images that result from the proposed strategy is compared to those of the original non-compressed frames, MJPEG compressed frames, and compressed frames using [KMHD19].

Figure 5.12 shows the recognition results for sample frames from the used datasets and demonstrates the competitiveness of our method to enhance the recognition accuracy at the destination. For all sequences, we achieve higher recognition accuracy compared to [KMHD19]. The results are still comparable to the original and MJPEG frames or even better in many cases compared to MJPEG. At first impression, results show that the compression quality degradation hurts the recognition accuracy. This conclusion is supported by the overall recognition results depicted in Figure 5.13 that represents the performance of the recognition process, for the entire dataset. Figure 5.13a plots the number of the detected objects and shows that unsurprisingly, original frames achieve the highest score for all the sequences. Our proposed strategy, overall, shows the second-best results. Preserving only a high quality compression of the ROI while ensuring a good ROI detection is sufficient to enable more accurate smart tasks at the destination like object recognition. As for the recognition accuracy, Figure 5.13b shows the superiority of our method which allows smart machine-based tasks at a significantly low bitrate and energy budgets (§5.2.1).

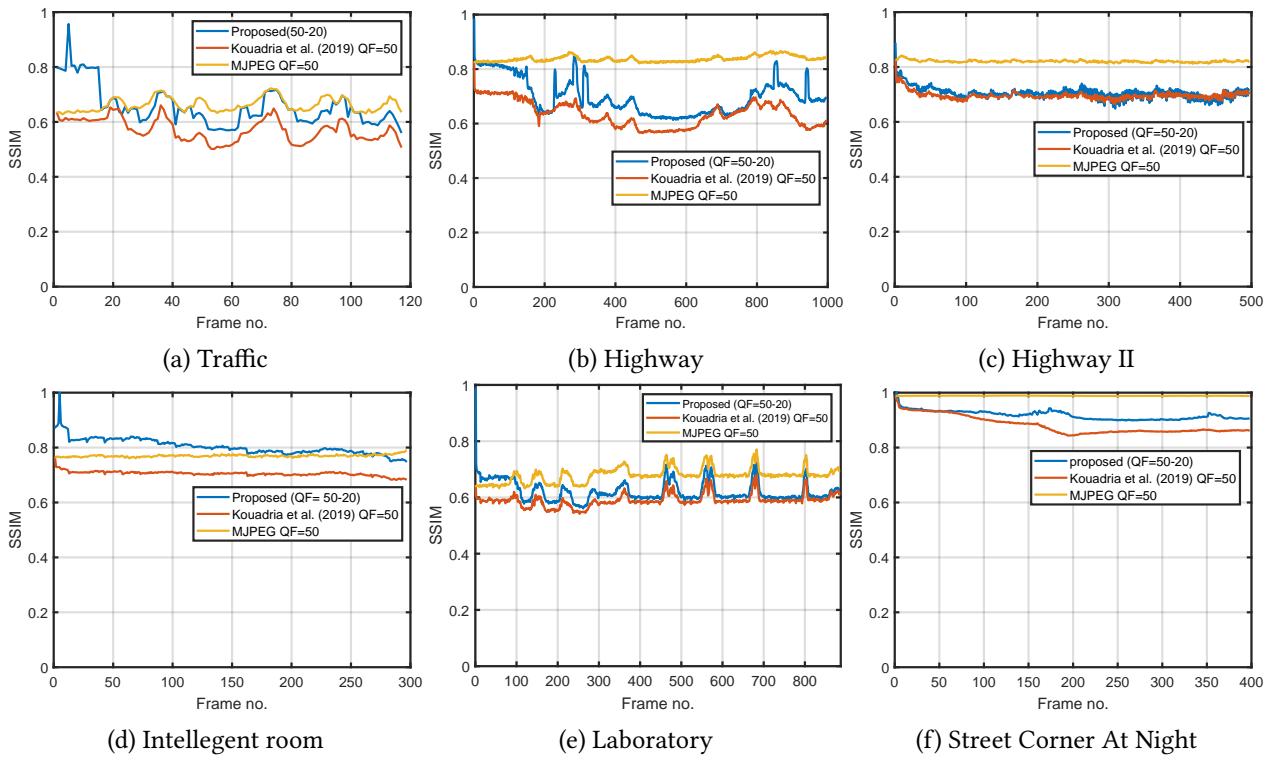


Figure 5.10: SSIM results for different sequences

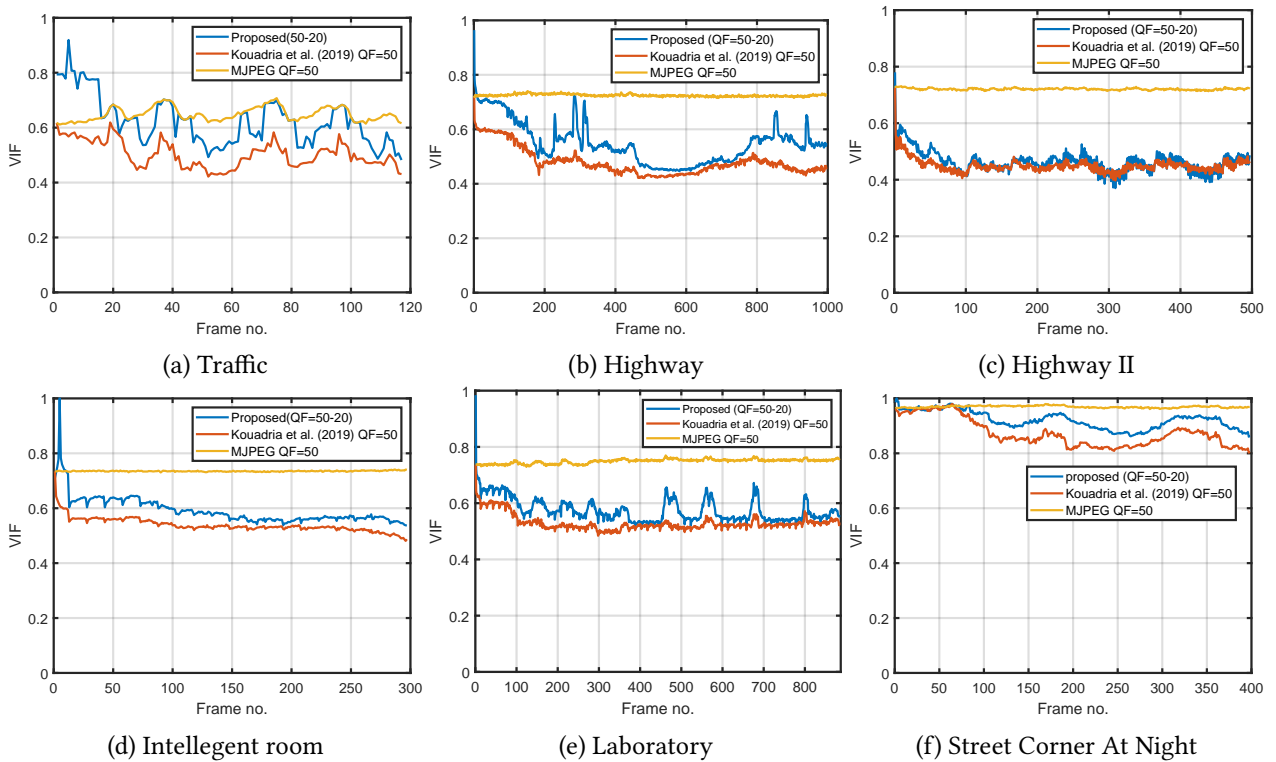


Figure 5.11: VIF results for different sequences

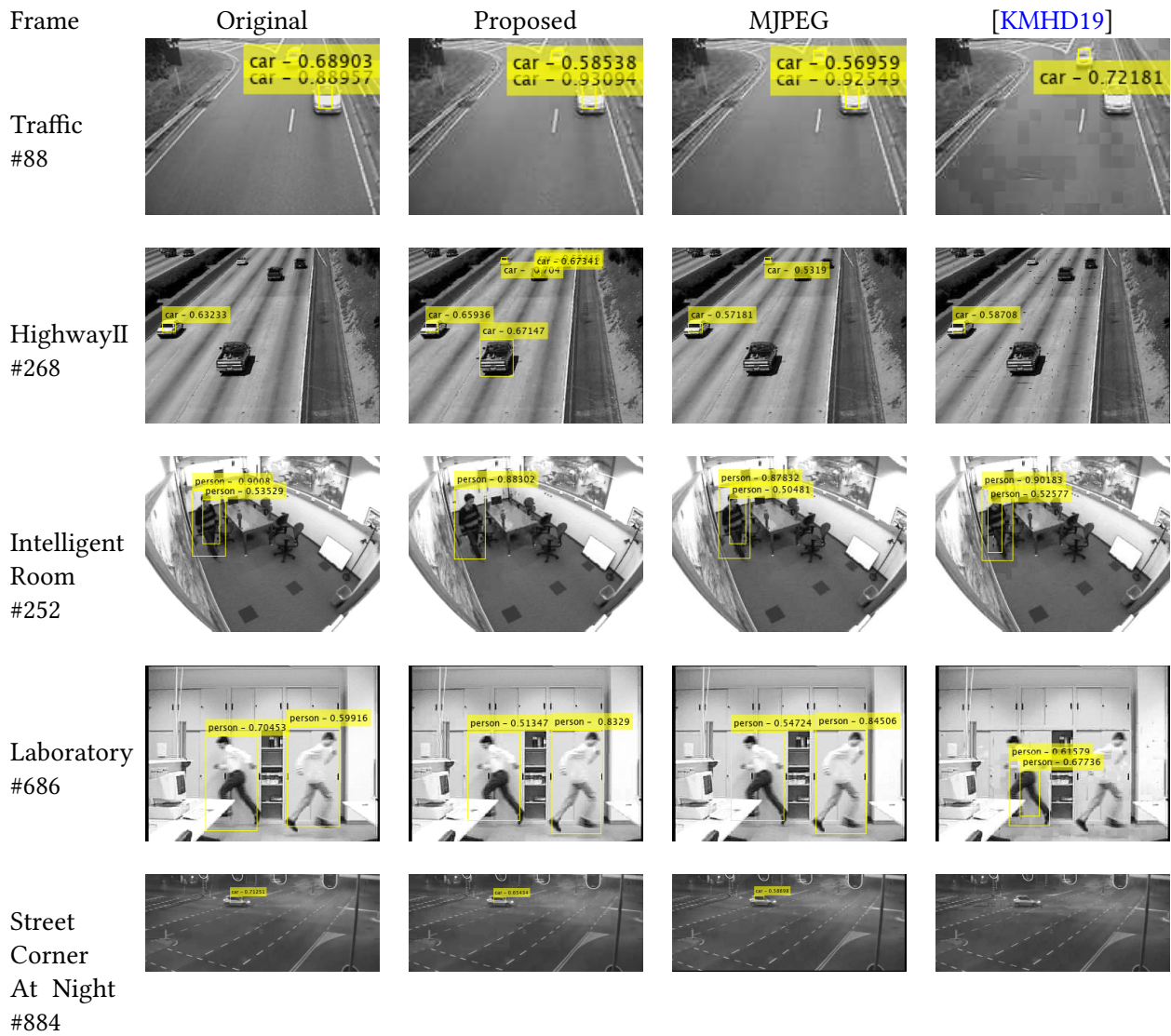


Figure 5.12: Bounding box insertion results for the used dataset

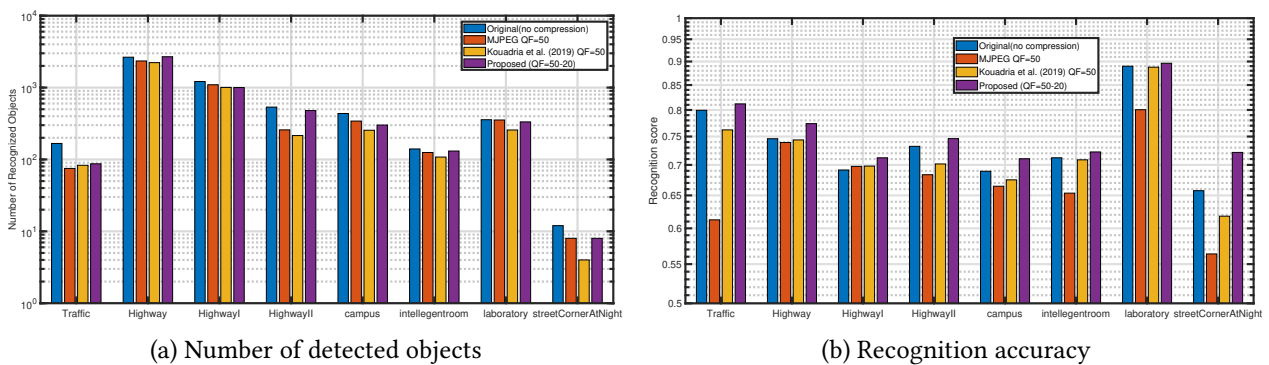


Figure 5.13: Performance of recognition for different sequences.

5.3 Conclusion

In this chapter, low-cost moving region detection strategies have been presented to address the limitations of constrained networks. Compared to conventional MJPEG, low bitrates are achieved and energy expenditure is significantly reduced with a slight sacrifice in the non-ROI blocks. It has been shown that this does not influence the intelligent tasks at the destination but enhances them by virtue of the content-aware strategy used.

The proposed ROI-based techniques can be adopted for large-scale video surveillance in an edge-cloud processing paradigm using WMSN, where network-based scenarios should be elaborated and evaluated. In fact, the assessment was made without considering the impact of network transmission. Therefore, these techniques have been integrated into SenseVid to consider their evaluation taking into account the impact of network losses on their robustness as part of the my research project (§ 6.5).

Part II

Scientific Project

Chapter 6

Digital Twin from Manufacture to Nature - Network Perspective

The Internet of Things (IoT) is experiencing strong growth in various fields and is constantly evolving, with a forecast of more than 125 billion connected objects in the world by 2030¹. These are mainly wireless sensors connected to the Internet but also any other physical or virtual object that can communicate via this global network. Today, there is not yet a universal IoT architecture. Standardization efforts are underway with international bodies competing to find a global and viable solution to what scientists summarize in 5Vs in relation to the big data : volume, velocity, variety, veracity and value.

For some years now, many standards have been issued by several international organizations and alliances to enable the development and deployment of wireless sensor networks in several application domains. ZigBee [WJZ16] and 6LoWPAN² are built on the IEEE 802.15.4 standard designed for Low Power Lossy Networks (LLN). Although ZigBee is a mature and a popular standard, it does not allow easy communication with other protocols. 6LoWPAN on the other hand was introduced to make it possible for LLN objects like sensors to be connected to the Internet of Things. It handles 802.15.4 devices as well as other ones on an IP network. A border router can connect the two worlds. Figure 6.1 depicts the 6LoWPAN network stack for LLNs that will be used throughout this project.

The distributed nature and the significant scale of the IoT make it complex and difficult to model accurately. This renders service provision challenging in the context of LLN networks when strict requirements are expected while ensuring energy efficiency. Most of networking problems are NP hard and as a result solved using carefully designed heuristics. However, these heuristics are often based on simple models and require lengthy tests and adjustments to achieve a practical realization [MAMK16]. Thanks to recent advances in GPU technology and cloud computing, machine learning (ML) returned to the front stage as a response to complex and challenging problems from various domains. While traditional heuristics produce "one-size fits all" solutions, ML is able to deal with complexity and allows to adapt to the actual network state (network dynamics) which avoids manual intervention.

Facilitated by this dramatic development of the IoT along with the rise of big data analytics, the last decade witnessed the revival of the concept of *Digital Twin* [BCC20]. In particular, the IoT holds huge potential to keep a digital twin consistent and synchronized with the physical entity it represents through its sensing technology coupled with the communication capabilities it provides. A *Digital Twin (DT)* can be viewed as a machine that is emulating or "twinning" the life of a physical entity [BCF19]. A DT is more than just a set of powerful models and simulators, it is a continuously evolving model that is always aware of the events happening in its physical twin (PT) throughout its lifecycle to supervise and optimize its functions.

¹ihsmarkit.com/

²IPv6 Low power Wireless Personal Area Networks

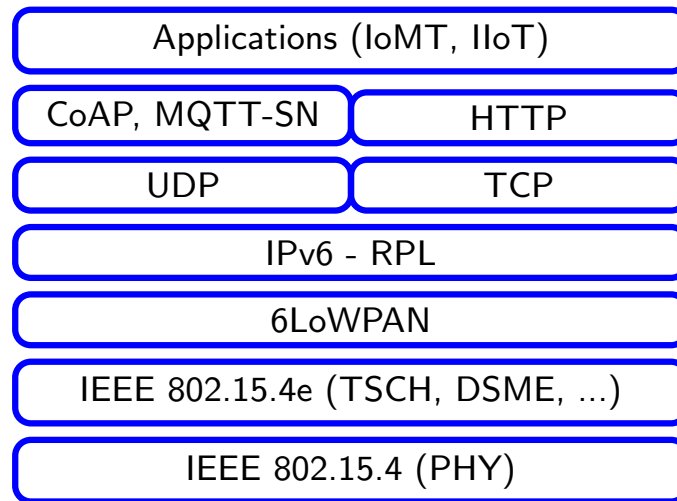


Figure 6.1: Typical Network Stack for LLNs

The major effort is underway to narrow any gap that may occur between the twins [VNT⁺22].

Digital twin is ranked three times in a row as one of the top ten most promising technological trends for the next decade [CBS⁺19]. The corresponding market size is foreseen to grow from approximately 11 to more than 150 Billion dollars by 2030³. DT is particularly promising in creating a continuously updated model of a physical system to enable rapid adaptation to dynamics mainly unpredicted and undesirable changes. A DT is characterized by four foundational elements, namely physical part, digital part, data feed and intervention [Cen22]. These foundational elements and their interactions are illustrated in Figure 6.2. The digital and physical twins in addition to the IoT ensuring the twins connection can be viewed, especially in industry 4.0 context, as a Cyber-Physical System (CPS) with continuous real-time interaction to efficiently mirror the physical system. With respect to CPS, Digital twining allows going beyond real-time optimization and control.

The major added value of digital twin identified in the literature can be summarized in what follows :

- Personalized products and services can be offered since the DT is specific rather than a general model.
- Efficient decision making along the physical twin lifecycle (design, operation, maintenance).
- Real-time monitoring and control are enabled by the bidirectional connection between the twins.
- Predictive maintenance can be improved by forecasting the future status of the physical twin based on smart analysis of collected data.
- What-if scenarios for evolution, uncertainty qualification and risk assessment are made possible since the DT can be fed by hypothetical data or even by evolving its model in simulation mode.

This chapter is organized as follows. Section 6.1 introduces the concept of Digital Twin-based Knowledge-Defined Wireless Sensor Networks (DT-based KD-WSN) and sets the architecture that will serve as a foundation for the answers sought to the issues raised in this project. As the expected solutions have to chiefly consider communication networks, Section 6.2 considers digital twining from a network perspective. Section 6.3 introduces the problem of DT modeling and the planned strategy regarding the problem of building a DT for the communication network. My research considers two application fields, namely Industry 4.0 and natural environment surveillance, that is Section 6.4 brings the idea of building a DT for the natural environment. With respect to this latter, the problem of knowledge extraction in a constrained environment is a challenging issue described in Section 6.5. The problem of communication resources allocation is the object of Section 6.6. Finally, Section 6.7 concludes this chapter by addressing the timeliness and positioning of this project.

³grandviewresearch.com

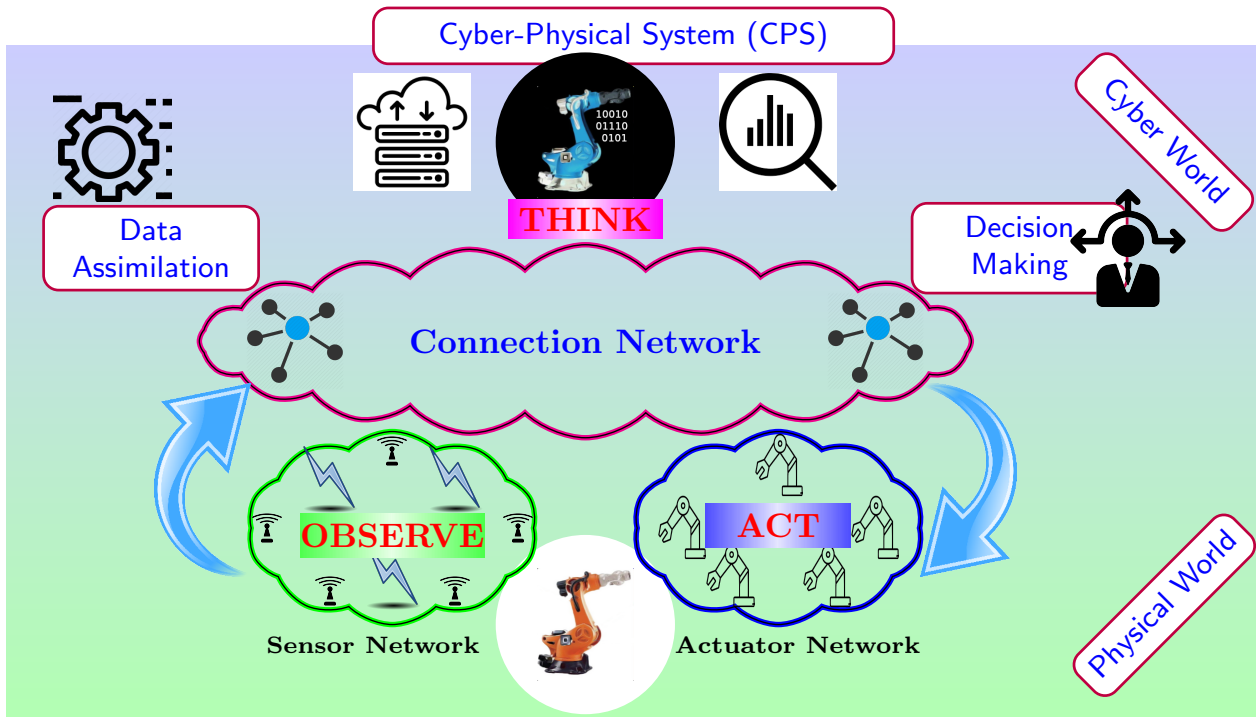


Figure 6.2: CPS-DT Architecture

6.1 Digital Twin-based Knowledge-Defined Wireless Sensor Networks (DT-based KD-WSN)

This project considers knowledge-defined networks through a digital twinning perspective in an attempt to achieve the added value, in the sense of "knowledge", that has been missing in my previous work for both application and network related data. A Knowledge Plane (KP) for the Internet [CPRW03] is proposed to allow for network design based on ML and cognitive systems. It consists in a separate construct in the Internet that would enable a high level view to provide services such as automation and anomaly detection. The idea appears good on paper, but significant challenges need to be addressed in order to make it a reality. Based on the emerging Software-Defined Networking (SDN) paradigm [KAMH17, JAAB⁺15] along with a centralized Network Analytics (NA) platform, authors of [MRNC⁺17] introduced the Knowledge-Defined Networking (KDN). SDN promotes the separation of control functions (how an equipment should transfer traffic) from the actual transfer of data. This results in a centralized controller with a global view of the network. Thus, the best decisions can be made to meet the different needs and requirements of users in terms of both quality of service (QoS) and user experience (QoE). In the last years, SDN has received significant attention from network researchers. SDN comes as a potential solution to network management, configuration, energy, scalability and many other issues affecting the IoT.

I propose, as shown in Figure 6.3, to adopt a four-plane SDN-like architecture following the cyber-physical system (CPS) model. Information from physical wireless sensors that constitute the **Data Plane (DP)** are fed back to a decision server. In addition to capturing data of interest, the sensors are able to perform a given number of moderately complex treatments with limited storing means. The gateway along with SDN controller, as one or separated entities, constitute the **Collect & Control Plane (CP)**. The SDN controller allows for network monitoring by sending commands to the devices in the data plane and collecting the required information from the physical network to build a centralized global view. This two-way connection allows for the realization of digital twins at higher plane for different physical assets of the DP. The gateway is in charge of gathering sensors application data and possibly applying treatments of medium complexity. Like the SDN controller, the gateway allows for the connection between the devices/assets in the data

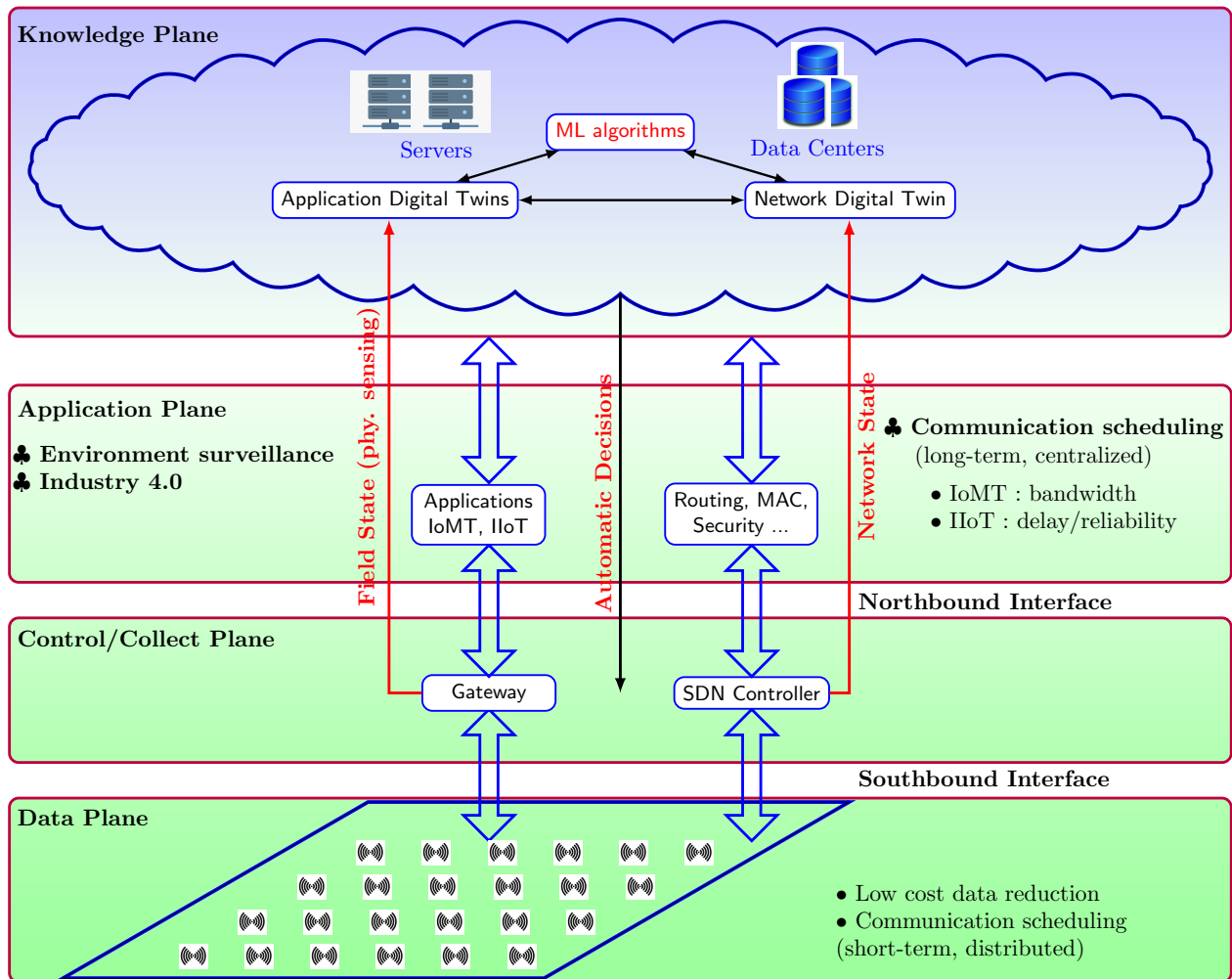


Figure 6.3: Four-plane DT-based KD-WSN Architecture.

plane and their corresponding digital twins. This level (CP) allows to have more computing resources while being close to both the source of the data and the end user. Moreover, it provides services on behalf of the **Application Plan (AP)**. Finally, I propose to realize the **Knowledge Plane (KP)** in the *cloud* that allows hosting the different digital twins and providing the necessary processing means to execute more powerful (ML) algorithms on the collected data.

This project aims to take a step forward to enable the KDN concept in the context of WSNs to consider not only knowledge for network management but also the knowledge that can be learned from the analysis of application data that is useful for the end users. Accordingly, the aim is to build a holistic digital twinning architecture where the communication network is integrated along with the other components of the system. In addition to the realization of the NDT⁴ (the digital twin of the communication network), one has to consider the network of digital twins (DTN⁵) to enable modeling of the interactions between the different DTs and PTs (§ 6.2). This research aims to investigate two use cases with distinct requirements, namely the Industrial Internet of Things (IIoT) and the Internet of Multimedia Things (IoMT). By addressing challenges associated with Industry 4.0 in the former and multimedia environment surveillance in the latter, this project intends to provide a concrete proof of concept.

⁴Network Digital Twin

⁵Digital Twin Network

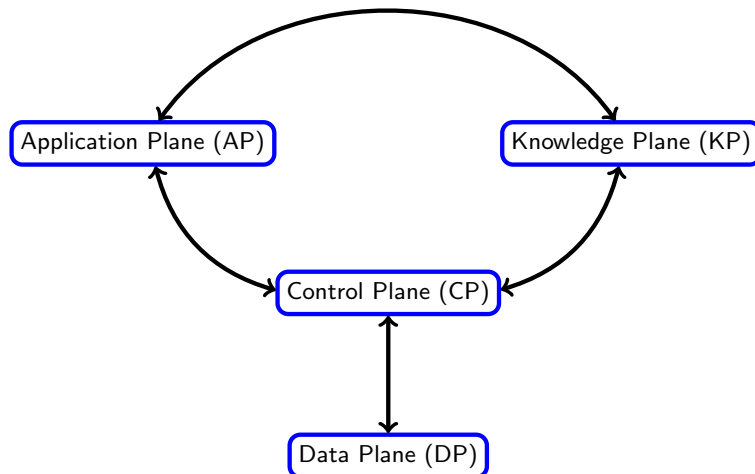


Figure 6.4: Interplane communication in the proposed architecture.

6.2 Digital Twinning and Communication Networks

Many Digital Twins of industrial systems exist nowadays. A wide range of industrial fields are concerned such as manufacturing [MPPU19, LZY⁺19], healthcare [BSdSvdH18], shipping [AG20], city management [FZYM21] and aerospace [MUMF21]. Despite the tremendous potential of DT-based systems and their growing number, having a perfect and synchronized real-time representation of any physical asset remains a challenging problem. The DT accuracy is highly dependent on the underlying communication networks especially for large scale systems. Adequate network services with good QoS/QoE are a prerequisite to achieve the expected functionalities with the desired performances. In spite of this, building a digital twin destined for communication networks has not received enough attention and is still in its infancy [VNT⁺22]. In our paper [KMR21], we proposed the concept of *Network Digital Twin* (NDT) in order to permit a closed-loop network management across the whole network lifecycle, from the design to the service phase. This allows to move from the current network design methodology to a more dynamic one where the output from both twins allows to improve the designed networking protocols and algorithms. At the service stage, the NDT will allow for real-time network monitoring, predictive maintenance mechanisms, and network diagnostics, etc. Additionally, I expect to consider the interactions between (and within) the different DTs and PTs in a holistic architecture.

Considering DT-based systems from a communication perspective is driven by the diverse interactions that take place within these systems, particularly in complex ones [AL⁺19]. In relation to the reference architecture outlined in Section 6.1, these communications can be broadly categorized into two main groups :

Interplane communications. These (Figure 6.4) can be qualified as *“vertical interactions”* since they occur between planes. The following are of particular interest in this project :

1. Communication between each digital twin, in the knowledge plane (KP), and its corresponding physical counterpart in the data plane (DP) is a fundamental element of the paradigm. It plays a crucial role in enabling synchronization between the twins. This communication operates bidirectionally, bridging the data and knowledge planes through the control/collect plane and potentially the application plane. Data related to the network and applications is transmitted to the KP where the DTs analyze and make decisions that translate into commands or, in certain instances, trigger reconfigurations that may require the transmission of firmware updates to the DP .
2. Communication between a digital twin (KP) and the real applications at the application plane (AP) whether or not related to the network. For instance, the NDT may consider translating application-level requirements into an appropriate demand for communication resources.

Intraplane communications. These take place between elements within one plane and can be qualified as "*horizontal interactions*". The most relevant to my research project are the following :

1. Communication between (sensor) nodes in the data plane (*DP*). These nodes constitute a WSN, the physical counterpart of the NDT. The NDT is in charge of optimizing the operation of the WSN by providing efficient and innovative solutions at the various levels of the communication stack throughout the whole lifecycle of the network.
2. Communication within the DTN that takes place between the different digital twins of the system, in particular between the NDT and other digital twins (ADT⁶) that mirror the different applications running on the underlying network. This communication takes place within the knowledge plane (*KP*) between DTs instead of direct interaction with the applications in the *AP* and the PTs in the *DP*. This allows substantial network load reduction as the communication does not involve the PTs. Information is reported only once, even in the presence of multiple DTs. Moreover, the information can be richer thanks to the data analysis performed by the DTs instead of raw data acquired from the PTs. Finally, cooperation between the digital twins not only becomes possible but also extends to the physical part, resulting in a tangible and efficient collaboration among the components of the physical system.
3. Communication between the digital twins and the (cloud) servers of the knowledge plane to benefit from the necessary computation and storage resources. Services based on (ML) data analysis, visualization and simulation models can be provided. One might consider implementing "*Siblings*" [RSK20] to perform simulations and run what-if scenarios for both service and model evolution to prevent problems and improve performance.

6.3 Digital Twin Modeling and Placement

While research on DT has significantly progressed over recent years, researchers still have a long way to go to narrow the gap between the digital twin and its physical counterpart. Obtaining a flawless replica of any physical object or phenomena poses substantial challenges. Main desired Properties of a DT [MLC20, Eri17, VNT⁺22] can be summarized as follows :

- **Representativeness.** The digital representation should be identical to the physical object or, at the very least, as similar as possible.
- **Promptness.** The digital twin must reflect the state of the physical twin in (or close to) real time.
- **Persistence.** The digital twin should exhibit persistence over time and capable of compensating for limitations and mitigating malfunctions of the physical twin.
- **Memorization.** The digital twin should possess the ability to store and represent both past and present data of the physical twin, effectively capturing and describing its behavior. This enables the digital twin to access historical information and leverage it for analysis, comparison, and decision-making processes.
- **Composability.** To analyze complex systems, it is essential to group their diverse components and examine both the composed object as a whole and the individual components separately. This approach allows for a comprehensive understanding of the system behavior, interactions, and dependencies, facilitating effective analysis and decision-making processes.
- **Context-awareness.** The digital twin should possess the ability to perceive and understand the context in which it operates. This contextual awareness equips the digital twin with valuable insights to make informed decisions, dynamically adapt to changes, and effectively interact with its physical counterpart and the broader ecosystem.
- **Replicability.** The digital representation should be replicable in different environments, allowing the creation of siblings that can be utilized for running what-if scenarios, among other purposes.

The continuous bidirectional connection between the two twins plays an important role in satisfying these

⁶Application Digital Twin

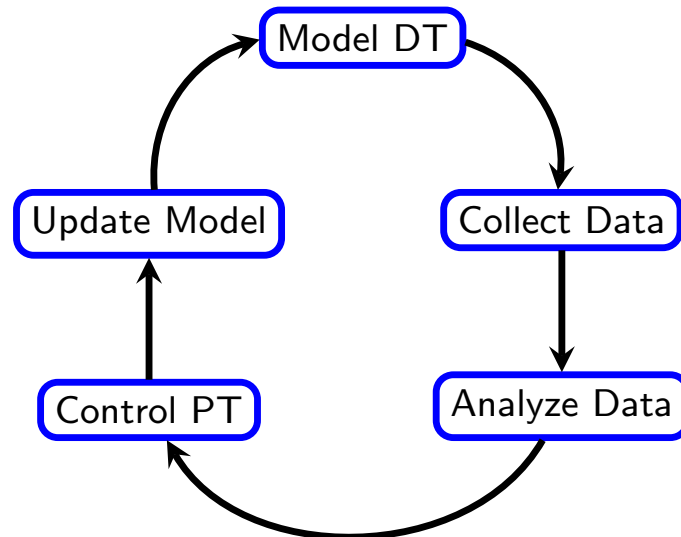


Figure 6.5: DT Modeling Process

properties ; otherwise, a DT would be no more than a set of powerful models, which we refer to as a *digital model*. Collected data from the real world are fed manually to the digital twin [Gri14]. When there is a one-way connection from the physical entity and its virtual representation, it is instead known as a *digital shadow*.

Incremental (Iterative) Modeling. One of the objectives of this research project is to build a network digital twin (NDT) to model the WSN used to collect the data from the physical world. To achieve these objectives, I suggest adopting an incremental (iterative) strategy that can be applied to build any DT (Figure 6.5). This approach is driven by the fact that achieving a flawless DT is almost impossible, particularly for complex systems characterized by a high degree of device heterogeneity, expansive geographical coverage, and the support of various applications [RMA⁺21]. Modeling the key aspects and features with respect to the application can be sufficient to obtain an operational DT. The well-known *Apollo 13 Mission* episode⁷, widely recognized as the pioneering implementation of a Digital Twin (DT), serves as compelling evidence that the process can yield significant benefits even when the employed models are not entirely accurate. Moreover, an incremental approach would allow for a step-by-step development process that can be applied to build and refine the DT over time. By incrementally adding and improving the components of the DT, continuous enhancement and adaptability to evolving requirements.

As an initial step, the adoption of a *digital model* based on "the known" can be considered. Depending on the characteristics of the PT and its intended application, this initial model may take the form of a physical (mathematical/statistical) model that is built upon established governing equations. These models are robust and enable predictions regarding the system response and behavior. Depending on the nature of the physical system, knowledge representation languages such as Petri nets and ontologies can be utilized during this stage [KMR23]. These models typically have universal validity and are capable of predicting any point covered by the model. However, they suffer from the following limitations :

- Extensive domain knowledge is required and "the known" is not sufficient since they are limited in capturing the full complexity and nuances of real-world systems.
- Mathematical or formal models rely on various hypotheses and complete assumptions about input/output must be made upfront, as a result a big chunk of the physics is ignored.

Subsequent steps (Figure 6.5) involve the collection of data to further mirror the actual state of the PT.

⁷blogs.sw.siemens.com/simcenter/apollo-13-the-first-digital-twin

Recent advances in IoT, especially in sensing technologies have led to the availability of cost-effective, lightweight, and high-performance sensors. This has enabled the collection of massive amounts of data from the physical environment. Moreover, the tremendous development of Cloud and HPC⁸ technologies has provided access to extensive storage and computational resources. This has facilitated the development of data-driven models, primarily leveraging ML techniques. These models enable the exploration of "the unknown" by producing models that can analyze the sensed data and infer new insights and knowledge from it. Nevertheless, ML-based models suffer from the following drawbacks that need to be considered, to name a few :

- The availability of an adequate volume of input data to train models with a satisfactory level of accuracy.
- ML models, particularly DL models, are often complex and lack interpretability. They operate as a black-box, providing predictions or outcomes without clear explanations.

Multilevel Digital Twinning. The actual implementation of a DT depends mainly on the PT nature, its target application and the intended services. The incremental approach assumes that the DT will become operational after a finite number of iterations, with its accuracy keeps improving as more data is collected. Meanwhile, the models may become increasingly complex requiring an ever greater amount of resources which can be definitely provided by the cloud but another issue arises. The responsiveness of the DT may become significantly slow which can affect the timeliness of the PT functioning. To achieve higher "promptness", one approach is to place the digital twin as close as possible to the PT, such as at the Fog or even Edge level. However, limited resources at these levels necessitate compromises in terms of accuracy, thereby affecting the DT "representativeness". This can be generalized to multiple DTs with different abstraction levels (granularities) and using different modeling frameworks located at different positions along the *Edge-Cloud Continuum*. The following optimization problems have to be jointly addressed with respect to multilevel digital twinning considering the four-plane architecture presented in § 6.1 :

- The problem of the optimal number of modeling levels to consider.
- The problem of temporal consistency between the DTs.
- The problem of the optimal placement of the different DTs.

6.4 From Industrial to Natural Environment Digital Twinning

In recent years, digital twinning research has been conducted in various domains, covering both "natural" and "built" environments. The term "natural" refers to ecological units that operate without any human intervention, encompassing elements such as the planet Earth and its subsystems like forests, lakes, etc. On the other hand, "built" environments refer to human-created structures designed to facilitate various activities. In this project, we will utilize the introduced DT-based KD-WSN architecture (§ 6.1) to address some issues encountered in the context of a human built environment, namely Industry 4.0, in addition to some challenges faced in natural environment surveillance applications. These problems will be chiefly tackled from a communication network perspective by considering its impact. The interaction between the NDT and the ADTs should be strengthened and the surrounding environment context to be taken into consideration [PZCG14, EAG21]. A particular emphasis will be devoted to the problems related to knowledge extraction (§ 6.5) and communication resource allocation (§ 6.6) in a highly constrained environment, the LLN.

The Industrial Internet of Things (IIoT) [SSH⁺18] is completely transforming current industrial system design. The fourth industrial revolution is underway with new functionalities in the sights such as real-time distant monitoring and control, big data analytics and predictive maintenance [ACQB21]. These features can be achieved through the adoption of wireless communication technologies such as sensor networks,

⁸High Performance Computing

which are crucial to ensure a fast and low-cost deployment of IIoT systems [ODK20]. They chiefly enable collecting the required data that contribute in the realization of digital twins of the physical assets that compose the industrial system. Digital twinning paradigm is expected to enable more efficient solutions as industrial systems are known to be complex. Regarding Industry 4.0, we already initiated the construction of a NDT aiming to meet the strict requirements in terms of energy and quality of service of industrial applications [KMR21, KMR22b, KMR22a]. The built DT will mainly serve to solve the problem of communication resource allocation detailed in § 6.6.

Human-built environments, such as industrial systems, exert a significant influence on the natural environment. Taking actions at various levels is crucial to protect and preserve Earth's ecosystems. A key aspect in this endeavor is the development of indicators or measures that facilitate the assessment of environmental changes, aiming to mitigate ecological damage. One effective approach to achieve this is through the utilization of WMSN⁹ [SHB⁺22, SMR⁺22] for environmental monitoring. Unlike the traditional method of relying solely on human observations for data collection, the use of wireless sensor networks offers compelling advantages and holds great promise in this context, enabling :

- Operation in remote locations with limited or difficult access, even in extreme conditions such as typhoons or hurricanes. This capability allows for data collection in areas that may be challenging or unsafe for human beings.
- Reduction in logistical and maintenance costs, particularly in cases where the target field is large and requires frequent or intensive data sampling. Wireless data transmission from sensors to a central collection station eliminates the need for manual data collection and prevents local storage devices from becoming overwhelmed.
- Unobtrusive observation of phenomena, particularly in the case of wildlife and bird monitoring. Observers can be located far away in their labs, eliminating disturbance to the observed targets.
- Real-time or near-real-time processing and delivery of collected data, even over an extended duration. The use of WSN eliminates the need for offline data processing, enabling timely analysis and decision-making based on the collected data.

Despite the undeniable benefits of wireless sensor networks in natural environments, there is still a major obstacle to overcome : the large-scale deployment of the WMSN in such environments. The natural surroundings present harsh and unpredictable circumstances that were previously unseen and not accounted for during pre-deployment testing, leading to potential bugs and performance degradation in the deployed WMSN. The complexities and uncertainties of the natural environment, which can negatively impact sensor outputs, degrade the quality of wireless links, and strain network nodes, cannot be fully captured and modeled solely through simulations and laboratory testbeds [RR07]. The LOFAR-agro project illustrates perfectly the problems we could face during the actual deployment of the network in a real environment [LBV06]. The project team reports an endless stream of hardware malfunctions, programming bugs, software incompatibilities when considering 100-node network and even when considering a short-scale deployment with 10 nodes. These issues were initially overlooked during simulations and can be imputed to the lack of continuous connection between the real world network and the design/validation process. By creating a digital twin of the wireless network, a "living model" that is kept constantly updated, decisions are, therefore, made based on current conditions rather than those of the original study. This approach allows for a more accurate representation of the network's behavior in real-world scenarios, enabling better decision-making and mitigating potential issues that may arise during large-scale deployment in natural environments.

Actual deployment of WMSN in a natural environment poses significant challenges. To address these challenges, I propose leveraging the NDT to mitigate the unexpected issues during the real deployment process. An iterative strategy can be followed (§ 6.3), starting with an initial solution that incorporates basic features. Based on the feedback from the physical network, the solution is continuously enhanced

⁹Wireless Multimedia Sensor Networks

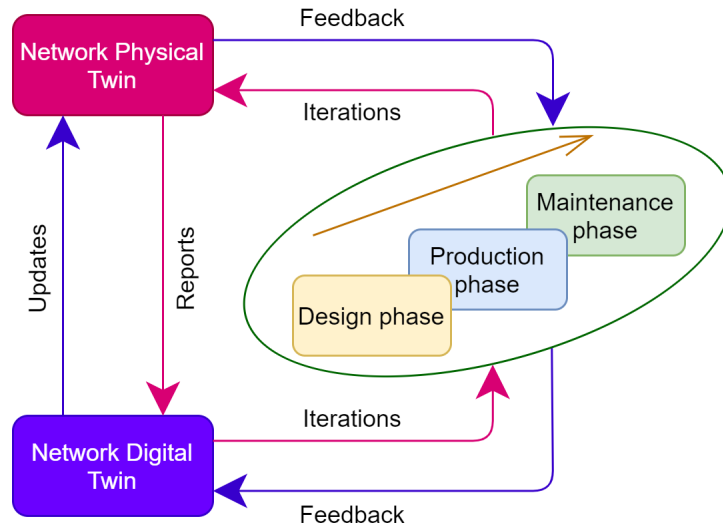


Figure 6.6: NDT throughout the whole network development process.

and enriched with new features. The iterative process is repeated as in Agile methodology until the network reaches full functionality. Throughout the entire life cycle of the WSN, the connection between the network twin and the physical network is maintained. As depicted in Figure 6.6, modeling and analysis can be tightly coupled with execution, enabling a cycle of continuous improvement and innovation. The digital twin enables proactive measures to enhance network reliability and address potential risks by predicting future network states using AI algorithms, for example. Improved performance can also be achieved by dynamically adjusting network configuration based on various options, adapting to evolving traffic and resource demands. Additionally, different solutions can be safely experimented with to determine the optimal network configuration without jeopardizing the operation of the physical network. This approach eliminates the risks associated with testing new network policies in a production environment and reduces costs since experiments can be conducted within the network digital twin. To sum up, by leveraging the NDT, the deployment of WMSNs in natural environments can be significantly improved, ensuring greater reliability, adaptability, and cost-effectiveness throughout the network operational life.

When it comes to monitoring the natural environment, the focus lies in the surveillance of waterbirds in their natural habitat. In this regard, I aim to develop an ADT that works in cooperation with the NDT. The aim is not to create a comprehensive ADT, but rather to focus on the most important blocks (including contextual elements) that are of interest for waterbird surveillance application (see § 6.5). Although the concept of DT is quite recent, it can be viewed as well-established in the industrial domain. In the natural domain, it is still in its infancy and raises issues of a mostly different nature [Bla21]. Some initial works have explored building digital twins for underwater ocean observation systems [BPH⁺21], forest ecosystems [BYV22], Earth's ecosystem [BSH21, DO22], river basin [WY22] and smart agriculture [AAG⁺20]. However, confusion between a digital shadow and a digital twin still prevails, and the foundational element of "interventions" when developing their DT systems is almost overlooked. Moreover, apart from [BPH⁺21], existing research tends solely to focus on developing the digital twin of the target environment, assuming that the monitoring infrastructure, including the WMSN, will be flawlessly deployed without any issues. However, as previously discussed, this is not always true, especially in large-scale deployments [KMR21]. This research is motivated by the absence of studies related to DT development specifically for bird monitoring. Its novelty resides in considering the interaction with the NDT and other DTs. Specifically, the applications requirements can be translated into an appropriate computation and communication resources allocation.

6.5 Knowledge Extraction for Natural Environment Surveillance

Waterbirds Surveillance Context. Wetlands, including marshes, lakes, wet meadows, . . . , encompass approximately six percent of the Earth’s surface. These unique ecosystems are renowned for their rich biodiversity and are among the most diverse habitats on our planet [SZ95]. Unfortunately, over the past century, more than half of the world’s wetlands have been lost. Today, these environments continue to face threats from urbanization, agricultural intensification and pollution. In 1986, France made a commitment to preserve the wetlands within its territory by signing the Ramsar Convention¹⁰, an international agreement adopted on 2 February 1971. Currently, France boasts 49 sites “Ramsar”) with the *Grand Est* region being particularly abundant in wetland areas. Notably, the *Étangs de la Champagne humide*, spanning an impressive 2.558 km², represents the largest Ramsar site on mainland France.

Wetlands provide a habitat for a remarkable array of animal and plant species. They serve as vital ecosystems, offering sanctuary to tens of thousands of waterbirds during winter or migration periods. With approximately 10,000 recognized bird species worldwide, avian populations act as responsive indicators of environmental changes and play a crucial role in maintaining biodiversity. Moreover, birds contribute significantly to environmental stability and security. The decline of certain avian species can disrupt the delicate balance of the food chain, jeopardizing environmental integrity and potentially impacting public health. Within the French wetlands¹¹, some waterbird species are threatened with extinction [BCKZ16]. Although some species can still be considered as breeding, others have sadly become extinct within France. This highlights the immense importance of wetlands and underscores the necessity for their preservation and diligent conservation efforts.

Monitoring fauna and flora, especially birds in their natural habitat, offers several benefits [Arc11] : (i) it provides a reliable indicator for assessing the population trends of endangered bird species in a particular area over time ; (ii) birds can serve as effective indicators for monitoring environmental and public health conditions ; (iii) effective monitoring can help prevent significant economic losses. To achieve this, a wireless multimedia sensor network (WMSN) [AMC07, Yan14] can be deployed in to monitor migratory birds in their natural habitat (wetlands). The network can incorporate acoustic and image sensors along with other presence detection sensors to identify, recognize and count the number of bird species, particularly those considered threatened. Birds vocalizations such as songs and cries can be used for species identification, while photographs can be taken to capture significant events and better analyze the individuals present in a specific spatio-temporal context.

Problem Statement. Monitoring waterbirds in their natural habitat using a wireless sensor network must consider issues related to massive data collection (multimedia) as well as automatic analysis of the collected data [GO04]. Once again, we encounter challenges related to the IoT 4V attributes. The collection of diverse and large-scale data, with high acquisition rates, using a resource-constrained infrastructure such as a WSN, presents a real challenge that requires significant efforts from the scientific community. These applications have specific needs in terms of quality of service, bandwidth and, not least, storage and processing capacities. Meeting these requirements often leads to substantial energy consumption.

In order to accommodate the high bandwidth requirements, there are two complementary solutions that should be jointly explored. The first solution involves increasing the available bandwidth through high-performance network services and protocols. These services may include optimized resource allocation mechanisms coupled with an efficient routing protocol (see § 6.6). The second solution consists in reducing the amount of visual data captured *at the source* before transmitting it to the base station while still preserving important information for analysis [Mai18b, AKM⁺23, AKHM23].

The analysis of the collected data using efficient algorithms is of a paramount importance to provide the expected added value to the application, particularly in tasks such as automatic recognition, classification

¹⁰International treaty to protect wetlands.

¹¹datazone.birdlife.org/country/france

and counting of birds. Conducted by a human, these tasks can be tedious and prone to inaccuracies. For example, ensuring the identification of identical birds observed at different times becomes challenging. Automatic detection and recognition algorithms can be used to fully exploit the collected data and minimize human intervention. This approach is particularly valuable for predicting environmental behavior, where avian species often serve as relevant indicators. To accomplish this, I expect to use deep learning-based object detection techniques [ZZXW19], specifically convolutional neural networks (CNNs) [ZZXW19]. These models can be trained to detect and classify both dynamic objects (such as animals and humans) and static objects (such as trees and water lakes) based on the images captured by the WMSN. The detected dynamic objects can be stored in a database along with relevant object information for further analysis and interpretation.

The objective is to establish an intelligent data collection and transmission system in an environment considered to be hostile. The harsh conditions prevalent in this environment inevitably impact the quality of data collected by the sensor nodes deployed in the area of interest. Transmission of data is particularly subject to significant packet loss, attributed to the constraints imposed by the surveillance infrastructure, causing damaging holes to appear in the received images. Moreover, during data capture, the resulting images are subject to a "blurring" effect essentially due to the natural movements of birds and the dynamic environment. Additionally, the adoption of low-cost compression techniques may introduce noticeable distortions due to the high compression levels required. Furthermore, the sensors themselves may produce additional noise in the captured data. These factors collectively affect the performance of the system. To address these challenges, the application of inpainting, denoising, and deblurring techniques becomes inevitable.

Addressing this challenge, a preliminary study has been conducted (§ 4.3), proposing a complete and efficient encoding-transmission-reconstruction chain [MSR⁺22]. In addition to employing a low-complexity image compression method, a well-suited packetization scheme is introduced. At the receiving end, more powerful resources are leveraged to apply deep learning models to compensate for the distortion caused by the adopted lossy compression as well as to fill in the gaps induced by packet losses. The obtained results show the effectiveness of the proposed chain. This work has to be pursued :

- Enhance the DL models by expanding their training dataset to include more images that exhibit loss patterns similar to those encountered in an LLN environment ;
- Consider the impact of image quality degradation on the performance and effectiveness of object recognition algorithms [FDBD21] ;
- Explore the feasibility and benefits of capturing and transmitting low-resolution images, and investigating the application of super-resolution models [GGW⁺19] to enhance image quality.
- Assess the significance of sending only ROIs or prioritizing their transmission with higher reliability to optimize resource utilization and enhance recognition accuracy.

6.6 Communication Resource Allocation : TSCH Communication Scheduling

Efficient resource allocation is of paramount importance in communication networks as it directly affects its overall performance. The management of available communication resources needs to be dynamic and adaptable to the fluctuations in wireless channels and traffic loads. Additionally, it is crucial to handle the QoS/E requirements of different applications while dealing with scarce resources. In wireless networks, communication resources allocation at the MAC layer can be performed using a random access protocol such as CSMA/CA¹². Although CSMA/CA is easy to implement and requires no explicit management, it has been observed to experience high packet loss rates [DMPFJ12]. This motivates proposing collision-free protocols based on a scheduling strategy such as TDMA¹³. TDMA-based protocols are more suitable to industrial applications where energy efficiency and strict QoS requirements in terms of delay, relia-

¹²Carrier-Sense Multiple Access with Collision Avoidance

¹³Time-Division Multiple Access

bility, determinism and robustness are crucial [SDK20]. In the context of LLNs, the 2012 IEEE 802.15.4e amendment [std12] introduced several channel access modes, including TSCH¹⁴ and DSME¹⁵ that have been integrated into the 2015 IEEE 802.15.4 standard [std16].

TSCH in a nutshell. TSCH protocol is designed to achieve high reliability while ensuring minimal power consumption in sensor devices. It benefits from a time-slotted multichannel-access mode to enable efficient resource utilization and increase network capacity through spatial reuse of time and frequency. The protocol also incorporates channel hopping, which helps mitigate interference and the effects of multipath fading. In TSCH, time synchronization is achieved using a slotframe structure that repeats over time. The slotframe is composed of a set of timeslots in which communication can occur. The duration of a timeslot is sufficient to accommodate the transmission of a maximum-length packet and the corresponding acknowledgment from the receiver. By activating the radio only during active slots, energy consumption is significantly reduced. Additionally, TSCH employs multiple channels, typically 16, with a schedule that allocates cells (timeslot, channel offset pairs) to nodes. By default, a cell is *dedicated* meaning that it is assigned to one particular node guaranteeing contention free communication. The IEEE 802.15.4e standard allows for a cell to be shared where collisions are dealt with using a CSMA-like backoff scheme. A different channel is guaranteed to be used in the same timeslot in successive frames if the slotframe size and the number of channels are relatively prime. Additionally, a subset of channels can be blacklisted to restrict the available channels for coexistence purposes.

6TiSCH. The interconnection of WSNs with the Internet is a crucial aspect in the process of the IIoT evolution. To bridge the gap between TSCH and 6LoWPAN networks, the IETF established the 6TiSCH¹⁶ Working Group (WG) to enable IPv6 connectivity for low-power industrial devices [VWC⁺19]. In particular, a 6TiSCH architecture was defined [Thu21] (Figure 6.7) in which the scheduling function (SF) and the 6top sublayer [WVW18] are considered as key building blocks. SF allows nodes to dynamically allocate cells, while the 6top sublayer is used to negotiate with neighbors to establish a coordinated schedule with common cells. MSF¹⁷ is considered as the reference SF [CVDD21], although other SFs can be defined to meet the specific requirements of different applications. 6TiSCH involves an abstract NME¹⁸ responsible for managing the device schedule and other related resources. The NME can collaborate with a PCE¹⁹ to minimize interaction and reduce the burden on the resource-constrained devices. This model is an adaptation of the DetNet²⁰ architecture in the context of TSCH, allowing for Traffic Engineering with deterministic properties.

TSCH Scheduling Problem. While the IEEE 802.15.4e standard defines how the MAC layer executes a schedule in the network, it does not specify how such a schedule should be constructed. The specification of the access schedule is left to higher protocol layers. Designing an optimal schedule is a complex problem known to be NP-hard, as established by previous research [GDP08]. As a result, the development of efficient scheduling algorithms remains an open challenge that requires further attention from both academic and industry researchers. Depending on the targeted application, a TSCH scheduler should consider the following main requirements/features :

- deterministic and possibly short latency ;
- reliable communication ;
- high throughput ;
- efficient usage of the available resources : bandwidth, energy , computation ;

¹⁴Time Slotted Channel Hopping

¹⁵Deterministic and Synchronous Multi-channel Extension

¹⁶IPv6 over the TSCH mode of IEEE 802.15.4e

¹⁷The Minimal Scheduling Function

¹⁸Network Management Entity

¹⁹Path Computation Element

²⁰Deterministic Networking

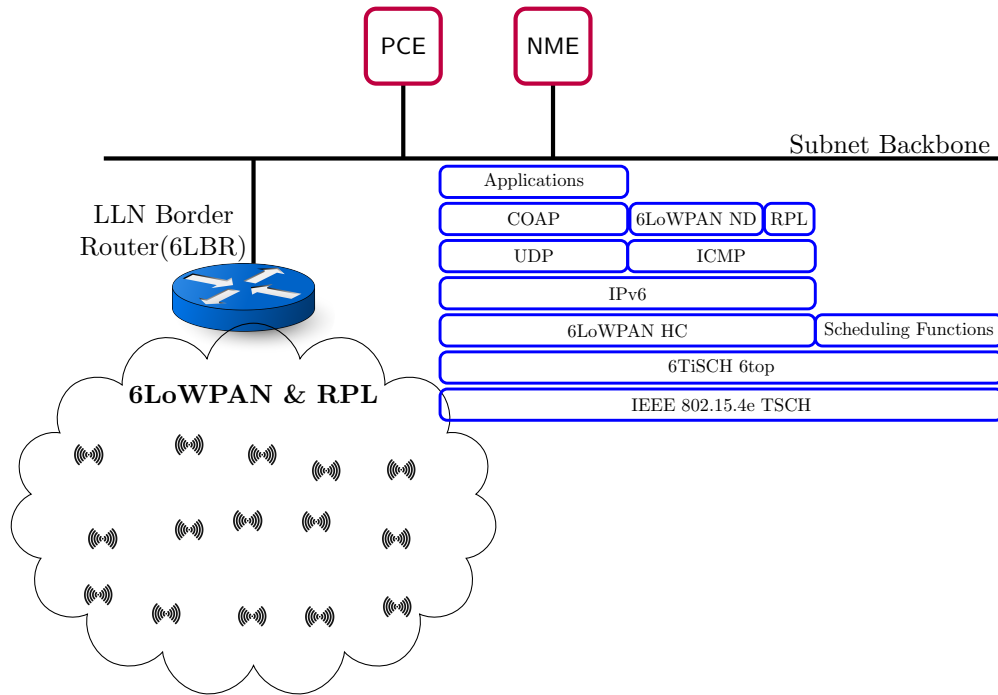


Figure 6.7: 6TiSCH High Level Architecture [Thu21]

- scalable (increasing number of nodes) and dynamic (topology changes, traffic demand evolution) scheduling algorithm ;
- heterogeneous traffic handling (traffic awareness) .

To fulfill the requirements of different applications, scheduling algorithms in the literature have employed various approaches and strategies, which can be classified into three groups [KSM⁺23], namely, centralized, distributed and autonomous protocols. In the first group, a central entity possessing a full knowledge of the network characteristics, is in charge of building the final schedule [PAD⁺12, JKWS16, GMMP15]. While these approaches have demonstrated their efficiency in terms of optimal schedule and traffic awareness, mainly for relatively static topologies, they suffer from the overhead of additional control messages required to make the central node aware of the network dynamics in a timely manner. As a result, they have been found to scale poorly in large and dynamic topologies. As a result, distributed approaches [CWWV16, MSL18] have gained popularity as they rely on negotiation among neighboring nodes. These distributed approaches are known to be more resilient to network dynamics (traffic and topology) while reducing the network overhead compared to centralized schemes. The autonomous category [DANLW15] encompasses schedulers that operate without the need for exchanging control messages. Instead, they exploit the existing stored data, such as cross-layer routing information [UKO22].

Toward a DT-based ML Hybrid Scheduling Algorithm. This part of my research project aims to address the problem of communication scheduling in the presence of *highly* heterogeneous traffic, which has not been sufficiently investigated in the context of the IEEE 802.15.4e standard. Most existing work has focused on low data rate traffic and has not addressed highly heterogeneous traffic [RVDA20, EKKK20, OEPP21]. However, it is crucial to address this issue since a wide range of current and future IoT applications require support for heterogeneous flows to meet the diverse requirements of end-users. In addition to scalar sensors that generate low-rate data, other sensors with much higher bandwidth requirements, such as multimedia sensors, are more than necessary in surveillance applications [MPH09, AKM⁺23]. In industry 4.0, Visual sensing is of utmost importance to create 3D visualization for the digital twin paradigm [HGZ18].

Highly heterogeneous traffic conditions are challenging due to the coexistence of multiple data flows with

varying rates and requirements within the same network. Hence, more effort must be made to ensure efficient communication. In our preliminary study [KSM⁺23], we have focused on evaluating decentralized scheduling algorithms under highly heterogeneous traffic conditions. Although some protocols have shown promising results, none have been able to fully accommodate the diverse needs of the heterogeneous flows. To address this issue, it is necessary to make scheduling on a per-flow basis depending on the application needs. For instance, light traffic originating from scalar sensors may require timeliness and reliability, while heavy traffic from visual sensors may prioritize bandwidth allocation with less emphasis on reliability. .

Based on the current state-of-the-art, promising solution to address the challenges of communication scheduling in highly heterogeneous traffic conditions could be a hybrid approach [APB⁺13, AR17]. This approach involves a centralized entity (the DT at the KP) that is responsible of providing a long-term allocation scheme while a short-term schedule is to be ensured at the edge (DP) in a decentralized strategy. The DT, utilizing the abundant resources of the cloud infrastructure, leverages powerful ML models to optimize the overall schedule, taking into account various factors such as traffic characteristics, network conditions, and application requirements. At the edge level, the short-term scheduling allows to deal with frequent changes and can make use of RL algorithms [KSM⁺22][NDNQK⁺19][PKKM20]. By combining the strengths of both approaches, this hybrid solution will enable the system to achieve the benefits of long-term optimization while maintaining flexibility and responsiveness to dynamic traffic conditions. This research direction opens up opportunities to develop efficient and adaptive communication scheduling mechanisms that can effectively handle highly heterogeneous traffic in IoT networks.

6.7 Project Timeliness and Positioning

The purpose of this section is to highlight the significance and relevance of my research project at various levels, including international, national, regional, and local contexts. Additionally, it explores potential funding strategies for supporting my future research endeavors.

My research project aligns with the objectives and vision of the MPSI²¹ department of CRAN for the upcoming years. It directly contributes to the development of the highly significant field of Industry 4.0. The identified research issues clearly contribute to the problem of modeling, especially using digital twins to address the challenges pertaining to both the network infrastructure and the targeted applications. This project aligns seamlessly with the anticipated progression of the ARN²² project, which seeks to strengthen its activities in network control with a specific emphasis on the SDN and KDN paradigms. A key aspect of this project's vision involves harnessing AI algorithms to optimize the functioning of communication networks, rendering them more intelligent, and ensuring their compatibility with environmental considerations. In my project the KDN paradigm is expected to be implemented using digital twins (§ 6.1).

In addition to collaborating with the members of the ARN team, my proposed research project offers ample opportunities for cooperation with other teams within the department, particularly the COPIL²³ project. Aiming to establish a common platform for conducting experiments with digital twins in cyber-physical systems, I recently joined the CRAN action "TwinForAll", led by William Derigent and Michaël David. "TwinForAll" will provide a solid foundation for fostering collaboration and knowledge exchange among researchers in the field of digital twins. There is significant potential for a fruitful partnership in the near future. The shared interests and expertise within the "TwinForAll" project will create an ideal environment for exploring common research objectives, sharing resources, and collectively advancing the field of digital twins.

The expected contributions of my research project align closely with the digital, industrial, and environmental transitions highlighted at the University of Lorraine, particularly within the "Cobots and Industry of

²¹Modélisation, Pilotage et Sûreté des systèmes Industriels

²²Autonomous & Resilient Networks

²³Modélisation des COonnaissances et PILotage des systèmes industriels cyber-physiques

the Future” initiative supported by the LUE²⁴. By addressing the challenges and opportunities presented by Industry 4.0, my project aims to contribute to the advancement of digital technologies and their integration into industrial processes. To secure funding for my research, it is essential to leverage the growing interest and adoption of Industry 4.0 principles among companies. The Grand’Est region has recently announced the ”Industry of the Future” plan, which provides financial support to companies seeking to incorporate Industry 4.0 concepts into their production processes. This presents an excellent opportunity to establish stronger connections between academia and industry, fostering collaborative partnerships that drive innovation and progress. As part of Action 30 ”*Soutien aux chaires industrielles*” of the Grand’Est region, an application for funding can be submitted, in partnership with a regional company. At the national level, artificial intelligence holds a prominent position among the five strategic priorities outlined in the ANR²⁵’s 2023 action plan and the ”*France 2030*” program. My research project aligns directly with these priorities and is in clear accord with the ANR’s established focus areas (PEPR²⁶). In particular, the ANR has identified communication networks as a key area of interest, encompassing advanced cloud and 5G technologies. Additionally, my project also resonates with the ANR’s focus on digital technology for agro-ecology, which addresses the intersection of digital innovation and sustainable practices.

Digital twinning has gained considerable attention within the French scientific community, particularly as a response to challenges hindering the effective implementation of Industry 4.0. In line with my project focusing on the network digital twin (NDT) for Industry 4.0, a PRCE²⁷ project titled ”Reliable Orchestration and improved availability for IIoT networks Using Standard internet protocols and digital Twin” has been submitted and successfully passed first step of the selection process. This collaborative project involves a consortium comprising ICube Labs (Strasbourg University) and notable companies such as Orange (Grenoble), Technology & Strategy (Schiltigheim), and Orisun (Strasbourg). Even though the project was not selected for funding, the experience gained from the collaboration remains valuable. It demonstrates a proactive approach towards addressing the challenges in wireless communication in the context of the Internet of Things and Industry 4.0. Moreover, it provides valuable insights and potential for future collaboration with a unique opportunity to engage in standardization efforts conducted by the RAW²⁸ working group of the IETF²⁹.

My research work aligns well with the research topics and initiatives promoted by national research groups (GDR) in France. Specifically, within the MACS³⁰ group, the action ”*Jumeaux Numériques*” (digital twins) is directly relevant to my project. The concept of digital twins and their application in various domains is an area of active interest and exploration within the MACS group. Furthermore, my project also relates to the research areas covered by the RSD³¹ group, specifically the actions ”*Énergie*” (Energy), ”*Plateformes*” (Platforms), and ”*Reproductibilité*” (Reproducibility). These actions encompass topics related to energy efficiency, platform development, and the reproducibility of research results, which are highly relevant to my work in the context of communication networks and digital twinning. Being aligned with these national research groups provides an opportunity for collaboration, knowledge sharing, and dissemination of research findings within the relevant scientific community in France.

At the international level, there are ongoing collaborative projects with Algerian universities that require further development, particularly in the area of natural environment surveillance. To strengthen these collaborations, a new PHC application is being prepared for submission. The collaboration involves working with K. Berkane, a Professor of theoretical physics from the University of Setif, to focus on developing efficient deep learning models with a specific emphasis on explainable artificial intelligence (XAI). With

²⁴Lorraine Université d’Excellence

²⁵Agence Nationale de Recherche

²⁶Programmes et équipements prioritaires de recherche

²⁷Projet de Recherche Collaborative Entreprise

²⁸Reliable and Available Wireless

²⁹Internet Engineering Task Force

³⁰Modélisation, analyse et conduite des systèmes dynamiques

³¹Réseaux et Systèmes Distribués

respect to this latter topic, a cooperation within the GENIAL³² consortium has been initiated with Professors M. S. Hossain from the University of Chittagong, Ah-Lian Kor from Leeds Beckett University, and Karl Andersson from Lulea University.

At the European level, I anticipate exploring funding programs and open calls within "Horizon Europe" especially in the domains of "Cluster 4: Digital, Industry and Space" and "Cluster 6: Food, Bioeconomy, Natural Resources, Agriculture and Environment". As the *Principal Investigator* for the University of Lorraine, I am actively involved in the preparation of *DaCenSus* (Data Centers - towards a Sustainable future) to establish a "Marie Skłodowska-Curie Industrial Doctoral Network Cooperation" in cooperation with the universities of Twente, Lulea, the Research Institute of Sweden, and the Spanish National Research Council. The consortium includes several industrial partners, among them Ericsson, Beeyon, Techbuyer, DECOM, etc. *DaCenSus* project aims to address the challenges posed by data centers (DCs) in terms of energy consumption, resource scarcity, societal impact, and data security. It seeks to develop technical and governance approaches to enhance the sustainability of DCs across their entire lifecycle. It also aims to train a multidisciplinary cohort of experts who can work collaboratively in the intersection of the digital and energy sectors.

³²Erasmus Mundus Joint Masters Degree

Part III

Curriculum Vitae

Chapter 7

Curriculum Vitae

Name : MAIMOUR

Surname : Moufida

Date of birth : September 14, 1975

Associate Professor

TELECOM Nancy - Université de Lorraine

Centre de Recherche en Automatique de Nancy (CRAN)

MPSI¹ Department - Modelling, Control and Safety of Industrial Systems

ARN team - Autonomous & Resilient Networks

Address 1 CRAN (UMR 7039)

Campus Sciences - BP 70239

54506 VANDOEUVRE Cedex

moufida.maimour@univ-lorraine.fr

Address 2 TELECOM Nancy

193 Av. Paul Muller

54600 Villers-lès-Nancy

moufida.maimour@telecomnancy.eu

Professional Experience

Sep. 2004- **Associate Professor**

TELECOM Nancy, Lorraine University

CRAN (Centre de Recherche en Automatique de Nancy)

CNRS (UMR 7039)

2003/2004 **Lecturer - ATER** (attachée temporaire de l'enseignement et de la recherche)

Institut Galilée, Paris 13 University

L2TI (Laboratoire de Traitement et Transport de l'Information)

¹Modélisation, Pilotage et Sécurité des systèmes Industriels

Education

- Nov. 2003** **Ph.D. Degree in Computer Science**
"Design, Analysis and Validation of Router-Assisted Reliable Multicast Potocols in Wide Area Networks"
LIP (Laboratoire Informatique du Parallélisme) at ENS Lyon & University Lyon I
Supervisors : CongDuc Pham & Pascale Vicat-Blanc
Defense Date : November 25, 2003.
Appreciation : With Honors (Mention : Très Honorable).
President : Serge Fdida (Professor, Sorbonne University)
Reviewers : Guy Leduc (University of Liège) & Jean-Jacques Pansiot (University of Strasbourg)
Examiners : Alain Milles (University Lyon I)& Vincent Roca (INRIA)
- Jul. 2000** **Research Master Degree (DEA - Diplôme des Études Approfondies)**
Fundamental Computer Science. Major "Networks, Systems, Computer Hardware and Parallel Computing"
ENS Lyon & University Lyon I
Master thesis "Performance Evaluation of Active Reliable Multicast Protocols"
Supervisors : CongDuc Pham and Bernard Tourancheau
- 03-07/1999** **R&D Internship**
LIGIM - University Lyon I. "Design of a Viewpoint Integration Model in a Collaborative CAD Environment"
- Jul. 1998** **Engineer Degree in Computer Science.**
University of Constantine (Algeria)
Top of class (each year)
- 1997/1998** **Half-time Engineer Internship** (ENAD corporation) "Fuzzy controller design for a chemical production system"
- 1993** **BAC "Baccalauréat"** - Major : Mathematics (Série C)
Appreciation (Mention) : Bien

Attended Training Courses

- "Mental Health First Aid - PPSM²", 2 days, Nov. 2022
- "Keysight Cybersecurity platform *BreakingPoint*", 3 days, Sept. 2022
- "Pedagogical day on skills : From defining to assessing skills", 6h, March 2021
- "Writing your own application for a promotion, reporting on a colleague's application", 2h, Jan. 2021
- "Support for thesis supervision", 2 days, Dec. 2020
- "Cybersecurity *cyber-range* of diateam", 2 days, Jul. 2019
- "Project Management" 1 day, 2009
- "Cisco CCNA Instructor Training" 5 days in 2006.

²Premiers Secours de Santé Mentale

Awards

- Best Paper Award from the IEEE ISCC'2003 Conference.
- Winner of BAF competition (1998) to obtain a Ph.D. scholarship in France (7 winners in Algeria national level)
- Top of Class Medal from the University of Constantine (Algeria)

7.1 Summary of Teaching/Administrative Activities

Hourly Volume over the last 8 years (HETD) :

2015/2016	2016/2017	2017/2018	2018/2019	2019/2020	2020/2021	2021/2022	2022/2023
269	285	287	280	270	117 ³	268	219

Main Teaching Themes

- **Communication Networks**
 - All communication stack layers (OSI, TCP/IP)
 - Network programming : sockets in java and C, ...
 - Preparation for Cisco CCNA1-4 certification.
- **Operating Systems (OS)**
 - Parallel algorithms, mutual exclusion, synchronization and deadlock problems, ...
 - System (C) programming (implementation of the above concepts).
 - Operating system design & Study of UNIX-like OS.
 - System and network administration.
- **Computer Architecture**
 - Computer system principles.
 - Computer architecture.
 - Assembly programming (x86, arm, ...).
- **Quantitative Performance Evaluation (Communication Networks)**
 - Simulation-based Evaluation (PARSEC, ns2, Cooja).
 - Analytical Evaluation (queuing models, Markov chains, ...).
- **Operational Research & Graph Theory**
 - Graph Theory : general principles, shortest path problem, maximal flow problem, ...
 - Operational Research : mainly linear programming.
- **Algorithms and programming** in Delphi/Pascal, Java, C & Shell

7.1.1 Teaching Activities Tables

TELECOM Nancy⁴ :

Module	Audience	Hourly Volume	Period
Operating Systems (Advanced)	2A	CM(10) TD(10) TP(4)	2005-
Operating Systems (Design)	2A FISA	CM(10) TD(12) TP(4)	2014-
Operating Systems (Programming)	2A	TD(6) TP(8)	2004-2007 2021-
Performance Evaluation	2A	TP(8)	2016-2020
Communication Networks	1A	TD(8) TP(8)	2021-
Assembly Programming (ARM)	1A	TP(16)	2021
Communication Networks (Advanced)	2A	TD/TP(18)	2004-2020

⁴nA : year n - \approx 130 students per class. FISA : Formation Initiale par Apprentissage \approx 24 students

Computer Architecture Fundamentals	1A	TD(16) TP(12)	2004-2020
	1A FISA	TD(16) TP(12)	2013-2020
Networks : Phy & MAC layers	2A	TD(4) TP(4)	2005-2020
Communication Networks (Advanced)	2A	TD(8) TP(8)	2004-2016
Cisco Certified Network Associate ⁵ 1-2	2A	CM(4) TD (10) TP(22)	2006-2013
Cisco Certified Network Associate 3-4	3A	CM(4) TD(6) TP(10)	2007-2014
C & Shell Programming	1A	CM(4) TD/TP(42)	2005-2006 2011-2013
Graph & Operational Research	2A	TD(22)	2004-2009
Evolution of Systems and Networks	2A	CM(3) TP(16)	2004-2007
Experimenting Advanced Networking	3A	TP(30)	2004-2007
Systems, Networks & Telecom	2A	TD(4) TP(6)	2004-2005
System & Network Administration	2A	CM(2) TP(8)	2004-2005

University of Lorraine :

Module	Audience	Hourly Volume	Period
Internet Networks	M1-EEAPR ⁶	30h CM/TD/TP	2005-2007

Institut Galilée (University Paris 13) :

Module	Audience	Hourly Volume	Period
8086 Assembly Programming	Telecom1 ⁷	24h TP	2003-2004
Networks and Data Transmission	Telecom2 ⁸	20h TD	2003-2004
Network Architecture	DEUST2 ⁹	72h CM/TD/TP	2003-2004

University Lyon 1 :

Module	Audience	Hourly Volume	Period
Simulation of Communication Networks	DESS ¹⁰	26h CM/TP	2002-2003
Quantitative Performance Evaluation (queuing theory)	DESS	6h CM/TD	2000-2003

⁵CCNA

⁷Ingénieurs Télécommunications 1st year

⁸Ingénieurs Télécommunications 2nd year

⁹DEUST IMaRI, 2nd year Installation et maintenance des réseaux informatiques Diplôme d'études universitaires supérieures techniques

¹⁰DESS Informatique, Image et Réseaux

Networks Simulation (Principles, PARSEC, ns2)	IUP ¹¹	34h CM/TD/TP	2002-2003
Algorithmics and Pascal programming	DEUG ¹²	39h TP	2002-2003
Communication Networks	IUP MIAG ¹³	18h TD	2000-2003
Communication Networks Simulation	DESS	10h TP	2000-2001

ENS Lyon :

Module	Audience	Hourly Volume	Period
Communication Networks	MIM2 ¹⁴	10h TD	2000-2003

7.1.2 Educational Responsibility

Since 2013, I am in charge of 2nd year internships (Master 1), "Assistant Engineer" - TELECOM Nancy. Duration : 8 to 17 weeks. Class of about 130 students, varying slightly from year to year. Main tasks :

- Sort and provide students with the received internship proposals.
- Validate the internship subjects and their duration.
- Follow-up the establishment of the internship agreements.
- Manage the internships supervision, in particular by assigning an academic tutor to each student.
- Solve the problems that may arise during internships.
- Manage the internship evaluation process : collect of the various evaluations from the supervisors (companies) and academic tutors (school).
- Constitute juries, organize and plan internship defense sessions.

7.1.3 Other Educational Activities**At TELECOM Nancy**

- Curriculum Lead for CCNA at ESIAL (ex-TELECOM Nancy) :
 - Management and enrollment of students in the program on the digital training platform.
 - Setting up the platform (network devices) for the CCNA program.
- 2nd year jury member (since 2014).
- Supervision of students internships, reports correction (1A, 2A) and theses (3A) (about 15 students/year) and visits to companies.
- Mentoring of apprenticeship students.
- Oral exams for the recruitment of future students.
- Supervision of last year (3A) industrial projects - up to 2 projects per year.
- Supervision of R&D projects (2A) - up to 2 projects per year.
- ...

At Lorraine University

- Academic partner of the consortium GENIAL (Erasmus Mundus Joint Masters Degree) :
 - Examination of students applications.

¹¹Maîtrise Informatique Appliquée aux Réseaux

¹²DEUG MASS : Mathématiques Appliquées aux Sciences Sociales

¹³Maîtrise Informatique Appliquée à la Gestion (dont un groupe de formation continue)

¹⁴Magistère de Mathématiques et d'Informatique, 2nd year

- Proposal and supervision of Master research theses.
- Project proposal & supervision for Master 1, Master 2 or Licence.
- Supervision of Master 2 interns with visits to companies (2005-2007).

7.1.4 International Activities

Upon invitations, I have given seminars (CM) to research master 2 & PhD students on two half-days.

University	Workshop Theme	Dates
Khenchela (Algeria)	Routing in WSNs	01/2017
Sétif (Algeria)	Routing in WSNs	05/2018
Sétif (Algeria)	High data rate accomodation in WSNs	01/2020
Batna (Algeria)	Digital Twinning for Natural Environments	12/2022

7.2 Supervision Activities and PhD Panel Participation

Summary :

- 5 defended PhD theses (2013 (2), 2022 (2), 2023 (1)) ;
- 5 in progress PhD theses (end expected in 2023 (1), 2024 (2), 2025 (2)) ;
- 2 Magister theses (Algerian degree) in 2012 ;
- 9 Research Master 2 (or DEA) defended ;
- 20 Research Master 1 Internships.

7.2.1 Defended PhD Thesis (5)

Ahcen Aliouat. Jan. 2020 - May. 2023 (41 months)

He is currently a post-doctoral fellow at IMT Atlantique, France.

- Title :** Study and Implementation of an Object-based Video Encoder for Embedded Wireless Video Surveillance Systems
- Defense date :** May 31, 2023
- University :** Annaba - Algeria
- Jury :** Benouaret Mohamed, Annaba University, President
Kouadria Nasreddine, Annaba University, Supervisor
Harize Saliha, Annaba University, Co-supervisor
Maimour Moufida, Lorraine University, Co-supervisor
Boumehez Farouk, Khenchela University, Examiner
Boukaache Abdenour, Guelma University, Examiner
- Supervised at :** 33%.
- with :** Kouadria N. & Harize S. (Annaba University- Algeria)
- Publications :** journals [1, 3], conferences [32, 33].

Sihem Benkhald. Oct. 2019 - Nov. 2022 (37 months)

She is currently a Lecturer in Computer Science at Khenchela University, Algeria

- Title :** A Multi-Level Interoperability Approach for Interconnected Objects in the Context of the Internet of Things
- Defense date :** November 14, 2022
- University :** Khenchela - Algeria
- Jury :** Nessah Djamel, Khenchela University, President
Hemam Mounir, Khenchela University, Supervisor
Maimour Moufida, Lorraine University, Co-supervisor
Benmerzoug Djamel, Constantine II University, Examiner
Maarouk Toufik Messaoud, Khenchela University, Examiner
Marir Toufik, OEB University, Examiner
Zianou Ahmed-Seghir, Khenchela University, Examiner
- Supervised at :** 50%.
- with :** M. Hemam (Khenchela University - Algeria)
- Publications :** journal [14], conference [39].

Souhila Kettouche. Nov. 2018 - Jun. 2022 (41 months)

She is currently a Lecturer in Computer Science at Skikda University, Algeria.

- Title :** Multipath Multichannel Routing for Wireless Multimedia Sensor Networks
- Defense date :** June 6, 2022
- University :** OEB University - Algeria
- Jury :** Moukhati Farid, OEB University, President
Derdouri Lakhdar, OEB University, Supervisor
Maimour Moufida, Lorraine University, Co-supervisor
Boutekkouk Fateh, OEB University, Examiner
Bourouis Abdelhabib, OEB University, Examiner
Merniz Salah, Constantine II University, Examiner
- Supervised at :** 80%.
- with :** L. Derdouri (OEB University)
- Publications :** journal [4], national journal [21], conferences [42, 41].

Houda Zeghilet. June 2009 - December 2013 (53 months)

She is *Associate Researcher* at CERIST¹⁵-Algiers.

- Title :** Routing in Wireless Multimedia Sensor Networks
- Defense date :** December 8, 2013
- Universitys :** Cotutelle Lorraine University & Algiers University (USTHB)
- Jury :** Samira Moussaoui, USTHB, President
Congduc Pham, UPPA (Pau), Reviewer
Benchaba Mahfoud, USTHB, Reviewer
Francis Lepage, Lorraine University, Supervisor
Nadjib Badache, USTHB, Supervisor
Moufida Maimour, Lorraine University, Co-supervisor
- Supervised at :** 60%.
- with :** F. Lepage (UL) & N. Badache (Algiers University)
- Publications :** journal [8], book chapter [24], conferences [48, 52, 53]

¹⁵Centre de Recherche sur l'Information Scientifique et Technique

Zahia Bidai. Jan. 2010 - June 2013 (41 months)

She is currently an Associate Professor at the University of Oran.

Title : QoS Routing for Multimedia Transport in Wireless Sensor Networks
Defense date : June 23, 2013
University : University of Oran- Algeria
Jury : K. Mustapha Rahmouni, University of Oran, President
Hafid Haffaf, Oran University, Supervisor
Moufida Maimour, Lorraine University, Co-supervisor
Nacéra Ghoulmi, University Badji Mokhtar, Annaba, Reviewer
Mohamed Benmohamed, University Mentouri, Constantine, Reviewer
Majdi Kaddour, Oran University, Examiner
Supervised at : 80%.
with : H. Haffaf (Oran University - Algeria)
Publications : journals [17, 7], conferences [45, 47, 49].

7.2.2 In progress PhD Thesis (5)

- Nov. 2020 -** Mehdi Kherbache. "Toward Optimized 802.15.4 Industrial Wireless Networks: Harnessing Machine Learning and Digital Twins"
Expected defense date : **December 6, 2023**
Co-supervised at **50%**.
Co-supervisor E. Rondeau (UL).
Publications : journals [5, 2], conferences [27, 28, 75, 38, 36, 37].
- Apr. 2021 -** Aya Sakhri. Cotutelle. "Deep Learning Migratory Birds Surveillance of the wetland Annaba/Tarf (Algeria) using WMSN"
Expected defense date **April 2024**
Co-supervised at **25%**.
Co-supervisors E. Rondeau (UL) and N. Doghmane (Annaba University).
Publications : national journal [20] conferences [73, 34, 30, 35]
- Apr. 2021 -** Oussama Hadji. "Deep Learning Surveillance Approach for birds surveillance"
Expected defense date **April 2024**
Co-supervised at **33%**.
Co-supervisor E. Rondeau (UL) and O. Kadri (University Batna II).
Publications : conferences [74, 31, 34]
- Jan. 2022 -** Chakir Bouarouguen. "Efficient Resource Management Protocol for the IOT"
Expected defense date **2025**
Co-supervised at **33%**.
Co-supervisor E. Rondeau, UL and O. Kadri, University Batna II.
Publications : conferences [72, 34]
- Jan. 2022 -** Mohamed Madani Hafidi. "Knowledge Representation of Interoperable Cyber-Physical Systems based on Deep Reinforcement Learning"
Expected defense date **2025**
Co-supervised at **50%**.
Co-supervisor M. Hemam, Khenchela University - Algeria
Publications : journals [13] conference [29]

7.2.3 Magister Thesis

- Jun. 2010 -** Yacine Baziz. "Development of an evaluation tool for video transmission protocols with applications to wireless sensor networks". Co-supervisor (60%) with B. Kechar and L. Sekhri (Oran University). Defense date **January 4, 2012**.
Jan. 2012
Publications : conferences [46, 48].
- Jun. 2010 -** Amine Belkhodja. "Distributed Source Coding (DSC) Use in Wireless Sensor Networks". Co-supervised (60%) with B. Kechar and L. Sekhri (Oran University). Defense Date **December 2, 2012**.
Dec. 2012

7.2.4 Research Master 2

- 01-06/2023** Arsalan Ahmed. "Digital Twins for Natural Environments: Case Study on a Wireless Multimedia Sensor Network for Waterbirds Monitoring"
 Co-supervised at **50%** with E. Rondeau
- 01-06/2022** Otabek Sobirov. "Energy Efficient Communication Scheduling for IoT-based Waterbirds Monitoring : Decentralized Strategies"
 Co-supervised at **50%** with E. Rondeau
Publication : journal [2], conference [37].
- 02-07/2020** Mehdi Kherbache. "SDN-based Centralized IEEE 802.15.4-TSCH Scheduler for Industry 4.0"
 Co-supervised (**50%**). Co-supervisor E. Rondeau
Publications : journal [5], conference [36]
- 01-06/2018** Khaoula Kalek. "Semantic Enrichment of Sensed Data"
 Co-supervised (**50%**). Co-supervisor M. Hemam (Université de Khenchela - Algeria)
Publication : conference [43].
- 01-06/2018** Fatima-Zohra Amara. "Semantic Enrichment of Sensed Data : Weather Forecasting Application"
 Co-supervised (**50%**) with M. Hemam (Khenchela University - Algeria)
Publications : journal [18], book chapter [23], conferences [43, 40].
- 01-06/2016** Asma AounAllah. "Development of an Ontology for WSN : Application to the Environment Surveillance"
 Co-supervised (**50%**). Co-supervisor M. Hemam (Khenchela University- Algeria)
Publication : conference [44].
- 02-08/2009** Mohamed Ali Mahmoud, "Performance Evaluation of WMSN Applications using CASTALIA".
 Co-supervised (**50%**). Co-supervisor F. Lepage
- 02-07/2007** Gilbert Habib, "Use of Directed Diffusion for Multipath Transport of a Video Flow in Wireless Sensor Networks"
 Co-supervised (**50%**). Co-supervisor F. Lepage
- 02-07/2005** Yang Guang, "Experimental Comparative Study of WSN Simulators".
 Co-supervised (**50%**). Co-supervisor F. Lepage

7.3 Scientific Projects

7.3.1 Funded Projects in Response to Call for Proposals

Partenariat Hubert Curien (PHC) Tassili

Organism/Agency	MEAE (Ministère de L'Europe et des Affaires Étrangères) & MESRI (Ministère de l'Enseignement Supérieur, de la Recherche et de l'Innovation) MESRS (Ministère Algérien de l'Enseignement Supérieur et de la Recherche Scientifique).
Title	MIGNON - MIGratory bird moNitoring using sensOr Networks : A machine learning approach PHC 21MDU323 & Campus France 46082TB
Period	2021-2023 (36 months)
Partners	CRAN (Lorraine University) 3 participants LASA (Annaba University) 6 participants LASTIC (Batna University) 4 participants
Funding	70 K€ including 35 K€ for CRAN. Algerian PhD students mobility funding (Algeria → France) as well as an associate professor (preparing HDR). Coordination missions for the coordinators.
Role	Principal Investigator (PI) at CRAN PhD students co-supervision : Aya Sakhri, Oussama Hadji, Chakir Bouarrougouen and Ahcen Aliouat.

Partenariat Hubert Curien (PHC) Tassili

Organism/Agency	MEAE (Ministère de L'Europe et des Affaires Étrangères) & MESRI (Ministère de l'Enseignement Supérieur, de la Recherche et de l'Innovation) MESRS (Ministère Algérien de l'Enseignement Supérieur et de la Recherche Scientifique).
Title	Cooperative Control using Wireless Sensor Networks for Surveillance Applications PHC 09MDU784 & EGIDE 20281UB
Period	2009-2012 (48 months)
Partners	CRAN (Lorraine University) 1 participant LIUPPA (University of Pau) 2 participants University of Oran (Algeria) 9 participants
Funding	80 K€. Algerian PhD students mobility funding (Algeria <i>rightarrow</i> France) as well as an associate professor (preparing HDR). Coordination missions for the coordinators.
Role	Principal Investigator (PI) at CRAN Visits to the University of Oran : 2 weeks in May 2010 and May 2012 Co-supervision of the PhD thesis of Zahia Bidai

Projet JCJC TCAP

Organism/Agency	ANR
Title	TCAP - Video Transport using Wireless Sensor Networks 06-JCJC-0072
Period	2006-2009 (36 months)
Partners	CRAN (Lorraine University) 5 participants LIUPPA (University of Pau) 6 participants
Funding	126 K€
Role	Principal Investigator (PI) at CRAN Co-supervision of the PhD thesis of Houda Zeguilet

BQR UHP Lorraine

Organism/Agency	University Henri Poincaré Région de Lorraine
Title	Optimized Image Capture and Transmission in Wireless Sensor Networks
Period	2006-2008
Partners	CRAN : 4 participants
Role	Participant

Action Incitative CRAN

Organism/Agency	CRAN
Title	Wireless Sensor Networks
Period	2005/2006
Partners	CRAN : 4 participants
Funding	5 K€: 10 sensor nodes notes
Role	Participant

European Project - DataGrid

Organism/Agency	European Union
Title	DataGrid - to provide distributed computing power in a transparent way to the end-user
Period	2001-2003
Partners	6 main : CERN (coordinateur), ESA, PPARC (UK), CNRS (France), INFN (Italie), NIKHEF (Pays-Bas) & 15 others from 10 countries
Funding	9.8 M€
Role	I took part in the WP7 (Network Services), to the task "Reliable Multicast" in which I had the responsibility to propose a work plan and make a state-of-the-art on the already existing reliable multicast protocols. An appropriate protocol is implemented and experimented on a local testbed then for long distance. I made a presentation (June, 22 th , 2001) at IN2P3 (Lyon) "An overview of reliable multicas protocols for the Grid and a proposition of task workplan". I participate in writing the D7.3d eliverable "DataGrid-07-D7-3-0113-1-8" Network Services : Requirements, Deployment and Use in Testbeds. 06-30-2002.

Projet RNTL¹⁶ e-Toile et RNRT¹⁷ VTHD++

Organism/Agency	Ministère de la Recherche et de l'industrie
Title	RNTL e-Toile Experimental Testbed - Grid Computing
Period	2002-2004
Partners	INRIA (ENS Lyon), IMAG, ENST, Institut Eurécom , FT R&D, SUN ...
Role	I took part in the task of developing and integrating an active reliable multicast protocol. DyRAM protocol (mftp) was integrated in the testbed VTHD++.

RESO

Organism/Agency	INRIA
Title	RESO - Protocols and Software for Optimized Network Interfacing
Period	2000-2003
Partner	RESO Team (INRIA/LIP - ENS Lyon)
Role	Participant

ACI GRID JCJC

Organism/Agency	Ministère de la recherche
Title	RESAM - Intelligence and Network Support for the Grid
Period	2001-2002 (2 years)
Partner	RESO team (INRIA/LIP - ENS Lyon)
Funding	200 KF
Role	I mainly took part in the task "Reliable Multicast Optimization" aiming to provide a reliable multipoint communication that reduces the latency on the Grid.

Réseaux actifs

Organism/Agency	ANVAR & EZUS Lyon I
Title	Active Networks & Experimental Testbed
Period	2001-2003
Partner	RESO team (INRIA/LIP - ENS Lyon)
Role	I took part in the setup of a local experimental testbed (hardware, software) to validate protocols that follow the active networking paradigm.

7.3.2 Funded Projects by Mutual Agreement**Partnership with ICOSI¹⁸ Lab. (University of Khenchela - Algeria)**

Theme	Design of Ontologies for environment surveillance and Industry 4.0
Period	since 2015
Funding	Khenchela University funded several visits of Algerian researchers at CRAN and my visit to Khenchela from 2-5 Jan. 2017
Role	co-supervision of the PhD thesis of M. M. Hafidi co-supervision of the PhD thesis of S. Benkhaled defended in 2022 collaboration with PhD student F. Z. Amara co-supervision of 3 research master theses
Publications	journals : [13, 14, 18], book chapter : [23], conferences : [29, 40, 39, 43, 44]

¹⁸Laboratoire d'Ingénierie des Connaissances et Sécurité Informatique

Partnership with RELA(CS)¹⁹ Lab. (OEB University - Algeria)

Theme	Multichannel Multipath Routing in the Internet of Multimedia Things
Period	since 2018
Funding	OEB University funded 1-month visit for PhD student S. Kettouche at CRAN
Role	co-supervision of the PhD thesis of S. Kettouche defended in 2022
Publications	journals : [4, 21], conferences : [41, 42]

Partnership with LASA²⁰ Lab. (Annaba University - Algeria)

Theme	Exploitation of machine learning methods for monitoring of migratory birds in the wetlands of the Annaba region.
Period	since 2019
Funding	Annaba University funded 2-week visit of an Algerian researcher at CRAN in 2019
Role	co-supervision of PhD students : Aya Sakhri, Ahcen Aliouat
Publications	journals : [3, 1], conferences : [20, 73, 32, 33, 34, 35]

Partnership with LASTIC²¹ Lab. (University Batna II - Algeria, a partner of the GENIAL²² consortium)

Theme	Resource Allocation in the IoT with Application to Waterbirds Surveillance.
Period	since 2021
Funding	University Batna II funded a 1-month visit of PhD student O. Hadji at CRAN in 2023
Role	co-supervision of PhD students : O. Hadji and C. Bouarrouguen
Publications	journal [2], [74, 72, 31, 34, 37]

7.4 Editorial Activities and Community Services

Research Visits

Upon invitations, each of the following visits was an opportunity to present the research work carried out at CRAN in general and in my team in particular.

- **Jan. 17-20, 2022.** University Batna II - Computer Science Departement (Algeria). LASTIC²³ Lab.
- **Jan. 8-15, 2020 & Apr. 28 - May 2, 2018.** Faculty of Sciences of University of Setif (Algeria). LRSD²⁴ Lab.
- **Jan. 2-5, 2017.** University of Khenchela - Computer Science Departement (Algeria). ICOSI²⁵ Lab.

Keynote Speaker

- **Sept. 18, 2022.** "Digital Twin : From Manufacture to Nature - Communication Networks Perspective". 5th International Conference on Advanced Aspects of Software Engineering (ICAASE'22).

¹⁹Research Laboratory on Computer Science's Complex Systems

²⁰Laboratoire d'Automatique et Signaux de Annaba

²¹Laboratoire des Systèmes et Technologies de L'Information et de la Communication

²²Erasmus Mundus Joint Masters Degree

²³Laboratoire des Systèmes et Technologies de L'Information

²⁴Laboratoire des Réseaux et des Systèmes Distribués

²⁵Laboratoire d'Ingénierie des Connaissances et Sécurité Informatique

Editorial Activities

• Editorial Board Membership

- 2020-2021 : The African Journal of Engineering Science and Technology ;
- since 2020 : Topics Board of MDPI journal "Sensors" ;
 - * Special Issue: "Intelligent Digital Twin-based IoT Applications: from Industry to Natural Environment"
- since 2018 : Mesford Publishers Inc "Current Analysis on Communication Engineering (CACE)" ;
- since 2018 : IASE "Annals of Electrical and Electronic Engineering (AEEE)" ;
- since 2017 : IASE "International Journal of Advanced and Applied Sciences (IJAAS)".

• TPC Member for the following conferences :

- Int. Conf. on Ambient Systems, Networks and Technologies (ANT) **2015, 2017-2023** ;
- Int. Workshop on Semantic Reasoning and Representation in IoT (IWSIoT) **2022** ;
- Tunisian-Algerian Joint Conference on Applied Computing (TACC) **2021-2022** ;
- Int. Conf. on Advanced Aspects of Software Engineering (ICAASE) **2020-2022** ;
- Int. Conf. on Computational Intelligence and Communication Networks (CICN) **2019-2022** ;
- Int. Conf. on Applied Machine Learning and Data Analytics (AMALDA) **2021** ;
- Int. Conf. on computer science's complex systems and their Applications (ICCSA) **2020, 2021** ;
- Int. Symposium on Personal, Indoor, and Mobile Radio Communications (PIMRC) **2008, 2011-2013, 2016, 2018-2021** ;
- Int. Conf. on Communication Systems and Network Technologies (CSNT) **2018,2020** ;
- Int. Conf. on Emerging Ubiquitous Systems and Pervasive Networks (EUSPN) **2014, 2016-2018** ;
- Global Summit on Computer & Information Technology (GSCIT) **2015, 2016** ;
- Int. Conf. on Communication and Computer Engineering (ICOCOE) **2015-2016** ;
- Int. Conf. on Advances in Computing, Communication and Informatics (ICACCI) **2016** ;
- Int. Conf. on Pattern Analysis and Intelligent Systems (PAIS) **2016** ;
- Int. Symp. on Women in Computing and Informatics (WCI) **2015** ;
- Global Summit on Computer and Information Technology (GSCIT) **2015** ;
- Int. Conf. on Emerging Networks and Systems Intelligence (EMERGING) **2011-2014** ;
- IEEE Asia Pacific Conference on Wireless and Mobile (APWiMob) **2014** ;
- IEEE/ACM Int. Conf. on Green Computing and Communications (GreenComm) **2010** ;...

• Review for International Conferences (in addition to the above mentoned) :

- IEEE Conference on Local Computer Networks (LCN) ;
- IEEE Symposium on Computers and Communications (ISCC) ;
- IEEE International Conference on Communications (ICC) ;
- IFIP Wireless and Mobile Networking Conference (WMNC) ;
- ...;

• Review for International Journals :

- **IEEE Access** (2019)
- **Elsevier**
 - * Fundamental Research (2022)
 - * Internet of Things (2020)
 - * Future Generation Computer Systems (2019)
 - * Adhoc Networks (2016, 2018, 2020, 2023)
 - * Computer Communication (2013, 2014)
 - * Performance Evaluation (2014)
- **MDPI**
 - * Applied Sciences (2023)
 - * Sensors (2016, 2017, 2019)
- **Springer**

- * SN Computer Science (2019, 2023)
- * Wireless Personal Communication (2015, 2016, 2017)
- * Journal of Heuristics (2014)
- * Wireless Networks (2012)
- **Inderscience**
 - * International Journal of Distributed Sensor Networks (2021, 2022)
 - * International Journal of Sensor Networks, special issue "Multimedia Data Applications in Wireless sensor networks" (2010)
 - * Journal of Communication Networks and Distributed Systems (IJCNSD). Special Issue on "Mobile, Multimedia, Ad Hoc & Sensor Networks" (2010)
- **King Saud University** Journal of King Saud University - Computer and Information Sciences (2019, 2023)
- **Emerald Publishing** International Journal of Pervasive Computing and Communications (2023)
- **SCIRP** Wireless Sensor Network (2018)
- **EURASIP** Journal on Wireless Communications and Networking (2013)

Ph.D. Panel Participation

- **PhD Panel Examiner Member** of Christian Salim. **University of Franche-Comté, France**. "Data Reduction based Energy-Efficient Approaches for Secure Priority-based Managed Wireless Video Sensor Networks". **December, 3rd 2018**.
- **PhD thesis External Examiner** of Shaamili Varsa G V **Anna University, Chennai, India**. "A balanced Energy Efficient Connected Dominating Set Algorithm using Compressive Sensing in WSN". Expected defense in **2023**.

Misc.

- **Follow-up Committee Member** of the PhD thesis of Marion Richardot. "Spatio-temporal interpolation and hybrid AI for biodiversity application". GeorgiaTech Lorraine, Metz. Expected defense in **2025**.
- **Reviewer of the Magister Thesis** of Nawel Bendimerad. **Université d'Oran, Algérie**. "Interference-free disjoint node multipath DyMO for IEEE 802.15.4 ZigBee/Standard networks". **May 2010**.

7.5 Publications and Scientific production

Software (*open source*)

- **mftp**²⁶, developed in Java to enable reliable multicast transfer of files based on active networks. Developed in collaboration with F. Bouhafs et C. Pham.
Reference publication : [12]
- **SenseVid**²⁷, developed in C++, a performance evaluation tool targeted to WWSN.
Reference publication : [6].

PhD Thesis in Computer Science

M. Maimour, "Design, Analysis and Validation of Router-assisted Reliable Multicast Protocols in Wide Area Networks", Ph.D. dissertation, Lyon I University, November 2023.

²⁶cpham.perso.univ-pau.fr/MULTICAST/index.html

²⁷w3.cran.univ-lorraine.fr/perso/moufida.maimour/SenseVid/sensevid.html

International Peer-Reviewed Journals (12 - JCR with IF)

- [1] A. Aliouat, N. Kouadria, S. Harize, and **M. Maimour**. An Efficient Low Complexity Region-of-Interest Detection for Video Coding in Wireless Visual Surveillance. *IEEE Access*, 11:26793–26806, 2023. **JCR, Q2, IF 3.476**.
- [2] M. Kherbache, O. Sobirov, **M. Maimour**, E. Rondeau, and A. Benyahia. Decentralized TSCH scheduling protocols and heterogeneous traffic: Over view and performance evaluation. *Internet of Things*, page 100696, 2023. **JCR, Q1, IF 5.711**.
- [3] A. Aliouat, N. Kouadria, **M. Maimour**, S. Harize, and N. Doghmane. Region-of-Interest Based Video Coding Strategy for Rate/Energy-constrained Smart Surveillance Systems Using WMSNs. *Ad Hoc Networks*, 140:103076, 2023. **JCR, Q2, IF 4.816**.
- [4] S. Kettouche, **M. Maimour**, and L. Derdouri. Disjoint Multipath RPL for QoE/QoS Provision in the Internet of Multimedia Things. *Computing*, 104(7):1677–1699, July 2022. **JCR, Q2, IF 2.42**.
- [5] M. Kherbache, **M. Maimour**, and E. Rondeau. When Digital Twin Meets Network Softwarization in the Industrial IoT: Real-Time Requirements Case Study. *Sensors*, 21(24):8194, December 2021. **JCR, Q2, IF 3.847**.
- [6] **M. Maimour**. SenseVid : A Traffic Trace based Tool for QoE Video Transmission Assessment Dedicated to Wireless Video Sensor Networks. *Simulation Modelling Practice and Theory*, 87:120–137, September 2018. **JCR, Q1, IF 4.199**.
- [7] **M. Maimour** and Z. Bidai. A Multipath Prefix Routing for Wireless Sensor Networks. *Wireless Personal Communications*, 91(1):313–343, November 2016. **JCR, Q4, IF 2.017**.
- [8] H. Zeghilet, **M. Maimour**, F. Lepage, and N. Badache. On the Use of Passive Clustering in Wireless Video Sensor Networks. *International Journal of Sensor Networks*, 11(2):67–80, 3 2012. **JCR, Q4, IF 1.264**.
- [9] F. Bouhafs, J.P. Gelas, L. Lefèvre, **M. Maimour**, C. Pham, P. Primet, and B. Tourancheau. Designing and evaluating an active grid architecture. *Future Generation Computer Systems*, 21(2):315–330, 2005. **JCR, Q1, IF 7.307**.
- [10] **M. Maimour** and C. Pham. A Survey of Active and Router-Assisted Reliable Multicast Solutions. In *Annals of Telecommunications*, volume 59, pages 543–564. Springer-Verlag, 2004. **JCR, Q3, IF 1.901**.
- [11] **M. Maimour** and C. Pham. Experimenting Active Reliable Multicast on Application-Aware Grids. *Journal of Grid Computing*, 2(1):71–83, 2004. **JCR, Q2, IF 4.674**.
- [12] **M. Maimour** and C. Pham. DyRAM: an Active Reliable Multicast Framework for Data Distribution. *Cluster Computing Journal*, 7(2):163–176, 2004. **JCR, Q2, IF 2.303**.

International Peer-Reviewed Journals (5 - JCR without IF)

- [13] M. Hafidi, M. Djezzar, M. Hemam, F. Z. Amara, and **M. Maimour**. Semantic Web and Machine Learning Techniques Addressing Semantic Interoperability In Industry 4.0. *International Journal of Web Information Systems*, August 2023.
- [14] S. Benkhaled, M. Hemam, and M. Djezzar **M. Maimour**. An Ontology-based Contextual Approach for Cross-domain Applications in Internet of Things. *Informatica-Journal of Computing and Informatics*, 3 2022.
- [15] **M. Maimour**. Interference-aware Metrics Impact on the Performance of Incremental Multipath Routing in WSNs. *Journal of High Speed Networks*, 26(3):225–240, 2020.

- [16] **M. Maimour**. Impact of Interference Aware Metrics on Iterative Multipath Routing for Industrial WSN. *Internet Technology Letters, Special Issue on Industrial Internet of Things*, 3(4):e159, July 2020.
- [17] Z. Bidai, **M. Maimour**, and H. Haffaf. Multipath extension of the ZigBee tree routing in cluster-tree wireless sensor networks. *International Journal of Mobile Computing and Multimedia Communications*, 4(2):30–48, 2012.

International Peer-Reviewed Journals (2 - Other)

- [18] F.Z. Amara, M. Hemam, M. Djezzar, and **M. Maimour**. Semantic Web and Internet of Things: Challenges, Applications and Perspectives. *Journal of ICT Standardization*, pages 261–292, 2022.
- [19] **M. Maimour**. Interference-aware multipath routing for WSNs: Overview and performance evaluation. *Applied Computing and Informatics*, 16(1/2):59–80, 3 2018.

National Peer-Reviewed Journals (3)

- [20] A. Sakhri, **M. Maimour**, S. Harize, E. Rondeau, and N. Doghmane. An energy efficient Monitoring system for endangered birds. *Synthèse - Revue des Sciences et de la Technologie*, 2023.
- [21] S. Kettouche, **M. Maimour**, and L. Derdouri. DM-RPL: Disjoint multipath RPL for bandwidth provision in the internet of multimedia things. *Revue de l'Information Scientifique et Technique*, 26(1):23–35, 2021.
- [22] **M. Maimour** and Cong-Duc Pham. Modélisation et évaluation des protocoles de multicast fiable dans le contexte des réseaux actifs. *Réseaux et Systèmes Répartis-Calculateurs Parallèles (RSR-CP), Special Issue on Performance of Networks and Systems*, 13(6), 2001.

Book Chapters (4)

- [23] F.Z. Amara, M. Hemam, M. Djezzar, and **M. Maimour**. *Tools, Languages, Methodologies for Representing Semantics on the Web of Things*, chapter Semantic Web Approach for Smart Health to Enhance Patient Monitoring in Resuscitation. Wiley, October 2022.
- [24] **M. Maimour**, H. Zeghilet, and F. Lepage. *Wireless Sensor Networks*, chapter Cluster-based Routing Protocols for Energy Efficiency in Wireless Sensor Networks. IN-TECH, December 2010.
- [25] C. Pham and **M. Maimour**. *Multimedia Multicast on the Internet*, chapter Congestion Control in Multicast Communication, pages 223–246. Number 7. Hermes, January 2007.
- [26] C. Pham and **M. Maimour**. *Multicast Multimédia dans l'Internet*, chapter Le contrôle de congestion dans les communications multicast. Number 7. Hermes, 2005.

International Peer-Reviewed Conferences (45)

- [27] IEEE, editor. *QL-TSCH-plus : A Q-learning Distributed Scheduling Algorithm for TSCH Networks*, October 2023.
- [28] M. Kherbache, **M. Maimour**, and E. Rondeau. An Advanced Assessment of Decentralized TSCH Schedulers: Unraveling the Implications of Heterogeneous Traffic Scenarios on Performance Efficacy. In *The 22nd World Congress of the IFAC World Congress*, Yokohama, Japan, June 2023.
- [29] M. Hafidi, M. Djezzar, M. Hemam, A. S. Zianou, and **M. Maimour**. Semantic Models and Machine Learning Approach in CPS : a Survey. In *1st International Workshop on Semantic Reasoning and Representation in IoT (IWSIoT'22)*, November 2022.

- [30] **M. Maimour**, A. Sakhri, E. Rondeau, M.O. Chida, C. Tounsi-Omezzine, and C. Zhang. Deep learning-based image restoration for low-power and lossy networks. In *5th Edition of the International Conference on Advanced Aspects of Software Engineering, ICAASE'22*, Constantine, Algeria, September 2022.
- [31] O. Hadji, O. Kadri, **M. Maimour**, E. Rondeau, and A. Benyahia. Region of interest and redundancy problem in migratory birds wild life surveillance. In *5th Edition of the International Conference on Advanced Aspects of Software Engineering, ICAASE'22*, Constantine, Algeria, September 2022.
- [32] A. Aliouat, N. Kouadria, **M. Maimour**, and S. Harize. Region-of-Interest based Video Coding Strategy for Low Bitrate Surveillance Systems. In IEEE, editor, *2022 19th International Multi-Conference on Systems, Signals and Devices (SSD)*, pages 1357–1362, Setif, Algeria, 6-10 May 2022.
- [33] A. Aliouat, N. Kouadria, S. Harize, and **M. Maimour**. Multi-Threshold-Based Frame Segmentation for Content-Aware Video Coding in WMSN. In *International Conference on Computing Systems and Applications*, pages 337–347. Springer, 2022.
- [34] A. Sakhri, O. Hadji, C. Bouarrouguen, **M. Maimour**, N. Kouadria, A. Benyahia, E. Rondeau, N. Doghmane, and S. Harize. Audio-Visual Low Power System for Endangered Waterbirds Monitoring. In IFAC, editor, *2nd Workshop on Integrated Assessment Modelling for Environmental Systems (IAMES)*, Tarbes, France, June 1-3 2022.
- [35] A. Sakhri, **M. Maimour**, E. Rondeau, N. Doghmane, and S. Harize. An Energy-Efficient WMSN-based System for Endangered Birds Monitoring. In *6th Symposium on Telematics Applications, TA'22*, Nancy, France, June 2022. IFAC.
- [36] M. Kherbache, **M. Maimour**, and E. Rondeau. Digital Twin Network for the IIoT using Eclipse Ditto and Hono. In *6th Symposium on Telematics Applications, TA'22*, Nancy, France, June 2022. IFAC.
- [37] M. Kherbache, O. Sobirov, **M. Maimour**, E. Rondeau, and A. Benyahia. Reinforcement Learning TDMA-Based MAC Scheduling in the Industrial Internet of Things: A Survey. In *6th Symposium on Telematics Applications, TA'22*, Nancy, France, June 2022. IFAC.
- [38] M. Kherbache, **M. Maimour**, and E. Rondeau. Network Digital Twin for the Industrial Internet of Things. In *2022 IEEE 23rd International Symposium on a World of Wireless, Mobile and Multimedia Networks (WoWMoM)*, pages 573–578. IEEE, 2022.
- [39] S. Benkhaled, M. Hemam, and **M. Maimour**. SDN-based Approaches for Heterogeneity and Interoperability in Internet of Things : An Overview. In *International Conference on Distributed Sensing and Intelligent Systems*, pages 489–499, Agadir, Morocco, February 2020. Springer. Published as a chapter in 2022.
- [40] F.Z. Amara, M. Hemam, M. Djeddar, and **M. Maimour**. Semantic Web Technologies for Internet of Things Semantic Interoperability. In *The International Conference on Information, Communication & Cybersecurity (ICI2C)*, pages 133–143. Springer, 2021.
- [41] S. Kettouche, **Maimour, M.**, and L. Derdouri. Bandwidth Provision Through Disjoint Multipath RPL in the IoMT. In *International Conference on Computer Science's Complex Systems and their Applications, ICCSA'21*, 2021.
- [42] S. Kettouche, **M. Maimour**, and L. Derdouri. QoE-based Performance Evaluation of Video Transmission using RPL in the IoMT. In *2019 7th Mediterranean Congress of Telecommunications (CMT)*, pages 1–4, Oct 2019.
- [43] M. Djeddar, M. Hemam, **M. Maimour**, F. Amara, K. Falek, and Z. A. Seghir. An approach for Semantic Enrichment of Sensor Data. In IEEE Algeria, editor, *The 3rd International Conference on Pattern Analysis and Intelligent Systems, PAIS*, Tebessa, Algeria, October 24-25 2018.

- [44] M. Hemam, M. Djezzar, **M. Maimour**, T. Djouad, and A. Aounallah. An Ontological Approach for Domain Knowledge Modeling and Querying in Wireless Sensor Networks. In IEEE Algeria, editor, *The 2nd International Conference on Pattern Analysis and Intelligent Systems, PAIS*, Khenchela, Algeria, November 16-17 2016.
- [45] Z. Bidai and **M. Maimour**. Interference-aware Multipath Routing Protocol for Video Transmission over ZigBee Wireless Sensor Networks. In IEEE, editor, *the 4th International Conference on Multimedia Computing and Systems*, Marrakesh, Morocco, April 14-16 2014. IEEE.
- [46] Y. Baziz, **M. Maimour**, and B. Kechar. EvalVSN : a New Tool for Video Quality Evaluation in Wireless Sensor Networks. In IEEE, editor, *the 4th International Conference on Multimedia Computing and Systems*, Marrakesh, Morocco, April 14-16 2014. IEEE.
- [47] Z. Bidai and **M. Maimour**. Multipath Routing for High-Data Rate Applications in ZigBee Wireless Sensor Networks. In *the 6th International Conference On New Technologies, Mobility & Security (NTMS'2014)*, pages 1–5, March 30-April 2 2014.
- [48] H. Zeghilet, Y. Baziz, **M. Maimour**, B. Kechar, and N. Badache. The Effects of Interference on Video Quality over Wireless Sensor Networks. In *2013 International Workshop on Communications and Sensor Networks*, volume 21, pages 436–441, Ontario, Canada, October 2013.
- [49] Z. Bidai, H. Haffaf, and **M. Maimour**. Node disjoint multi-path routing for ZigBee cluster-tree wireless sensor networks. In *Multimedia Computing and Systems (ICMCS), 2011 International Conference on*, pages 1–6, April 2011.
- [50] C. Pham, **M. Maimour**, K. Fellah, B. Kechar, and H. Haffaf. Increasing Network Lifetime of Surveillance System with Dynamic Risk-based Scheduling and Mobility of Sensors. In *IROS'10 Workshop on Robots and Sensors integration in future rescue INFORMATION system (ROSIN'10)*, October 18th 2010.
- [51] **M. Maimour**, K. Fellah, B. Kechar, C. Pham, and H. Haffaf. Minimizing Energy Consumption Through Mobility in Wireless Video Sensor Networks. In *The Second International Conference on Emerging Network Intelligence, EMERGING 2010*, October 25 - 30 2010.
- [52] H. Zeghilet, **M. Maimour**, F. Lepage, and N. Badache. Using passive clustering to enhance video quality in wireless sensor networks. In *WD'09: Proceedings of the 2nd IFIP conference on Wireless days*, pages 90–95, Piscataway, NJ, USA, 2009. IEEE Press.
- [53] H. Zeghilet, N. Badache, and **M. Maimour**. Energy efficient cluster-based routing in wireless sensor networks. In *ISCC*, pages 701–704, 2009.
- [54] **M. Maimour**, C. Pham, and D. Hoang. A Congestion Control Framework for Handling Video Surveillance Traffics on WSN. In *International Workshop on Pervasive Multimedia Sensor Networks (PMSN'09)*, Vancouver, Canada, August 29th-31st 2009.
- [55] **M. Maimour**. Maximally Radio-Disjoint Multipath Routing for Wireless Multimedia Sensor Networks. In *Proceedings of the 4th ACM workshop on Wireless multimedia networking and performance modeling colocated with MSWIM'08*, Vancouver, Canada, 27-31 October 2008.
- [56] **M. Maimour**, C. Pham, and J. Amelot. Load Repartition for Congestion Control in Multimedia Wireless Sensor Networks with Multipath Routing. In *IEEE International Symposium on Wireless Pervasive Computing*, Santorini, Greece, 7-9 May 2008.
- [57] **M. Maimour**. Multipath Routing Protocol for Layered Video Transport in Wireless Sensor Networks. In *Workshop on Wireless Sensor Networks in conjunction with NOTERE 2007*, Marrakesh, Morocco, June 2007.

- [58] V. Lecuire, C. Duran-Faundez, T. Holl, N. Krommenacker, **M. Maimour**, and M. David. Energy consumption analysis of a simple image transmission protocol in wireless sensor networks. In *6th IEEE International Workshop on Factory Communication Systems, WFCS'2006*, pages 215–218, Torino, Italy, June 2006.
- [59] **M. Maimour** and C. Pham. Dealing with Heterogeneity in a Fully Reliable Multicast Protocol. In *in the 11th IEEE International Conference on Networks (ICON'03)*, Sydney, Australia, September 28th - October 1st 2003.
- [60] **M. Maimour** and C. Pham. A RTT-based Partitioning Algorithm for a Multi-Rate Reliable Multicast Protocol. In *6th IEEE International Conference on High Speed Networks and Multimedia Communications HSNMC'03*, Estoril, Portugal, July 23-25 2003.
- [61] **M. Maimour** and C. Pham. AMCA: an Active-based Multicast Congestion Avoidance Algorithm. In *the 8th IEEE Symposium on Computers and Communications (ISCC 2003)*, pages 747–754, Kemer-Antalya, Turkey, July 2003. **Best Paper Award**.
- [62] **M. Maimour** and C. Pham. A New Active-based Multicast Congestion Avoidance Algorithm. In *Canadian Conference on Electrical and Computer Engineering (CCECE'03)*, Montreal, Canada, May 4-7 2003.
- [63] **M. Maimour** and C. Pham. Towards an application-aware communication framework for computational grids. In *Proceedings of the Asian Computing Science Conference (ASIAN 2002)*, Hanoi, Vietnam, December 2002.
- [64] **M. Maimour** and C. Pham. An Analysis of a Router-based Loss Detection Service for Active Reliable Multicast Protocols. In *Proceedings of the 11th IEEE International Conference on Networks*, Singapore, August 2002.
- [65] **M. Maimour**, J. Mazuy, and C. Pham. The Cost of Active Services in Active Reliable Multicast. In *Proceedings of the 4th IEEE Annual International Workshop on Active Middleware Services (AMS 2002)*, pages 67–72, Edinburg, UK, July 2002.
- [66] **M. Maimour** and C. Pham. Dynamic Replier Active Reliable Multicast (DyRAM). In *Proceedings of the 7th IEEE Symposium on Computers and Communications (ISCC 2002)*, pages 275–282, Taormina, Sicily, July 2002.
- [67] **M. Maimour** and C. Pham. A Loss Detection Service for Active Reliable Multicast Protocols. In *Proceedings of the International Network Conference (INC'2002)*, Plymouth, UK, July 2002.
- [68] **M. Maimour** and C. Pham. An Active Reliable Multicast Framework for the Grids. In *Proceedings of the International Conference on Computational Science (ICCS 2002)*, volume 2330 of *Lecture Notes in Computer Science*, pages 588–597, April 2002.
- [69] L. Lefèvre, C. Pham, P. Primet, B. Tourancheau, B. Gaidioz, J.P. Gelas, and **M. Maimour**. Active Networking Support for the Grid. In Noaki Wakamiya Ian W. Marshall, Scott Nettles, editor, *IFIP-TC6 Third International Working Conference on Active Networks, IWAN 2001*, volume 2207 of *Lecture Notes in Computer Science*, pages 16–33, October 2001. ISBN: 3-540-42678-7.
- [70] **M. Maimour** and C. Pham. Active Reliable Multicast for Efficient Data Distribution on an Internet-based Grid Computing Infrastructure. In *Proceedings of the International Conference on Internet Computing (IC'2001)*, pages 437–443, Monte Carlo Hotel, Las Vegas, USA, June 2001.
- [71] **M. Maimour** and C. Pham. A Throughput Analysis of Reliable Multicast Protocols in an Active Networking Environment. In *Proceedings of the Sixth IEEE Symposium on Computers and Communications (ISCC 2001)*, pages 151–158, Hammamet, Tunisia, July 2001.

National Conferences (4)

- [72] C. Bouarouguene, **M. Maimour**, O. Kadri, E. Rondeau, and A. Benyahia. DNN Inference Splitting and Offloading in the Internet of Things : A Survey. In *1er Congrès annuel de la Société d'Automatique de Génie Industriel et de Productique SAGIP 2023*, Marseille, France, June 2023.
- [73] A. Sakhri, **M. Maimour**, N. Doghmane, and E. Rondeau. Performance Evaluation of a WMSN-based System for Endangered Bird Monitoring. In *1er Congrès annuel de la Société d'Automatique de Génie Industriel et de Productique SAGIP 2023*, Marseille, France, June 2023.
- [74] O. Hadji, A. Benyahia, **M. Maimour**, E. Rondeau, and O. Kadri. Proposed System for Efficient Wildlife Monitoring Using WSN and Image Processing. In *1er Congrès annuel de la Société d'Automatique de Génie Industriel et de Productique SAGIP 2023*, Marseille, France, June 2023.
- [75] M. Kherbache, **M. Maimour**, and E. Rondeau. IoT Network Digital Twins modeling using Petri-Nets. In *1er Congrès annuel de la Société d'Automatique de Génie Industriel et de Productique SAGIP 2023*, Marseille, France, June 2023.

Research Reports (10) - INRIA, LIP/ENS, Deliverables

- [76] **M. Maimour**. Virtualisation et problèmes d'allocation des ressources dans l'IoT : Approche basée sur l'apprentissage profond. Rapport d'activité de crct, Université de Lorraine, Mai 2021.
- [77] **M. Maimour**. Performance Evaluation of DyRAM using NS. Technical Report 2004-12, LIP/ENS research report, March 2004.
- [78] **M. Maimour**. Accomodating Heterogeneity in a Multicast Session Through a Receiver-based Data Replication Scheme. Technical Report RR2004-06, LIP/ENS research report, January 2004.
- [79] **M. Maimour** and C. Pham. Dealing with Heterogeneity in an Active-based Multicast Congestion Avoidance Protocol. Technical Report RR2003-20, LIP/ENS research report, March 2003. Also available as an INRIA research report RR-4796.
- [80] **M. Maimour** and C. Pham. A RTT-based Partitioning Algorithm for a Multi-rate Reliable Multicast Protocol. Technical Report RR2003-16, LIP/ENS research report, March 2003. Also available as an INRIA research report RR-4779.
- [81] **M. Maimour** and C. Pham. AMCA : An Active-Based Multicast Congestion Avoidance Algorithm. Technical Report RR2003-07, LIP/ENS research report, January 2003. Also available as an INRIA research report RR-4689.
- [82] **M. Maimour** and C. Pham. An Analysis of a Router-based Loss Detection Service for Active Reliable Multicast Protocols. Technical Report RR2003-06, LIP/ENS research report, November 2002. Also available as an INRIA research report RR-4636.
- [83] **M. Maimour** and C. Pham. Dynamic Replier Active Reliable Multicast (DyRAM). Technical Report RR2003-05, LIP/ENS research report, November 2002.
- [84] **M. Maimour** and C. Pham. A Throughput Analysis of Reliable Multicast Protocols in an Active Networking Environment. Technical Report TR01-2001, RESAM research report, January 2001.
- [85] A Alessandrini, H Blom, F Bonnassieux, T Ferrari, R Hughes-Jones, M Goutelle, R Harakaly, Y Li, **M Maimour**, C Pham, P Primet, et al. Network services: requirements, deployment and use in testbeds. Technical Report D7.3 DataGRID, 2002.



Bibliography

- [80211] “IEEE standard for local and metropolitan area networks—part 15.4: Low-rate wireless personal area networks (LR-WPANs),” *IEEE Std 802.15.4-2011 (Revision of IEEE Std 802.15.4-2006)*, pp. 1–314, Sept 2011.
- [AAG⁺20] P. Angin, M. H. Anisi, F. Göksel, C. Gürsoy, and A. Büyükgülcü, “Agrilora: a digital twin framework for smart agriculture,” *J. Wirel. Mob. Networks Ubiquitous Comput. Dependable Appl.*, vol. 11, no. 4, pp. 77–96, 2020.
- [AAMS08] H. S. Aghdasi, M. Abbaspour, M. Moghadam, and Samei, “An energy-efficient and high-quality video transmission architecture in wireless video-based sensor networks,” *Sensors*, vol. 8, pp. 4529–4559, August 2008.
- [ABF⁺15] C. Adjih, E. Baccelli, E. Fleury, G. Harter, N. Mitton, T. Noel, R. Pissard-Gibollet, F. Saint-Marcel, G. Schreiner, J. Vandaele *et al.*, “Fit iot-lab: A large scale open experimental iot testbed,” in *2015 IEEE 2nd World Forum on Internet of Things (WF-IoT)*. IEEE, 2015, pp. 459–464. [Online]. Available: www.iot-lab.info
- [ABV⁺12] R. Alexander, A. Brandt, J. Vasseur, J. Hui, K. Pister, P. Thubert, P. Levis, R. Struik, R. Kelsey, and T. Winter, “RPL: IPv6 Routing Protocol for Low-Power and Lossy Networks,” RFC 6550, Mar. 2012.
- [ACQB21] M. I. M. Abdulla, M. Chetto, A. Queudet, and L. Belouaer, “On designing cyber-physical-social systems with energy-neutrality and real-time capabilities,” in *2021 4th IEEE International Conference on Industrial Cyber-Physical Systems (ICPS)*, 2021, pp. 369–374.
- [AFT⁺22] R. Antonio, S. Faria, L. M. Tavora, A. Navarro, and P. Assuncao, “Learning-based compression of visual objects for smart surveillance,” in *2022 Eleventh International Conference on Image Processing Theory, Tools and Applications (IPTA)*. IEEE, 2022, pp. 1–6.
- [AG20] V. Arrichiello and P. Gualeni, “Systems engineering and digital twin: a vision for the future of cruise ships design, production and operations,” *International Journal on Interactive Design and Manufacturing (IJIDeM)*, vol. 14, no. 1, pp. 115–122, 2020.
- [AKHM22] A. Aliouat, N. Kouadria, S. Harize, and M. Maimour, “Multi-Threshold-Based Frame Segmentation for Content-Aware Video Coding in WMSN,” in *International Conference on Computing Systems and Applications*. Springer, 2022, pp. 337–347.
- [AKHM23] —, “An Efficient Low Complexity Region-of-Interest Detection for Video Coding in Wireless Visual Surveillance,” *IEEE Access*, vol. 11, pp. 26 793–26 806, 2023.
- [AKM⁺23] A. Aliouat, N. Kouadria, M. Maimour, S. Harize, and N. Doghmane, “Region-of-Interest Based Video Coding Strategy for Rate/Energy-constrained Smart Surveillance Systems Using WMSNs,” *Ad Hoc Networks*, vol. 140, p. 103076, 2023.

-
- [AKMH22] A. Aliouat, N. Kouadria, M. Maimour, and S. Harize, "Region-of-Interest Based Video Coding Strategy for Low Bitrate Surveillance Systems," in *2022 19th International Multi-Conference on Systems, Signals and Devices (SSD)*, IEEE, Ed., Setif, Algeria, 6-10 May 2022, pp. 1357–1362.
- [AL⁺19] R. Ala-Laurinaho *et al.*, "Sensor data transmission from a physical twin to a digital twin," Master's thesis, Aalto University School of Engineering, 2019.
- [Ali23] A. Aliouat, "Étude et mise en œuvre d'un encodeur vidéo basé-objet pour des systèmes de vidéosurveillance sans fils embarqués," Ph.D. dissertation, Badji Mokhtar University, Annaba, Algeria, ?Mai 2023.
- [AM19] D. ADHIKARY and D. K. MALLICK, "Energy-aware on-demand fuzzy-unequal clustering protocol for wireless sensor networks," *Journal of Engineering Science and Technology*, vol. 14, no. 3, pp. 1200–1219, 2019.
- [AMC07] I. F. Akyildiz, T. Melodia, and K. R. Chowdhury, "A survey on wireless multimedia sensor networks," *Computer Networks*, vol. 51, no. 4, pp. 921–960, 3 2007.
- [ANT19] E. M. Ahrar, M. Nassiri, and F. Theoleyre, "Multipath aware scheduling for high reliability and fault tolerance in low power industrial networks," *Journal of Network and Computer Applications*, vol. 142, pp. 25–36, 2019.
- [AP19] S. Arjunan and S. Pothula, "A Survey on Unequal Clustering Protocols in Wireless Sensor Networks," *Journal of King Saud University-Computer and Information Sciences*, vol. 31, no. 3, pp. 304–317, 2019.
- [APB⁺13] N. Accettura, M. R. Palattella, G. Boggia, L. A. Grieco, and M. Dohler, "Decentralized traffic aware scheduling for multi-hop low power lossy networks in the internet of things," in *2013 IEEE 14th International Symposium on "A World of Wireless, Mobile and Multimedia Networks"(WoWMoM)*. IEEE, 2013, pp. 1–6.
- [AR17] A. Aijaz and U. Raza, "DeAMON: A decentralized adaptive multi-hop scheduling protocol for 6TiSCH wireless networks," *IEEE Sensors Journal*, vol. 17, no. 20, pp. 6825–6836, 2017.
- [Arc11] F. Archaux, "On methods of biodiversity data collection and monitoring," *Revue Science Eaux & Territoires, Public policy and biodiversity*, no. 03bis, pp. 70–75, 3 2011.
- [Arm18] Arm, "Cortex M3 datasheet," <https://iot-lab.github.io/assets/misc/docs/iot-lab-m3/stm32f103re.pdf>, 2018.
- [ARS15] K. R. Anupama, C. S. S. Reddy, and M. V. Shenoy, "FlexEye – A Flexible Camera Mote for Sensor Networks," *2015 2nd International Conference on Signal Processing and Integrated Networks (SPIN)*, pp. 1010–1015, 2015.
- [ASM15] S. A. Alvi, G. A. Shah, and W. Mahmood, "Energy efficient green routing protocol for internet of multimedia things," in *2015 IEEE Tenth International Conference on Intelligent Sensors, Sensor Networks and Information Processing (ISSNIP)*. IEEE, 2015, pp. 1–6.
- [ATM13] J. Albath, M. Thakur, and S. Madria, "Energy constraint clustering algorithms for wireless sensor networks," *Ad Hoc Networks*, vol. 11, no. 8, pp. 2512–2525, 2013.
- [ATM⁺14] F. Awad, E. Taqieddin, M. Mowafi, O. Banimelhem, and A. AbuQdais, "A simulation testbed to jointly exploit multiple image compression techniques for wireless multimedia sensor networks," in *International Symposium on Wireless Communications Systems (ISWCS)*, Barcelona, 2014, pp. 905–911.

-
- [B⁺11] A. Boulis *et al.*, *Castalia: A simulator for wireless sensor networks and body area networks*, NICTA: National ICT Australia, <https://github.com/boulis/Castalia> - last accessed 2019-12-12, 2011.
- [BAB20] I. Bouderbal, A. Amamra, and M. A. Benatia, "How Would Image Down-Sampling and Compression Impact Object Detection in the Context of Self-driving Vehicles ?" in *International Conference on Computing Systems and Applications*. Springer, 2020, pp. 25–37.
- [BBKS20] I. Bouacheria, Z. Bidai, B. Kechar, and F. Sailhan, "Leveraging Multi-Instance RPL Routing Protocol to Enhance the Video Traffic Delivery in IoMT," *Wireless Personal Communications*, pp. 1–30, 2020.
- [BCC20] G. Büchi, M. Cugno, and R. Castagnoli, "Smart factory performance and industry 4.0," *Technological Forecasting and Social Change*, vol. 150, p. 119790, 2020.
- [BCF19] B. R. Barricelli, E. Casiraghi, and D. Fogli, "A Survey on Digital Twin: Definitions, Characteristics, Applications, and Design Implications," *IEEE Access*, vol. 7, pp. 167 653–167 671, 2019.
- [BCKZ16] G. F. Barrowclough, J. Cracraft, J. Klicka, and R. M. Zink, "How many kinds of birds are there and why does it matter?" *PLOS ONE*, vol. 11, no. 11, pp. 1–15, 11 2016.
- [BCM11] V. C. Borges, M. Curado, and E. Monteiro, "The impact of interference-aware routing metrics on video streaming in wireless mesh networks," *Ad Hoc Networks*, vol. 9, no. 4, pp. 652 – 661, 2011, multimedia Ad Hoc and Sensor Networks.
- [BFZA16] I. Bennis, H. Fouchal, O. Zytoune, and D. Aboutajdine, "Carrier sense aware multipath geographic routing protocol," *Wireless Communications and Mobile Computing*, vol. 16, no. 9, pp. 1109–1123, 2016.
- [BHM11] Z. Bidai, H. Haffaf, and M. Maimour, "Node Disjoint Multipath Routing for ZigBee Cluster-Tree Wireless Sensor Networks," in *International Conference on Multimedia Computing and Systems (ICMCS)*, April 2011, pp. 1–6.
- [Bid13] Z. Bidai, "Routage avec qualité de service pour le transport multimédia dans les réseaux de capteurs sans fil," Ph.D. dissertation, Oran University, Algeria, June 2013.
- [BJE⁺10] Y. Benezeth, P.-M. Jodoin, B. Emile, H. Laurent, and C. Rosenberger, "Comparative study of background subtraction algorithms," *Journal of Electronic Imaging*, vol. 19, no. 3, p. 033003, 2010.
- [BKH08] Z. Bidai, B. Kechar, and H. Haffaf, "Node disjoint multipath routing protocol supporting quality of service in wireless sensor networks," in *in Proceedings of International Conference on Web Information Technologies (ICWIT'08)*, Sidi Bel Abbes, Algeria, 29-30 June 2008, pp. 281–286.
- [BL20] H. Bouzebiba and M. Lehsaini, "FreeBW-RPL: A New RPL Protocol Objective Function for Internet of Multimedia Things," *Wireless Personal Communications*, pp. 1–21, 2020.
- [Bla21] G. S. Blair, "Digital twins of the natural environment," *Patterns*, vol. 2, no. 10, p. 100359, 2021.
- [BLT93] E. M. Bakker, J. Leeuwen, and R. B. Tan, "Prefix routing schemes in dynamic networks," *Computer Networks and ISDN Systems*, vol. 26, no. 4, pp. 403 – 421, 1993.

-
- [BM14a] Z. Bidai and M. Maimour, "Interference-aware Multipath Routing Protocol for Video Transmission over ZigBee Wireless Sensor Networks," in *the 4th International Conference on Multimedia Computing and Systems*, IEEE, Ed. Marrakesh, Morocco: IEEE, April 14-16 2014.
- [BM14b] —, "Multipath routing for high-data rate applications in zigbee wireless sensor networks," in *the 6th International Conference On New Technologies, Mobility & Security (NTMS'2014)*, March 30-April 2 2014, pp. 1–5.
- [BMH12] Z. Bidai, M. Maimour, and H. Haffaf, "Multipath Extension of the ZigBee Tree Routing in Cluster-tree Wireless Sensor Networks," *International Journal of Mobile Computing and Multimedia Communications*, vol. 4, no. 2, pp. 30–48, 2012.
- [BMK14] Y. Baziz, M. Maimour, and B. Kechar, "EvalVSN : A New Tool for Video Quality Evaluation in Wireless Sensor Networks," in *the 4th International Conference on Multimedia Computing and Systems*, IEEE, Ed. Marrakesh, Morocco: IEEE, April 14-16 2014.
- [BPCM09] V. C. Borges, D. Pereira, M. Curado, and E. Monteiro, "Routing metric for interference and channel diversity in multi-radio wireless mesh networks," in *Ad-Hoc, Mobile and Wireless Networks*. Springer, 2009, pp. 55–68.
- [BPH⁺21] A. Barbie, N. Pech, W. Hasselbring, S. Flögel, F. Wenzhöfer, M. Walter, E. Shchekinova, M. Busse, M. Türk, M. Hofbauer *et al.*, "Developing an Underwater Network of Ocean Observation Systems with Digital Twin Prototypes - A Field Report from the Baltic Sea," *IEEE Internet Computing*, vol. 26, no. 3, pp. 33–42, 2021.
- [BPO⁺22] F. Bhering, D. Passos, L. S. Ochi, K. Obraczka, and C. Albuquerque, "Wireless Multipath Video Transmission: when IoT Video Applications Meet Networking - a Survey," *Multimedia Systems*, vol. 28, no. 3, pp. 831–850, 2022.
- [BS10] L. Buttyán and P. Schaffer, "Position-based aggregator node election in wireless sensor networks," *International Journal of Distributed Sensor Networks*, vol. 6, no. 1, p. 679205, 2010.
- [BSdSvdH18] K. Bruynseels, F. Santoni de Sio, and J. van den Hoven, "Digital twins in health care: ethical implications of an emerging engineering paradigm," *Frontiers in genetics*, vol. 9, p. 31, 2018.
- [BSH21] P. Bauer, B. Stevens, and W. Hazeleger, "A digital twin of earth for the green transition," *Nature Climate Change*, vol. 11, no. 2, pp. 80–83, 2021.
- [BYV22] L. Buonocore, J. Yates, and R. Valentini, "A proposal for a forest digital twin framework and its perspectives," *Forests*, vol. 13, no. 4, p. 498, 2022.
- [CBS⁺19] D. Cearley, B. Burke, D. Smith, N. Jones, A. Chandrasekaran, and C. Lu, "Top 10 strategic technology trends for 2020," Gartner, Stamford, CT, USA, Technical Report, 2019.
- [Cen22] Centre for Digital Built Britain, "What are connected digital twins?" University of Cambridge, Tech. Rep., 2022.
- [CLMY07] M. Chen, V. C. M. Leung, S. Mao, and Y. Yuan, "Directional geographical routing for real-time video communications in wireless sensor networks," *Comput. Commun.*, vol. 30, no. 17, pp. 3368–3383, Nov. 2007.
- [CN22] R. Chiwariro and T. . N, "Quality of Service Aware Routing Protocols in Wireless Multimedia Sensor Networks: Survey," *International Journal of Information Technology*, vol. 14, no. 2, pp. 789–800, 2022.
- [CP99] S. D. C. Perkins, E. Royer, "Ad hoc on demand distance vector (aodv) routing," 1999.

-
- [CPRW03] D. D. Clark, C. Partridge, J. C. Ramming, and J. T. Wroclawski, "A knowledge plane for the internet," in *Proceedings of the 2003 conference on Applications, technologies, architectures, and protocols for computer communications*, 2003, pp. 3–10.
- [CVDD21] T. Chang, M. V. X. Vilajosana, S. Duquennoy, and D. R. Dujovne, "6TiSCH Minimal Scheduling Function (MSF)," RFC 9033, May 2021.
- [CWWV16] T. Chang, T. Watteyne, Q. Wang, and X. Vilajosana, "Llsf: Low latency scheduling function for 6tisch networks," in *2016 International Conference on Distributed Computing in Sensor Systems (DCOSS)*. IEEE, 2016, pp. 93–95.
- [DABM03] D. S. J. De Couto, D. Aguayo, J. Bicket, and R. Morris, "A high-throughput path metric for multi-hop wireless routing," in *Proceedings of the 9th ACM International Conference on Mobile Computing and Networking (MobiCom '03)*, San Diego, California, 9 2003.
- [DANLW15] S. Duquennoy, B. Al Nahas, O. Landsiedel, and T. a. Watteyne, "Orchestra: Robust mesh networks through autonomously scheduled tsch," in *Proceedings of the 13th ACM conference on embedded networked sensor systems*, 2015, pp. 337–350.
- [DFL08] C. Duran-Faundez and V. Lecuire, "Error Resilient Image Communication with Chaotic Pixel Interleaving for Wireless Camera Sensors," ser. REALWSN '08. New York, NY, USA: Association for Computing Machinery, 2008, pp. 21–25.
- [DGG14] M. De Gregorio and M. Giordano, "Change detection with weightless neural networks," in *Proceedings of the IEEE conference on computer vision and pattern recognition workshops*, 2014, pp. 403–407.
- [DGV04] A. Dunkels, B. Gronvall, and T. Voigt, "Contiki - a lightweight and flexible operating system for tiny networked sensors," in *29th annual IEEE international conference on local computer networks*. IEEE, 2004, pp. 455–462.
- [DHC05] P. Ding, J. Holliday, and A. Celik, "Distributed energy efficient hierarchical clustering for wireless sensor networks," in *IEEE International Conference on Distributed Computing in Sensor Systems(DCOSS'05)*, Marina Del Rey, CA, 6 2005.
- [DMPFJ12] P. Di Marco, P. Park, C. Fischione, and K. H. Johansson, "Analytical modeling of multi-hop ieee 802.15.4 networks," *IEEE Transactions on Vehicular Technology*, vol. 61, no. 7, pp. 3191–3208, 2012.
- [DO22] J. P. Duque Ordoñez, "Towards a digital twin of the italian coast," 2022.
- [DPZ04] R. Draves, J. Padhye, and B. Zill, "Routing in multi-radio, multi-hop wireless mesh networks," in *MobiCom '04: Proceedings of the 10th annual international conference on Mobile computing and networking*, ACM. New York, NY, USA: ACM, 2004, pp. 114–128.
- [Dun11] A. Dunkels, "The contikimac radio duty cycling protocol," Swedish Institute of Computer Science, Tech. Rep., 2011.
- [EAG21] H. Elayan, M. Aloqaily, and M. Guizani, "Digital Twin for Intelligent Context-Aware IoT Healthcare Systems," *IEEE Internet of Things Journal*, vol. 8, no. 23, pp. 16 749–16 757, 2021.
- [EHD00] A. Elgammal, D. Harwood, and L. Davis, "Non-parametric model for background subtraction," in *European conference on computer vision*. Springer, 2000, pp. 751–767.
- [EKKK20] A. Elsts, S. Kim, H.-S. Kim, and C. Kim, "An Empirical Survey of Autonomous Scheduling Methods for TSCH," *IEEE Access*, vol. 8, pp. 67 147–67 165, 2020.

-
- [ELJP⁺20] A. C. Estrin, T. Lagos Jenschke, G. Z. Papadopoulos, J. Ignacio Alvarez-Hamelin, and N. Montavont, "Thorough Investigation of multipath Techniques in RPL based Wireless Networks," in *2020 IEEE Symposium on Computers and Communications (ISCC)*, 2020, pp. 1–7.
- [Eri17] S. O. Erikstad, "Merging physics, big data analytics and simulation for the next-generation digital twins," *High-Performance Marine Vehicles*, pp. 141–151, 2017.
- [EYG⁺16] M. E. E. D. A. El, A. A. Youssif, A. Z. Ghalwash *et al.*, "Energy aware and adaptive cross-layer scheme for video transmission over wireless sensor networks," *IEEE Sensors Journal*, vol. 16, no. 21, pp. 7792–7802, 2016.
- [FDBD21] Y. Fang, S. Du, L. Boubchir, and K. Djouani, "Detecting african hoofed animals in aerial imagery using convolutional neural network," *IAES International Journal of Robotics and Automation*, vol. 10, no. 2, p. 133, 2021.
- [FLE06] E. Felemban, C.-G. Lee, and E. Ekici, "Mmspeed: Multipath multi-speed protocol for qos guarantee of reliability and timeliness in wireless sensor networks," *IEEE Transactions on Mobile Computing*, vol. 5, no. 6, pp. 738–754, 6 2006.
- [FZYM21] C. Fan, C. Zhang, A. Yahja, and A. Mostafavi, "Disaster city digital twin: A vision for integrating artificial and human intelligence for disaster management," *International Journal of Information Management*, vol. 56, p. 102049, 2021.
- [GBRP03] S. Gwalani, E. Belding-Royer, and C. Perkins, "Aodv-pa: Aodv with path accumulation," in *Communications, 2003. ICC '03. IEEE International Conference on*, vol. 1, May 2003, pp. 527–531 vol.1.
- [GBS19] N. Ghosh, I. Banerjee, and R. S. Sherratt, "On-demand fuzzy clustering and ant-colony optimisation based mobile data collection in wireless sensor network," *Wireless Networks*, vol. 25, no. 4, pp. 1829–1845, 2019.
- [GDP08] S. Gandham, M. Dawande, and R. Prakash, "Link scheduling in wireless sensor networks: Distributed edge-coloring revisited," *Journal of Parallel and Distributed Computing*, vol. 68, no. 8, pp. 1122–1134, 2008.
- [GGSE01] D. Ganesan, R. Govindan, S. Shenker, and D. Estrin, "Highly-resilient, energy-efficient multipath routing in wireless sensor networks," *ACM SIGMOBILE Mobile Computing and Communications Review*, vol. 5(4), pp. 11–25, 2001.
- [GGW⁺19] J. Guo, X. Gong, W. Wang, X. Que, and J. Liu, "Sasrt: semantic-aware super-resolution transmission for adaptive video streaming over wireless multimedia sensor networks," *Sensors*, vol. 19, no. 14, p. 3121, 2019.
- [GJBM17] D. Ghrab, I. Jemili, A. Belghith, and M. Mosbah, "Correlation-free multipath routing for multimedia traffic in wireless sensor networks," in *Ad-hoc, Mobile, and Wireless Networks. ADHOC-NOW 2017. Lecture Notes in Computer Science*, A. Puliafito, D. Bruneo, S. Distefano, and F. Longo, Eds. Springer, 2017, vol. 10517.
- [GK00] P. Gupta and P. R. Kumar, "The capacity of wireless networks," *IEEE TRANSACTIONS ON INFORMATION THEORY*, vol. 46, no. 2, pp. 388–404, 2000.
- [GMMP15] L. Galluccio, S. Milardo, G. Morabito, and S. Palazzo, "SDN-WISE: Design, prototyping and experimentation of a stateful sdn solution for wireless sensor networks," in *Computer Communications (INFOCOM), 2015 IEEE Conference on*. IEEE, 2015, pp. 513–521.

-
- [GO04] K. J. Gaston and M. A. O'Neill, "Automated species identification: why not?" *Philosophical Transactions of the Royal Society of London. Series B: Biological Sciences*, vol. 359, no. 1444, pp. 655–667, 2004.
- [Goy01] V. K. Goyal, "Multiple description coding: Compression meets the network," *Signal Processing Magazine, IEEE In Signal Processing Magazine, IEEE*, vol. 19, no. 5, pp. 74–93, 2001.
- [GP16] V. Gupta and R. Pandey, "An improved energy aware distributed unequal clustering protocol for heterogeneous wireless sensor networks," *Engineering Science and Technology, an International Journal*, vol. 19, no. 2, pp. 1050–1058, 2016.
- [Gri14] M. Grieves, "Digital twin: manufacturing excellence through virtual factory replication," *White paper*, vol. 1, pp. 1–7, 2014.
- [GS08] M. Genetzakis and V. A. Siris, "A contention-aware routing metric for multi-rate multi-radio mesh networks," in *Communications Society Conference on Sensor, Mesh and Ad Hoc Communications and Networks (SECON'08)*. IEEE, 2008, pp. 242–250.
- [GS18] K. Goyal and J. Singhai, "Review of background subtraction methods using gaussian mixture model for video surveillance systems," *Artificial Intelligence Review*, vol. 50, no. 2, pp. 241–259, 2018.
- [HAM21] I. M. Hameed, S. H. Abdulhussain, and B. M. Mahmmod, "Content-based image retrieval: A review of recent trends," *Cogent Engineering*, vol. 8, no. 1, p. 1927469, 2021.
- [HCWW14] H. Huang, X. Cao, R. Wang, and Y. Wen, "A qos-aware routing algorithm based on ant-cluster in wireless multimedia sensor networks," *Science China Information Sciences*, vol. 57, no. 10, pp. 1–16, 2014.
- [HGZ18] Y. He, J. Guo, and X. Zheng, "From surveillance to digital twin: Challenges and recent advances of signal processing for industrial internet of things," *IEEE Signal Processing Magazine*, vol. 35, no. 5, pp. 120–129, 2018.
- [HHHH22] M. A. Hossain, M. I. Hossain, M. D. Hossain, and E.-N. Huh, "DFC-D: A dynamic weight-based multiple features combination for real-time moving object detection," *Multimedia Tools and Applications*, pp. 1–32, 2022.
- [HJL17] J. Hou, R. Jadhav, and Z. Luo, "Optimization of Parent-node Selection in RPL-based Networks," Internet Engineering Task Force, Internet-Draft draft-hou-roll-rpl-parent-selection-00, Mar. 2017, work in Progress.
- [HKK⁺04] V. Handziski, A. KÄ¶pke, H. Karl, C. Frank, and W. Drytkiewicz, "Improving the energy efficiency of directed diffusion using passive clustering." in *EWSN*, ser. Lecture Notes in Computer Science, vol. 2920, Berlin, Germany, 2004, pp. 172–187.
- [HM95] N. R. Harvey and S. Marshall, "Rank-order morphological filters: A new class of filters," in *IEEE Workshop on nonlinear signal and image processing*, 1995, pp. 975–978.
- [HPCK07] J. Ha, H. Park, S. Choi, and W. Kwon, "EHRP: Enhanced hierarchical routing protocol for zigbee mesh networks," in *IEEE Communications Letters*, vol. 11, 2007, pp. 1028–1030.
- [HSA16] A. Hossain, C. J. Sreenan, and R. D. P. Alberola, "Neighbour-disjoint multipath for low-power and lossy networks," *ACM Transactions on Sensor Networks (TOSN)*, vol. 12, no. 3, p. 23, 2016.

-
- [IGE⁺03] C. Intanagonwiwat, R. Govindan, D. Estrin, J. Heidemann, and F. Silva, "Directed diffusion for wireless sensor networking," *IEEE/ACM Transactions on Networking (TON)*, vol. 11, no. 1, pp. 2–16, 2003.
- [IS07] K. Iwanicki and M. V. Steen, "On hierarchical routing in wireless sensor networks," in *IPSN*, 2007, p. 133144.
- [ITN15] O. Iova, F. Theoleyre, and T. Noel, "Exploiting multiple parents in RPL to improve both the network lifetime and its stability," in *2015 IEEE International Conference on Communications (ICC)*. IEEE, 2015, pp. 610–616.
- [IZZE17] P. Isola, J.-Y. Zhu, T. Zhou, and A. A. Efros, "Image-to-image translation with conditional adversarial networks," in *Proceedings of the IEEE conference on computer vision and pattern recognition*, 2017, pp. 1125–1134.
- [JAAB⁺15] Y. Jararweh, M. Al-Ayyoub, E. Benkhelifa, M. Vouk, A. Rindos *et al.*, "SDIoT: a software defined based internet of things framework," *Journal of Ambient Intelligence and Humanized Computing*, vol. 6, no. 4, pp. 453–461, 2015.
- [JBM12] A. Jayashree, G. Biradar, and V. Mytri, "Energy efficient prioritized multipath qos routing over wmsn," *International Journal of Computer Applications*, vol. 46, no. 17, pp. 33–39, 2012.
- [JJKD09] N. Javaid, A. Javaid, I. A. Khan, and K. Djouani, "Performance study of etx based wireless routing metrics," in *2009 2nd International Conference on Computer, Control and Communication*, 2009, pp. 1–7.
- [JKWS16] Y. Jin, P. Kulkarni, J. Wilcox, and M. Sooriyabandara, "A centralized scheduling algorithm for ieee 802.15. 4e tsch based industrial low power wireless networks," in *2016 IEEE Wireless Communications and Networking Conference*. IEEE, 2016, pp. 1–6.
- [JMB01] D. B. Johnson, D. A. Maltz, and J. Broch, *DSR: The Dynamic Source Routing Protocol for Multi-Hop Wireless Ad Hoc Networks*. Addison-Wesley, 2001, ch. 5, pp. 139–172.
- [KAMH17] H. I. Kobo, A. M. Abu-Mahfouz, and G. P. Hancke, "A survey on software-defined wireless sensor networks: Challenges and design requirements." *IEEE Access*, vol. 5, no. 1, pp. 1872–1899, 2017.
- [KD18] L. Kong and R. Dai, "Efficient video encoding for automatic video analysis in distributed wireless surveillance systems," *ACM Transactions on Multimedia Computing, Communications, and Applications (TOMM)*, vol. 14, no. 3, pp. 1–24, 2018.
- [Kes91] S. Keshav, *A control-theoretic approach to flow control*. ACM, 1991, vol. 21, no. 4.
- [Ket22] S. Kettouche, "Multipath Multichannel Routing for Wireless Multimedia Sensor Networks," Ph.D. dissertation, Larbi Ben M'hidi University, Oum Oum El Bouaghi, Algeria, June 2022.
- [KG02] T. J. Kwon and M. Gerla, "Efficient flooding with passive clustering (pc) in ad hoc networks," *SIGCOMM Comput. Commun. Rev.*, vol. 32, no. 1, pp. 44–56, 2002.
- [KK00] B. Karp and H. T. Kung, "Gpsr: greedy perimeter stateless routing for wireless networks," in *Proceedings of the 6th annual international conference on Mobile computing and networking*, ser. MobiCom '00. New York, NY, USA: ACM, 2000, pp. 243–254.
- [KKK16] M. U. K. Khan, A. Khan, and C.-M. Kyung, "EBSCam: Background subtraction for ubiquitous computing," *IEEE Transactions on Very Large Scale Integration (VLSI) Systems*, vol. 25, no. 1, pp. 35–47, 2016.

-
- [KKP⁺07] T. Kim, D. Kim, N. Park, S.-E. Yoo, and T. Lopez, "Shortcut tree routing in zigbee networks," in *Wireless Pervasive Computing, 2007. ISWPC '07. 2nd International Symposium on*, Feb 2007.
- [KKPB16] H.-S. Kim, H. Kim, J. Paek, and S. Bahk, "Load balancing under heavy traffic in RPL routing protocol for low power and lossy networks," *IEEE Transactions on Mobile Computing*, vol. 16, no. 4, pp. 964–979, 2016.
- [KMD19] S. Kettouche, M. Maimour, and L. Derdouri, "QoE-based Performance Evaluation of Video Transmission using RPL in the IoMT," in *2019 7th Mediterranean Congress of Telecommunications (CMT)*, Oct 2019, pp. 1–4.
- [KMD21a] —, "Bandwidth Provision Through Disjoint Multipath RPL in the IoMT," in *International Conference on Computer Science's Complex Systems and their Applications, ICCSA'21*, 2021.
- [KMD21b] —, "DM-RPL: Disjoint multipath RPL for bandwidth provision in the internet of multimedia things," *Revue de l'Information Scientifique et Technique*, vol. 26, no. 1, pp. 23–35, 2021.
- [KMD22] —, "Disjoint Multipath RPL for QoE/QoS Provision in the Internet of Multimedia Things," *Computing*, vol. 104, no. 7, pp. 1677–1699, July 2022.
- [KMHD19] N. Kouadria, K. Mechouek, S. Harize, and N. Doghmane, "Region-of-interest based image compression using the discrete tchebichef transform in wireless visual sensor networks," *Computers & Electrical Engineering*, vol. 73, pp. 194–208, 2019.
- [KMM15a] J. H. Ko, B. A. Mudassar, and S. Mukhopadhyay, "An Energy-efficient Wireless Video Sensor Node for Moving Object Surveillance," *IEEE Transactions on Multi-Scale Computing Systems*, vol. 1, no. 1, pp. 7–18, 2015.
- [KMM15b] —, "An energy-efficient wireless video sensor node for moving object surveillance," *IEEE Transactions on Multi-Scale Computing Systems*, vol. 1, no. 1, pp. 7–18, 2015.
- [KMR21] M. Kherbache, M. Maimour, and E. Rondeau, "When Digital Twin Meets Network Softwarization in the Industrial IoT: Real-Time Requirements Case Study," *Sensors*, vol. 21, no. 24, p. 8194, 12 2021.
- [KMR22a] —, "Digital Twin Network for the IIoT using Eclipse Ditto and Hono," in *6th Symposium on Telematics Applications, TA'22*. Nancy, France: IFAC, 6 2022.
- [KMR22b] —, "Network Digital Twin for the Industrial Internet of Things," in *2022 IEEE 23rd International Symposium on a World of Wireless, Mobile and Multimedia Networks (WoWMoM)*. IEEE, 2022, pp. 573–578.
- [KMR23] —, "IoT Network Digital Twins modeling using Petri-Nets," in *1er Congrès annuel de la Société d'Automatique de Génie Industriel et de Productique SAGIP 2023*, Marseille, France, June 2023.
- [KNM18a] J. H. Ko, T. Na, and S. Mukhopadhyay, "An Energy-quality Scalable Wireless Image Sensor Node for Object-based Video Surveillance," *IEEE Journal on Emerging and Selected Topics in Circuits and Systems*, vol. 8, no. 3, pp. 591–602, 2018.
- [KNM18b] —, "An energy-quality scalable wireless image sensor node for object-based video surveillance," *IEEE Journal on Emerging and Selected Topics in Circuits and Systems*, vol. 8, no. 3, pp. 591–602, 2018.
- [Ko18] J. H. Ko, "Resource-aware and robust image processing for intelligent sensor systems," Ph.D. dissertation, Georgia Institute of Technology, 2018.

-
- [KRW03] J. Klaue, B. Rathke, and A. Wolisz, "Evalvid - a framework for video transmission and quality evaluation," in *In Proc. of the 13th International Conference on Modelling Techniques and Tools for Computer Performance Evaluation*, 2003, pp. 255–272, <http://www.tkn.tu-berlin.de/research/evalvid/>.
- [KSM⁺22] M. Kherbache, O. Sobirov, M. Maimour, E. Rondeau, and A. Benyahia, "Reinforcement Learning TDMA-Based MAC Scheduling in the Industrial Internet of Things: A Survey," in *6th Symposium on Telematics Applications, TA'22*. Nancy, France: IFAC, 6 2022.
- [KSM⁺23] —, "Decentralized TSCH Scheduling Protocols and Heterogeneous Traffic: Overview and Performance Evaluation," *Internet of Things*, p. 100696, 2023.
- [LA10] A. R. Lari and B. Akbari, "Network-adaptive multipath video delivery over wireless multimedia sensor networks based on packet and path priority scheduling," in *Proceedings of the 2010 International Conference on Broadband, Wireless Computing, Communication and Applications*, ser. BWCCA '10. Washington, DC, USA: IEEE Computer Society, 2010, pp. 351–356.
- [LBB09] R. Langar, N. Bouabdallah, and R. Boutaba, "Mobility-aware clustering algorithms with interference constraints in wireless mesh networks," *Computer Networks*, vol. 53, no. 1, pp. 25–44, 2009.
- [LBV06] K. Langendoen, A. Baggio, and O. Visser, "Murphy loves potatoes: Experiences from a pilot sensor network deployment in precision agriculture," in *Proceedings 20th IEEE international parallel & distributed processing symposium*. IEEE, 2006, pp. 8–pp.
- [LC13] B.-Y. Li and P.-J. Chuang, "Geographic energy-aware non-interfering multipath routing for multimedia transmission in wireless sensor networks," *Information Sciences*, vol. 249, pp. 24 – 37, 2013.
- [LCS⁺21] J. Liang, J. Cao, G. Sun, K. Zhang, L. Van Gool, and R. Timofte, "SwinIR: Image restoration using swin transformer," in *Proceedings of the IEEE/CVF International Conference on Computer Vision*, 2021, pp. 1833–1844.
- [LDFH⁺06] V. Lecuire, C. Duran-Faundez, T. Holl, N. Krommenacker, M. Maimour, and M. David, "Energy Consumption Analysis of a Simple Image Transmission Protocol In Wireless Sensor Networks," in *6th IEEE International Workshop on Factory Communication Systems, WFCS'2006*, Torino, Italy, 6 2006, pp. 215–218.
- [LEA00] *Energy-efficient communication protocol for wireless sensor networks*, Hawaii, January 2000.
- [LG95] C. R. Lin and M. A. Gerla, "A distributed control scheme in multi-hop packet radio networks for voice/data traffic support," in *Proceedings of IEEE GLOBECOM*, 1995, pp. 1238–1242.
- [LG01] S.-J. Lee and M. Gerla, "Split multipath routing with maximally disjoint paths in ad hoc networks," in *Communications, 2001. ICC 2001. IEEE International Conference on*, vol. 10. IEEE, 2001, pp. 3201–3205.
- [LGB⁺13] X. Liu, J. Guo, G. Bhatti, P. Orlik, and K. Parsons, "Load balanced routing for low power and lossy networks," in *2013 IEEE Wireless Communications and Networking Conference (WCNC)*, 2013, pp. 2238–2243.
- [LJKPM21] T. Lagos Jenschke, R.-A. Koutsiamanis, G. Z. Papadopoulos, and N. Montavont, "ODESe: On-demand selection for multi-path RPL networks," *Ad Hoc Networks*, vol. 114, 2021.

-
- [LJXY19] H. Liu, B. Jiang, Y. Xiao, and C. Yang, "Coherent Semantic Attention for Image Inpainting," in *Proceedings of the IEEE/CVF International Conference on Computer Vision*, 2019, pp. 4170–4179.
- [LKHL19] S. Li, J. G. Kim, D. H. Han, and K. S. Lee, "A survey of energy-efficient communication protocols with QoS guarantees in wireless multimedia sensor networks," *Sensors*, vol. 19, no. 1, p. 199, 2019.
- [LKLL07] S. Li, S. Kulkarni, C. Liu, and A. Lim, "Edge: A routing algorithm for maximizing throughput and minimizing delay in wireless sensor networks," in *Proceedings of the 26th Military Communications Conference (MILCOM'07)*, 2007.
- [LKR⁺09] D.-U. Lee, H. Kim, M. Rahimi, D. Estrin, and J. D. Villasenor, "Energy-efficient image compression for resource-constrained platforms," *IEEE Transactions on Image Processing*, vol. 18, no. 9, pp. 2100–2113, 2009.
- [LLM89a] C. Loeffler, A. Ligtenberg, and G. S. Moschytz, "Practical fast 1-d dct algorithms with 11 multiplications," in *Acoustics, Speech, and Signal Processing, 1989. ICASSP-89., 1989 International Conference on*, May 1989, pp. 988–991 vol.2.
- [LLM89b] —, "Practical fast 1-D DCT algorithms with 11 multiplications," in *International Conference on Acoustics, Speech, and Signal Processing.* IEEE, 1989, pp. 988–991.
- [LLZ⁺06] X. Liao, S. Li, P. Zhu, S. Peng, W.-F. Cheng, and D. Dong, "Path selection of reliable data delivery in wireless sensor networks," in *WASA*, 2006, pp. 163–174.
- [Lou05] W. Lou, "An efficient n-to-1 multipath routing protocol in wireless sensor networks," in *IEEE International Conference on Mobile Adhoc and Sensor Systems Conference*. Washington, DC: IEEE, 2005, pp. 672–679.
- [LRCL08] S. Li, N. R., L. C., and A. Lim, "Delay-constrained high throughput protocol for multi-path transmission over wireless multimedia sensor networks," in *9th IEEE International Symposium on a World of Wireless, Mobile and Multimedia Networks (WOWMOM'08)*, 2008.
- [LRK⁺17] M. A. Lodhi, A. Rehman, M. M. Khan, M. Asfand-e yar, and F. B. Hussain, "Transient multipath routing protocol for low power and lossy networks." *KSII Transactions on Internet & Information Systems*, vol. 11, no. 4, 2017.
- [LT83] J. Leeuwen and R. B. Tan, "Routing with compact routing tables," Department of Computer Science, University of Utrecht, Utrecht, Tech. Rep. RUU-CS-83-16, 1983.
- [LT95] —, "Compact routing methods: A survey," in *DEPT. OF COMPUTER SCIENCE, UTRECHT UNIVERSITY*. University Press, 1995, pp. 99–109.
- [LW06] Y. Lu and V. W. Wong, "An energy-efficient multipath routing protocol for wireless sensor networks," *Wiley International Journal of Communication Systems, special issue on Energy-efficient Networks Protocols and Algorithms for Wireless Sensor Networks*, 2006.
- [LWM22] L. Li, X. Wang, and X. Ma, "Design of a location-based opportunistic geographic routing protocol," *Computer Communications*, vol. 181, pp. 357–364, 2022.
- [LZY⁺19] J. Leng, H. Zhang, D. Yan, Q. Liu, X. Chen, and D. Zhang, "Digital twin-driven manufacturing cyber-physical system for parallel controlling of smart workshop," *Journal of ambient intelligence and humanized computing*, vol. 10, no. 3, pp. 1155–1166, 2019.

-
- [MAH07] M. Mamun-or-Rashid, M. M. Alam, and C. S. Hong, "Energy conserving passive clustering for efficient routing in wireless sensor network," in *9th International Conference on Advanced Communication Technology*, February 2007, pp. 982–986.
- [Mai07] M. Maimour, "Multipath Routing Protocol for Layered Video Transport in Wireless Sensor Networks," in *Workshop on Wireless Sensor Networks in conjunction with NOTERE 2007*, Marrakesh, Morocco, 6 2007.
- [Mai08] —, "Maximally Radio-Disjoint Multipath Routing for Wireless Multimedia Sensor Networks," in *Proceedings of the 4th ACM workshop on Wireless multimedia networking and performance modeling colocated with MSWIM'08*, Vancouver, Canada, 27-31 October 2008.
- [Mai18a] —, "Interference-aware Multipath Routing for WSNs: Overview and Performance Evaluation," *Applied Computing and Informatics*, vol. 16, no. 1/2, pp. 59–80, Mar. 2018.
- [Mai18b] —, "SenseVid: A Traffic Trace based Tool for QoE Video Transmission Assessment Dedicated to Wireless Video Sensor Networks," *Simulation Modelling Practice and Theory*, vol. 87, pp. 120–137, 9 2018.
- [Mai20a] —, "Impact of Interference Aware Metrics on Iterative Multipath Routing for Industrial WSN," *Internet Technology Letters, Special Issue on Industrial Internet of Things*, vol. 3, no. 4, p. e159, July 2020.
- [Mai20b] —, "Interference-aware Metrics Impact on the Performance of Incremental Multipath Routing in WSNs," *Journal of High Speed Networks*, vol. 26, no. 3, pp. 225–240, 2020.
- [MAMK16] H. Mao, M. Alizadeh, I. Menache, and S. Kandula, "Resource management with deep reinforcement learning," in *Proceedings of the 15th ACM Workshop on Hot Topics in Networks*. ACM, 2016, pp. 50–56.
- [MB16] M. Maimour and Z. Bidai, "A Multipath Prefix Routing for Wireless Sensor Networks," *Wireless Personal Communications*, vol. 91, no. 1, pp. 313–343, 2016.
- [MCL⁺14] D. Min, S. Choi, J. Lu, B. Ham, K. Sohn, and M. N. Do, "Fast global image smoothing based on weighted least squares," *IEEE Transactions on Image Processing*, vol. 23, no. 12, pp. 5638–5653, 2014.
- [MK18] F. Mortazavi and M. Khansari, "An energy-aware RPL routing protocol for internet of multimedia things," in *Proceedings of the International Conference on Smart Cities and Internet of Things*, ser. SCIOT '18. New York, NY, USA: ACM, 2018, pp. 11:1–11:6.
- [MKZH08a] A. Mammeri, A. Khoumsi, D. Ziou, and B. Hadjou, "Energy-efficient transmission scheme of jpeg images over visual sensor networks," in *Local Computer Networks, 2008. LCN 2008. 33rd IEEE Conference on*, Oct 2008, pp. 639–647.
- [MKZH08b] —, "Modeling and Adapting JPEG to the Energy Requirements of VSN," in *Computer Communications and Networks, 2008. ICCCN '08. Proceedings of 17th International Conference on*, 2008, pp. 1–6.
- [MLC20] R. Minerva, G. M. Lee, and N. Crespi, "Digital twin in the IoT context: a survey on technical features, scenarios, and architectural models," *Proceedings of the IEEE*, vol. 108, no. 10, pp. 1785–1824, 2020.
- [MLWSW07] Y. Ming Lu and V. W. S. Wong, "An energy-efficient multipath routing protocol for wireless sensor networks: Research articles," *Int. J. Commun. Syst.*, vol. 20, no. 7, pp. 747–766, 7 2007.

-
- [Mot] *Tmote Sky Datasheet*, Moteiv Corporation. [Online]. Available: <http://sentilla.com/files/pdf/eol/tmote-sky-datasheet.pdf>
- [MPA08] M. Maimour, C. Pham, and J. Amelot, "Load Repartition for Congestion Control in Multimedia Wireless Sensor Networks with Multipath Routing," in *IEEE International Symposium on Wireless Pervasive Computing*, Santorini, Greece, 7-9 May 2008.
- [MPH09] M. Maimour, C. Pham, and D. Hoang, "A Congestion Control Framework for Handling Video Surveillance Traffics on WSN," in *2009 International Conference on Computational Science and Engineering*, vol. 2, 2009, pp. 943–948.
- [MPPU19] C. Mandolla, A. M. Petruzzelli, G. Percoco, and A. Urbinati, "Building a digital twin for additive manufacturing through the exploitation of blockchain: A case analysis of the aircraft industry," *Computers in Industry*, vol. 109, pp. 134–152, 2019.
- [MR04] V. Mhatre and C. Rosenberg, "Design guidelines for wireless sensor networks: communication, clustering and aggregation," *Ad Hoc Networks*, vol. 2, no. 1, pp. 45–63, January 2004.
- [MRNC⁺17] A. Mestres, A. Rodriguez-Natal, J. Carner, P. Barlet-Ros, E. Alarcón, M. Solé, V. Muntés-Mulero, D. Meyer, S. Barkai, M. J. Hibbett *et al.*, "Knowledge-defined networking," *ACM SIGCOMM Computer Communication Review*, vol. 47, no. 3, pp. 2–10, 2017.
- [MSL18] E. Municio, K. Spaey, and S. Latré, "A distributed density optimized scheduling function for iee 802.15. 4e tsch networks," *Transactions on Emerging Telecommunications Technologies*, vol. 29, no. 7, p. e3420, 2018.
- [MSR⁺22] M. Maimour, A. Sakhri, E. Rondeau, M. Chida, C. Tounsi-Omezzine, and C. Zhang, "Deep Learning-based Image Restoration for Low-power and Lossy Networks," in *5th Edition of the International Conference on Advanced Aspects of Software Engineering, ICAASE'22*, Constantine, Algeria, Sep. 2022.
- [MT14] M. N. Moghadam and H. Taheri, "High throughput load balanced multipath routing in homogeneous wireless sensor networks," in *2014 22nd Iranian Conference on Electrical Engineering (ICEE)*. IEEE, 2014, pp. 1516–1521.
- [MUMF21] F. G. Medina, A. W. Umpierrez, V. MartÁnez, and H. Fromm, "A maturity model for digital twin implementations in the commercial aerospace oem industry," in *2021 10th International Conference on Industrial Technology and Management (ICITM)*, 2021, pp. 149–156.
- [MWQ⁺07] Y. MAO, F. WANG, L. QIU, S. S. LAM, and J. M. SMITH, "S4: Small state and small stretch routing protocol for large wireless sensor networks," in *USENIX NSDI*, Cambridge, MA, USA, 4 2007.
- [MZL10] M. Maimour, H. Zeghilet, and F. Lepage, *Sustainable Wireless Sensor Networks*. Intech, December 2010, ch. Cluster-based Routing Protocols for Energy-Efficiency in Wireless Sensor Networks, pp. 167–188.
- [NDNQK⁺19] H. Nguyen-Duy, T. Ngo-Quynh, F. KOJIMA, T. Pham-Van, T. Nguyen-Duc, and S. Luongoudon, "RL-TSCH: A Reinforcement Learning Algorithm for Radio Scheduling in TSCH 802.15.4e," in *2019 International Conference on Information and Communication Technology Convergence (ICTC)*, 2019, pp. 227–231.
- [NK17] T. Noguchi and T. Kobayashi, "Adaptive location-aware routing with directional antennas in mobile adhoc networks," in *International Conference on Computing, Networking and Communications (ICNC)*. IEEE, 2017, pp. 1006–1011.

-
- [ns2] “Network simulator 2,” <http://www.isi.edu/nsnam/ns>.
- [NSC21] H. N. Noura, O. Salman, and R. Couturier, “A Deep Learning Scheme for Efficient Multimedia IoT Data Compression,” 2021, arXiv preprint arXiv:2105.09280.
- [NWRK04] N. T. Nguyen, A.-I. A. Wang, P. Reiher, and G. Kuenning, “Electric-field-based routing: a reliable framework for routing in manets,” *ACM SIGMOBILE Mobile Computing and Communications Review*, vol. 8, no. 2, pp. 35–49, 2004.
- [ODK20] S. S. Oyewobi, K. Djouani, and A. M. Kurien, “A review of industrial wireless communications, challenges, and solutions: A cognitive radio approach,” *Transactions on Emerging Telecommunications Technologies*, vol. 31, no. 9, p. e4055, 2020.
- [OEFP21] C. Orfanidis, A. Elsts, P. Pop, and X. Fafoutis, “Tsch evaluation under heterogeneous mobile scenarios,” *IoT*, vol. 2, no. 4, pp. 656–668, 2021.
- [omn] “Omnet++, discrete event simulator.” [Online]. Available: <https://omnetpp.org/>
- [ORSHDF⁺11] E. Orellana-Romero, J. SanMartin-Hernandez, C. Duran-Faundez, V. Lecuire, and C. Aguilera, “Sim-lit: A simulation framework for image quality assessment in wireless visual sensor networks under packet loss conditions,” in *Computer Science Society (SCCC), 2011 30th International Conference of the Chilean*, 2011, pp. 202–209.
- [PAD⁺12] M. Palattella, N. Accettura, M. Dohler, L. Grieco, and G. Boggia, “Traffic aware scheduling algorithm for reliable low-power multi-hop iee 802.15.4e networks,” in *IEEE International Symposium on Personal, Indoor and Mobile Radio Communications, PIMRC*, 09 2012.
- [PB94] C. E. Perkins and P. Bhagwat, “Highly dynamic destination-sequenced distance-vector routing (dsv) for mobile computers,” in *ACM SIGCOMM computer communication review*, vol. 24, no. 4. ACM, 1994, pp. 234–244.
- [Pet97] G. Peterson, “Arnold’ Cat Map,” *Math Linear Algebra*, vol. 45, pp. 1–7, 1997.
- [Pha12] C. Pham, “videosense: a simulation model of image sensors under omnet++/castalia,” 6 2012. [Online]. Available: <http://cpham.perso.univ-pau.fr/WSN-MODEL/wvsn-castalia.html>
- [PHST00] M. R. Pearlman, Z. J. Haas, P. Sholander, and S. S. Tabrizi, “On the impact of alternate path routing for load balancing in mobile ad hoc networks,” in *Mobile and Ad Hoc Networking and Computing, 2000. MobiHOC. 2000 First Annual Workshop on*. IEEE, 2000, pp. 3–10.
- [PKKM20] H. Park, H. Kim, S.-T. Kim, and P. Mah, “Multi-Agent Reinforcement-Learning-Based Time-Slotted Channel Hopping Medium Access Control Scheduling Scheme,” *IEEE Access*, vol. 8, pp. 139 727–139 736, 2020.
- [PTK08] I. Politis, M. Tsagkaropoulos, and S. Kotsopoulos, “Optimizing video transmission over wireless multimedia sensor networks,” in *GLOBECOM’08*, 2008, pp. 117–122.
- [PZCG14] C. Perera, A. Zaslavsky, P. Christen, and D. Georgakopoulos, “Context Aware Computing for The Internet of Things: A Survey,” *IEEE Communications Surveys & Tutorials*, vol. 16, no. 1, pp. 414–454, 2014.
- [QSH09] W. Qiu, E. Skafidas, and P. Hao, “Enhanced tree routing for wireless sensor networks,” *Ad hoc networks*, vol. 7, no. 3, pp. 638–650, 2009.
- [RBI⁺05] M. Rahimi, R. Baer, O. Iroezi, J. Garcia, J. Warrior, D. Estrin, and M. Srivastava, “Cyclops: in situ image sensing and interpretation in wireless sensor networks,” in *Proc. of the ACM Conf. on Embedded Networked Sensor Systems (SenSys)*, San Diego, CA, November 2005.

-
- [RCP23] M. A. Ribeiro, I. A. Carvalho, and A. H. Pereira, “The widest k-set of disjoint paths problem,” *RAIRO-Operations Research*, vol. 57, no. 1, pp. 87–97, 2023.
- [RDB⁺11] M. Radi, B. Dezfouli, K. Bakar, S. A. Razak, and M. Nematbakhsh, “Interference-aware multipath routing protocol for qos improvement in event-driven wireless sensor networks,” *Tsinghua Sci. Tech*, vol. 16, no. 5, pp. 475–490, 2011.
- [RDB⁺14] M. Radi, B. Dezfouli, K. A. Bakar, S. A. Razak, and T. Hwee-Pink, “Im2pr: interference-minimized multipath routing protocol for wireless sensor networks,” *Wireless Networks*, vol. 20, no. 7, pp. 1807–1823, 2014.
- [RMA⁺21] L. Raes, P. Michiels, T. Adolphi, C. Tampere, T. Dalianis, S. Mcaleer, and P. Kogut, “Duet: a framework for building secure and trusted digital twins of smart ci ties,” *IEEE Internet Computing*, pp. 1–9, 2021.
- [RQADG16] I. Romdhani, M. Qasem, A. Y. Al-Dubai, and B. Ghaleb, “Cooja simulator manual,” Edinburgh Napier University, Tech. Rep., 2016.
- [RR07] M. Ringwald and K. Romer, “Deployment of sensor networks: Problems and passive inspection,” in *2007 Fifth Workshop on Intelligent Solutions in Embedded Systems*. IEEE, 2007, pp. 179–192.
- [RSK20] A. Rasheed, O. San, and T. Kvamsdal, “Digital twin: Values, challenges and enablers from a modeling perspective,” *IEEE Access*, vol. 8, pp. 21 980–22 012, 2020.
- [RVDA20] F. Righetti, C. Vallati, S. K. Das, and G. Anastasi, “An Evaluation of the 6TiSCH Distributed Resource Management Mode,” *ACM Trans. Internet Things*, vol. 1, no. 4, 7 2020.
- [RZS⁺13] D. Rosário, Z. Zhao, C. Silva, E. Cerqueira, and T. Braun, “An omnet++ framework to evaluate video transmission in mobile wireless multimedia sensor networks,” in *Proceedings of the 6th International ICST Conference on Simulation Tools and Techniques*. ICST (Institute for Computer Sciences, Social-Informatics and Telecommunications Engineering), 2013, pp. 277–284.
- [SA18] G. Suseela and Y. Asnath Vicky Phamila, “Energy efficient image coding techniques for low power sensor nodes: A review,” *Ain Shams Engineering Journal*, vol. 9, no. 4, pp. 2961 – 2972, 2018.
- [SB06] H. R. Sheikh and A. C. Bovik, “Image Information and Visual Quality,” *IEEE Transactions on image processing*, vol. 15, no. 2, pp. 430–444, 2006.
- [SBM06] A. P. Subramanian, M. M. Buddhikot, and S. Miller, “Interference aware routing in multi-radio wireless mesh networks,” in *Wireless Mesh Networks, 2006. WiMesh 2006. 2nd IEEE Workshop on*. IEEE, 2006, pp. 55–63.
- [SC17] J. C. SanMiguel and A. Cavallaro, “Networked computer vision: the importance of a holistic simulator,” *Computer*, vol. 50, no. 7, pp. 35–43, 2017.
- [SDE18] M. F. Savaş, H. Demirel, and B. Erkal, “Moving object detection using an adaptive background subtraction method based on block-based structure in dynamic scene,” *Optik*, vol. 168, pp. 605–618, 2018.
- [SDK20] P. Z. Sotenga, K. Djouani, and A. M. Kurien, “Media access control in large-scale internet of things: A review,” *IEEE Access*, vol. 8, pp. 55 834–55 859, 2020.
- [SF⁺68] I. Sobel, G. Feldman *et al.*, “A 3×3 isotropic gradient operator for image processing,” *a talk at the Stanford Artificial Project in*, pp. 271–272, 1968.

-
- [SG99] C. Stauffer and W. E. L. Grimson, "Adaptive background mixture models for real-time tracking," in *Proceedings. 1999 IEEE computer society conference on computer vision and pattern recognition (Cat. No PR00149)*, vol. 2. IEEE, 1999, pp. 246–252.
- [SGG13] K. Sha, J. Gehlot, and R. Greve, "Multipath Routing Techniques in Wireless Sensor Networks: A Survey," *Wireless Personal Communications*, vol. 70, no. 2, pp. 807–829, 2013.
- [SH05] S. Soro and W. Heinzelman, "Prolonging the lifetime of wireless sensor networks via unequal clustering," in *5th International Workshop on Algorithms for Wireless, Mobile, Ad Hoc and Sensor Networks (IEEE WMAN '05)*, Denver, Colorado, 4 2005.
- [SHB⁺22] A. Sakhri, O. Hadji, C. Bouarrouguen, M. Maimour, N. Kouadria, A. Benyahia, E. Rondeau, N. Doghmane, and S. Harize, "Audio-Visual Low Power System for Endangered Waterbirds Monitoring," in *2nd Workshop on Integrated Assessment Modelling for Environmental Systems (IAMES)*, IFAC, Ed., Tarbes, France, 6 2022.
- [SHL⁺12] Y. Shen, W. Hu, J. Liu, M. Yang, B. Wei, and C. T. Chou, "Efficient background subtraction for real-time tracking in embedded camera networks," in *Proceedings of the 10th ACM Conference on Embedded Network Sensor Systems*, 2012, pp. 295–308.
- [SHY⁺15] Y. Shen, W. Hu, M. Yang, J. Liu, B. Wei, S. Lucey, and C. T. Chou, "Real-time and robust compressive background subtraction for embedded camera networks," *IEEE Transactions on Mobile Computing*, vol. 15, no. 2, pp. 406–418, 2015.
- [SK85] N. Santoro and R. Khatib, "Labeling and implicit routing in networks," *The Computer Journal*, vol. 28, no. 1, pp. 5–8, 1985.
- [SM17] S. S. Sengar and S. Mukhopadhyay, "Moving object detection based on frame difference and W4," *Signal, Image and Video Processing*, vol. 11, no. 7, pp. 1357–1364, 2017.
- [SMR⁺22] A. Sakhri, M. Maimour, E. Rondeau, N. Doghmane, and S. Harize, "An Energy-Efficient WMSN-based System for Endangered Birds Monitoring," in *6th Symposium on Telematics Applications, TA'22*. Nancy, France: IFAC, 6 2022.
- [SR15] M. Subasri and R. Ramesh, "Neighbor table based shortcut tree routing in zigbee wireless networks," *Int. J. Adv. Eng.*, vol. 1, no. 3, pp. 367–372, 2015.
- [SRK04] P. Seeling, M. Reisslein, and B. Kulapala, "Network performance evaluation using frame size and quality traces of single-layer and two-layer video: A tutorial," *Communications Surveys Tutorials, IEEE*, vol. 6, no. 3, pp. 58–78, 3 2004.
- [SSC11] E. Sun, X. Shen, and H. Chen, "A low energy image compression and transmission in wireless multimedia sensor networks," *Procedia Engineering*, vol. 15, pp. 3604–3610, 2011.
- [SSH⁺18] E. Sisinni, A. Saifullah, S. Han, U. Jennehag, and M. Gidlund, "Industrial internet of things: Challenges, opportunities, and directions," *IEEE transactions on industrial informatics*, vol. 14, no. 11, pp. 4724–4734, 2018.
- [SSK⁺07] K.-Y. Shin, J. Song, J. Kim, M. Yu, and P. S. Mah, "Rear: reliable energy aware routing protocol for wireless sensor networks," in *The 9th international conference on advanced communication technology*, vol. 1. IEEE, 2007, pp. 525–530.
- [std12] I. std., "802.15.4e, Part. 15.4: Low-Rate Wireless Personal Area Networks (LR-WPANs) Amendment 1: MAC sublayer," IEEE Standard for Information Technology, Standard, 4 2012.

-
- [std16] —, “Ieee standard for low-rate wireless networks,” IEEE standard for Information Technology, Standard, 2016.
- [SZ95] J. Skinner and S. Zalewski, *Fonctions et valeurs des zones humides méditerranéennes*. Medwet, 1995.
- [TBZBO12] B. Tavli, K. Bicakci, R. Zilan, and J. M. Barcelo-Ordinas, “A survey of visual sensor network platforms,” *Multimedia Tools and Applications*, vol. 60, no. 3, pp. 689–726, 2012.
- [TD18] V. Tsakanikas and T. Dagiuklas, “Video surveillance systems-current status and future trends,” *Computers & Electrical Engineering*, vol. 70, pp. 736–753, 2018.
- [Tel04] A. Telea, “An Image Inpainting Technique Based on the Fast Marching Method,” *Journal of graphics tools*, vol. 9, no. 1, pp. 23–34, 2004.
- [Teu78] J. Teuhola, “A compression method for clustered bit-vectors,” *Information processing letters*, vol. 7, no. 6, pp. 308–311, 1978.
- [THT08] J.-Y. Teo, Y. Ha, and C.-K. Tham, “Interference-minimized multipath routing with congestion control in wireless sensor network for high-rate streaming,” *IEEE Trans. Mobile Comput.*, vol. 7, no. 9, p. 1124–1137, 2008.
- [Thu12] P. Thubert, “Objective Function Zero for the Routing Protocol for LowPower and Lossy Networks (RPL),” RFC 6552, Mar. 2012.
- [Thu21] —, “An Architecture for IPv6 over the Time-Slotted Channel Hopping Mode of IEEE 802.14 (6TiSCH),” RFC 9030, 5 2021.
- [TMHW16] W. Tang, X. Ma, J. Huang, and J. Wei, “Toward improved RPL: A congestion avoidance multipath routing protocol with time factor for wireless sensor networks,” *Journal of Sensors*, 2016.
- [TMP16] G. Tarter, L. Mottola, and G. P. Picco, “Directional antennas for convergecast in wireless sensor networks: Are they a good idea ?” in *International Conference on Mobile Ad Hoc and Sensor Systems (MASS)*. IEEE, 2016, pp. 172–182.
- [TPD02] C. N. Taylor, D. Panigrahi, and S. Dey, “Design of an adaptive architecture for energy efficient wireless image communication,” in *Embedded processor design challenges*. Springer, 2002, pp. 260–273.
- [TPLT09] C.-H. Tsai, M.-S. Pan, Y.-C. Lu, and Y.-C. Tseng, “Self-learning routing for zigbee wireless mesh networks,” in *IEEE Asia-Pacific Wireless Communications Symposium (APWCS)*, 2009.
- [Tra99] T. D. Tran, “A fast multiplierless block transform for image and video compression,” in *Image Processing, 1999. ICIP 99. Proceedings. 1999 International Conference on*, vol. 3, 1999, pp. 822–826 vol.3.
- [TYM17] Y. Tahir, S. Yang, and J. McCann, “BRPL: Backpressure RPL for high-throughput and mobile IoTs,” *IEEE Transactions on Mobile Computing*, vol. 17, no. 1, pp. 29–43, 2017.
- [TZ01] M. Thorup and U. Zwick, “Compact routing schemes,” in *Proceedings of the thirteenth annual ACM symposium on Parallel algorithms and architectures*. ACM, 2001, pp. 1–10.
- [UKO22] A. R. Urke, O. Kure, and K. Ovsthus, “A Survey of 802.15.4 TSCH Schedulers for a Standardized Industrial Internet of Things,” *Sensors*, vol. 22, no. 1, 2022.

-
- [VDP22] R. Vinodha, S. Durairaj, and S. Padmavathi, “Energy-Efficient Routing Protocol and Optimized Passive Clustering in WSN for SMART Grid Applications,” *International Journal of Communication Systems*, vol. 35, no. 1, p. e5019, 2022.
- [VKP⁺12] J. Vasseur, M. Kim, K. Pister, N. Dejean, and D. Barthel, “Routing Metrics Used for Path Calculation in Low-Power and Lossy Networks,” RFC 6551, Mar. 2012.
- [VNT⁺22] M. Vaezi, K. Noroozi, T. D. Todd, D. Zhao, G. Karakostas, H. Wu, and X. Shen, “Digital Twins from a Networking Perspective,” *IEEE Internet of Things Journal*, 2022.
- [VWC⁺19] X. Vilajosana, T. Watteyne, T. Chang, M. Vućinić, S. Duquennoy, and P. Thubert, “Ietf 6tisch: A tutorial,” *IEEE Communications Surveys & Tutorials*, vol. 22, no. 1, pp. 595–615, 2019.
- [WBSS04] Z. Wang, A. Bovik, H. Sheikh, and E. Simoncelli, “Image quality assessment: from error visibility to structural similarity,” *Image Processing, IEEE Transactions on*, vol. 13, no. 4, pp. 600–612, 2004.
- [WC07] G. Wu and T.-c. Chiueh, “Passive and accurate traffic load estimation for infrastructure-mode wireless lan,” in *Proceedings of the 10th ACM Symposium on Modeling, analysis, and simulation of wireless and mobile systems*. ACM, 2007, pp. 109–116.
- [WDHN04] J. Wu, S. Dulman, P. Havinga, and T. Nieberg, “Multipath routing with erasure coding for wireless sensor networks,” in *ProRISC 2004, 15th Annual Workshop on Circuits, Systems and Signal Processing*, Veldhoven, the Netherlands, 25-26 November 2004, pp. 181–188.
- [WH01a] K. Wu and J. Harms, “On-demand multipath routing for mobile ad hoc networks,” in *Proceedings of EPMCC*, 2001, pp. 1–7.
- [WH01b] —, “Performance study of a multipath routing method for wireless mobile ad hoc networks,” in *Proceedings of the Ninth International Symposium in Modeling, Analysis and Simulation of Computer and Telecommunication Systems*, ser. MASCOTS ’01. Washington, DC, USA: IEEE Computer Society, 2001, pp. 99–107.
- [WJP⁺14] Y. Wang, P.-M. Jodoin, F. Porikli, J. Konrad, Y. Benezeth, and P. Ishwar, “Cdnnet 2014: An expanded change detection benchmark dataset,” in *Proceedings of the IEEE conference on computer vision and pattern recognition workshops*, 2014, pp. 387–394.
- [WJZ16] C. Wang, T. Jiang, and Q. Zhang, *ZigBee network protocols and applications*. Auerbach Publications, 2016.
- [WP18] H. Wei and Q. Peng, “A block-wise frame difference method for real-time video motion detection,” *International Journal of Advanced Robotic Systems*, vol. 15, no. 4, p. 1729881418783633, 2018.
- [WQB⁺22] G. Wu, M. Qin, T. M. Bae, S. Li, Y. Fang, and Y.-K. Chen, “Region of interest quality controllable video coding techniques,” Mar. 15 2022, uS Patent 11,277,626.
- [WS99] J. Wu and L. Sheng, “Deadlock-free routing in irregular networks using prefix routing,” in *IN PROCEEDINGS OF PARALLEL AND DISTRIBUTED COMPUTING SYSTEMS*, 1999, pp. 424–430.
- [WVW18] Q. Wang, X. Vilajosana, and T. Watteyne, “6TiSCH Operation Sublayer (6top) Protocol (6P),” RFC 8480, Nov. 2018.

-
- [WY22] L. Wenzheng and Z. Yifeng, "Concept, key technologies and challenges of digital twin river-basin," in *2022 IEEE 12th International Conference on Electronics Information and Emergency Communication (ICEIEC)*. IEEE, 2022, pp. 117–122.
- [WZ10] Z. Wang and J. Zhang, "Interference aware multipath routing protocol for wireless sensor networks," in *GLOBECOM Workshops (GC Wkshps), 2010 IEEE*. IEEE, 2010, pp. 1696–1700.
- [WZZW18] Z. Wang, L. Zhang, Z. Zheng, and J. Wang, "Energy balancing RPL protocol with multipath for wireless sensor networks," *Peer-to-Peer Networking and Applications*, vol. 11, no. 5, pp. 1085–1100, 2018.
- [Yan14] K. Yang, *Wireless sensor networks*. Springer, 2014.
- [YF04] O. Younis and S. Fahmy, "Heed: A hybrid, energy-efficient, distributed clustering approach for ad hoc sensor networks," *IEEE Trans. Mob. Comput.*, vol. 3, no. 4, pp. 366–379, 2004.
- [yuv] "Yuv video sequences." [Online]. Available: <http://trace.eas.asu.edu/yuv/index.html>
- [YYG01] D. E. Y. Yu and R. Govindan, "Geographical and energy-aware routing: a recursive data dissemination protocol for wireless sensor networks," UCLA Computer Science Department, Tech. Rep. UCLA-CSD TR-01-0023, May 2001.
- [ZBM⁺13] H. Zeghilet, Y. Baziz, M. Maimour, B. Kechar, and N. Badache, "The Effects of Interference on Video Quality over Wireless Sensor Networks," in *2013 International Workshop on Communications and Sensor Networks*, vol. 21, Ontario, Canada, October 2013, pp. 436–441.
- [ZBS09] W. Zijian, E. Bulut, and B. K. Szymanski, "Energy efficient collision aware multipath routing for wireless sensor networks," in *Proceedings of the IEEE International Conference on Communications (ICC'09)*, IEEE, Ed., Dresden, Germany, 6 2009, pp. 91–95.
- [Zeg13] H. Zeghilet, "Le Routage dans les Réseaux de Capteurs Multimédia," Ph.D. dissertation, Lorraine University & USTHB, Algeria, December 2013.
- [ZHKS04] G. Zhou, T. He, S. Krishnamurthy, and J. A. Stankovic, "Impact of radio irregularity on wireless sensor networks," in *Proceedings of the 2nd international conference on Mobile systems, applications, and services*. ACM, 2004, pp. 125–138.
- [Zig04] "Zigbee alliance. zigbee document 02130r9: Network specification," 7 2004.
- [Ziv04] Z. Zivkovic, "Improved adaptive gaussian mixture model for background subtraction," in *Proceedings of the 17th International Conference on Pattern Recognition, 2004. ICPR 2004.*, vol. 2. IEEE, 2004, pp. 28–31.
- [ZL20] L. Zhao and S. Li, "Object Detection Algorithm Based on Improved YOLOv3," *Electronics*, vol. 9, no. 3, p. 537, 2020.
- [ZLK⁺17] B. Zhou, A. Lapedriza, A. Khosla, A. Oliva, and A. Torralba, "Places: A 10-million Image Database for Scene Recognition," *IEEE Transactions on Pattern Analysis and Machine Intelligence*, 2017.
- [ZMLB12] H. Zeghilet, M. Maimour, F. Lepage, and N. Badach, "On the Use of Passive Clustering in Wireless Video Sensor Networks," *International Journal of Sensor Networks*, vol. 11, no. 2, pp. 67–80, 2012.
- [ZVDH06] Z. Zivkovic and F. Van Der Heijden, "Efficient adaptive density estimation per image pixel for the task of background subtraction," *Pattern recognition letters*, vol. 27, no. 7, pp. 773–780, 2006.

-
- [ZWY17] L. Zhu, R. Wang, and H. Yang, “Multi-path data distribution mechanism based on rpl for energy consumption and time delay,” *Information*, vol. 8, no. 4, p. 124, 2017.
- [ZZXW19] Z.-Q. Zhao, P. Zheng, S.-t. Xu, and X. Wu, “Object detection with deep learning: A review,” *IEEE transactions on neural networks and learning systems*, vol. 30, no. 11, pp. 3212–3232, 2019.

Résumé.

Les réseaux de capteurs sans fil (RCSF) sont un élément fondamental de l'Internet des objets. Bien que les RCSF soient traditionnellement destinés à des applications à faible débit, il existe un nombre croissant d'applications nécessitant des débits élevés en raison de l'émergence des capteurs multimédia ainsi que l'augmentation du nombre de capteurs et de leurs fréquences d'acquisition. Afin de prendre en charge ces applications, un protocole de routage multichemin efficace est proposé. Par ailleurs, le problème de l'interférence entre chemins multiples est également traité.

Les réseaux de capteurs vidéo sans fil représentent un domaine d'application qui pose des défis importants à cause de l'utilisation intensive des ressources lors de la capture, de l'encodage et de la transmission d'une vidéo. Pour optimiser l'utilisation de la bande passante sans compromettre l'efficacité des tâches d'analyse de l'utilisateur final, une chaîne complète et efficace d'encodage-transmission-reconstruction est proposée. Elle comprend principalement des stratégies de réduction des données peu complexes à la source et l'utilisation de modèles d'apprentissage profond à la destination pour compenser la distorsion causée par la perte due à la compression et à la transmission sur le réseau.

Mon futur projet de recherche se focalise principalement sur *les réseaux définis par la connaissance (KDN)* avec l'utilisation de jumeaux numériques. L'objectif est de construire une architecture globale de jumeaux numériques où le réseau de communication est intégré avec les autres composants du système. Cette recherche vise à explorer deux domaines d'application avec des exigences distinctes : l'Industrie 4.0 et la surveillance de l'environnement.

Abstract.

Wireless Sensor Networks (WSN) form an essential building block of the rapidly growing *Internet of Things (IoT)*. While WSNs have traditionally been designed for low-rate applications, there is an increasing need for high data rate sensing and reporting. Modern applications are witnessing an increase in the number of sensors and their data acquisition frequency including multimedia sensors. To handle high data rate applications, a low-state, low-overhead yet efficient multipath routing protocol is proposed. Additionally, the problem of interpath interference in multipath routing is carefully addressed to optimize the overall network performance.

Wireless Video Sensor Networks (WVSN) constitute a distinctive application domain characterized by resource-intensive tasks, namely, video capture, encoding, and transmission. To optimize bandwidth utilization while ensuring the effectiveness of end-user analysis tasks, a complete and efficient encoding-transmission-reconstruction chain is proposed. This mainly involves employing low-cost data reduction strategies at the source, complemented by the utilization of deep learning models at the destination to address distortions resulting from compression and network transmission losses.

My future research project primarily focuses on *Knowledge-Defined Networks (KDN)* to implement using digital twins. The primary goal is to build a holistic digital twinning architecture that integrates the communication network with other system components. This research aims to explore two application domains, namely Industry 4.0 and environmental surveillance, each with its specific requirements and challenges.